Fruitful Foundations: Novel insights into community composition and succession in the hydroponic strawberry rhizosphere microbiome

Grace Laevens

Thesis submitted to the University of Ottawa
in partial Fulfillment of the requirements for the
Master of Science in Biology.

Department of Biology
Faculty of Science
University of Ottawa

© Grace Laevens, Ottawa, Canada, 2026

Acknowledgements

I would like to sincerely thank everyone who supported me and this project. First, thank you to my supervisor Dr. Allyson MacLean for your guidance and commitment during all aspects of this project. I am thankful for your expertise, enthusiasm, and that you saw as much value in this project as I did. Thank you to the Symbiosis Lab team, specifically Nedishtha, Kris, and Emily, for your physical and emotional support during my time in Ottawa. Thank you Michelle in particular; it was my distinct pleasure to learn with and work alongside you for as long as I had the opportunity. Thank you to the Natural Sciences and Engineering Research Council of Canada (NSERC), the Mitacs Accelerate program, and Ceragen Inc. for their financial support of this research.

To my friends and family, without whom I would never have embarked upon this path in the first place, I would like to express my sincerest gratitude. To my family, thank you for fostering my interest in science from the beginning. To my dearest friends, Cailyn, Sayward, and Kirsten, thank you all for commiserating *and* celebrating with me. To Matthew, thank you for making the bad days good, and the good days better.

Last but certainly not least, I dedicate this thesis to the entire Ceragen team, past and present, without which this work would simply not exist. Danielle, thank you for pursuing this dream to the *very* best of your abilities. Matt, thank you for your unwavering optimism. Ben, thank you for introducing me to the special "joy" that only bioinformatics can provide. Thank you Soufiane and Hannah for being the best microbiologist duo the world has ever seen. Ashley, thank you for your expert advice in all things. Finally, thank you to all of the co-op students who supported the various phases of this project, especially Carina Leung, Brianna Thomas, Sydney Milton, William Dolson, and Acadia Reiser. I am a better scientist for having known each of you.

Abstract

As the global population increases, the productivity of food production systems must also increase. In Canada, strawberry production has declined significantly over several years, highlighting the need for strategies that increase fruit yield and production stability. Microbial inoculants, especially when used in controlled environment agriculture (CEA), present a possible strategy for increasing strawberry yields by leveraging naturally occurring symbiotic relationships between rhizosphere microorganisms and host plants. However, research into developing an effective microbial inoculant for hydroponic strawberries has been unfruitful, in part because the hydroponic strawberry rhizosphere is poorly understood.

In this study, soil samples were added to hydroponic strawberries as an initial source of microbial diversity to influence community assembly. The objectives of this research were to describe community composition, succession, and persistence of bacteria, fungi, and oomycetes within the hydroponic strawberry rhizosphere using 16S and ITS ribosomal RNA (rRNA) amplicon sequencing. Microbial succession was evident, with numerous differentially abundant taxa between initial and final timepoints. However, no microbial taxa were significantly associated with changes in yield. This study also identifies a candidate core microbiome for hydroponic strawberries. The commercial implications of these findings are discussed. Overall, these findings form a foundational understanding of the hydroponic strawberry rhizomicrobiome, and suggest several novel strategies for development of an effective inoculant for hydroponic strawberry production.

Key Words: hydroponic, controlled environment agriculture (CEA), strawberry, rhizosphere, microbiome, microbial succession, plant growth-promoting microorganisms (PGPM), yield, core microbiome, amplicon sequencing, 16S, ITS

Table of Contents

Fruitful Foundations: Novel insights into the hydroponic strawberry rhizosphere microbiome i
Acknowledgements ii
Abstract iii
Table of Contents iv
List of Tables vi
List of Figures vii
List of Abbreviations ix
Chapter 1: Introduction 1
1.1 Trends and challenges in Canadian strawberry production 1
1.2 Controlled environment agriculture 2
1.3 The role of microorganisms in the rhizosphere 3
1.4 Trends in the hydroponic rhizosphere 7
1.5 PGPM for hydroponic strawberries 7
1.6 Microbial persistence and succession, and their implications for inoculant development 9
1.7 Research objectives 10
Chapter 2: Methodology 10
2.1 Hydroponic strawberry plant trial design and maintenance 10
2.2 Addition of soil to hydroponic strawberry systems 13
2.3 Root sample collection and selection for analysis 14
2.4 Sample processing and sequencing 15
2.5 Bioinformatic analysis of amplicon sequencing data 17
Chapter 3: Results 18
3.1 Assessing the impact of soil addition on the hydroponic strawberry rhizomicrobiome 18
3.2 Examining microbial succession in the hydroponic strawberry rhizomicrobiome 28
3.3 Investigating associations between microbial abundances and fruit yield 39
Chapter 4: Discussion and Conclusions 42
4.1 Microbial community composition varies between soil samples and hydroponic systems 42
4.2 Soil addition had minimal long-term impact on the hydroponic strawberry rhizomicrobiome 44
4.3 Microbial succession of rare taxa occurs, while a core microbiome remains consistent 46
4.3.1 The role of stochastic and deterministic processes in the strawberry rhizomicrobiome 47
4.3.2 Discrepancies between time-series and growth-state succession analyses 49
4.3.3 Proposing a candidate beneficial core rhizosphere microbiome of hydroponic strawberries 50
4.3.4 Applying new insights of succession and core microbiome membership in the hydroponic strawberry rhizomicrobiome 56
4.4 No genera were significantly associated with changes in yield 57
4.5 Limitations and future directions 58

4.6 Concluding remarks …… 61
References …… 63
Appendix A: Supplementary Figures …… 99
Appendix B: Supplementary Tables ……... 110
Appendix C: Full-Resolution Figures …… 119

List of Tables

Table 3.1. Summary of number of significant differentially abundant taxa (effect >|1|, FDR <0.05) between pairwise treatment and timepoint comparisons…… 23
Table 4.1. Summary of relevant literature for highly prevalent, highly abundant taxa with respect to their ecological role in strawberry production, demonstrated persistence in hydroponic cropping systems, and evidence of plant growth-promoting (PGP) phenotypes……... 53
Supplementary Table B1. Hydroponic strawberry nutrient solutions for three developmental stages……... 110
Supplementary Table B2. PCR reagents and primer sequences for separate amplification of 16S and ITS rRNA amplicons…….. 110
Supplementary Table B3. PCR cycling specifications for amplification of 16S and ITS rRNA amplicons…….. 111
Supplementary Table B4. Summary of bacterial differential abundance between soil and hydroponic sample groups…… 112
Supplementary Table B5. Summary of fungal/oomycete differential abundance between soil and hydroponic sample groups……... 114
Supplementary Table B6. Summary of effect size and FDR for significant differentially abundant bacterial genera between growth states……. 115
Supplementary Table B7. Summary of microbial differential abundance between week two and week eight sample groups……. 116
Supplementary Table B8. Summary of yield and vegetative growth results for plants selected for analysis…… 117
Supplementary Table B9. Nutrient content (ppm) in soil samples and hydroponic nutrient solution……... 118

List of Figures

Figure 1.1. Summary of direct and indirect plant growth-promoting mechanisms used by microorganisms of the rhizosphere……. 5
Figure 2.1. Experimental workflow for characterization of the hydroponic strawberry rhizosphere microbiome via molecular methods…….. 11
Figure 3.1. Pairwise principal component analysis (PCA) and ALDEx2 effect plots for genus-level 16S CLR abundance data from control (n = 6) and inoculated treatment (n = 6) groups at week eight……... 21
Figure 3.2. Pairwise principal component analysis (PCA) and ALDEx2 effect plots for genus-level ITS CLR abundance data from control (n = 6) and inoculated treatment (n = 6) groups at week eight……... 22
Figure 4.1. Principal component analysis (PCA) and ALDEx2 effect plots for genus-level 16S CLR abundance data from initial soil sample (n = 3) and week eight inoculated root samples (n = 18)..... 24
Figure 4.2. Principal component analysis (PCA) and ALDEx2 effect plots for genus-level ITS CLR abundance data from initial soil samples (n = 3) and week eight inoculated root samples (n = 18)..... 25
Figure 5.1.Summarizing magnitude of bacterial differential abundance between initial soil samples and week eight hydroponic treatment samples…….. 26
Figure 5.2.Summarizing magnitude of fungal and oomycete differential abundance between initial soil samples and week eight hydroponic treatment samples…….. 27
Figure 6.1. Bacterial community composition of baseline microbiome samples…….. 31
Figure 6.2. Fungal and oomycete community composition of baseline microbiome samples……... 32
Figure 7.1. Principal component analysis (PCA) of genus-level 16S CLR abundance at three strawberry growth stages……... 33
Figure 7.2. Principal component analysis (PCA) of genus-level ITS CLR abundance at three strawberry growth stages……... 34
Figure 8.1. Summary of hydroponic strawberry rhizomicrobiome bacterial composition with respect to assigned growth stage…… 35
Figure 8.2. Summary of hydroponic strawberry rhizomicrobiome fungal and oomycete community composition with respect to assigned growth stage…… 36
Figure 9.1. Summary of hydroponic strawberry rhizomicrobiome bacterial community composition with respect to time in weeks…… 37
Figure 9.2. Summary of hydroponic strawberry rhizomicrobiome fungal community composition with respect to time in weeks…… 38
Figure 10.1. Comparison of bacterial community composition between high- and low-yielding strawberry plants from all experimental groups at week eight……. 40
Figure 10.2. Comparison of fungal/oomycete community composition between high- and low-yielding strawberry plants from all experimental groups at week eight……... 41
Supplementary Figure A1. Schematic of hydroponic strawberry cropping systems….. 99
Supplementary Figure A2. Scree plots for Figure 3.1 PCAs……... 100
Supplementary Figure A3. Scree plots for Figure 3.2 PCAs……... 101
Supplementary Figure A4. Scree plots for Figure 4.1 (G) and 4.2 (H) PCAs……. 102
Supplementary Figure A5. Scree plots for Figure 7.1 (I) and 7.2 (J) PCAs…… 103

Supplementary Figure A6. Scree plots for Figure 9.1A (K) and 9.2A (L) PCAs…… 104
Supplementary Figure A7. Scree plots for Figure 10.1A (M) and 10.2A (N) PCAs….. 105
Supplementary Figure A8. Growth state tracking for the no-soil control strawberry plants……... 106
Supplementary Figure A9. Growth state tracking for Field treatment strawberry plants……... 107
Supplementary Figure A10. Growth state tracking for Garden treatment strawberry plants……... 108
Supplementary Figure A11. Growth state tracking for Wetland treatment strawberry plants……... 109

List of Abbreviations

ACC deaminase	1-aminocyclopropane-1-carboxylate deaminase
ALDEx2	ANOVA-like differential expression version 2
BCP Group	*Burkholderia-Caballeronia-Paraburkholderia* tri-genus group
CEA	Controlled environment agriculture
CFIA	Canadian Food Inspection Agency
CLR	Center log ratio
CO_2	Carbon dioxide
DNA	Deoxyribonucleic acid
dNTPs	Deoxynucleotide triphosphates
dS/m	Deci Siemens per meter
EC	Electrical conductivity
FDR	False discovery rate
GAs	Gibberellins
GC content	Guanidine-cytosine content
GC-SM	Gas chromatography-mass spectrometry
GLM	Generalized linear model
IAA	Indole acetic acid
OMAFA	Ontario Ministry of Agriculture, Food, and Agribusiness
ONT	Oxford Nanopore Technologies
PCA	Principle component analysis
PCR	Polymerase chain reaction
PGP	Plant growth-promoting
PGPB	Plant growth-promoting bacteria
PGPF	Plant growth-promoting fungi
PGPM	Plant growth-promoting microorganisms

ppm	Parts per million
qPCR	Quantitative polymerase chain reaction
Rhizomicrobiome	Rhizosphere microbiome
RO	Reverse osmosis
rRNA	Ribosomal ribonucleic acid
VOCs	Volatile organic compounds
WHO	World Health Organization

Chapter 1: Introduction

1.1 Trends and challenges in Canadian strawberry production

The global population is predicted to approach 10 billion by 2050[1]. This 16% increase in population will place further strain on already-insufficient global food production systems[2]. A 2015 study estimated that global food production must increase by at least 0.5% each year to meet this predicted demand[3]. However, we have already fallen short of that goal; an estimated 2.33 billion people experience moderate to severe food insecurity each year, and 88% of countries do not have sufficient fresh produce to meet recommended intake per capita[3,4]. Therefore, there is a growing need for advancements that increase food production.

Traditional, soil-based agriculture alone is unlikely to cover the deficit in food demand for several reasons. First, at current productivity levels, 50-100% of habitable land not already used for agriculture would need to be repurposed for agricultural use[5]. This is unreasonable and unsustainable, as it leaves no allowance for further population growth. Second, erosion, acidification, compaction, salinization, and pollution have already decreased the productivity of more than 50% of existing farmland, and this trend is expected to continue[6]. Third, climate change is increasing weather variability and global temperatures; increases in temperature have been linked to an increased frequency of phytopathogen infections, resulting in decreased crop yields[6]. Thus, we are in need of novel strategies that increase the production of fresh produce.

Canadian strawberry production decreased by 66% between 1995 and 2023, largely due to the three reasons outlined above[7,8]. Specifically, arable farmland in Canada decreased by more than 8% between 2001 and 2021 as farmland was developed for urban use[9]. The earlier onset of spring, combined with late-spring frosts, is a serious threat to flowering crops in Canada, such as strawberries. Early springs coax earlier flowering in many strawberry cultivars, but frost

damage to flowers and developing fruits can significantly decrease yield for the entire season[10,11]. Finally, changes to the North American climate now permit soil-borne pathogens, such as *Verticillium, Fusarium, Phytophthora,* and *Rhizoctonia*, to persist for longer periods[12]. The recommended crop rotation interval before reusing the same land for strawberry production is now 5-7 years[12]. As a result of increased challenges associated with outdoor, soil-based production, Canadian strawberry production is transitioning toward controlled environment agriculture[13].

1.2 Controlled environment agriculture

Controlled environment agriculture (CEA) is the cultivation of crops under partially or completely controlled conditions, ranging from "low-tech" options, such as hoop houses, to "high-tech" options, such as hydroponic greenhouses[14]. Hydroponic agriculture is a type of CEA that uses water-based nutrient solutions and non-soil substrates to grow crops[5]. In general, hydroponic systems can generate higher crop yields and consume less water and fertilizer[5]. Hydroponic agriculture has several advantages for strawberry production specifically. First, hydroponic agriculture bypasses the need for lengthy crop rotation schedules and reduces reliance on chemical pesticides as the hydroponic systems can be sterilized between growing cycles to significantly reduce microbial and insect pest loads[12]. Second, hydroponic greenhouses confer a year-round growing season by maintaining optimal temperature and lighting conditions inside, despite seasonal changes outside. This is particularly advantageous for Canadian strawberry production, because Canada's outdoor growing season is shorter and it's yields are lower than those of southern-grown strawberries (e.g., California)[12]. However, hydroponic greenhouses are expensive to operate, sensitive to technological failure, and conducive to

phytopathogen accumulation during the growing season[15-17]. Fortunately, plant growth-promoting microorganisms can alleviate some of the challenges associated with hydroponic agriculture.

1.3 The role of microorganisms in the rhizosphere

Microorganisms are naturally abundant in the rhizosphere, which is the area in, on, and around plant roots[18]. Microorganisms of the rhizosphere, or rhizomicrobes, may be beneficial, neutral, or harmful. Beneficial rhizomicrobes include plant growth-promoting microorganisms (PGPM)[18]. PGPM participate in symbiosis with plants; host plants provide root exudates as a nutrient source, while PGPM promote plant growth, control phytopathogen populations, and regulate plant stress[18,19]. The term PGPM is an umbrella term that encompasses both bacteria and fungi that promote plant growth (PGPB and PGPF, respectively)[20,21]. Neutral rhizomicrobes are also known as commensalists, which theoretically confer neither benefit nor harm to the host plant[22]. However, in practice, it is difficult to prove that a microorganism truly has no effect on the host plant; thus the classification of commensalists in the rhizomicrobiome is a topic of debate[22]. Harmful rhizomicrobes, also known as phytopathogens, colonize plant tissues and have a negative impact on plant growth[23]. Both PGPM and phytopathogens may use a variety of mechanisms to alter the growth of their host plants.

There exists a wide variety of strategies that microorganisms use to promote plant growth (Figure 1.1); these strategies can be broadly classified as either direct or indirect mechanisms[18]. Direct PGPM mechanisms involve the growth-promoting microbe and the host plant and include increased nutrient acquisition, phytohormone production, and stress regulation[18]. PGPM may increase the bioavailability of nitrogen, phosphate, and iron via nitrogen fixation, the production

of phosphate-solubilizing acids and enzymes, and release of iron-sequestering siderophores, respectively[18]. PGPM may also produce phytohormones (auxins, cytokinins, and gibberellins) or enzymes, such as ACC deaminase, that regulate phytohormones to enhance growth and reduce stress[18,24,25]. Growth promotion by direct PGPM mechanisms is well documented in literature[26-36].

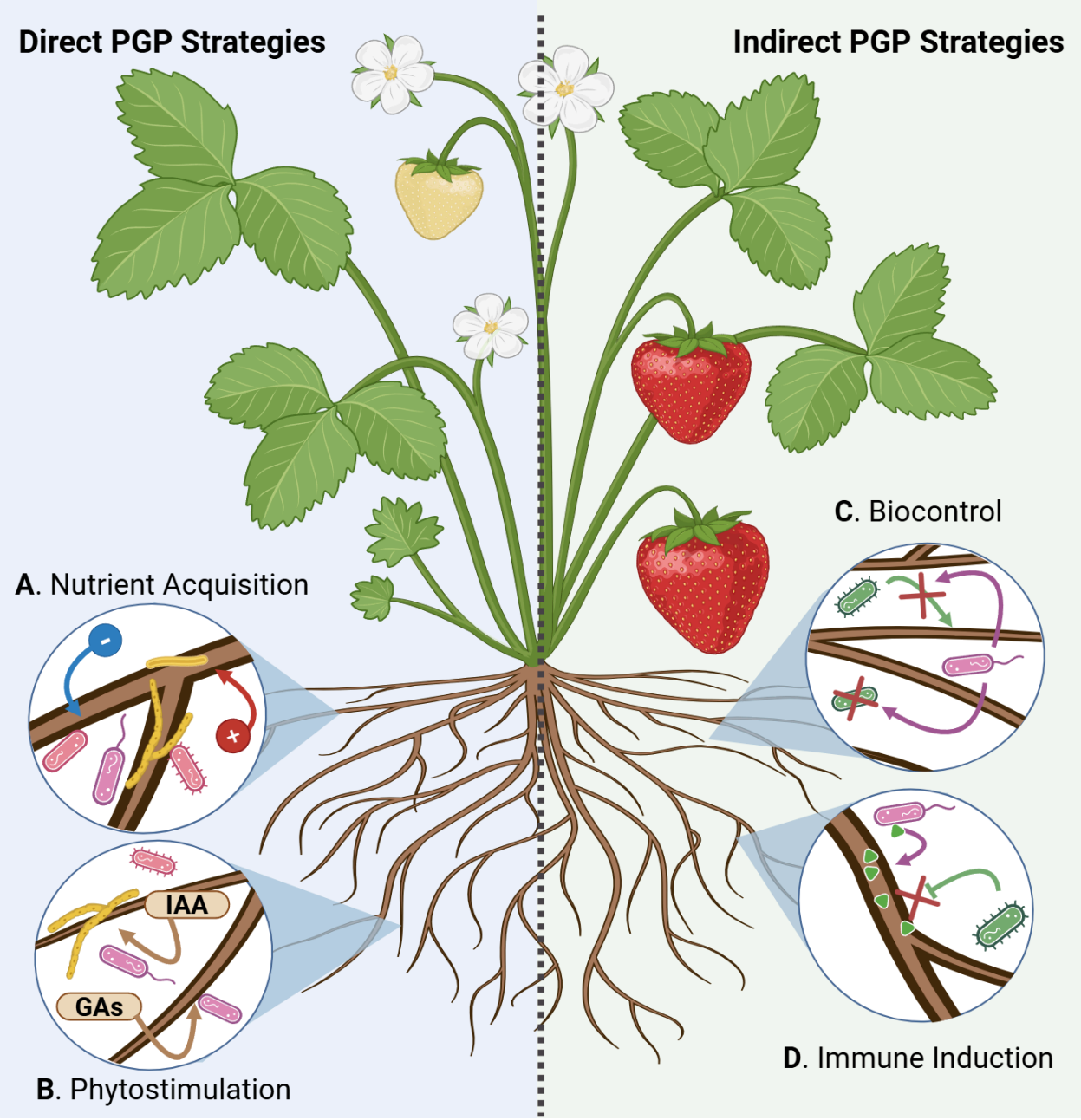


Figure 1.1. Summary of direct and indirect plant growth-promoting mechanisms used by microorganisms of the rhizosphere. Briefly, nutrient acquisition (A) and phytohormone production (i.e. phytostimulation) (B) are examples of direct methods; PGPM may produce and/or deliver nutrients and phytohormones to the host plant. Biocontrol of phytopathogens (C) and immune induction in the host plant (D) are examples of indirect methods, where PGPM activity benefits the host plant by preventing or decreasing the magnitude of phytopathogen infection and symptomology. Figure adapted in BioRender from (Laevens et al., 2024), originally published under a CC BY license.

Indirect mechanisms involve a PGPM that prevents phytopathogen infection of the host plant, thereby indirectly promoting plant growth[18]. PGPM may produce antimicrobial compounds, hydrolytic enzymes, quorum-quenching enzymes, or simply outcompete phytopathogens for resources and space in the rhizosphere, thus preventing phytopathogen growth[5]. Alternatively, secretion of certain volatile organic compounds (VOCs) by PGPM can induce systemic resistance in plants; this primes the host plant defense systems and reduces the risk of phytopathogen infection[21]. Growth promotion by indirect PGPM mechanisms is also well documented in literature[37-41].

Phytopathogens may be biotrophic, necrotrophic, or hemibiotrophic. Biotrophic phytopathogens infect living plant tissue and siphon off nutrients without killing the host plant by secreting effector molecules that inhibit plant defence mechanisms[20]. Biotrophic phytopathogens, such as *Podosphaera xanthii*, the causative agent of powdery mildew in strawberries, generally cause milder symptoms and less yield loss than their necrotrophic counterparts[20]. Necrotrophic phytopathogens infect and kill host tissues, causing necrosis. The necrotrophic pathway often involves the secretion of cell-wall-degrading enzymes that lyse plant cells, causing necrosis[20,21]. The exact symptoms of necrosis vary with the phytopathogen and host plant but can include root, crown, and fruit rot, as well as vascular wilt and blights[20]. Many phytopathogens exhibit both biotrophic and necrotrophic phases and are known as hemibiotrophs[20,21]. Necrotrophic and hemibiotrophic phytopathogens, such as *Botrytis cinerea*, *Xanthomonas fragariae*, and *Neopestalotiopsis*, species are particularly devastating in strawberry production because they can remain undetected and asymptomatic in fruit tissue until ripening begins, at which point fruit rot causes significant yield loss[20, 21,42,43].

1.4 Trends in the hydroponic rhizosphere

The soil rhizosphere is well studied relative to the hydroponic rhizosphere[44-46]. However, the hydroponic rhizosphere is physicochemically different from the soil rhizosphere and therefore exerts different selective pressures on the rhizomicrobiome; thus, trends observed in the soil rhizosphere cannot always be applied to the hydroponic rhizosphere[47]. Hydroponic rhizospheres experience different pH, dissolved oxygen levels, nutrient concentration and nutrient bioavailability than soil-based cropping systems[47]. Hydroponic rhizosphere conditions can also vary with the choice of substrate; inorganic substrates (e.g., stonewool) are metabolically inert, while organic substrates (e.g., coco coir) act as sources of organic matter for members of the rhizomicrobiome[47]. Additionally, some studies suggest that optimal lighting, temperature, and CO_2 levels in CEA systems may increase the production of photosynthetically fixed carbon by hydroponically grown plants, thereby increasing the exudation of carbon-containing compounds[48]. Similarly, some studies have observed decreased lipid exudation by hydroponic plants relative to soil-grown plants; this may be due to the hydrophobic nature of the hydroponic environment[48]. These differences in physicochemical conditions and root exudation likely account for some of the observed differences in rhizomicrobiome community composition in comparative studies of soil and hydroponic systems[49-51].

1.5 PGPM for hydroponic strawberries

PGPM are frequently formulated into and sold as biological inoculants for use in both soil-based and hydroponic agricultural operations[52]. Often, the first step in designing a microbial inoculant is to isolate microorganisms from a crop's rhizosphere[53]. In some studies, researchers inoculate hydroponic systems with rhizosphere soil as a diverse initial source of plant-associated

microorganisms and then allow the hydroponic systems to select for microorganisms that can survive (i.e., persist) in the hydroponic rhizosphere before isolating individual microorganisms[54]. Then, isolates are evaluated for plant growth-promoting (PGP) potential based on *in vitro* biochemical assays and whole-genome sequencing[55,56]. Microorganisms that demonstrate PGP activity *in vitro* or possess genes associated with PGP traits are then used in inoculated plant trials to assess their ability to promote plant growth *in planta*[5]. Single isolates or consortia that consistently perform well in plant trials can then be considered for commercialization and must be registered with the Canadian Food Inspection Agency (CFIA) as an agricultural fertilizer to be used in Canadian greenhouses.

Despite the plethora of commercial inoculants available for use in Canada, there is a lack of effective options for commercial-scale hydroponic strawberry production due to a combination of factors. First, many existing microbial inoculants are based on microorganisms originally isolated from the soil rhizosphere and formulated for use in soil-based agriculture. Given the numerous physicochemical differences between soil and hydroponic environments, soil-derived microorganisms cannot always persist in the hydroponic rhizosphere and are often ineffective in hydroponic systems[47,48,57-62]. Second, the ability of PGPM to colonize the rhizosphere can be crop- and cultivar-specific, such that inoculants designed for one crop are frequently ineffective for other crops[59,63-65]. Thus, a commercial inoculant intentionally designed for use in hydroponic strawberries is more likely to persist and function in the hydroponic strawberry rhizosphere than inoculants that are not.

1.6 Microbial persistence and succession, and their implications for inoculant development

Microbial persistence and microbial succession are two integral concepts in PGPM inoculant development. Persistence is defined as the ability of a microorganism to colonize and survive in a given environment over time[66]. Microbial succession is the change in microbial community composition over time [67]. Microbial persistence and succession in the rhizosphere are influenced by stochastic and deterministic processes[67]. Stochastic processes, such as dispersal and ecological drift, are random, while deterministic processes are driven by selective pressures, such as resource availability[67]. In the rhizosphere, the primary resources are root exudates produced by the host plant[68]. The composition and quantity of root exudates vary over time in synchrony with plant development[47,68]. This trend has previously been observed in several plant species, including *Arabidopsis*, *Medicago*, maize, pea, wheat, and sugar beet, though not yet been described in hydroponic strawberries[69-75]. Root exudates are considered the primary deterministic driver of rhizomicrobiome assembly[44]; changes in root exudation can alter the ability of each microorganism to persist and thus can influence overall microbial succession[76]. Therefore, microbial inoculants must be able to colonize and persist in the target rhizosphere despite microbial succession.

Defining the core rhizosphere microbiome is a reasonable first step in developing a persistent inoculant for hydroponic strawberries. The collection of rhizosphere microorganisms that persists across all stages of growth is often referred to as the core microbiome[77]. Core rhizosphere microbiomes are usually composed of relatively few taxa (<50) compared to the total number of microorganisms in the rhizosphere (often >1,000) and can be used to hypothesize the functional effect of rhizomicrobiome composition on plant growth[77-79]. By definition, core microbiome members of the hydroponic strawberry rhizosphere are capable of persisting in the

hydroponic environment, despite microbial succession. Core microbiome members with *in vitro* PGP potential may be particularly promising candidates for use in inoculated plant trials.

1.7 Research objectives

The goal of this project is to form a foundational understanding of the hydroponic strawberry rhizomicrobiome. Thus, the objectives of this project are to (1) assess the impact of soil inoculation on hydroponic strawberry rhizomicrobiome community composition, (2) describe microbial succession in the rhizomicrobiome and identify a core microbiome for the first time, and (3) identify any associations between microbial abundance and fruit yield. The results of these analyses will inform future research into the development of a microbial inoculant that promotes growth in hydroponic strawberries. The development of such an inoculant would increase Canadian strawberry production and help alleviate global food insecurity.

Chapter 2: Methodology

2.1 Hydroponic strawberry plant trial design and maintenance

This hydroponic strawberry trial was designed to closely resemble commercial greenhouse conditions such that the observations in this study are as applicable as possible to the long-term goal of developing a microbial inoculant for commercial hydroponic strawberry production. The plant trial took place between June 13th and August 27th, 2024 and contained three inoculated treatments and one uninoculated "no-soil" control group (Figure 2.1). Prior to planting, frozen tray plants of the "Lycia" cultivar (NovaFruit, Quebec) were thawed at room temperature, rinsed in water to remove excess propagation substrate, and treated with Nova©

antifungal (Plant Products, #20950) and Floramite© (Plant Products, #40090) antimite solutions according to manufacturer instructions to minimize risk of phytopathogen and pest infection. Strawberry Pots (MeteorSystems) were assembled with two plants and two litres of coco coir substrate. Each hydroponic system contained 12 pots with one drip stake per pot. Supplementary figure A1 (Appendix A) depicts the drip irrigation hydroponic set up in detail. Plants were allowed to grow for five days to ensure successful establishment in the hydroponic systems, then pots were distributed between the four experimental groups according to plant size such that each system contained 24 plants of similar size distribution. This was done to prevent an unequal distribution of plant sizes between groups, which could have influenced yield results. Green lacewings and *Aphidoletes* (The Bug Lady, #22710 & #23742) were deployed shortly after planting as a preventative measure against aphids.

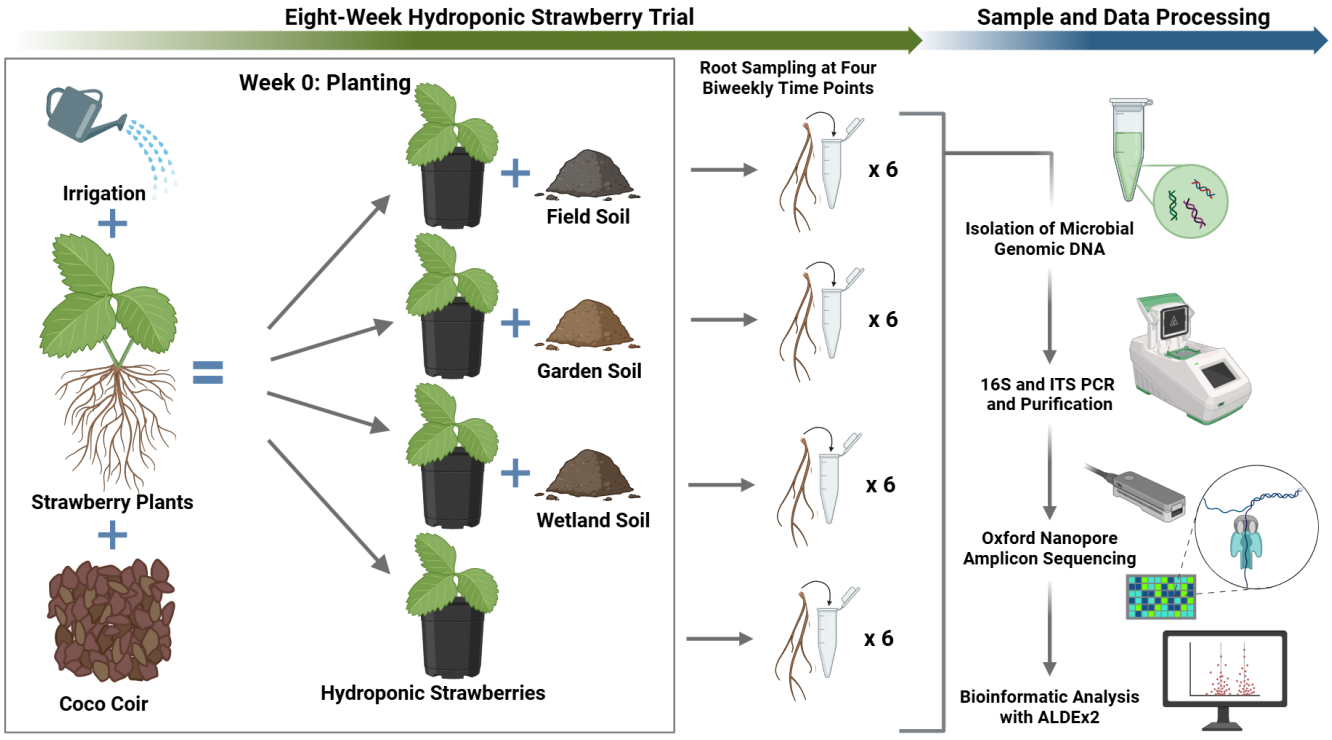


Figure 2.1. Experimental workflow for characterization of the hydroponic strawberry rhizosphere microbiome via molecular methods. Briefly, the workflow began with an eight-week hydroponic strawberry plant trial, followed by extensive sample processing and data analysis. Figure generated with BioRender.

All four hydroponic systems were housed in the same growth chamber and subjected to the same growth conditions and maintenance schedule for the duration of the trial. A 16-hour light, 8-hour dark photoperiod was maintained using ArizeLife2 GE lights (1 BRI, 2 PPF spectrum per shelf). Growth chamber conditions were maintained at 24 °C during light periods and 16.5 °C during dark periods, 65% humidity, and ~800 ppm CO_2. Flowers were hand-pollinated (Amazon, #B01D5G88ZE) every 2-3 days[80]. Senesced leaves and reproductive stolons (i.e., runners) were pruned weekly to minimize habitat for phytopathogenic fungi and to prevent establishment of daughter plants, respectively. Nutrient solution was replenished every 2-3 days, and changed weekly with one of three nutrient solution recipes based on the growth state and thus nutritional needs of the plants (Supplementary table B1, Appendix B). The coco coir substrate was flushed every 30 days with 15 L of fresh RO water to maintain electrical conductivity (EC) below 2.2 dS/m, according to industry standards[81].

Mass (g) and count of marketable berries produced per plant were recorded throughout the trial as a measure of yield. In this trial, ripe berries were classified as “marketable” when they were uniformly red, with no visible lesions or deformities (i.e., Canadian No. 1 grade requirements)[82]. The growth state of each plant was determined weekly via visual inspection, based on the following criteria: “vegetative” for plants that had not yet produced a mature flower, “flowering” began at observation of first mature, receptive flower, “fruiting” began at observation of first developing marketable berry (i.e., all petals have fallen away and berry is uniformly green with no visual imperfections), and “post-harvest” when all berries had been harvested and no new flowers or berries were developing. The trial was concluded after eight weeks, at which point the majority of developing fruits were ripe and few new flowers were being produced. Shoot fresh weight (g) and height (cm) were recorded for each plant at the

conclusion of the trial. Root weight per plant could not be assessed because the root systems from co-potted plants were too entangled to reliably separate from one another and from the substrate.

2.2 Addition of soil-based inoculant to hydroponic strawberry systems

Five days after planting, three of the hydroponic systems were inoculated with soil (i.e., June 18th, 2024). With permission, soil samples were collected from an agricultural soybean field (43.56138º N, 80.49062º W) and wetland (43.48356ºN, 80.56622º S). A third soil sample was donated from a residential strawberry garden (Kitchener, Ontario, Canada). Soil samples were collected from the rhizosphere of dominant plant species at each site using sterile instruments and containers, then used to inoculate the hydroponic systems later that same day. One soil sample was added to each of three hydroponic systems in the following manner: (1) the soil sample was split into equal-weight halves in sterile 500 mL beakers and 100 mL of sterile RO water was added to each beaker to generate a soil slurry, (2) one soil slurry was added to each of two nutrient solution reservoirs per hydroponic system and mixed thoroughly with a sterilized spatula, (3) the drip irrigation system was activated for 30 seconds to immediately deliver soil to the root zone of each plant in the hydroponic systems. The fourth hydroponic system received equivalent irrigation with nutrient solution containing no soil to account for extra nutrient delivery caused by soil inoculation. A subsample of each soil sample was reserved and stored at -80 °C until subsequent nutrient quantification by a third-party lab (A&L Canada Laboratories, London, Ontario). Inoculated treatment groups will henceforth be referred to by their soil sample source (i.e., “Field,” “Garden,” and “Wetland”) and the no-soil negative control will be referred to as the uninoculated control.

2.3 Root sample collection and selection for analysis

A small sample of root was collected from each healthy plant each week resulting in a total of 768 root samples. Briefly, the root samples contained both primary and secondary root with adherent coco coir substrate and were collected in sterile 1.5 mL microcentrifuge tubes (BioBasic, #BT620-NS.SIZE.1PK) using ethanol-sterilized forceps. The inclusion of both primary and secondary root in each sample was done to represent possible differences in rhizomicrobiome composition within the strawberry root system that may arise due to differences in root exudation based on root type[83]. Root samples were collected from the no-soil control treatment before the soil inoculated treatments and the forceps were re-sterilized in between all samples to minimize cross-contamination within and between treatments. Weekly root samples were collected at the same time of day to account for potential variation in the rhizomicrobiome caused by the host plant circadian clock[84]. Additionally, baseline microbiome samples were collected from three young strawberry plants prior to planting, coco coir substrate, irrigation water, and each of the three soil samples to act as source-community reference points in the downstream microbiome analysis. All samples were stored at -80 °C until processing.

Due to budgetary constraints, only a subset of all 768 root samples were processed. With a constraint of around 100 samples, the number of timepoints (n = 4) and the number of plants per timepoint (n = 24, 6/treatment) were optimized to allow the most robust comparisons within and between timepoints as possible to support the research objectives. Alternatively, processing root samples from 12 plants per treatment at two timepoints would not have been as informative regarding microbial succession, while processing three samples per treatment at eight timepoints would have been insufficient for yield analysis via generalized linear modelling.

Root samples were selected for analysis based on yield and position of their source plant in the plant trial. Three high- and three low-yielding plants per treatment were selected for analysis. This selection was then adjusted to ensure no two plants from the same pot were analyzed. The rhizomicrobiomes of co-potted plants may be more similar to one another than to the rhizomicrobiomes of other pots due to close proximity; this could have skewed the analysis if not accounted for[85]. Sample selection was further adjusted such that two high-yielding plants were located on the bottom shelf and one was located on the top shelf of the hydroponic system; likewise for the selected low-yielding plants. The top shelves received roughly 50% less irrigation than bottom shelves (data not shown) because the shelves were supplied by identical pumps, which generated identical maximum pressure, but the pump supplying the top shelf delivered less nutrient solution due to increased elevation. Thus, this criteria for sample selection was included to account for differences in irrigation between shelves of the hydroponic systems which may have caused differences in rhizomicrobiome composition[73,86].

2.4 Sample processing and sequencing

First, microbial genomic DNA was extracted from all samples (n = 104) using the DNeasy PowerSoil Pro Kit (Qiagen, #47014) according to the manufacturer protocol and stored at -80 °C prior to PCR. Specifically, 100 mg of sample was used for all root and baseline microbiome samples, with the exception of root samples collected in week two and RO water baseline samples. For week two root samples, sample collection was physically constrained by small plant size, so microbial genomic DNA was isolated from 50 mg of tissue. DNA was extracted from 15 mL of RO water using a sterile syringe and 0.22 μm filter; the filter paper was

then used as the starting material for DNA extraction. DNA extraction, PCR, and gel electrophoresis were performed for an unused filter to confirm sterility of the filter paper.

16S and ITS amplicons were amplified from microbial genomic DNA according to tables B2 and B3. PCR products were immediately purified to remove remaining enzyme, unused primers, and dNTPs using the QIAquick PCR Purification Kit (Qiagen, #28106) according to manufacturer protocol with the following deviations: (1) buffer EB was heated to 60 °C to increase elution efficiency, (2) 600 µL of buffer PE was used because the recommended 700 µL exceeded column capacity, (3) columns were dried via centrifugation for an additional 5 minutes in a fresh 2 mL collection tube to minimize residual ethanol. Successful amplification and purification were confirmed via gel electrophoresis (5 µL purified PCR product, 1% (w/v) agarose) and Nanodrop spectrophotometer. Purified PCR products that met yield and quality thresholds (i.e., yield >20 ng/µL, A260/A280 = 1.6-2.0, and A260/A230 = 2.0-2.2) were stored at -20 °C prior to sequencing (ONT, 2025). PCR and purification were repeated as necessary until high quality 16S and ITS PCR products were obtained for all 104 samples.

Amplicon sequencing was performed for all 208 purified PCR samples via Oxford Nanopore MinION (ONT, United Kingdom). The Native Barcoding Kit 96 (SQK-NBD114.96) was used according to manufacturer protocol[87] with three deviations: (1) 3.75 µL of end-prepped DNA was carried forward for barcode ligation instead of the recommended 0.75 µL, (2) the barcode ligation reaction was incubated for 60 minutes instead of the recommended 20 minutes, (3) 14 µL of prepared library was loaded, instead of the recommended 12 µL. All of these deviations were optimizations to increase sequencing success for low-yield amplicon samples. Base-calling was performed with Dorado[88]. Quality-filtering was performed using Chopper, to exclude reads with a mean Q-score less than 10 or read length less than 800 bp[89].

SILVA and Unite databases were used with Kraken2 to generate genus- and species-level count matrices for 16S and ITS amplicons, respectively[90-92].

2.5 Bioinformatic analysis of amplicon sequencing data

Downstream bioinformatic and statistical analyses were performed in R using ALDEx2 (v1.42)[93]. Before investigating the research objectives, three filtering schemes (strict, intermediate, and lenient) were applied and assessed via differential abundance analysis in ALDEx2 to confirm robustness of the data to subsetting[94]. The filtering schemes were based on both prevalence and mean abundance thresholds, where prevalence was the proportion of samples the taxa was detected in, and mean abundance was the mean count for a given taxa across all samples. ITS data were further filtered to include only the following fungal and oomycete phyla: *Ascomycota, Basidiobolomycota, Basidiomycota, Blastocladiomycota, Calcarisporiellomycota, Chytridiomycota, Entomophthoromycota, Entorrhizomycota, Glomeromycota, Kickxellomycota, Monoblepharomycota, Mortierellomycota, Mucoromycota, Neocallimastigomycota, Oomycota, Olpidiomycota, Sanchytriomycota, Zoopagomycota*. This filtering was performed because the ITS primers used in this study (ITS1catta, ITS4ngsuni) amplify a broad range of eukaryotes, including fungi and oomycetes, but also plants, nematodes, and protists[95]. Indeed, ITS sequences from strawberry (i.e., *Fragaria*) and peat-moss substrate (i.e., *Sphagnum*) made up significant proportions of each sample. However, the dynamics of fungi and oomycetes in the hydroponic strawberry rhizosphere are much more relevant to the long-term goal of this research and thus they were the focus of the analysis.

Large overlap of retained taxa and correlation of effect sizes between filtering schemes (data not shown) were evidence that trends in the data were stable despite filtering. The

intermediate filtering scheme (prevalence >10%, mean count >10) was used for subsequent 16S and ITS analysis, as was fungi/oomycete filtering for the ITS dataset. Filtered counts were then CLR-transformed in ALDEx2 and CLR-abundance data was used as input data for principal component analysis (PCA) and effect size calculations. The Benjamini-Hochberg correction of p-values for false discovery rate (FDR) was used. Both genus- and species-level analyses were performed and the most statistically supported versions are presented below. Order-level analyses and above were not performed as conclusions drawn from such results would not be as applicable to the commercial-nature of the research objectives.

Chapter 3: Results

Sequencing of 16S and ITS amplicons from 96 strawberry root and eight baseline microbiome samples revealed numerous insights into community composition and dynamics within the hydroponic strawberry rhizomicrobiome. The results for each of the study objectives are presented below. Greater-resolution versions of multi-panel figures are presented in Appendix C.

3.1 Assessing the impact of soil addition on the hydroponic strawberry rhizomicrobiome

Given the variety of microorganisms in the initial soil samples, and the unique selective pressures within the hydroponic rhizosphere, the first objective of this study is to investigate the outcome of soil inoculation in the hydroponic strawberry rhizosphere. Figures 3.1 and 3.2 summarize differences in microbial community composition between the no-soil control and inoculated treatment groups at week eight. Significant overlap on PCAs (Figure 3.1A-C, 3.2A-C) indicates a lack of statistical support for control and treatment groupings. No significant

differentially abundant taxa are identified based on effect size and FDR (Figure 1.1D-F, 1.2D-F). Further, there were few significant differences between genus-level microbiomes in pairwise combinations of the inoculated treatments and non-soil control at each timepoint (Table 3.1). Taken together, these results suggest that a single inoculation event was insufficient to significantly alter bacterial, or fungal/oomycete communities of the hydroponic strawberry microbiome eight weeks post-treatment.

While we do not observe differences between control and treatment groups, we do observe numerous significant differences between soil and hydroponic samples. Figures 4.1 and 4.2 summarize differences between the three initial soil samples (field, garden, and wetland-derived soil) and hydroponic root samples after eight weeks. Clear axes of separation in PCAs (Figure 4.1A, 4.2A) and numerous significant differentially abundant taxa in effect plots (Figure 4.1B, 4.2B) indicate substantial difference between soil inoculant and hydroponic root samples at both community- and genus-levels. The identity of these differentially abundant taxa and magnitude of difference between groups are summarized in Figures 5.1 and 5.2 for bacterial and fungal/oomycete communities, respectively, and in Supplementary Tables B4 and B5.

Briefly, sixteen bacterial genera and three fungal genera were detected at relatively high abundance in both soil and hydroponic samples: *Sphingobium, Hyphomicrobium, Flavobacterium, Chthoniobacter, Rhodoplanes, Ferruginibacter, Chryseolinea, Fimbriiglobus, Nocardioides, Terrimicrobium, Luteolibacter, Gemmata, Tepidisphaera, Reyranella, Mycobacterium, Bradyrhizobium*, *Podospora, Colletotrichum, and Coprinopsis*. Twelve bacterial genera, eleven fungal genera, and one oomycete genus were enriched in soil samples, and depleted in hydroponic samples: *Zavarzinella, Methyloceanibacter, Paenibacillus, Microlunatus, Gaiella, Vibrio, Stenotrophobacter, Roseimicrobium, Flavisolibacter, Ramlibacter, Patulibacter,*

Candidatus Tremblaya, *Cladosporium, Akanthomyces, Syncephalis, Schizothecium, Neosetophoma, Clonostachys, Mucor, Ganoderma, Psathyrella, Marquandomyces, Betamyces*, and *Globisporangium*. In contrast, four bacterial and seven fungal genera were depleted in soil samples and enriched in hydroponic samples: *Spirochaeta, Methylphilus, Methylovorus, Chroococcopsis, Simocybe, Tubeufia, Achroceratosphaeria, Archaeorhizomyces, Hohenbuehelia, Rhodosporidiobolus,* and *Neohelicosporium*.

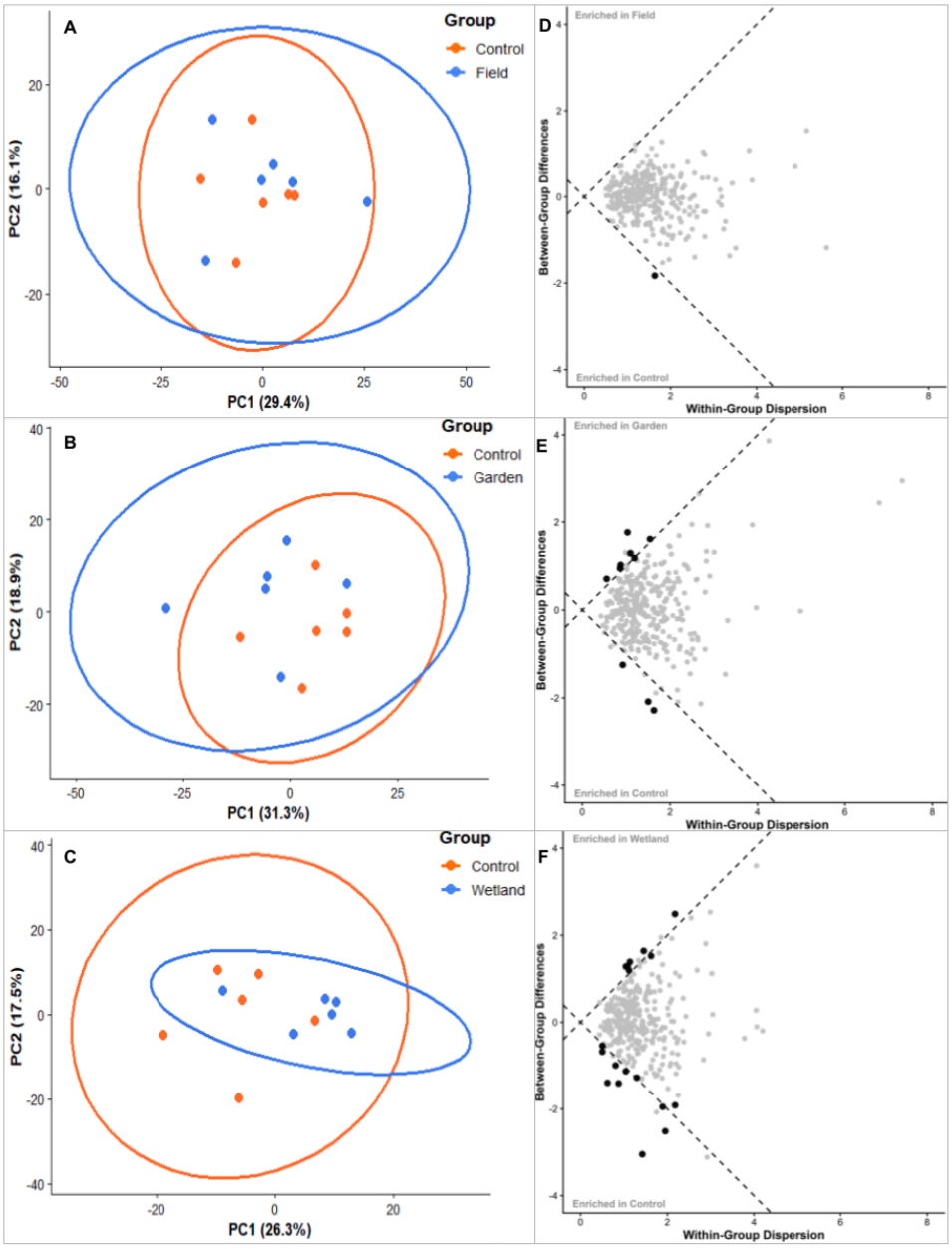


Figure 3.1. Pairwise principal component analysis (PCA) and ALDEx2 effect plots for genus-level 16S CLR abundance data from control (n = 6) and inoculated treatment (n = 6) groups at week eight. In PCAs (A-C), each point represents the bacterial community of one sample; orange and blue ellipses represent 95% confidence intervals for control (n = 6) and specified treatment groups (n = 6), respectively. Scree plots are in Supplementary Figure A2. In effect plots (D-F), each point represents a genus plotted according to between-group difference and within-group dispersion at week eight. Black points indicate genera with effect size >|1| and FDR >0.05. Red points, though none are identified in these analyses, indicate genera with effect size >|1| and FDR <0.05.

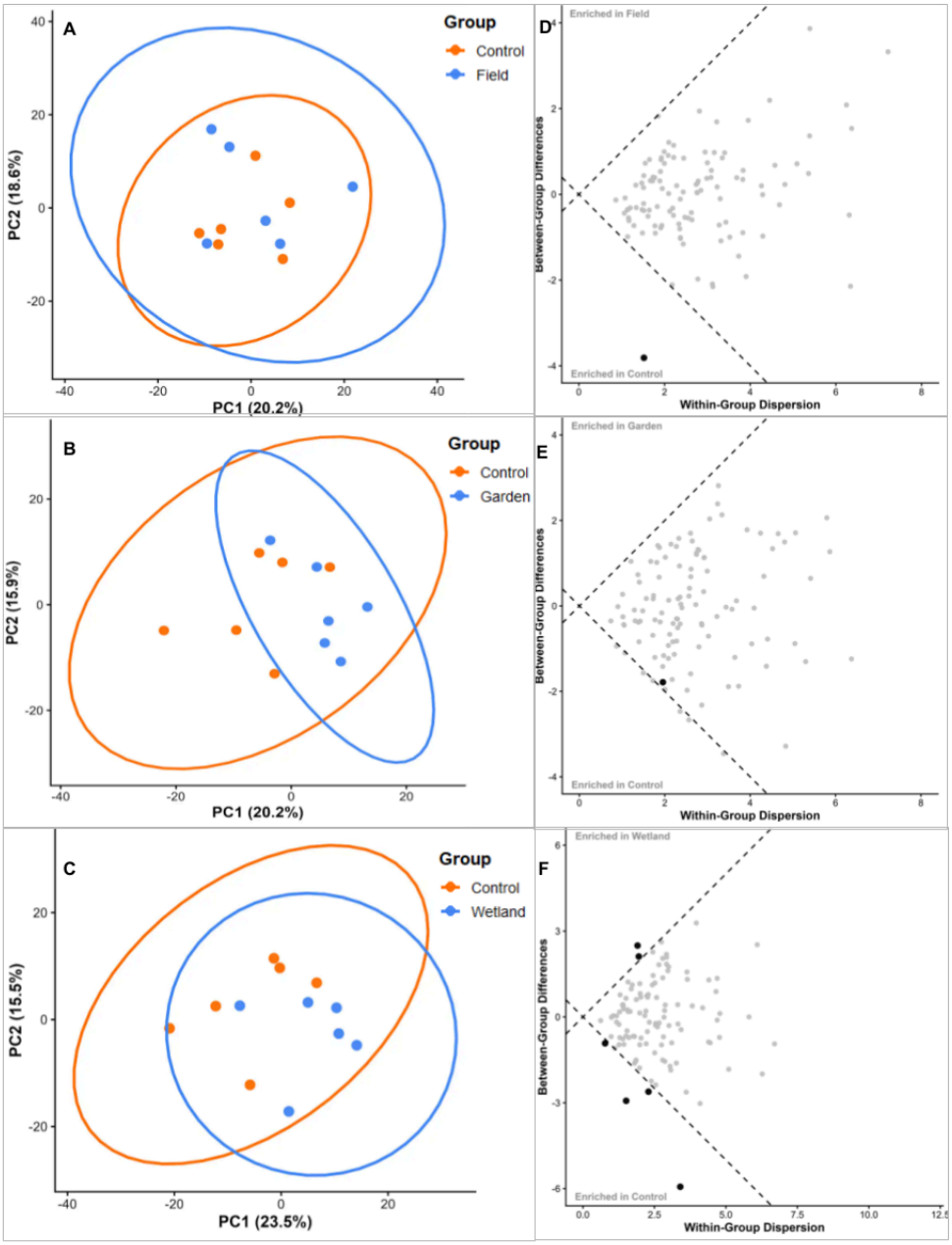


Figure 3.2. Pairwise principal component analysis (PCA) and ALDEx2 effect plots for genus-level ITS CLR abundance data from control (n = 6) and inoculated treatment (n = 6) groups at week eight. In PCAs (A-C), each point represents the bacterial community of one sample; orange and blue ellipses represent 95% confidence intervals for control and specified treatment groups, respectively. Associated scree plots are in Supplementary Figure A3. In effect plots (D-F), each point represents a genus plotted according to between-group difference and within-group dispersion at week eight. Black points indicate genera with effect size >|1| and FDR >0.05. Red points, though none are identified in these analyses, indicate genera with effect size >|1| and FDR <0.05.

Table 3.1. Summary of number of significant differentially abundant taxa (effect >|1|, FDR <0.05) between pairwise treatment and timepoint comparisons. Effect size and FDR were calculated in ALDEx2 as previously described.

		Control			
		Week 2	Week 4	Week 6	Week 8
Field	Week 2	0			
	Week 4		0		
	Week 6			2[A]	
	Week 8				0
Garden	Week 2	0			
	Week 4		0		
	Week 6			1[B]	
	Week 8				0
Wetland	Week 2	0			
	Week 4		0		
	Week 6			1[C]	
	Week 8				0

		Field			
		Week 2	Week 4	Week 6	Week 8
Garden	Week 2	0			
	Week 4		2[E]		
	Week 6			0	
	Week 8				0
Wetland	Week 2	6[D]			
	Week 4		3[F]		
	Week 6			0	
	Week 8				0

		Garden			
		Week 2	Week 4	Week 6	Week 8
Wetland	Week 2	0			
	Week 4		1[G]		
	Week 6			0	
	Week 8				0

(A) Pui enriched in Field at week six. *Rhodotorula* enriched in Control at week six.
(B) *Olpidium* enriched in week six Control relative to week six Garden.
(C) *Rhodotorula* enriched in week six Control relative to week six Wetland.
(D) *Phenylobacterium, Granulicella, Puia, Mucilaginibacter, Terriglobus,* and *Edaphobacter* enriched in week two Wetland, relative to week two Field.
(E) *Cthoniobacter* and *Nocardioides* enriched in week four Garden, relative to week four Field.
(F) *Luteolibacter*, *Duganella*, and *Rurimicrobium* enriched in week four Wetland, relative to week four Field.
(G) *Luteolibacter* enriched in week four Wetland, relative to week four Garden.

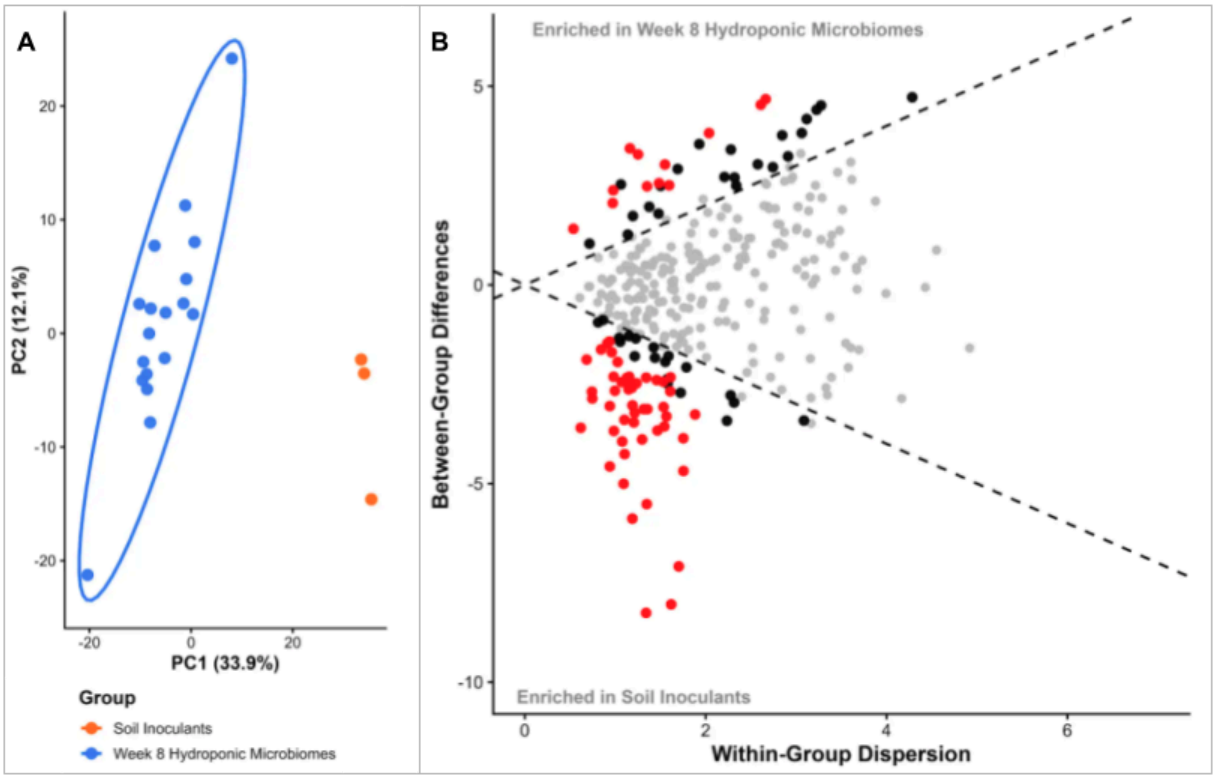


Figure 4.1. Principal component analysis (PCA) and ALDEx2 effect plots for genus-level 16S CLR abundance data from initial soil sample (n = 3) and week eight inoculated root samples (n = 18). In the PCA (A), each point represents the bacterial community of one sample. Week eight hydroponic samples are coloured in blue. Soil samples are coloured in orange and lack an ellipse due to small sample size. The associated scree plot is in Supplementary Figure A4. In the effect plot (B), each point represents a genus plotted according to between-group difference and within-group dispersion. Location of points outside of the dashed lines indicates enrichment of that taxon in one group, relative to the other, as labelled on the effect plot. Both black and grey points indicate statistical insignificance (FDR >0.05). Black points indicate genera with effect size >|1|, while grey points indicate genera with effect size <|1|. Red points indicate significant differentially abundant genera, with effect size >|1| and FDR <0.05. Effect size and FDR value for significant taxa are listed in Supplementary Table B4.

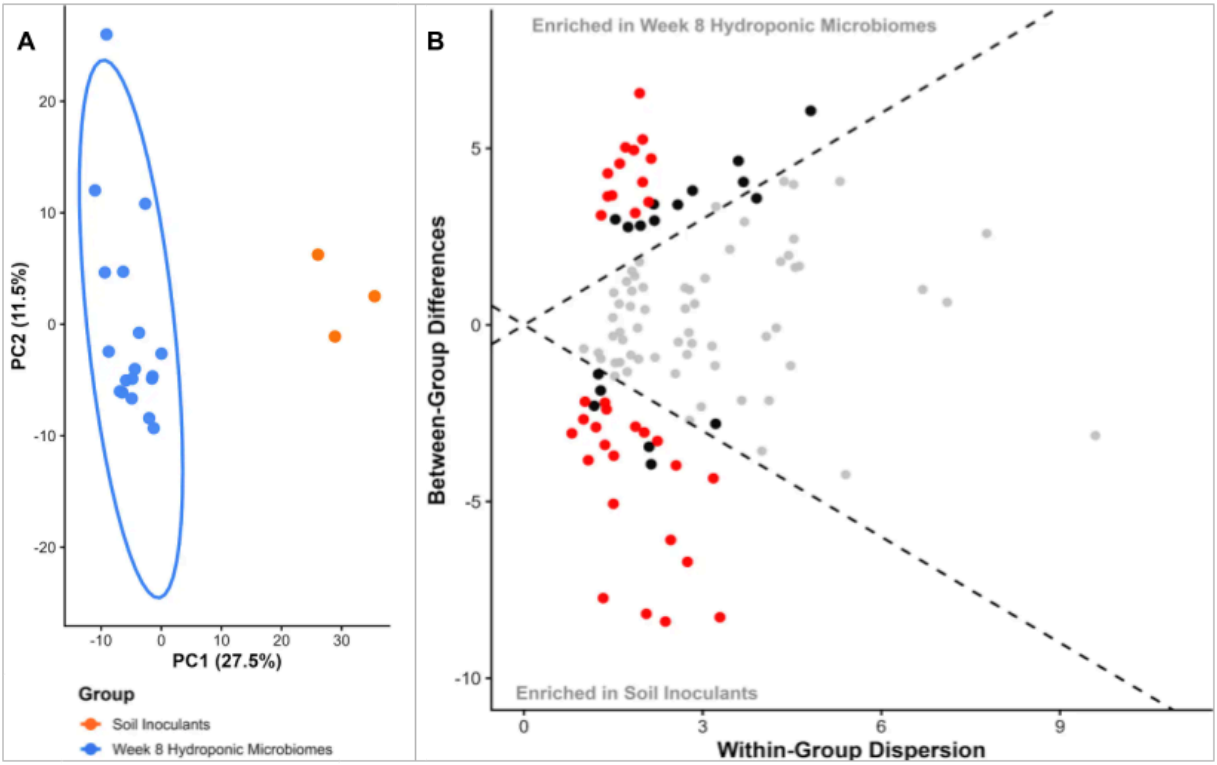


Figure 4.2. Principal component analysis (PCA) and ALDEx2 effect plots for genus-level ITS CLR abundance data from initial soil samples (n = 3) and week eight inoculated root samples (n = 18). In the PCA (A), each point represents the fungal/oomycete community of one sample. Week eight hydroponic samples are coloured in blue. Soil samples are coloured in orange and lack an ellipse due to small sample size. The associated scree plot is in Supplementary Figure A4. In the effect plot (B), each point represents a genus plotted according to between-group difference and within-group dispersion. Location of points outside of the dashed lines indicates enrichment of that taxon in one group, relative to the other, as labelled on the effect plot. Both black and grey points indicate statistical insignificance (FDR >0.05). Black points indicate genera with effect size >|1|, while grey points indicate genera with effect size <|1|. Red points indicate significant differentially abundant genera, with effect size >|1| and FDR <0.05. Effect size and FDR value for significant taxa are listed in Supplementary Table B5.

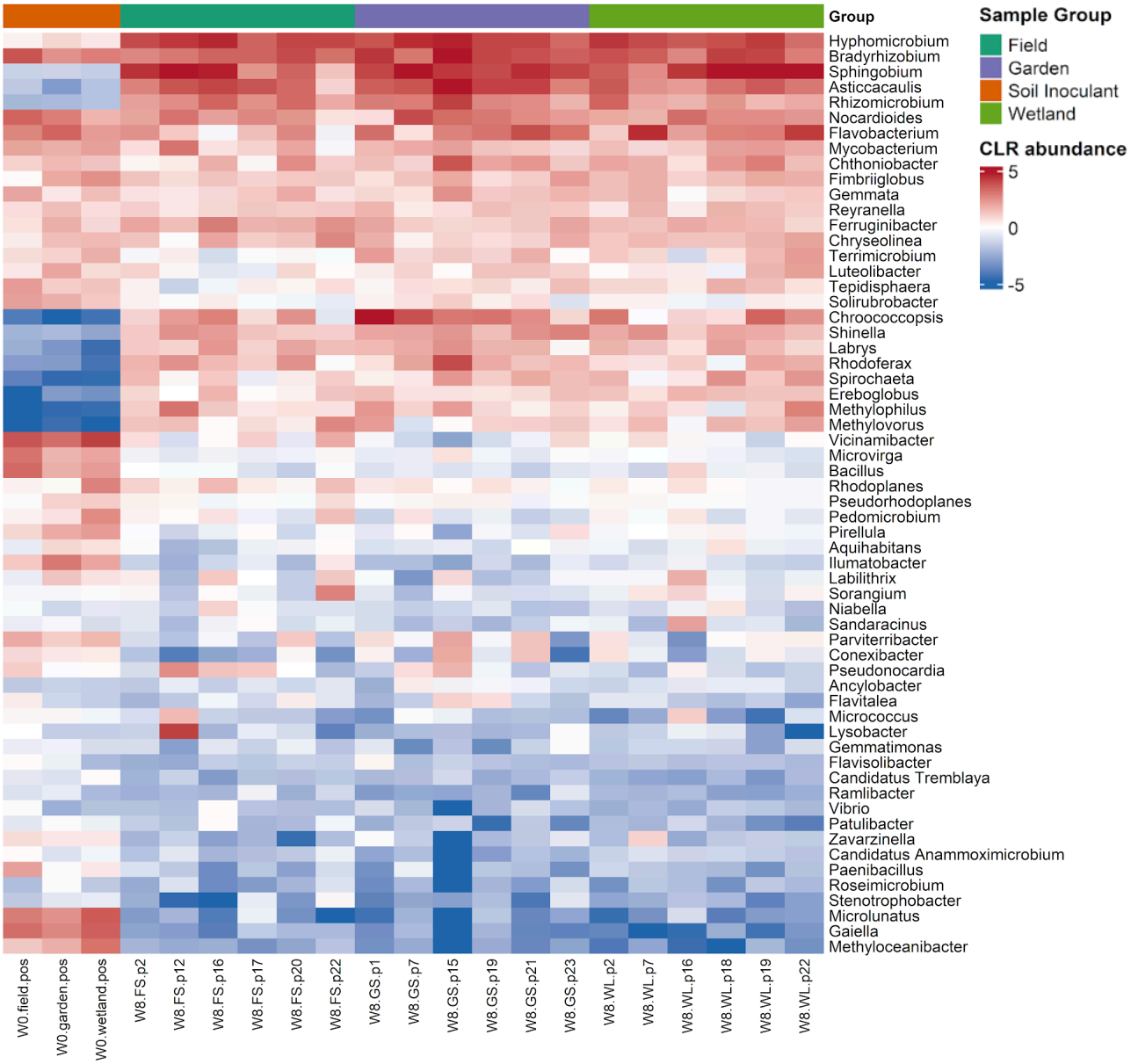


Figure 5.1.Summarizing magnitude of bacterial differential abundance between initial soil samples and week eight hydroponic treatment samples. Each row represents a significant differentially abundant bacterial genera identified in Figure 4.1B (i.e. effect size >|1|, FDR <0.05). Each column represents one sample; sample name is listed at the bottom of the figure, and sample group is summarized by the coloured bar across the top. Red and blue tile colours represent high or low CLR abundance, which can be interpreted in relative terms, as higher or lower than the geometric mean of the dataset, respectively.

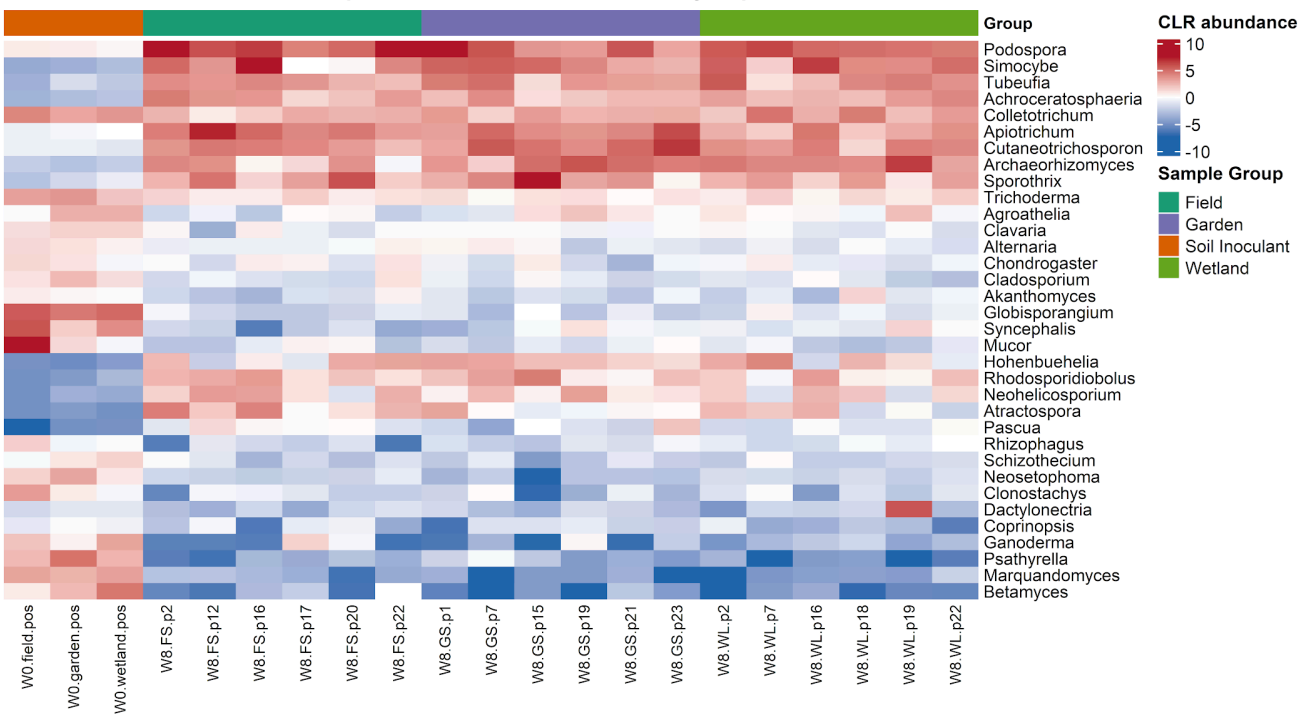


Figure 5.2.Summarizing magnitude of fungal and oomycete differential abundance between initial soil samples and week eight hydroponic treatment samples. Each row represents a significant differentially abundant genera identified in Figure 4.2B (i.e. effect size >|1|, FDR <0.05). Each column represents one sample; sample name is listed at the bottom of the figure, and sample group is summarized by the coloured bar across the top. Red and blue tile colours represent high or low CLR abundance, which can be interpreted in relative terms, as higher or lower than the geometric mean of the dataset, respectively.

3.2 Examining microbial succession in the hydroponic strawberry rhizomicrobiome

Microbial succession in the rhizomicrobiome has been described for several commercially-relevant crops, but not for hydroponic strawberries[70-73,96-101]. Therefore, as the second objective of this study, we assessed change in bacterial and fungal/oomycete communities over time and in response to growth state of the host plant. Figures 6.1 and 6.2 summarize community composition of the baseline microbiome samples; effectively, these communities are the starting material for ecological forces to act on in the hydroponic rhizosphere. Figures 7.1 and 7.2 summarize changes in bacterial and fungal/oomycete community composition in the hydroponic systems across three growth states (vegetative, flowering, fruiting). In these PCAs, there is partial differentiation between vegetative and fruiting groups suggesting a possible shift with growth state while a core microbiome is maintained. Notably, the flowering group is highly variable in both 16S and ITS datasets. Despite evidence of change at the community-level, few bacteria and zero fungal/oomycete taxa were identified as differentially abundant between growth states at the genus-level (Supplementary Table B6).

Given the few significant differences in rhizomicrobiome community composition across growth states, the next step was to assess similarities in order to identify candidate core microbiome members for hydroponic strawberries (Figure 8.1, 8.2). Bacterial and fungal/oomycete community composition is largely consistent across growth states (Figure 8.1A, 8.2A), as expected based on PCA (Figure 7.1, 7.2). This study uses a conservative definition of core membership; specifically, detection in at least 90% of samples (i.e. prevalence) and mean relative abundance of at least 1%. The prevalence-abundance plots identify 20 bacterial genera and 21 fungal/oomycete genera as candidate core microbiome members (Figure 8.1B, 8.2B).

Core occupancy heat maps elaborate on the distribution of observed relative abundance for each core candidate (Figure 8.1C, 8.2C).

Majority of bacterial core candidates are detected at varying levels of relative abundance, while fungal core candidates are most frequently detected at less than 1% relative abundance, and less frequently detected at levels above 1%. *Pseudomonas, Rhizobium, Flavobacterium, Acinetobacter, Streptomyces, Cadophora, Leucosporidium, Serendipita, Podospora, Penicillium, Pseudogymnoascus, Cutaneotrichosporon,* and *Nectria* were present in 100% of samples and mean relative abundance greater than 2%, with *Pseudomonas* and *Cadophora* being the most prevalent and abundant bacterial and fungal genera, respectively. Similarly, *Pseudomonas* and *Cadophora* were both dominant genera in the uninoculated root baseline community prior to planting (Figures 6.1, 6.2). *Pedosphaera, Bradyrhizobium, Mucilaginibacter*, *Chroococcopsis, Mesorhizobium, Terrimonas, Apiotrichum, Coniochaeta, Rhodotorula, Mortierella, Achroceratosphaeria* and *Pythium* were identified in 100% of samples, at greater than 1% abundance. *Burkholderia-Caballeronia-Paraburkholderia* (aka. BCP Group), *Sphingobium, Novosphingobium, Devosia, Hyphomicrobium, Asticcacaulis, Simocybe, Olpidium,* and *Phytophthora* were observed in more than 90% of samples, with a mean relative abundance between 2-5%. *Sphingomonas, Rhodanobacter, Phenylobacterium, Sporothrix, Tubeufia, Exophiala,* and *Mycochaetophora* were detected in more than 90% of samples, with a mean relative abundance between 1-2%.

Next, microbial succession was analyzed with respect to time by assessing changes in bacterial and fungal/oomycete community composition across four biweekly timepoints. Time point PCA groups (Figure 9.1A, 9.2A) are slightly more statistically supported than their growth state counterparts (Figure 8.1A, 8.2A). Numerous taxa are identified as differentially abundant

between week two and week eight samples (Figure 9.1B, 9.2B). Differentially abundant taxa are listed in Supplementary Table B7. Of these differentially abundant taxa, seven bacterial and two fungal genera are enriched at both week two and week eight timepoints: *Oleiharenicola, Schlesneria, Acidovorax, Asticcacaulis, Comamonas, Luteolibacter, Methylotenera, Mortierella,* and *Aspergillus*. No significant differentially abundant taxa appear at both relatively high abundance in week two then relatively low abundance in week eight. In other words, taxa that are enriched in week two maintain relatively average abundance or higher in week eight samples. Two bacterial genera and one fungal genus were depleted in week two, and enriched in week eight: *Zoogloea, Hohenbuehelia,* and *Rhodosporidiobolus*. Time-series stacked bar charts (Figure 9.1C, 9.2C) capture comparable trends as observed in growth state stacked bar charts (Figure 8.1A, 8.2A). Overall, this study observes significant change in community composition over time as evidence of microbial succession in the hydroponic strawberry rhizomicrobiome.

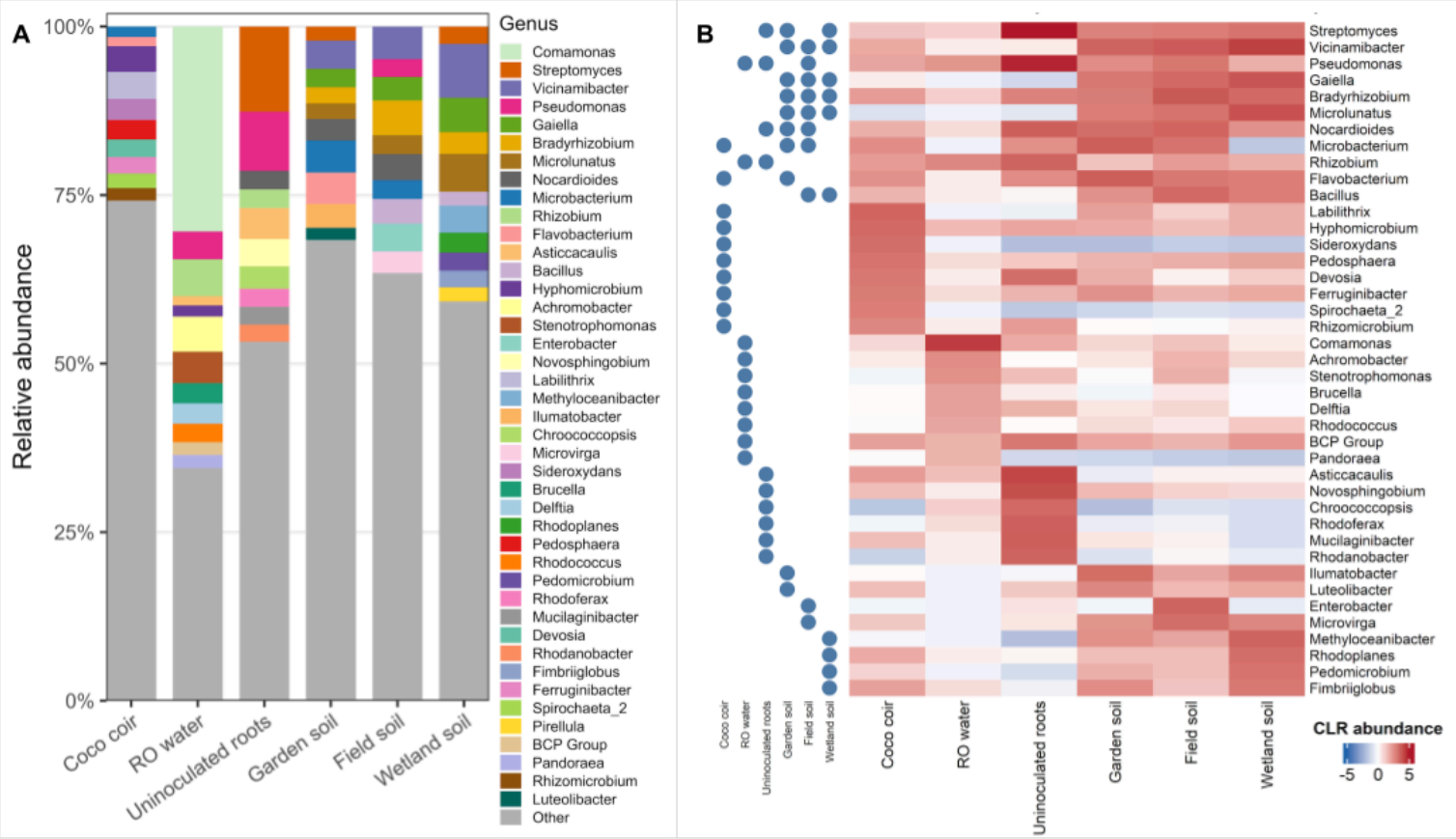


Figure 6.1. Bacterial community composition of baseline microbiome samples. The stacked bar chart (A) summarizes relative bacterial abundance for the ten most abundant genera per baseline sample, with all other genera collapsed into the "Other" category. Note, "BCP Group" is an acronym for the tri-genus group "*Burkholderia- Caballeronia-Paraburkholderia*." In the heat map (B), each row represents one of the top ten relatively abundant genera identified in A. In the dot-map, dots indicate which baseline communities each taxa was within the top ten genera for relative abundance. Tile colours of red and blue indicate high or low CLR abundance per sample, which can be interpreted in relative terms, as higher or lower than the geometric mean abundance (white) of the dataset, respectively.

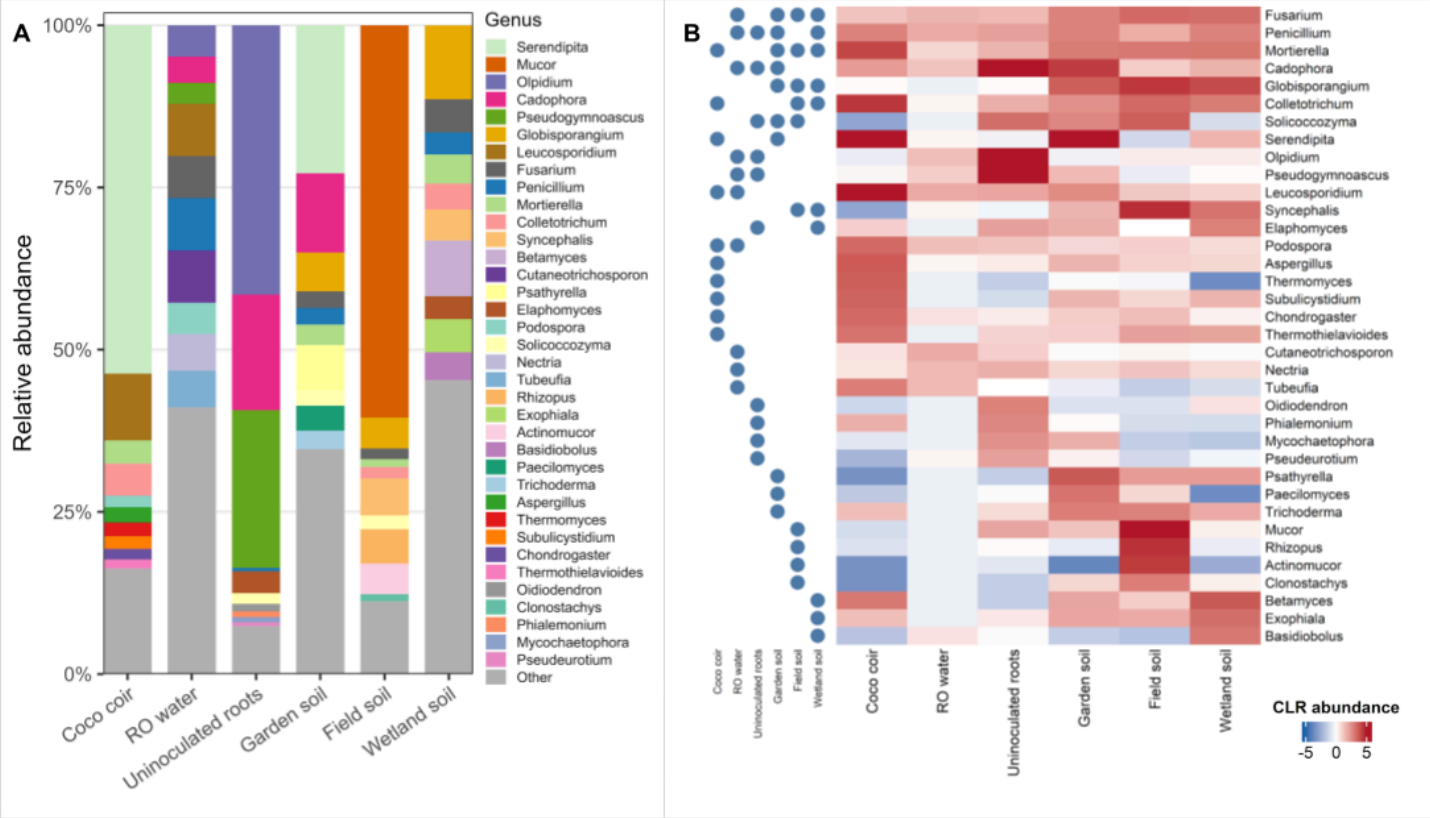


Figure 6.2. Fungal and oomycete community composition of baseline microbiome samples. The stacked bar chart (A) summarizes relative fungal/oomycete abundance for the ten most abundant genera per baseline sample, with all other genera collapsed into the "Other" category. In the heat map (B), each row represents one of the top ten relatively abundant genera identified in A. In the dot-map, dots indicate which baseline communities each taxa was within the top ten genera for relative abundance. Tile colours of red and blue indicate high or low CLR abundance per sample, which can be interpreted in relative terms, as higher or lower than the geometric mean abundance (white) of the dataset, respectively.

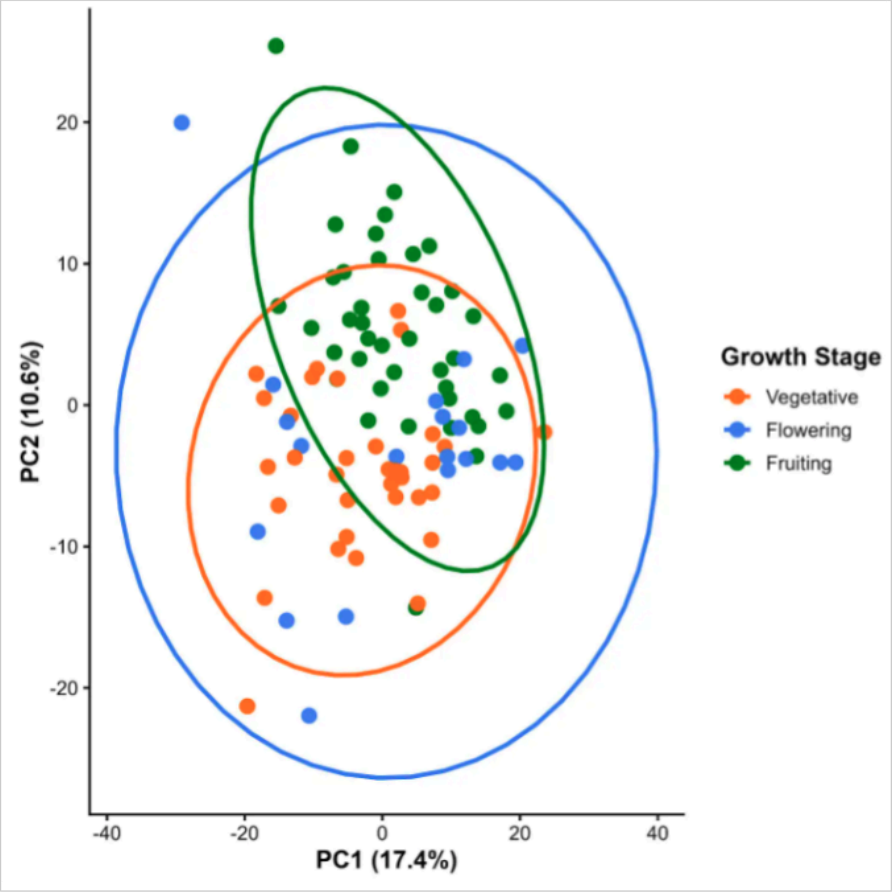


Figure 7.1. Principal component analysis (PCA) of genus-level 16S CLR abundance at three strawberry growth stages. Each point represents the bacterial community of one sample. Sample points are coloured based on growth stage with a corresponding ellipse representing the 95% confidence interval: orange for vegetative (n = 34) , blue for flowering (n = 19), and green for fruiting (n = 41). It is important to note that two hydroponic root samples are excluded from this analysis because the plants transitioned to a "post-harvest" state in week eight; these two samples do not meet criteria to be included in the three growth state groups described here, and n = 2 is too small to include post-harvest as a fourth growth state in this analysis. Raw growth state data is summarized in Supplementary Figures A8-A11. Associated scree plot is in Supplementary Figure A5.

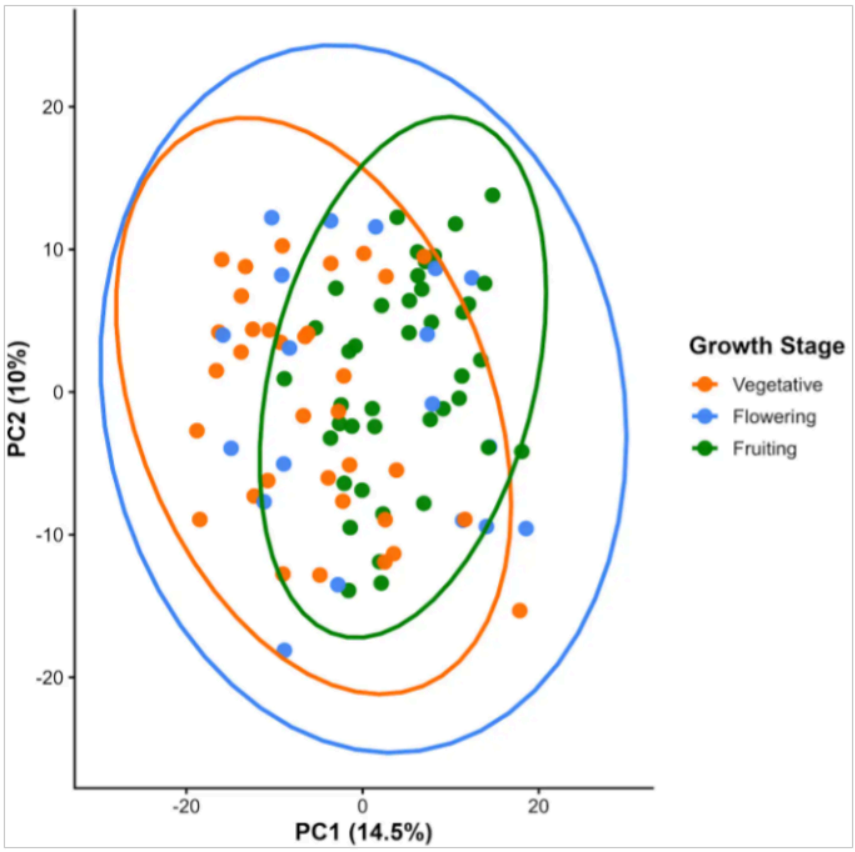


Figure 7.2. Principal component analysis (PCA) of genus-level ITS CLR abundance at three strawberry growth stages. Each point represents the fungal/oomycete community of one sample. Sample points are coloured based on growth stage with a corresponding ellipse representing the 95% confidence interval: orange for vegetative (n = 34) , blue for flowering (n = 19), and green for fruiting (n = 41). Again, please note that two hydroponic root samples are excluded from this analysis because the plants transitioned to a "post-harvest" state in week eight. Raw growth state data is summarized in Supplementary Figures A8-A11. Associated scree plot is in Supplementary Figure A5.

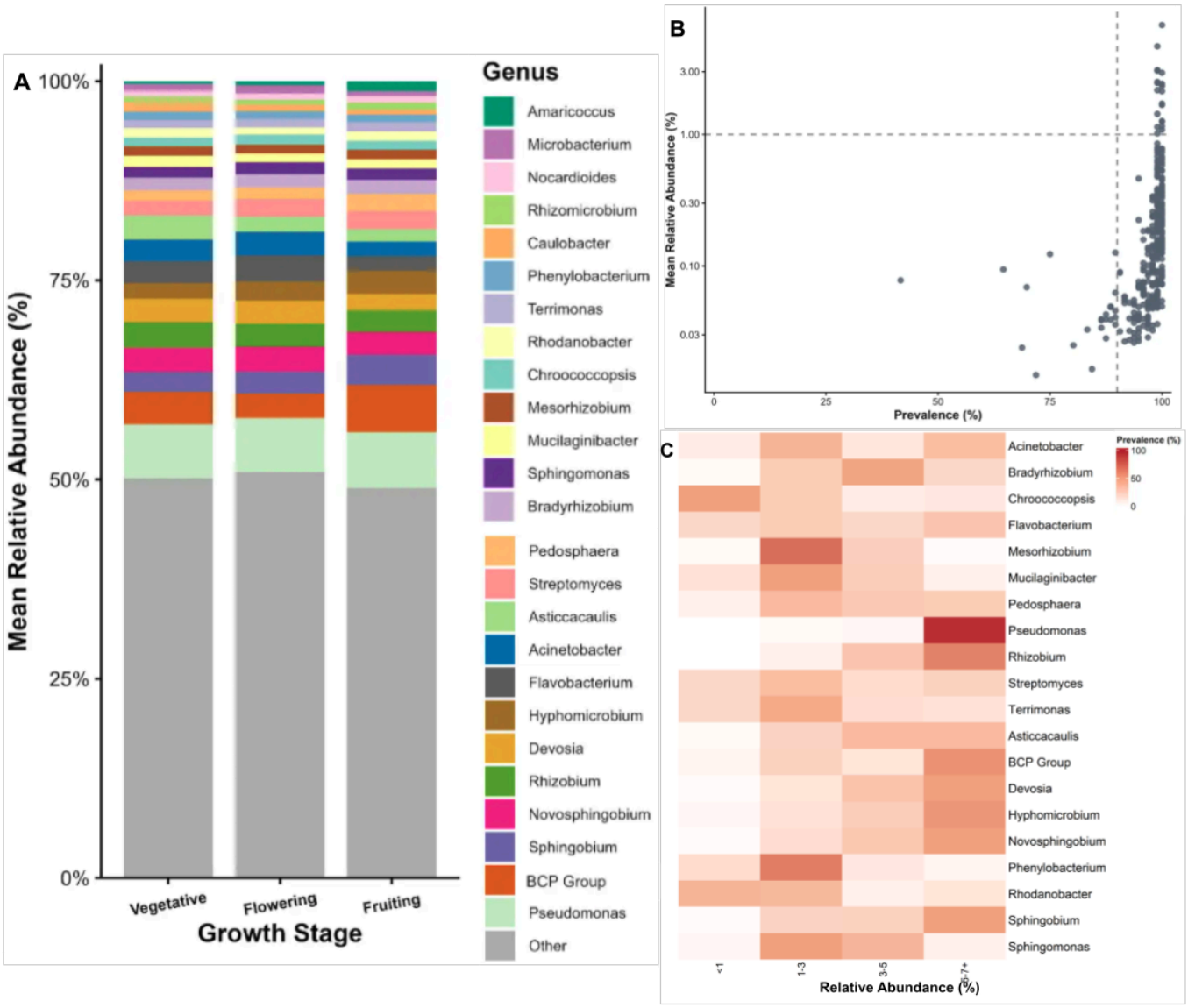


Figure 8.1. Summary of hydroponic strawberry rhizomicrobiome bacterial composition with respect to assigned growth stage. The stacked bar chart (A) summarizes mean relative abundance (%) of the top 25 most abundant bacterial genera at three strawberry growth stages. Left to right, the bars summarize data for all samples collected at vegetative (n = 34), flowering (n = 19), and fruiting (n = 41) growth stages. The 25 most abundant genera are ordered top to bottom in the legend and each bar. All other genera are collapsed into the "Other" category. Note, "BCP Group" is an acronym for the tri-genus group "*Burkholderia- Caballeronia-Paraburkholderia*." In the prevalence-abundance plot (B) each dot represents a bacterial genus plotted according to prevalence (%) and mean relative abundance (%) across all samples (n = 94). Taxa that surpass both dashed thresholds are highly prevalent (i.e. detected in ≥ 90% of samples) and highly abundant (i.e. ≥ 1% mean relative abundance). The core occupancy heat map (C) visualizes the magnitude of prevalence in each category of mean relative abundance (%) for candidate core taxa identified in panel B.

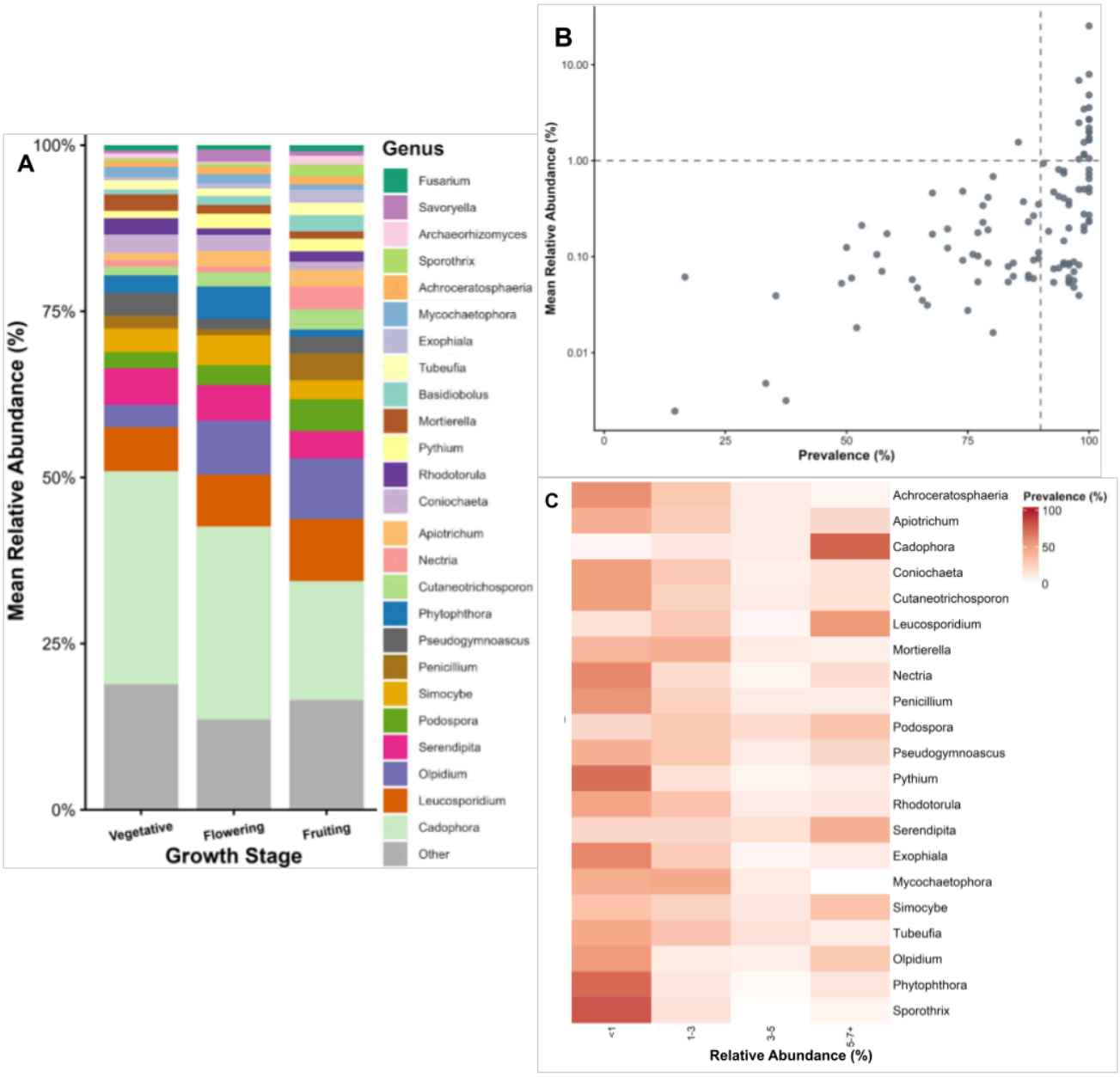


Figure 8.2. Summary of hydroponic strawberry rhizomicrobiome fungal and oomycete community composition with respect to assigned growth stage. The stacked bar chart (A) summarizes mean relative abundance (%) of the top 25 most abundant genera at three strawberry growth stages. Left to right, the bars summarize data for all samples collected at vegetative (n = 34), flowering (n = 19), and fruiting (n = 41) growth stages. The 25 most abundant genera are ordered top to bottom in the legend and each bar. All other genera are collapsed into the "Other" category. In the prevalence-abundance plot (B) each dot represents a eukaryotic genus plotted according to prevalence (%) and mean relative abundance (%) across all samples (n = 94). Taxa that surpass both dashed thresholds are highly prevalent (i.e. detected in ≥ 90% of samples) and highly abundant (i.e. ≥ 1% mean relative abundance). The core occupancy heat map (C) visualizes the magnitude of prevalence in each category of mean relative abundance (%) for candidate core taxa identified in panel B.

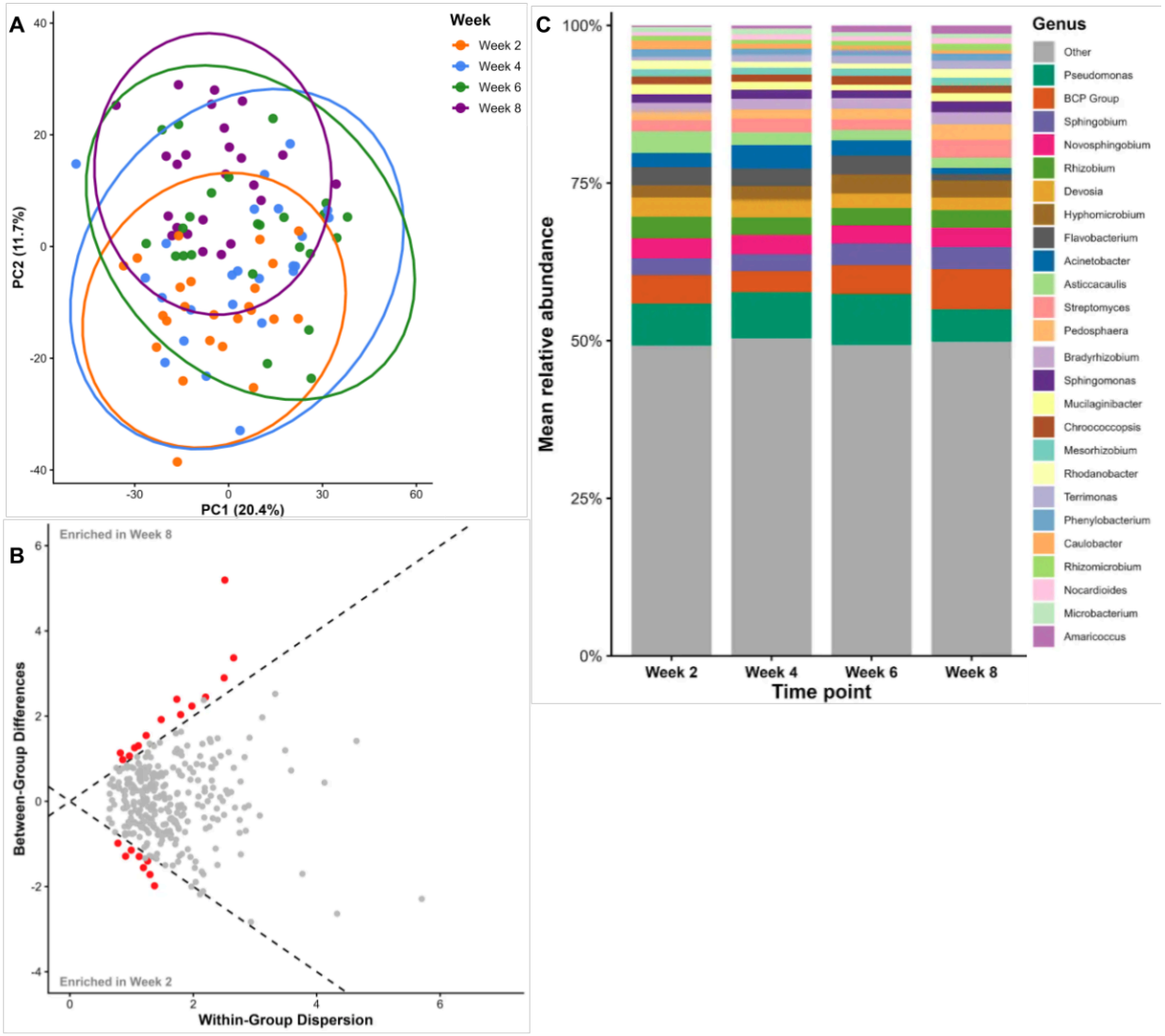


Figure 9.1. Summary of hydroponic strawberry rhizomicrobiome bacterial community composition with respect to time in weeks. Principal component analysis (A) summarizes species-level 16S CLR abundance data grouped by biweekly timepoint (n = 24) for week two (orange), week four (blue), week six (green), and week eight (purple) with corresponding 95% confidence interval ellipses. The associated scree plot is in Supplementary figure A6. In the ALDEx2 effect plot (B), each point represents a bacterial genus, plotted based on median within-group dispersion (i.e. variance) and median between-group difference of 16S CLR abundance data between week two and week eight timepoints. Location of points outside of the dashed lines indicates enrichment of that taxon in one group, relative to the other, as labelled on the plot. Both black and grey points indicate statistical insignificance (FDR >0.05), with effect sizes of >|1| and <|1|, respectively. Red points denote significant differentially abundant taxa, with effect size >|1| and FDR <0.05. The stacked bar chart (C) summarizes mean relative abundance (%) for the top 25 most abundant genera at the four biweekly timepoints. All other genera are collapsed into the "Other" category. Note, "BCP Group" is an acronym for the tri-genus group "*Burkholderia- Caballeronia-Paraburkholderia*."

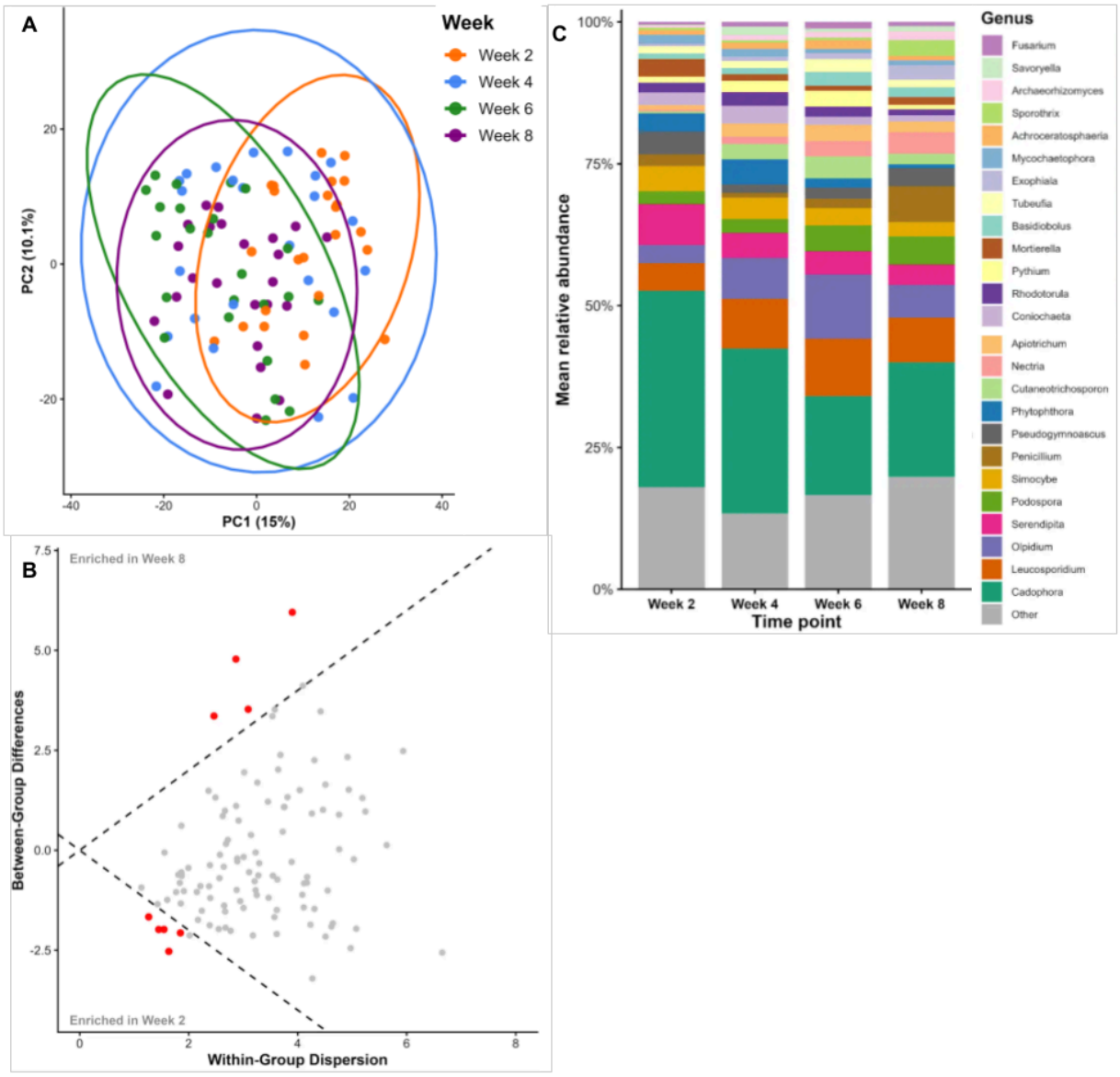


Figure 9.2. Summary of hydroponic strawberry rhizomicrobiome fungal community composition with respect to time in weeks. Principal component analysis (A) summarizes species-level ITS CLR abundance data grouped by biweekly timepoint (n = 24) for week two (orange), week four (blue), week six (green), and week eight (purple) with corresponding 95% confidence interval ellipses. The associated scree plot is in Supplementary figure A6. In the ALDEx2 effect plot (B), each point represents a eukaryotic genus, plotted based on median within-group dispersion (i.e. variance) and median between-group difference of ITS CLR abundance data between week two and week eight timepoints. Location of points outside of the dashed lines indicates enrichment of that taxon in one group, relative to the other, as labelled on the plot. Both black and grey points indicate statistical insignificance (FDR >0.05), with effect sizes of >|1| and <|1|, respectively. Red points denote significant differentially abundant taxa, with effect size >|1| and FDR <0.05. The stacked bar chart (C) summarizes mean relative abundance (%) for the top 25 most abundant genera at the four biweekly timepoints. All other genera are collapsed into the "Other" category.

3.3 Investigating associations between microbial abundances and fruit yield

There are numerous studies that assess the ability of microorganisms to promote plant growth in a variety of commercially important crops, yet no commercial inoculant for hydroponic strawberries is currently available in the market[5,20,21]. Therefore, the final objective of this study is to identify microorganisms associated with high or low strawberry yield. If identified, taxa associated with high yield may be suitable candidates for development of an inoculant for hydroponic strawberries. Figures 10.1 and 10.2 describe 16S and ITS CLR abundance data with respect to berry yield, using microbiome data from the three "high" and three "low" yielding plants. Recall, cumulative yield was one factor considered during sample selection. Significant overlap of high- and low-yielding groups in PCAs (Figure 10.1A, 10.2A) is evidence of similarity in microbial communities at the species-level. Similarly, effect plots (Figure 10.1B, 10.2B) identify zero significant differentially abundant taxa between groups of high- and low-yielding strawberry plants. Therefore, it is no surprise that generalized linear modelling (GLM) identifies no taxa significantly associated with either high or low yield (Figure 10.1C, 10.2C).

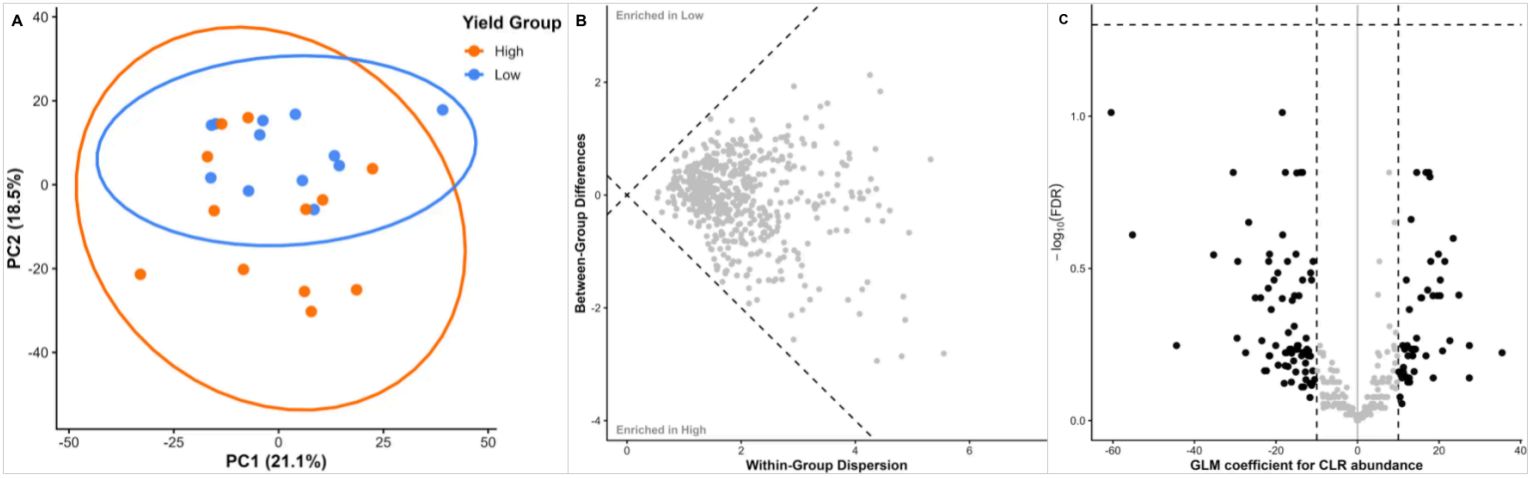


Figure 10.1. Comparison of bacterial community composition between high- and low-yielding strawberry plants from all experimental groups at week eight. Principal component analysis (A) summarizes species-level 16S CLR abundance data grouped by yield category; orange and blue correspond to high- and low-yielding plant samples, respectively. The associated scree data is in Supplementary figure A7. In the ALDEx2 effect plot (B), each point represents a bacterial species, plotted based on median within-group dispersion (i.e. variance) and median between-group difference of 16S CLR abundance data for sample groups of high- and low-yielding plants. Location of points outside of the dashed lines indicates enrichment of that taxon in one group, relative to the other, as labelled on the plot. Both black and grey points indicate statistical insignificance (FDR >0.05), with effect sizes of >|1| and <|1|, respectively. Red points denote significant differentially abundant taxa, with effect size >|1| and FDR <0.05; no red points are observed in this figure. The volcano plot (C) summarizes associations between fruit yield (g) and genus-level 16S CLR abundance at week eight. Each point represents one bacterial genus, plotted according to Gaussian GLM coefficient on the x-axis and log-transformed FDR value on the y-axis. The horizontal dashed threshold represents FDR = 0.05. The vertical dashed thresholds represent the GLM coefficients at which a taxon is associated with a yield increase or decrease of 5 g per 1-unit increase in CLR abundance. Black and grey points indicate statistical insignificance (FDR >0.05), with GLM coefficients >|5| or <|5|, respectively. Red points denote significantly associated taxa with FDR <0.05 and GLM coefficient >|5|; no red points are observed in this figure. Raw yield data is listed in Supplementary Table B8.

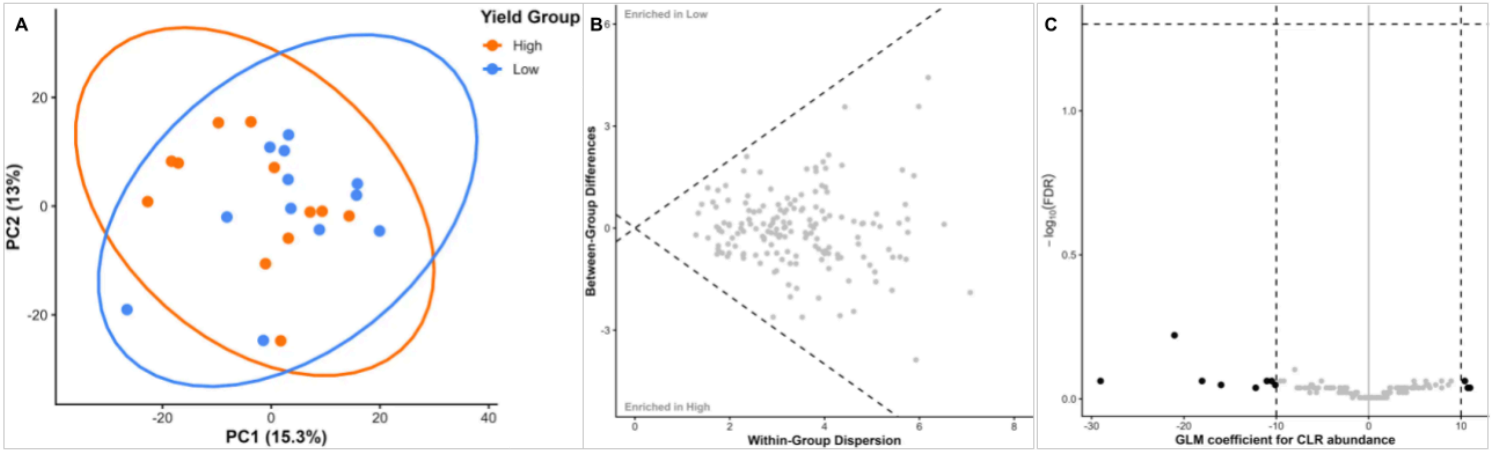


Figure 10.2. Comparison of fungal/oomycete community composition between high- and low-yielding strawberry plants from all experimental groups at week eight. Principal component analysis (A) summarizes species-level ITS CLR abundance data grouped by yield category; orange and blue correspond to high- and low-yielding plant samples, respectively. The associated scree data is in Supplementary figure A7. In the ALDEx2 effect plot (B), each point represents a eukaryotic species, plotted based on median within-group dispersion (i.e. variance) and median between-group difference of ITS CLR abundance data for sample groups of high- and low-yielding plants. Location of points outside of the dashed lines indicates enrichment of that taxon in one group, relative to the other, as labelled on the plot. Both black and grey points indicate statistical insignificance (FDR >0.05), with effect sizes of >|1| and <|1|, respectively. Red points denote significant differentially abundant taxa, with effect size >|1| and FDR <0.05; no red points are observed in this figure. The volcano plot (C) summarizes associations between fruit yield (g) and genus-level 16S CLR abundance at week eight. Each point represents one bacterial genus, plotted according to Gaussian GLM coefficient on the x-axis and log-transformed FDR value on the y-axis. The horizontal dashed threshold represents FDR = 0.05. The vertical dashed thresholds represent the GLM coefficients at which a taxon is associated with a yield increase or decrease of 5 g per 1-unit increase in CLR abundance. Black and grey points indicate statistical insignificance (FDR >0.05), with GLM coefficients >|5| or <|5|, respectively. Red points denote significantly associated taxa with FDR <0.05 and GLM coefficient >|5|; no red points are observed in this figure. Raw yield data is listed in Supplementary Table B8.

Chapter 4: Discussion and Conclusions

4.1 Microbial community composition varies between soil samples and hydroponic systems

There were substantial compositional differences between the initial soil samples and final hydroponic rhizomicrobiome communities, with 94 microbial genera identified as differentially abundant between soil and hydroponic samples. Thirty-six bacteria and seven fungal genera were enriched in soil samples relative to hydroponic samples, but were relatively highly abundant in both groups, just to a lesser degree in hydroponic samples. These taxa may be slightly better suited to the soil environment than the hydroponic environment, or they simply may not be recruited to the same abundance in the strawberry rhizosphere specifically.

Contrastingly, 12 bacterial, 11 fungal and one oomycete genera were relatively highly abundant in the soil samples, but depleted in hydroponic root samples. Of these, "*Candidatus Tremblaya", Methyloceanibacter, Microlunatus, Patulibacter, Zavarzinella, Betamyces, Ganoderma, Neosetophoma, Psathyrella, Schizothecium,* and *Syncephalis* have not previously been reported in the strawberry rhizomicrobiome; depletion of these taxa in hydroponic samples in this study may indicate that they are unable to colonize the strawberry rhizosphere. Similarly, "*Candidatus Tremblaya", Roseimicrobium, Zavarzinella, Betamyces, Psathyrella, Schizothecium* and *Syncephalis* have not previously been detected in any hydroponic root microbiome, while the remaining hydroponic-depleted taxa have, including *Flavisolibacter*[50], *Gaiella*[50], *Paenibacillus*[102], *Ramlibacter*[103], *Roseimicrobium*[103], *Stenotrophobacter*[104], *Vibrio*[105,106], *Akanthomyces*[107], *Cladosporium*[108], *Clonostachys*[109], *Globisporangium*[110], and *Mucor*[111]. These discrepancies indicate that while these taxa may colonize the strawberry rhizosphere, they may not persist in the hydroponic environment due to differences in environmental conditions[21,47].

Finally, numerous taxa were enriched in hydroponic samples, due to relatively low or intermediate abundance in the soil, and relatively high abundance in hydroponic samples: ten bacterial genera and ten fungal genera. These hydroponic-enriched taxa may have been selectively recruited by the strawberry host, and may be well suited to the hydroponic rhizosphere[77,112,113]. It is also highly possible that these taxa were introduced to the hydroponic rhizosphere via irrigation water, coco coir substrate, or on the unsterilized strawberry roots themselves, not from the soil samples, and thus appear depleted in the soil samples by default. Indeed, *Cutaneotrichon* and *Tubeufia* were dominant genera in the baseline irrigation water community, *Asticcacaulis* were dominant in the microbial community of the roots prior to planting, and *Rhizomicrobium*, *Rhodoferax*, *Spirochaeta* and *Chroococcopsis* were dominant genera in the coco coir baseline community.

Interestingly, *Bacillus* and *Trichoderma* were enriched in the soil samples, and do not appear at relatively high abundance in the hydroponic samples. Roy (2026) and colleagues reported a similar observation, where *Bacillus* were abundant in soil-based strawberry roots, but depleted in the hydroponic counterparts[50]. *Bacillus* and *Trichoderma* isolates are frequently included in commercial inoculants used by hydroponic greenhouse growers, including RootShield©, RootShield Plus©, Rhapsody©, and Serenade©[114,115]. Many of the isolates included in existing commercial inoculants are derived from soil, and we have demonstrated in the present study that soil-based microorganisms do not always colonize the hydroponic rhizosphere to the same degree. The results of the present study indicate that these genera may not be as well suited to the hydroponic strawberry rhizosphere as they are for other crops, which calls into question the potential efficacy of *Bacillus*- and *Trichoderma*-based products in

hydroponic strawberry production. Therefore, the efficacy of existing commercial inoculants for promoting hydroponic strawberry growth should be assayed empirically, and not be assumed.

4.2 Soil addition had minimal long-term impact on the hydroponic strawberry rhizomicrobiome

It is well known that soil supports highly diverse communities of bacterial and eukaryotic microorganisms, especially rhizosphere soil[116,117]. Contrastingly, there is a long-standing misconception that hydroponic crops do not support their own microbiome[118]. Recent literature demonstrates that this is not true, yet the hydroponic rhizosphere microbiome differs considerably from the soil rhizosphere microbiome due to differences in physiochemical properties such as availability of nutrients and organic matter, pH, temperature, accumulation of salts, and dissolved oxygen[21,47]. Given the high microbial diversity in soil samples, and the unique selective pressures within the hydroponic rhizosphere, the first objective of this study is to investigate the effect of soil addition within the hydroponic strawberry rhizosphere. Overall, there are few statistically significant differences in microbial abundance between inoculated treatments and the uninoculated control group across all timepoints. There are three possible biological explanations for this observation.

First, thorough microbial colonization of the rhizosphere prior to soil addition may have prevented establishment of soil-based microorganisms. Existing studies demonstrate that the order of arrival of microorganisms into the rhizosphere influences their ability to colonize; this is known as priority effect[119]. Priority effect occurs as early-arriving taxa consume the available resources, occupy the available space, or otherwise alter the environment in a way that changes conditions for later-arriving taxa (i.e. niche preemption and modification)[120]. In this study, the young strawberry plants were not sterilized prior to planting, and thus retained some native root

microbiome. Further, treatments were inoculated five days after planting. It is possible that microorganisms from the native root, coco coir, and water microbiomes colonized the hydroponic rhizosphere during the five day period between planting and soil-addition, leaving little remaining space and resources for incoming soil-based microorganisms to utilize.

It is important to note that the decision not to sterilize strawberry tray plants prior to planting was intentional, not an oversight. A 2024 meta-analysis concluded that PGPM studies that use sterilized plants and substrates generally report better results than studies that use non-sterilized plants and substrates, such as greater plant growth-promotion and greater persistence of inoculum microorganisms[121]. However, the goal of this research is to develop a microbial inoculant for commercial use. Thus, the experimental plant trial was specifically designed to resemble common commercial practice where strawberry tray plants and substrates are not sterilized prior to planting.

Second, the soil samples contained a variety of bacteria, fungi, and oomycetes (Figures 6.1, 6.2). It is possible that differential establishment of soil-based microorganisms in the hydroponic microbiome inflated within-group variation. This would have been exacerbated by pre-colonization of the rhizosphere by native microorganisms[121]. In this study, the threshold for differential abundance is effect size >|1|, calculated as the ratio of between-group difference and within-group variation[93]. As within-group variation increases, effect size decreases and taxa are not identified as differentially abundant. Despite its reputation for accuracy, ALDEx2 is known to be conservative in identifying differentially abundant taxa for this reason[122].

Third, it is possible that the strawberry plants themselves selectively recruited a similar rhizomicrobiome community, regardless of soil treatment. Existing research has demonstrated that many plant species do recruit a functionally similar core microbiome even under different

environmental conditions[77,112,113]. Specifically, this has recently been demonstrated for strawberries, where soil-based strawberry roots from four regions of Chile possessed a functionally similar rhizomicrobiome, despite differences in soil type and nutrient conditions[123]. Indeed, we see a common core microbiome of highly-prevalent, highly-abundant microorganisms across all treatments and growth stages in the present study (Section 4.3.3).

The important takeaway from these results is that a single perturbation of the microbiome, in this case addition of a diverse collection of soil-based, plant-associated microorganisms, did relatively little to alter the hydroponic strawberry rhizomicrobiome in the long-term. Based on literature, different dosing strategies, such as addition of soil earlier in plant development or repeated applications of soil, may have conferred different results[124,125]. For example, de Oliveira and colleagues (2024) demonstrated that biweekly inoculation with *Azospirillum brasilense* resulted in greater growth-promotion in strawberry than single and monthly inoculation treatments over a 10 week plant trial[125]. Therefore, timing, frequency, and size of dose are important considerations for future research in designing a microbial inoculant for hydroponic strawberries.

4.3 Microbial succession of rare taxa occurs, while a core microbiome remains consistent

Microbial succession has been thoroughly described in the rhizosphere of a variety of crops including soil-based strawberries, but not yet in hydroponic strawberries[70-73,96-101]. Similarly, the rhizosphere core microbiome is a useful tool for hypothesizing the functional role of the rhizomicrobiome, but has not previously been described for hydroponic strawberries[79]. Therefore, the second objective of this research is to describe both succession and a candidate

core microbiome of bacteria, fungi, and oomycete members of the hydroponic rhizomicrobiome of strawberries.

4.3.1 The role of stochastic and deterministic processes in the strawberry rhizomicrobiome

In the present study, eight bacterial genera and five fungal genera are enriched in the young strawberry rhizomicrobiome. Early-enrichment may be the result of deterministic selection acting in a variety of ways. First, these microorganisms may be better suited to utilize root exudates released by young strawberry plants than mature strawberry plants[68]. This has been examined in the *Arabidopsis* rhizomicrobiome, where greater exudation of sugars by young plants and secondary metabolites by mature plants were each associated with changes in rhizosphere community composition and metabolism[70]. An analogous trend may exist in the hydroponic strawberry rhizosphere, though this remains undescribed. Second, early-enriched taxa may be able to colonize quickly, establishing themselves at relatively high abundance before the microbiome becomes competitive. Indeed, *Acidovorax*[127], *Comamonas*[128], *Delftia*[129], *Methylobacillus*[130], *Mortierella*[131], and *Aspergillus*[132] have relatively short doubling times, permitting rapid growth and enrichment early-on. Finally, early-enriched microorganisms may be transient taxa that aid in community assembly but become outcompeted in later plant growth stages[133]. For example, early-enriched fungal genera *Trechispora*[134], *Ophiostoma*[135], *Mortierella*[136] and *Aspergillus*[137] are known saprophytes. Saprophytic fungi are common in organic hydroponic substrates, including coco coir (i.e. ground coconut husk)[138]. Fungi-mediated degradation of organic matter may be important early-on in rhizomicrobiome assembly by releasing nutrients that are bioavailable to both host plant and rhizomicrobial community[139]. All thirteen taxa enriched in week two relative to week eight are also relatively

highly or intermediately abundant in week eight communities, but to a lesser degree; this is strong evidence of persistence of these taxa in the hydroponic strawberry rhizomicrobiome.

In contrast, fourteen bacterial genera and four fungal genera are enriched in the mature strawberry rhizomicrobiome. *Oleiharenicola* and *Schlesneria* were highly abundant relative to both week two and week eight communities, but more so in week eight, while the remaining taxa were relatively low or intermediately abundant in week two communities. Enrichment in week eight may be the product of deterministic or stochastic processes, or a combination of both. Deterministic selection may be acting in two ways. Taxa enriched in week eight may be 1) better adapted to utilize root exudates released by mature strawberry plants, or 2) in possession of traits that confer a competitive advantage in the hydroponic microbiome specifically[70]. For example, motility and adhesion are advantageous microbial traits in the hydroponic rhizosphere[56]. Adhesion allows microorganisms to resist displacement by high-flow irrigation and motility enables microorganisms to relocate to favourable microenvironments when they are displaced by irrigation, or when competition becomes intense[140,141]. For non-motile fungi, the production of mycelium provides similar advantages in the hydroponic environment[20]. Numerous late-enriched bacterial genera exhibit motility, including *Schlesneria*[142], *Gimesia*[143], *Zoogloea*[144], *Chondromyces*[145], *Polyangium*[146], *Pseudaminobacter*[147], and *Skermanella*[148]. The following week eight-enriched taxa exhibit adhesion via specialized appendages or biofilm formation: *Gimesia*[143], *Schlesneria*[149], *Amaricoccus*[150], *Skermanella*[151], *Hohenhuehelia*[152] and *Rhodosporidiobolus*[153]. Thus, phenotypes of motility and adhesion may be conferring a selective advantage in the hydroponic strawberry microbiome. Some of the late-enriched taxa are considered slow-growing, including *Amaricoccus*[154], *Gimesia*[155], *Nectria*[156], *Solirubrobacter*[157], *Hohenbuehelia*[158], *Chondromyces*[159], *Polyangium*[160], *Mariniblastus*[161],

and *Pseudaminobacter*[162]. For these taxa, it is possible that enrichment in week eight is the product of slow but consistent growth and dispersal over time, rather than either deterministic or stochastic mechanisms.

Stochastic processes are likely also influencing succession in the strawberry rhizomicrobiome. Dini-Andreote and colleagues (2014) posit that succession is dominated early-on by stochasticity when a wide variety of microorganisms are capable of surviving in a given environment[67]. Indeed, the soil samples contained a wide variety of microorganisms, many of which have previously demonstrated persistence in hydroponic environments, including *Sphingobium, Hyphomicrobium, Bradyrhizobium*[54], *Lysobacter*[49], *Gaiella*[163], *Flavisolibacter*[164], and *Paenibacillus*[21] to name a few. Stochastic succession in the young strawberry rhizomicrobiome may have had a cascading effect, impacting the mature strawberry rhizomicrobiome as well. Therefore, the observed enrichment of taxa in both week two and week eight rhizomicrobiomes may have been influenced by random chance, in addition to biology. Truthfully, stochasticity in microbial succession is a confounding variable that may contribute to the observed reproducibility concerns in plant microbiome research[165].

4.3.2 Discrepancies between time-series and growth-state succession analyses

Root exudation patterns can vary with plant developmental stage[70,71]. The quantity and composition of root exudates has a significant impact on the rhizomicrobiome community[68,75]. Therefore, we expect rhizomicrobiome community composition to vary with strawberry growth stage. At the genus level, *Methylotenera* and *Edaphobaculum* are enriched during vegetative and flowering growth states, relative to the fruiting stage, while *Amaricoccus* and *Polyangium* are enriched during fruiting relative to the vegetative stage (Supplementary Table B6). At the

community level, bacterial and fungal/oomycete communities both demonstrate greater variance in the flowering stage. Similar observations have been noted in literature; Micallef (2009) and Lundberg (2014) and colleagues both demonstrate that rhizosphere communities converge after the flowering stage[73,77]. Overall, rhizomicrobiome succession in response to strawberry growth state is not statistically well-supported in this hydroponic study.

Interestingly, time-series analysis provides a more statistically-supported analysis than growth-state analysis does. A potential limitation of this study is that growth stage was determined via visual inspection, which may not have captured the breadth of variation in physiological state. Quantitative methods for assessing growth state based on metabolic and phytohormone profiling exist and may have produced different results[166,167]. Regardless, visual inspection remains the standard in commercial greenhouses, and this study used well-defined criteria for classification. Briefly, growth state was determined weekly via visual inspection based on the following criteria: "vegetative" for plants that have not yet produced a mature flower, "flowering" at observation of first mature flower, "fruiting" at observation of first developing, marketable berry (i.e. all petals have fallen away and developing berry is uniformly green with no visual imperfections). Growth state likely contributed to microbiome structure overall, but the effect may have been obscured by microbiome variation within growth state groups. Raw growth state data is summarized in Supplementary Figures A8-A11.

4.3.3 Proposing a candidate beneficial core rhizosphere microbiome of hydroponic strawberries

This study identifies 20 bacterial, 19 fungal, and 2 oomycete genera that were present in at least 90% of all samples with a mean relative abundance greater than 1%. Table 4.1 summarizes the results of relevant literature for observed highly-prevalent, highly-abundant

microorganisms with respect to hydroponic strawberry production and PGP-ability. High prevalence and abundance across all samples, regardless of growth stage and treatment, is evidence that these taxa effectively colonized the hydroponic strawberry rhizosphere in this experiment. Indeed, members of nearly all of the highly-prevalent, highly-abundant genera have previously demonstrated persistence in the hydroponic rhizomicrobiome.

Of these, species of 11 genera have demonstrated the ability to promote growth in strawberries, including seven bacterial genera, *Acinetobacter*[168], *Burkholderia*[169], *Paraburkholderia*[170], *Pseudomonas*[103,171-174], *Rhizobium*[175], *Sphingobium*[176], *Streptomyces*[177,178], and four fungal general, *Exophiala*[179], *Penicillium*[180], *Rhodotorula*[181,182], and *Serendipita*[183]. In lieu of strawberry-specific literature for the remaining 33 genera, literature assessing their PGP-ability in other crops or *in vitro* can be used to hypothesize possible PGP-ability in strawberries.

It is not unexpected to see several novel observations in this analysis. Recall, the soil samples used in this study were specifically selected to introduce microbial diversity with the intention of identifying unique microorganisms that can colonize the hydroponic strawberry rhizosphere. For nine highly-prevalent, highly-abundant taxa identified in this study, this is the first report of persistence in the hydroponic rhizomicrobiome of any plant: *Chroococcopsis*, *Apiotrichum, Podospora, Sporothrix, Achroceratosphaeria, Leucosporidium, Mycochaetophora, Simocybe,* and *Tubeufia*. Similarly, nine taxa identified in this study have not previously been reported in a strawberry rhizomicrobiome, including six saprobic fungal genera: *Chroococcopsis, Hyphomicrobiome, Pedosphaera, Achroceratosphaeria, Cutaneotrichosporon, Leucosporidum, Mycochaetophora, Simocybe,* and *Tubeufia*. As saprobes, several of these genera likely appear at relatively high abundance in this study because their members are capable of degrading the coco

coir substrate as a nutrient source. That is not to say that the presence of these fungi in the rhizosphere is not beneficial; in fact, the release of nutrients from fungal degradation of coco coir may have supported the growth of other microorganisms in the rhizosphere as previously discussed[138,139]. Several of these taxa may also be absent from literature because fungal communities are understudied relative to bacterial communities in the hydroponic environment[20].

Ilyonectria, Olpidium, Phytophthora, and *Pythium* were among highly-prevalent, highly-abundant taxa, but will not be considered as members of the beneficial core microbiome. These taxa are phytopathogens known to cause symptoms of root rot in strawberries[20,184-186]. The presence of phytopathogens in this study is unsurprising; hydroponic monocultures with recirculating nutrient solution, such as in this study, are prone to phytopathogen accumulation[187]. Interestingly, *Olpidium* was one of the dominant fungal genera on the strawberry roots prior to planting, likely causing the high prevalence and abundance of *Olpidium* throughout the hydroponic trial (Figure 6.2). Detection of these taxa in the hydroponic strawberry rhizomicrobiome can indicate potential pathogen infection, certainly so if coupled with visual symptoms such as black/brown roots and crowns and wilting[20]. No symptoms of root rot were observed in this experiment. This may indicate that the observed relative abundances were insufficient to cause an active infection, or that beneficial members of the rhizomicrobiome were exerting biocontrol or inducing resistance in the strawberry plants[20]. Indeed, members of *Flavobacterium* and *Streptomyces* have exhibited biocontrol of *Phytophthora* and *Pythium* species, respectively[188,189].

Table 4.1. Summary of relevant literature for highly prevalent, highly abundant taxa with respect to their ecological role in strawberry production, demonstrated persistence in hydroponic cropping systems, and evidence of plant growth-promoting (PGP) phenotypes. Hydroponic studies were preferentially included where possible; non-hydroponic studies are presented where necessary. Genera of the BCP group are discussed separately, as *Burkholderia, Caballerona,* and *Paraburkholderia*. Similarly, *Nectria* is an out-dated genera, and literature is presented for *Ilyonectria* and *Thelonectria* instead.

			Evidence of PGP Traits			
Genera	Ecological Role in Strawberry	Persistence in Hydroponics	Phytohormone Production	Nutrient Acquisition	Stress Regulation	Biocontrol & Immune Induction
Bacteria						
Acinetobacter	PGPM[168]	Yes[190]	[191,192]	[39,192]	[191-193]	[39,41]
Burkholderia	PGPM[169]	Yes[194]	[195,196]	[195,197, 198]	[195,199, 200]	[197,198, 201]
Paraburkholderia	PGPM[170]	Yes[202]	[203]	[204]	[202,205]	[204]
Pseudomonas	PGPM[103,171-174]	Yes[21,206]	[207]	[32, 208]	[32]	[209-212]
Rhizobium	PGPM[175]	Yes[21,213,214]	[215]	[34,216, 217]	[218]	[217]
Sphingobium	PGPM[176]	Yes[54,219-222]	[221,223,224]	[223,225]	[224,226]	[226,227]
Streptomyces	PGPM[177,178]	Yes[228-230]	[178,231,232]	[178]	[231]	[177,178, 233]
Asticcacaulis	Detected, but undescribed[106, 234]	Yes[106,234,235]	[236]	[236]		[236]
Bradyrhizobium	Detected, but undescribed[237]	Yes[54,220,234,238]	[169,239,240]	[217,241, 242]	[243,244]	[217]
Caballeronia	Detected, but undescribed[50]	Yes[50,228]		[245]	[246]	
Devosia	Detected, but undescribed[108]	Yes[247]	[248]	[248]	[247]	[108]
Flavobacterium	Detected, but undescribed[249]	Yes[54,234,238,250]	[251,252]	[252]	[253]	[189]
Mesorhizobium	Detected, but undescribed[50]	Yes[50]	[254]	[254]	[255]	[256]
Mucilaginibacter	Detected, but undescribed[257]	Yes[258,259]	[260]		[260,261]	

Genera	Ecological Role in Strawberry	Persistence in Hydroponics	Evidence of PGP Traits			
			Phytohormone Production	Nutrient Acquisition	Stress Regulation	Biocontrol & Immune Induction
Phenylobacterium	Detected, but undescribed[266]	Yes[238]	[267]	[267,268]		
Rhodanobacter	Detected, but undescribed[103]	Yes[259]	[269,270]	[269,270]	[269]	[271]
Sphingomonas	Detected, but undescribed[272, 273]	Yes[54,274]	[275,276]	[275,276]	[275,276]	[276,277, 278]
Terrimonas	Detected, but undescribed[50]	Yes[50,221]	[279]	[279]		[280,281]
Chroococcopsis	Previously undetected	No Evidence				
Hyphomicrobium	Previously undetected	Yes[54,219,220]	[282]	[282]		
Pedosphaera	Previously undetected	Yes[283]				
Fungi						
Exophiala	PGPM[179]	Yes[284]	[285,286]		[285]	[179]
Penicillium	PGPM[180]	Yes[20,287]	[288,289]	[288-291]	[289,292]	[37,288,290,293,294]
Rhodotorula	PGPM[181,182]	Yes[221]	[295,296]	[297]	[296]	[182]
Serendipita (formerly *Piriformospora indica*)	PGPM[183]	Yes[298,299]	[300]	[300,301]	[302]	[303]
Apiotrichum	Detected, but undescribed[176]	No Evidence	[304]			[305]
Cadophora	Detected, but undescribed[237]	Yes[186]		[306,307]		[307,308]
Coniochaeta	Detected, but undescribed[228]	Yes[131,228]	[309]			[310]
Mortierella	Detected, but undescribed[311]	Yes[228,284]	[312]	[313-315]	[312]	[316,317]
Podospora	Detected, but undescribed[237, 318]	No Evidence				

Genera	Ecological Role in Strawberry	Persistence in Hydroponics	Evidence of PGP Traits			
			Phytohormone Production	Nutrient Acquisition	Stress Regulation	Biocontrol & Immune Induction
Sporothrix	Detected, but undescribed[318]	No Evidence				[322]
Thelonectria (formerly within *Nectria*)	Detected, but undescribed[228]	Yes[186,228]				
Achroceratosphaeria	Previously undetected	No Evidence				
Cutaneotrichosporon	Previously undetected	Yes[323]				
Leucosporidium	Previously undetected	No Evidence				
Mycochaetophora	Previously undetected	No Evidence				
Simocybe	Previously undetected	No Evidence				
Tubeufia	Previously undetected	No Evidence				
Ilyonectria (formerly within *Nectria*)	Phytopathogen [186]	Yes[186,228]				
Olpidium	Phytopathogen [184]	Yes[284]				
Oomycetes						
Phytophthora	Phytopathogen [20]	Yes[324]				
Pythium	Phytopathogen [185,325]	Yes[20]				

4.3.4 Applying new insights of succession and core microbiome membership in the hydroponic strawberry rhizomicrobiome

The observations of succession and core microbiome in this study have several implications on the development and use of a microbial inoculant for hydroponic strawberries. For example, defining the core microbiome is a useful first step in investigating the functional role of the rhizosphere microbiome in hydroponic strawberry production. This understanding can be applied to choose candidate inoculant microorganisms that fill functional roles and persist in the hydroponic strawberry rhizomicrobiome[79]. Thus, this study presents the following 29 genera for consideration as beneficial candidate core microbiome members in the hydroponic strawberry rhizosphere: *Acinetobacter, Burkholderia, Paraburkholderia, Pseudomonas, Rhizobium, Sphingobium, Streptomyces, Asticcacaulis, Bradyrhizobium, Caballeronia, Devosia, Flavobacterium, Mesorhizobium, Mucilaginibacter, Novosphingobium, Phenylobacterium, Rhodanobacter, Sphingomonas, Terrimonas, Hyphomicrobium, Exophiala, Penicillium, Rhodotorula, Serendipita, Apiotrichum, Cadophora, Coniochaeta, Mortierella,* and *Pseudogymnoascus*. These genera are a subset of all highly-prevalent, highly-abundant taxa identified in this study for which there is literature evidence of 1) persistence in the hydroponic rhizosphere and 2) PGP-ability in strawberries, in other crops, or *in vitro* (Table 4.1), and are suitable candidates for future inoculated plant trials.

This study describes several changes in hydroponic strawberry microbiome composition over time. A simple but important takeaway from this is that the microbiome is dynamic, not static. Changes in rhizosphere community composition may adversely impact the ability of inoculant microorganisms to colonize. This is not acknowledged by existing commercial inoculants but future research into developing a microbial inoculant should take this into

consideration. Molecular methods, such as amplicon sequencing or qPCR, should be used to confirm presence and quantify abundance of inoculant microorganisms throughout the strawberry growth cycle. Additionally, it may be fruitful to test multiple dosing strategies (e.g. inoculation frequency, volume, timing) to optimize persistence and abundance of inoculum microorganisms in the rhizomicrobiome. And always, when assessing new and existing literature, keep in mind that the number and timing of sampling events will influence the nature of the conclusions.

4.4 No genera were significantly associated with changes in yield

There are numerous studies that assess the ability of microorganisms to promote plant growth[20,21]. However, many studies neglect to measure commercially relevant end-points, such as yield[5,20,21]. A 2024 meta-analysis found that yield is reported in less than 2% of PGPM research[121]. Therefore, the final objective of this research is to identify any associations between microbial abundance and strawberry yield. Overall, this study finds no individual bacterial, fungal, or oomycete genera that are significantly associated with increases or decreases in yield. This observation does not mean that there are truly no microorganisms influencing yield.

Both biological and statistical factors may have acted together to cause this result. First, this study used entire soil communities to inoculate the hydroponic rhizosphere, rather than a concentrated dose of a single PGPM or phytopathogenic isolate. Differential establishment of soil-based microorganisms between strawberry plants within each treatment may have diluted any associations beyond the significance threshold. Further, week eight samples from all four experimental groups (one uninoculated control, three inoculated treatments) were collapsed into one global analysis (n = 24) because within-treatment sample sizes (n = 6) were too small for

robust analysis via GLM. Since there were no significant differences in microbial community composition between experimental groups in week eight (Table 3.1), this was statistically valid. However, as a result, treatment group may be a slight confounding variable in this analysis; if any taxa associated with yield in only one experimental group, they were not detected. Finally, this analysis used a linear model that identifies linear associations. Therefore, if any taxa influenced yield at intermediate abundance, with no effect on yield at either high or low extreme, they would be undetected by this model.

It is possible that a genus-level analysis was too reductionist in this application. We know that many host plants selectively recruit a functionally similar core microbiome (i.e. functional compensation theory), regardless of environmental conditions, and that many soil and rhizomicrobiome communities exhibit functional redundancy[44,77,112,113]. Therefore, if strawberry plants selectively recruit microorganisms to their rhizomicrobiome to fulfill specific functions, regardless of taxonomy, this may also confuse a genetic analysis. A community-level transcriptomic analysis may have been a more effective tool to elucidate the impact of the rhizomicrobiome community on strawberry fruit yield. Azarbad & Junker (2024) found that consortia promote plant-growth more reliably than single-isolates[121]. Combined with the results of this study, we can hypothesize that community-level engineering may be a more fruitful strategy for increasing hydroponic strawberry production.

4.5 Limitations and future directions

This study is subject to some limitations of technical, statistical, and biological nature that should be noted. First, DNA extraction, PCR, and Oxford Nanopore sequencing each impose their own biases on the final sequenced datasets. Many DNA extraction methods are known to be

biased against organisms with cell walls, such as gram-positive bacteria and most fungi, causing an underrepresentation of these organisms in the extracted DNA[326,327]. Sequences with high GC content are harder to denature, and thus less likely to be amplified via PCR, resulting in an underrepresentation in the PCR products[328]. Finally, Oxford Nanopore sequencing has a higher error rate (~ Q20, or 99% accuracy) than other popular sequencing platforms, such as Illumina MiSeq (~ Q30, or 99.9% accuracy)[329,330]. In this study, technical limitations were accounted for by treating all samples identically. We can confidently compare samples within this study, but the existence of these technical biases should be considered when comparing these results to similar studies.

Statistically, this study is limited by sample size. Microbiome datasets can be difficult to analyze statistically due to their high dimensionality and compositional nature[122,331,332]. Many existing and popular tools for microbiome analysis are not compositionally appropriate, and thus suffer from negative correlation bias, spurious correlation, and inconsistencies when the data are subset[332,333]. Nearing and colleagues (2022) described trends for 14 different analysis tools and found that ALDEx2, which is one of few compositionally-appropriate tools for analyzing sequencing datasets, can be conservative in the number of significant differences it identifies[122]. Thus, a larger sample size (e.g. more samples at more timepoints) may have increased statistical power in identifying significant differences, especially if soil-derived microorganisms established differentially between rhizospheres, as suspected. The same study also demonstrated that different analysis tools may produce wildly different conclusions from the same dataset[122]. This should be considered when comparing microbiome research across studies that use different analysis methods.

Further, there are several biological limitations in this study. First, the soil samples contained nutrients that may have altered plant growth, and thus rhizomicrobiome composition. Supplementary table B9 demonstrates that the amount of each nutrient contained in the soil samples is relatively little compared to the content of the nutrient solution. Thus the impact of soil-based nutrients was likely minimal. Second, the results of this study may be specific to the strawberry cultivar used in this study: June-bearing Lycia (NovaFruit, Quebec). Existing research has demonstrated that rhizomicrobiome composition can be cultivar-dependent[29,65]. Others posit that this is due to differences in host plant genotype, causing differences in root exudation patterns[44]. Finally, eight weeks is a comparatively short amount of time, considering many commercial greenhouses keep their strawberry crop for several months, or up to two years in some cases. Existing literature demonstrates that trends observed in short-, mid-, and long-term rhizomicrobiome studies can vary[121]. Overall, follow up experiments in this area of research should include multiple commercially-popular cultivars, such as Jewel and Albion[12], and assess a longer growth period to determine if the observations in this study are true trends in the overall hydroponic strawberry rhizosphere.

Finally, this study cannot confidently draw conclusions about the functional role of microorganisms in the strawberry rhizosphere based on amplicon sequencing data alone. We can, and do, use literature to hypothesize the role of core taxa (Table 4.1), but without transcriptomic analysis it is inappropriate to comment on functional roles with a high degree of certainty. Numerous studies have demonstrated discrepancies between microbial genotype and phenotype when it comes to plant growth-promoting traits[52,334]. Thus, gene content and even *in vitro* biochemical assays are not always accurate predictors of PGP-ability *in planta*. Further, this study generally reports genus-level resolution, and genera contain a wide variety of species-level

variation. PGP-traits detected in some members of a genus are not necessarily common to all members of that genus. Indeed, some genera contain known PGPM and phytopathogenic species, such as *Pseudomonas*, *Fusarium*, and *Pythium*[20,21,335,336]. A time-series metatranscriptomic analysis of rhizomicrobial activity coupled with GC-SM analysis of root exudate content, analogous to Chaparro and colleagues (2014) research with *Arabidopsis*, would be a powerful follow-up experiment to investigate the functional role of microbial members in the hydroponic strawberry rhizosphere[71].

4.6 Concluding remarks

This study reveals numerous novel insights into the nature and complexity of the hydroponic strawberry rhizomicrobiome in a commercially-relevant way. First, soil addition had relatively little impact on long-term rhizomicrobiome composition. This suggests that the rhizomicrobiome may be more difficult to engineer than previously thought. Second, this study describes, for the first time, microbial succession in the hydroponic strawberry rhizosphere. The occurrence of succession in the rhizomicrobiome should be considered when designing and implementing microbial inoculants for use in hydroponic strawberry production. Additionally, this study presents a candidate core microbiome for hydroponic strawberries. Core microbiome members demonstrate persistence in the rhizomicrobiome, and isolates of these genera that demonstrate *in vitro* PGP-ability are good candidates for future research into inoculant development. Finally, the lack of significant association between fruit yield and microbial abundance suggests that genus- and species-level rhizomicrobiome composition may not be as influential as community composition overall. Taken together, these results suggest that the best inoculant may not be a single isolate, but rather a series or consortium of microorganisms

designed to promote growth at each developmental stage of the strawberry plant. The results of this research should be considered in efforts to develop inoculants for hydroponic strawberries to ensure future efforts are not “fruitless.”

References

1. United Nations. 2022. World population projected to reach 9.8 billion in 2050, and 11.2 billion in 2100. Available from https://www.un.org/en/desa/world-population-projected-reach-98-billion-2050-and-112-billion-2100.
2. Kalmpourtzidou, A., Eilander, A., and Talsma, E.F. 2020. Global Vegetable Intake and Supply Compared to Recommendations: A Systematic Review. Nutrients **12**(6): 1558. doi:10.3390/nu12061558.
3. Grafton, R.Q., Williams, J., and Jiang, Q. 2015. Food and water gaps to 2050: preliminary results from the global food and water system (GFWS) platform. Food Sec. **7**(2): 209–220. doi:10.1007/s12571-015-0439-8.
4. WHO. 2024. Hunger numbers stubbornly high for three consecutive years as global crises deepen: UN report. Available from https://www.who.int/news/item/24-07-2024-hunger-numbers-stubbornly-high-for-three-consecutive-years-as-global-crises-deepen--un-report.
5. Stegelmeier, A.A., Rose, D.M., Joris, B.R., and Glick, B.R. 2022. The use of PGPB to promote plant hydroponic growth. Plants **11**(20): 2783. doi:10.3390/plants11202783.
6. Díaz-Rodríguez, A.M., Salcedo Gastelum, L.A., Félix Pablos, C.M., Parra-Cota, F.I., Santoyo, G., Puente, M.L., Bhattacharya, D., Mukherjee, J., and De Los Santos-Villalobos, S. 2021. The current and future role of microbial culture collections in food security worldwide. Front. Sustain. Food Syst. **4**: 614739. doi:10.3389/fsufs.2020.614739.
7. OMAFA. 2024. Strawberry: harvested area, marketed production, farm value, average price & yield, Ontario 1979-2023. Available from https://data.ontario.ca/dataset/ontario-strawberry-production-and-yield/resource/1190bf0f-9447-45a9-a217-0846fbae4238.
8. Statistics Canada. 2022. Strawberry fields forever? Statistics Canada. Available from https://www.statcan.gc.ca/o1/en/plus/1300-strawberry-fields-forever [accessed 5 October 2023].
9. Statistics Canada. 2022. Land use, census of agriculture historical data. Available from https://www150.statcan.gc.ca/t1/tbl1/en/tv.action?pid=3210015301.
10. Brown, D.M., and Blackburn, W.J. 1987. Impacts of freezing temperatures on crop production in Canada. Can. J. Plant Sci. **67**(4): 1167–1180. doi:10.4141/cjps87-156.

11. Qiu, H., Yan, Q., Yang, Y., Huang, X., Wang, J., Luo, J., Peng, L., Bai, G., Zhang, L., Zhang, R., Fu, Y.H., Wu, C., Peñuelas, J., and Chen, L. 2024a. Flowering in the Northern Hemisphere is delayed by frost after leaf-out. Nat Commun **15**(1): 9123. doi:10.1038/s41467-024-53382-3.
12. Hodgdon, E.A., Conner, D.S., McDermott, L.G., Pritts, M.P., Handley, D.T., Orde, K.M., and Grube Sideman, R. 2024. A Current View on Strawberry Production Practices and Trends in the Northeastern United States and Canada. hortte **34**(5): 574–584. doi:10.21273/HORTTECH05457-24.
13. Statistics Canada. 2025. Production and value of greenhouse vegetables. Government of Canada. doi:10.25318/3210045601-ENG.
14. Cowan, N., Ferrier, L., Spears, B., Drewer, J., Reay, D., and Skiba, U. 2022. CEA Systems: the means to achieve future food security and environmental sustainability? Front. Sustain. Food Syst. **6**: 891256. doi:10.3389/fsufs.2022.891256.
15. Suárez-Cáceres, G.P., Pérez-Urrestarazu, L., Avilés, M., Borrero, C., Lobillo Eguíbar, J.R., and Fernández-Cabanás, V.M. 2021. Susceptibility to water-borne plant diseases of hydroponic vs. aquaponics systems. Aquaculture **544**: 737093. doi:10.1016/j.aquaculture.2021.737093.
16. Sumalan, R.L., Stroia, N., Moga, D., Muresan, V., Lodin, A., Vintila, T., and Popescu, C.A. 2020. A cost-effective embedded platform for greenhouse environment control and remote monitoring. Agronomy **10**(7): 936. doi:10.3390/agronomy10070936.
17. Verdoliva, S.G., Gwyn-Jones, D., Detheridge, A., and Robson, P. 2021. Controlled comparisons between soil and hydroponic systems reveal increased water use efficiency and higher lycopene and β-carotene contents in hydroponically grown tomatoes. Scientia Horticulturae **279**: 109896. doi:10.1016/j.scienta.2021.109896.
18. Glick, B.R. 2020. Beneficial plant interactions. *In* Introduction to plant growth-promoting bacteria. Springer Nature Switzerland, Switzerland. pp. 1–38. Available from https://doi.org/10.1007/978-3-030-44368-9.
19. Walker, T.S., Bais, H.P., Groteworld, E., and Vivanco, J.M. 2003. Root exudation and rhizosphere biology. Plant Physiology **132**(1): 44–51. doi:https://doi.org/10.1104/pp.102.019661.
20. Laevens, G.C.S., Dolson, W.C., Drapeau, M.M., Telhig, S., Ruffell, S.E., Rose, D.M., Glick, B.R., and Stegelmeier, A.A. 2024. The Good, the Bad, and the Fungus: Insights into the Relationship Between Plants, Fungi, and Oomycetes in Hydroponics. Biology **13**(12): 1014. doi:10.3390/biology13121014.

21. Thomas, B.O., Lechner, S.L., Ross, H.C., Joris, B.R., Glick, B.R., and Stegelmeier, A.A. 2024. Friends and Foes: Bacteria of the Hydroponic Plant Microbiome. Plants **13**(21): 3069. doi:10.3390/plants13213069.
22. Ghosh, A.R. 2013. Appraisal of Microbial Evolution to Commensalism and Pathogenicity in Humans. Clin Med Insights Gastroenterol **6**: CGast.S11858. doi:10.4137/CGast.S11858.
23. Espinosa-Palomeque, B., Jiménez-Pérez, O., Ramírez-Gottfried, R.I., Preciado-Rangel, P., Buendía-García, A., Sifuentes, G.Z., Sariñana-Navarrete, M.A., and Rivas-García, T. 2025. Biocontrol of Phytopathogens Using Plant Growth Promoting Rhizobacteria: Bibliometric Analysis and Systematic Review. Horticulturae **11**(3): 271. doi:10.3390/horticulturae11030271.
24. Patten, C.L., and Glick, B.R. 2002. Role of *Pseudomonas putida* indoleacetic acid in development of the host plant root system. Appl Environ Microbiol **68**(8): 3795–3801. doi:10.1128/AEM.68.8.3795-3801.2002.
25. Taiz, L., Zeiger, E., Møller, I.M., and Murphy, A. 2018. Chapter 12: signals and signal transduction. *In* Fundamentals of Plant Physiology, 1st edition. Oxford University Press, New York. pp. 341–367.
26. Babu, A.G., Kim, S.W., Yadav, D.R., Hyum, U., Adhikari, M., and Lee, Y.S. 2015. Penicillium menonorum: a novel fungus to promote growth and nutrient management in cucumber plants. Mycobiology **43**(1): 49–56. doi:10.5941/MYCO.2015.43.1.49.
27. Del Amor, F.M., Serrano-Martínez, A., Fortea, M.I., Legua, P., and Núñez-Delicado, E. 2008. The effect of plant-associative bacteria (Azospirillum and Pantoea) on the fruit quality of sweet pepper under limited nitrogen supply. Scientia Horticulturae **117**(3): 191–196. doi:10.1016/j.scienta.2008.04.006.
28. Großkinsky, D.K., Tafner, R., Moreno, M.V., Stenglein, S.A., García De Salamone, I.E., Nelson, L.M., Novák, O., Strnad, M., Van Der Graaff, E., and Roitsch, T. 2016. Cytokinin production by Pseudomonas fluorescens G20-18 determines biocontrol activity against Pseudomonas syringae in Arabidopsis. Sci Rep **6**(1): 23310. doi:10.1038/srep23310.
29. Ibiang, S.R., Sakamoto, K., and Kuwahara, N. 2020. Performance of tomato and lettuce to arbuscular mycorrhizal fungi and Penicillium pinophilum EU0013 inoculation varies with soil, culture media of inoculum, and fungal consortium composition. Rhizosphere **16**: 100246. doi:10.1016/j.rhisph.2020.100246.
30. Kang, S.M., Hamayun, M., Khan, M.A., Iqbal, A., and Lee, I.-J. 2019. Bacillus subtilis JW1 enhances plant growth and nutrient uptake of Chinese cabbage through gibberellins

secretion. Journal of Applied Botany and Food Quality: 172-178 Pages. Journal of Applied Botany and Food Quality. doi:10.5073/JABFQ.2019.092.023.

31. Kennedy, C., Rudnick, P., MacDonald, M.L., and Melton, T. 2015. Azotobacter. *In* Bergey's Manual of Systematics of Archaea and Bacteria, 1st edition. *Edited by* W.B. Whitman. Wiley. pp. 1–33. doi:10.1002/9781118960608.gbm01207.
32. Mei, C., Chretien, R.L., Amaradasa, B.S., He, Y., Turner, A., and Lowman, S. 2021. Characterization of phosphate solubilizing bacterial endophytes and plant growth promotion in vitro and in greenhouse. Microorganisms **9**(9): 1935. doi:10.3390/microorganisms9091935.
33. Mukherjee, B., Roy, S., Parvin, N., Tarafdar, S., and Dutta, S. 2022. Characterization of a potent plant growth promoting fungal strain Aspergillus fumigatus MCC 1721 with special reference to indole-3-acetic acid production. Plant Sci. Today **10**(1): 210–223. doi:10.14719/pst.1991.
34. Patil, A., Kale, A., Ajane, G., Sheikh, R., and Patil, S. 2017. Plant Growth-Promoting Rhizobium: Mechanisms and Biotechnological Prospective. *In* Rhizobium Biology and Biotechnology. *Edited by* A.P. Hansen, D.K. Choudhary, P.K. Agrawal, and A. Varma. Springer International Publishing, Cham. pp. 105–134. doi:10.1007/978-3-319-64982-5_7.
35. Segarra, G., Casanova, E., Avilés, M., and Trillas, I. 2010. Trichoderma asperellum strain T34 controls Fusarium wilt disease in tomato plants in soilless culture through competition for iron. Microb Ecol **59**(1): 141–149. doi:10.1007/s00248-009-9545-5.
36. Yamaguchi, S. 2008. Gibberellin metabolism and its regulation. Annu. Rev. Plant Biol. **59**(1): 225–251. doi:10.1146/annurev.arplant.59.032607.092804.
37. Ibiang, S.R., Usami, T., and Sakamoto, K. 2021. Reduction of verticillium wilt in tomato by an arbuscular mycorrhizal fungus - Rhizophagus intraradices and an endophytic fungus - Penicillium pinophilum is cultivar dependent. Rhizosphere **20**: 100440. doi:10.1016/j.rhisph.2021.100440.
38. Punja, Z.K., Tirajoh, A., Collyer, D., and Ni, L. 2019. Efficacy of Bacillus subtilis strain QST 713 (rhapsody) against four major diseases of greenhouse cucumbers. Crop Protection **124**: 104845. doi:10.1016/j.cropro.2019.104845.
39. Rokhbakhsh-Zamin, F., Sachdev, D., Kazemi-Pour, N., Engineer, A., Pardesi, K.R., Zinjarde, S.S., Dhakephalkar, P.K., and Chopade, B.A. 2011. Characterization of Plant-Growth-Promoting Traits of Acinetobacter Species Isolated from Rhizosphere of Pennisetum glaucum. Journal of Microbiology and Biotechnology **21**(6): 556–566. doi:10.4014/jmb.1012.12006.

40. Srinivasan, R., Prabhu, G., Prasad, M., Mishra, M., Chaudhary, M., and Srivastava, R. 2020. Penicillium. *In* Beneficial Microbes in Agro-Ecology. Elsevier. pp. 651–667. doi:10.1016/B978-0-12-823414-3.00032-0.
41. Trotel-Aziz, P., Couderchet, M., Biagianti, S., and Aziz, A. 2008. Characterization of new bacterial biocontrol agents Acinetobacter, Bacillus, Pantoea and Pseudomonas spp. mediating grapevine resistance against Botrytis cinerea. Environmental and Experimental Botany **64**(1): 21–32. doi:10.1016/j.envexpbot.2007.12.009.
42. López, P., Pastrana, A.M., Marin, M.V., Borrero, C., Peres, N.A., and Avilés, M. 2026. Molecular characterization reveals three Neopestalotiopsis species causing strawberry disease outbreaks in Spain. Front. Plant Sci. **17**: 1830265. doi:10.3389/fpls.2026.1830265.
43. Puławska, J., Kałużna, M., Warabieda, W., Pothier, J.F., Gétaz, M., and Van Der Wolf, J.M. 2020. Transcriptome analysis of Xanthomonas fragariae in strawberry leaves. Sci Rep **10**(1): 20582. doi:10.1038/s41598-020-77612-y.
44. Regmi, R., and Gupta, V.S.R. 2025. Advances in understanding microbial communities in the rhizosphere. *In* Burleigh Dodds Series in Agricultural Science. *Edited by* University of Guelph, Canada and K.E. Dunfield. Burleigh Dodds Science Publishing Limited. pp. 129–174. doi:10.19103/AS.2024.0136.18.
45. Thepbandit, W., and Athinuwat, D. 2024. Rhizosphere Microorganisms Supply Availability of Soil Nutrients and Induce Plant Defense. Microorganisms **12**(3): 558. doi:10.3390/microorganisms12030558.
46. Watt, M. 2009. The rhizosphere: biochemistry and organic substances at the soil–plant interface. 2nd edn. Annals of Botany **104**(4): ix–x. doi:10.1093/aob/mcp166.
47. Alsanius, B.W., and Wohanka, W. 2019. Root Zone Microbiology of Soilless Cropping Systems. *In* Soilless Culture. Elsevier. pp. 149–194. doi:10.1016/B978-0-444-63696-6.00005-0.
48. De Haas, B., Dhooghe, E., and Geelen, D. 2025. Root Exudates in Soilless Culture Conditions. Plants **14**(3): 479. doi:10.3390/plants14030479.
49. Kuryntseva, P., Pronovich, N., Galieva, G., Galitskaya, P., and Selivanovskaya, S. 2025. Exploring the Role of Vertical and Horizontal Pathways in the Formation of Lettuce Plant Endospheric Bacterial Communities: A Comparative Study of Hydroponic and Soil Systems. Horticulturae **11**(7): 762. doi:10.3390/horticulturae11070762.
50. Roy, M., Han, D., Lee, D., Kang, B., and Choi, K. 2026. Cultivation system and plant health influence root-associated bacterial community structure and interaction networks in strawberry. Sci Rep **16**(1): 13270. doi:10.1038/s41598-026-45642-7.

51. Wei, X., Wang, L., Zhang, H., Sun, X., Yang, S., Li, J., Tan, L., and Zhong, Q. 2025. The interaction between rhizosphere microbial community structure and metabolites significantly affects the growth and development of hydroponically cultivated chives. Rhizosphere **33**: 101020. doi:10.1016/j.rhisph.2025.101020.
52. Samonty, I., Hasan, Md.Z., Hossain, Md.R., and Mahamud, A.G.M.S.U. 2025. The PGPB paradox: A critical review of field performance and practical constraints in agriculture. World J Microbiol Biotechnol **41**(9): 321. doi:10.1007/s11274-025-04552-y.
53. Ferreira, M.C., De Carvalho, C.R., Bahia, M., Barreto, D.L.C., Azevedo, R.N., Cota, B.B., Zani, C.L., De Oliveira Santos, A.R., Rosa, C.A., and Rosa, L.H. 2021. Plant-associated Fungi: Methods for Taxonomy, Diversity, and Bioactive Secondary Metabolite Bioprospecting. *In* The Plant Microbiome. *Edited by* L.C. Carvalhais and P.G. Dennis. Springer US, New York, NY. pp. 85–112. doi:10.1007/978-1-0716-1040-4_9.
54. Mejia, G., Jara-Servin, A., Hernández-Álvarez, C., Romero-Chora, L., Peimbert, M., Cruz-Ortega, R., and Alcaraz, L.D. 2025. Rhizosphere microbiome influence on tomato growth under low-nutrient settings. FEMS Microbiology Ecology **101**(3): fiaf019. doi:10.1093/femsec/fiaf019.
55. Batista, B.D., Bonatelli, M.L., and Quecine, M.C. 2021. Fast Screening of Bacteria for Plant Growth Promoting Traits. *In* The Plant Microbiome. *Edited by* L.C. Carvalhais and P.G. Dennis. Springer US, New York, NY. pp. 61–75. doi:10.1007/978-1-0716-1040-4_7.
56. Hirsch, M., Burges, P.L., Migueliz, L., Villarreal, N.M., and Marina, M. 2024. Isolation of beneficial bacteria from strawberry (Fragaria x ananassa, Duch). Potentialities for fungal disease control and plant growth promotion. Plant Growth Regul **102**(1): 135–152. doi:10.1007/s10725-023-00989-z.
57. Azizoglu, U., Yilmaz, N., Simsek, O., Ibal, J.C., Tagele, S.B., and Shin, J.-H. 2021. The fate of plant growth-promoting rhizobacteria in soilless agriculture: future perspectives. 3 Biotech **11**(8): 382. doi:10.1007/s13205-021-02941-2.
58. Calvo-Bado, L.A., Petch, G., Parsons, N.R., Morgan, J.A.W., Pettitt, T.R., and Whipps, J.M. 2006. Microbial community responses associated with the development of oomycete plant pathogens on tomato roots in soilless growing systems. J Appl Microbiol **100**(6): 1194–1207. doi:10.1111/j.1365-2672.2006.02883.x.
59. Haghshenas, M., Van Delden, S.H., and Nazarideljou, M.J. 2024. Effects of nutrient solution strength, PGPB, and mycorrhizal inoculation on growth,yield, and quality of strawberry. Turkish Journal of Agriculture and Forestry **48**(3): 390–401. doi:10.55730/1300-011X.3189.

60. Maboko, M.M., Bertling, I., and Du Plooy, C.P. 2013. Arbuscular mycorrhiza has limited effects on yield and quality of tomatoes grown under soilless cultivation. Acta Agriculturae Scandinavica, Section B - Soil & Plant Science **63**(3): 261–270. doi:10.1080/09064710.2012.755219.
61. Martínez, F., Palencia, P., Weiland, C., and Oliveira, J.A. 2015. RESPONSE OF TWO STRAWBERRY CULTIVARS TO INOCULATION WITH ARBUSCULAR MYCORRHIZAL FUNGUS IN DIFFERENT SOILS. Acta Hortic. (1099): 153–158. doi:10.17660/ActaHortic.2015.1099.15.
62. Palencia, P., Martinez, F., and Weiland, C. 2013. EFFECT OF ARBUSCULAR MYCORRHIZAL FUNGI ON QUALITY OF STRAWBERRY FRUIT IN SOILLESS GROWING SYSTEM. Acta Hortic. (1013): 493–498. doi:10.17660/ActaHortic.2013.1013.61.
63. Sowik, I., Borkowska, B., and Markiewicz, M. 2016. The activity of mycorrhizal symbiosis in suppressing Verticillium wilt in susceptible and tolerant strawberry (Fragaria x ananassa Duch.) genotypes. Applied Soil Ecology **101**: 152–164. doi:10.1016/j.apsoil.2016.01.021.
64. Vestberg, M. 1992. The effect of vesicular-arbuscular mycorrhizal inoculation on the growth and root colonization of ten strawberry cultivars. AFSci **1**(5): 527–535. doi:10.23986/afsci.72457.
65. Zhang, K., Bonito, G., Hsu, C.-M., Hameed, K., Vilgalys, R., and Liao, H.-L. 2020. Mortierella elongata Increases Plant Biomass among Non-Leguminous Crop Species. Agronomy **10**(5): 754. doi:10.3390/agronomy10050754.
66. Knights, H.E., Ramachandran, V.K., Jorrin, B., Ledermann, R., Parsons, J.D., Aroney, S.T.N., and Poole, P.S. 2024. *Rhizobium* determinants of rhizosphere persistence and root colonization. The ISME Journal **18**(1): wrae072. doi:10.1093/ismejo/wrae072.
67. Dini-Andreote, F., Stegen, J.C., Van Elsas, J.D., and Salles, J.F. 2015. Disentangling mechanisms that mediate the balance between stochastic and deterministic processes in microbial succession. Proc. Natl. Acad. Sci. U.S.A. **112**(11). doi:10.1073/pnas.1414261112.
68. Sasse, J., Martinoia, E., and Northen, T. 2018. Feed Your Friends: Do Plant Exudates Shape the Root Microbiome? Trends in Plant Science **23**(1): 25–41. doi:10.1016/j.tplants.2017.09.003.
69. Baudoin, E., Benizri, E., and Guckert, A. 2002. Impact of growth stage on the bacterial community structure along maize roots, as determined by metabolic and genetic

fingerprinting. Applied Soil Ecology **19**(2): 135–145. doi:10.1016/S0929-1393(01)00185-8.

70. Chaparro, J.M., Badri, D.V., Bakker, M.G., Sugiyama, A., Manter, D.K., and Vivanco, J.M. 2013. Root Exudation of Phytochemicals in Arabidopsis Follows Specific Patterns That Are Developmentally Programmed and Correlate with Soil Microbial Functions. PLoS ONE **8**(2): e55731. doi:10.1371/journal.pone.0055731.
71. Chaparro, J.M., Badri, D.V., and Vivanco, J.M. 2014. Rhizosphere microbiome assemblage is affected by plant development. The ISME Journal **8**(4): 790–803. doi:10.1038/ismej.2013.196.
72. Houlden, A., Timms-Wilson, T.M., Day, M.J., and Bailey, M.J. 2008b. Influence of plant developmental stage on microbial community structure and activity in the rhizosphere of three field crops: Plant and growth stage effects on microbial populations. FEMS Microbiology Ecology **65**(2): 193–201. doi:10.1111/j.1574-6941.2008.00535.x.
73. Micallef, S.A., Channer, S., Shiaris, M.P., and Colón-Carmona, A. 2009. Plant age and genotype impact the progression of bacterial community succession in the Arabidopsis rhizosphere. Plant Signaling & Behavior **4**(8): 777–780. doi:10.4161/psb.4.8.9229.
74. Mougel, C., Offre, P., Ranjard, L., Corberand, T., Gamalero, E., Robin, C., and Lemanceau, P. 2006. Dynamic of the genetic structure of bacterial and fungal communities at different developmental stages of *Medicago truncatula* Gaertn. cv. Jemalong line J5. New Phytologist **170**(1): 165–175. doi:10.1111/j.1469-8137.2006.01650.x.
75. Song, M., Zhang, X., Yang, J., Gao, C., Wei, Y., Chen, S., and Liesche, J. 2022. *Arabidopsis* plants engineered for high root sugar secretion enhance the diversity of soil microorganisms. Biotechnology Journal **17**(11): 2100638. doi:10.1002/biot.202100638.
76. Badri, D.V., Chaparro, J.M., Zhang, R., Shen, Q., and Vivanco, J.M. 2013. Application of Natural Blends of Phytochemicals Derived from the Root Exudates of Arabidopsis to the Soil Reveal That Phenolic-related Compounds Predominantly Modulate the Soil Microbiome. Journal of Biological Chemistry **288**(7): 4502–4512. doi:10.1074/jbc.M112.433300.
77. Lundberg, D.S., Lebeis, S.L., Paredes, S.H., Yourstone, S., Gehring, J., Malfatti, S., Tremblay, J., Engelbrektson, A., Kunin, V., Rio, T.G.D., Edgar, R.C., Eickhorst, T., Ley, R.E., Hugenholtz, P., Tringe, S.G., and Dangl, J.L. 2012. Defining the core Arabidopsis thaliana root microbiome. Nature **488**(7409): 86–90. doi:10.1038/nature11237.
78. Bulgarelli, D., Rott, M., Schlaeppi, K., Ver Loren Van Themaat, E., Ahmadinejad, N., Assenza, F., Rauf, P., Huettel, B., Reinhardt, R., Schmelzer, E., Peplies, J., Gloeckner,

F.O., Amann, R., Eickhorst, T., and Schulze-Lefert, P. 2012. Revealing structure and assembly cues for Arabidopsis root-inhabiting bacterial microbiota. Nature **488**(7409): 91–95. doi:10.1038/nature11336.

79. Santoyo, G. 2022. How plants recruit their microbiome? New insights into beneficial interactions. Journal of Advanced Research **40**: 45–58. doi:10.1016/j.jare.2021.11.020.
80. Miranda, P.S., Lima, Z.C.M., Pérez-Maluf, R., and Moreira, A.A. 2024. Pollination of flowers of the San Andreas strawberry cultivar. Pesq. agropec. bras. **59**: e03434. doi:10.1590/s1678-3921.pab2024.v59.03434.
81. Sun, Y., Niu, G., Wallace, R., Masabni, J., and Gu, M. 2015. Relative Salt Tolerance of Seven Strawberry Cultivars. Horticulturae **1**(1): 27–43. doi:10.3390/horticulturae1010027.
82. Fruit and Vegetable Dispute Resolution Corporation (FVDRC). 2026. Fresh Fruit and Vegetable Grade Requirements. Compendium, FVDRC, Canada. Available from https://fvdrc.com/wp-content/uploads/2026/02/FFVGR_2026Feb6_ENGLISH.pdf.
83. Galindo-Castañeda, T., Hartmann, M., and Lynch, J.P. 2024. Location: root architecture structures rhizosphere microbial associations. Journal of Experimental Botany **75**(2): 594–604. doi:10.1093/jxb/erad421.
84. Hubbard, C.J., Brock, M.T., Van Diepen, L.T.A., Maignien, L., Ewers, B.E., and Weinig, C. 2018. The plant circadian clock influences rhizosphere community structure and function. The ISME Journal **12**(2): 400–410. doi:10.1038/ismej.2017.172.
85. Zhang, B., Jiao, S., Zhu, G., Chen, H., Cai, Y., and Chang, S.X. 2023a. Neighboring plant community attributes drive rhizobiome assemblages of a focal plant in a Kobresia meadow. Geoderma **432**: 116409. doi:10.1016/j.geoderma.2023.116409.
86. Simmons, T., Caddell, D.F., Deng, S., and Coleman-Derr, D. 2018. Exploring the Root Microbiome: Extracting Bacterial Community Data from the Soil, Rhizosphere, and Root Endosphere. JoVE (135): 57561. doi:10.3791/57561.
87. ONT. 2025. Ligation sequencing amplicons - Native Barcoding Kit 96 V14 (SQK-NBD114.96). Protocol. Available from https://nanoporetech.com/document/ligation-sequencing-amplicons-native-barcoding-v14-sqk-nbd114-96.
88. ONT. 2026. Dorado. Oxford Nanopore Technologies. Available from https://github.com/nanoporetech/dorado.
89. De Coster, W., D'Hert, S., Schultz, D.T., Cruts, M., and Van Broeckhoven, C. 2018. NanoPack: visualizing and processing long-read sequencing data. Bioinformatics **34**(15): 2666–2669. doi:10.1093/bioinformatics/bty149.

90. Abarenkov, K., Nilsson, R.H., Larsson, K.-H., Taylor, A.F.S., May, T.W., Frøslev, T.G., Pawlowska, J., Lindahl, B., Põldmaa, K., Truong, C., Vu, D., Hosoya, T., Niskanen, T., Piirmann, T., Ivanov, F., Zirk, A., Peterson, M., Cheeke, T.E., Ishigami, Y., Jansson, A.T., Jeppesen, T.S., Kristiansson, E., Mikryukov, V., Miller, J.T., Oono, R., Ossandon, F.J., Paupério, J., Saar, I., Schigel, D., Suija, A., Tedersoo, L., and Kõljalg, U. 2024. The UNITE database for molecular identification and taxonomic communication of fungi and other eukaryotes: sequences, taxa and classifications reconsidered. Nucleic Acids Research **52**(D1): D791–D797. doi:10.1093/nar/gkad1039.
91. Quast, C., Pruesse, E., Yilmaz, P., Gerken, J., Schweer, T., Yarza, P., Peplies, J., and Glöckner, F.O. 2012. The SILVA ribosomal RNA gene database project: improved data processing and web-based tools. Nucleic Acids Research **41**(D1): D590–D596. doi:10.1093/nar/gks1219.
92. Wood, D.E., Lu, J., and Langmead, B. 2019. Improved metagenomic analysis with Kraken 2. Genome Biol **20**(1): 257. doi:10.1186/s13059-019-1891-0.
93. Fernandes, A.D., Reid, J.N., Macklaim, J.M., McMurrough, T.A., Edgell, D.R., and Gloor, G.B. 2014. Unifying the analysis of high-throughput sequencing datasets: characterizing RNA-seq, 16S rRNA gene sequencing and selective growth experiments by compositional data analysis. Microbiome **2**(1): 15. doi:10.1186/2049-2618-2-15.
94. Zhou, R., Ng, S.K., Sung, J.J.Y., Goh, W.W.B., and Wong, S.H. 2023. Data pre-processing for analyzing microbiome data – A mini review. Comput Struct Biotechnol J **21**: 4804–4815. doi:10.1016/j.csbj.2023.10.001.
95. PacBio. 2024. Full-length HiFi sequencing of eukaryotic ITS and rRNA amplicons. Application note, PacBio. Available from https://www.pacb.com/wp-content/uploads/Application-note-Full-length-HiFi-sequencing-of-eukaryotic-ITS-and-rRNA-amplicons.pdf.
96. Aleklett, K., Rosa, D., Pickles, B.J., and Hart, M.M. 2022. Community Assembly and Stability in the Root Microbiota During Early Plant Development. Front. Microbiol. **13**: 826521. doi:10.3389/fmicb.2022.826521.
97. Barajas, H.R., Martínez-Sánchez, S., Romero, M.F., Álvarez, C.H., Servín-González, L., Peimbert, M., Cruz-Ortega, R., García-Oliva, F., and Alcaraz, L.D. 2020. Testing the Two-Step Model of Plant Root Microbiome Acquisition Under Multiple Plant Species and Soil Sources. Front. Microbiol. **11**: 542742. doi:10.3389/fmicb.2020.542742.
98. Huang, Y., Xiao, X., Huang, H., Jing, J., Zhao, H., Wang, L., and Long, X.-E. 2018. Contrasting beneficial and pathogenic microbial communities across consecutive

cropping fields of greenhouse strawberry. Appl Microbiol Biotechnol **102**(13): 5717–5729. doi:10.1007/s00253-018-9013-6.

99. Lobanov, V., Keesman, K.J., and Joyce, A. 2022. Plants Dictate Root Microbial Composition in Hydroponics and Aquaponics. Front. Microbiol. **13**: 848057. doi:10.3389/fmicb.2022.848057.

100. Rosberg, A. 2014. Dynamics of Root Microorganisms in Closed Hydroponic Cropping Systems. Doctoral Thesis, Swedish University of Agricultural Sciences, Alnarp. Available from https://pub.epsilon.slu.se/11393/1/rosberg_ak_140804.pdf.

101. Zhang, Y., Gao, X., Shen, Z., Zhu, C., Jiao, Z., Li, R., and Shen, Q. 2019. Pre-colonization of PGPR triggers rhizosphere microbiota succession associated with crop yield enhancement. Plant Soil **439**(1–2): 553–567. doi:10.1007/s11104-019-04055-4.

102. Helbig, J. 2001. Biological Control of *Botrytis cinerea* Pers. ex Fr. in Strawberry by *Paenibacillus polymyxa*. Journal of Phytopathology **149**(6): 371–371. doi:10.1046/j.1439-0434.2001.00371.x.

103. Nam, J.H., Thibodeau, A., Qian, Y.L., Qian, M.C., and Park, S.H. 2023. Multidisciplinary evaluation of plant growth promoting rhizobacteria on soil microbiome and strawberry quality. AMB Expr **13**(1): 18. doi:10.1186/s13568-023-01524-z.

104. Li, W., Liu, Q., and Chen, P. 2018. Effect of long-term continuous cropping of strawberry on soil bacterial community structure and diversity. Journal of Integrative Agriculture **17**(11): 2570–2582. doi:10.1016/S2095-3119(18)61944-6.

105. Feng, L., Yu, S., Jin, W., Xiao, C., Qiao, Y., and Yang, G. 2024. The role of hydroponic solution of *Ulva fasciata* in modulating the antibiotic resistance of *Vibrio alginolyticus*. Journal of Applied Microbiology **135**(12): lxae281. doi:10.1093/jambio/lxae281.

106. Zhang, X., Ling, C., Wu, X., Fan, S., Liang, Q., and Zhou, F. 2023b. Bacterial diversity and function shift of strawberry root in different cultivation substrates. Rhizosphere **26**: 100696. doi:10.1016/j.rhisph.2023.100696.

107. Canassa, F., D'Alessandro, C.P., Sousa, S.B., Demétrio, C.G., Meyling, N.V., Klingen, I., and Delalibera, I. 2020. Fungal isolate and crop cultivar influence the beneficial effects of root inoculation with entomopathogenic fungi in strawberry. Pest Management Science **76**(4): 1472–1482. doi:10.1002/ps.5662.

108. Yang, J., Wei, S., Su, D., Zhang, Z., Chen, S., Luo, Z., Shen, X., Lai, Y., Jamil, A., Tong, J., and Cui, X. 2020. Comparison of the Rhizosphere Soil Microbial Community Structure and Diversity Between Powdery Mildew-Infected and Noninfected Strawberry

Plants in a Greenhouse by High-Throughput Sequencing Technology. Curr Microbiol **77**(8): 1724–1736. doi:10.1007/s00284-020-01948-x.

109. Xie, Z., Ourry, M., and Meyling, N.V. 2025. Above- and below-ground applications of fungal biocontrol agents have variable effects on two-spotted spider mites in three strawberry cultivars. Biocontrol Science and Technology **35**(12): 1409–1428. doi:10.1080/09583157.2025.2567984.

110. Shrestha, U., Dee, M.E., Ownley, B.H., and Butler, D.M. 2023. First Report of Strawberry Black Root Rot Caused by *Globisporangium sylvaticum* in Tennessee, U.S.A. Plant Disease **107**(9): 2890. doi:10.1094/PDIS-01-23-0007-PDN.

111. Olimi, E., Kusstatscher, P., Wicaksono, W.A., Abdelfattah, A., Cernava, T., and Berg, G. 2022. Insights into the microbiome assembly during different growth stages and storage of strawberry plants. Environmental Microbiome **17**(1): 21. doi:10.1186/s40793-022-00415-3.

112. Eberly, J.O., Hurd, A., Oli, D., Dyer, A.T., Seipel, T.F., and Carr, P.M. 2024. Compositional profiling of the rhizosphere microbiome of Canada thistle reveals consistent patterns across the United States northern Great Plains. Sci Rep **14**(1): 18016. doi:10.1038/s41598-024-69082-3.

113. Tkacz, A., Cheema, J., Chandra, G., Grant, A., and Poole, P.S. 2015. Stability and succession of the rhizosphere microbiota depends upon plant type and soil composition. The ISME Journal **9**(11): 2349–2359. doi:10.1038/ismej.2015.41.

114. Plant Products. 2026. Rootshield WP (1.36 kg). Available from https://plantproducts.com/ca-en/products/rootshield-wp-136-kg.

115. Plant Products. 2026. Rhapsody ASO (9.46 L). Available from https://plantproducts.com/ca-en/products/rhapsody-aso-946-l-1.

116. Fierer, N., and Jackson, R.B. 2006. The diversity and biogeography of soil bacterial communities. Proc. Natl. Acad. Sci. U.S.A. **103**(3): 626–631. doi:10.1073/pnas.0507535103.

117. Vilonen, L., Thompson, A., Adams, B., Ayres, E., Franco, A.L.C., and Wall, D.H. 2026. Characterising Soil Eukaryotic Diversity From NEON Metagenomics Datasets. Molecular Ecology Resources **26**(1): e70062. doi:10.1111/1755-0998.70062.

118. Thomas, P., Knox, O.G.G., Powell, J.R., Sindel, B., and Winter, G. 2023. The Hydroponic Rockwool Root Microbiome: Under Control or Underutilised? Microorganisms **11**(4): 835. doi:10.3390/microorganisms11040835.

119. Kong, Z., Li, T., Glick, B.R., and Liu, H. 2025. Priority effects of inoculation timing of plant growth-promoting microbial inoculants: role, mechanisms and perspectives. Plant Soil **513**(2): 1675–1687. doi:10.1007/s11104-025-07291-z.

120. Fukami, T. 2015. Historical Contingency in Community Assembly: Integrating Niches, Species Pools, and Priority Effects. Annu. Rev. Ecol. Evol. Syst. **46**(1): 1–23. doi:10.1146/annurev-ecolsys-110411-160340.

121. Azarbad, H., and Junker, R.R. 2024. Biological and experimental factors that define the effectiveness of microbial inoculation on plant traits: a meta-analysis. ISME Communications **4**(1): ycae122. doi:10.1093/ismeco/ycae122.

122. Nearing, J.T., Douglas, G.M., Hayes, M.G., MacDonald, J., Desai, D.K., Allward, N., Jones, C.M.A., Wright, R.J., Dhanani, A.S., Comeau, A.M., and Langille, M.G.I. 2022. Microbiome differential abundance methods produce different results across 38 datasets. Nat Commun **13**(1): 342. doi:10.1038/s41467-022-28034-z.

123. Farkas, C., Guerra, M., Heredia, A.A., and Castro, J.F. 2025. Comparative metagenomics of wild and cultivated Fragaria chiloensis reveals major rhizosphere microbiome shifts linked to stress adaptation. Current Research in Microbial Sciences **9**: 100460. doi:10.1016/j.crmicr.2025.100460.

124. Boyle, J.A., Simonsen, A.K., Frederickson, M.E., and Stinchcombe, J.R. 2021. Priority effects alter interaction outcomes in a legume–rhizobium mutualism. Proc. R. Soc. B. **288**(1946): 20202753. doi:10.1098/rspb.2020.2753.

125. De Oliveira, A.J.M., Cavalcanti, V.P., Rodrigues, F.A., Dos Santos, V.L., Julio, A.D.L., Molina, Y.C., Pasqual, M., Martins, A.D., Fufato, L., and Dória, J. 2024. Application Frequency and Colonization of the Rhizosphere of Strawberry (Fragaria x ananassa Duchesne) Plants by Azospirillum Brasilense. J Plant Growth Regul **43**(4): 986–997. doi:10.1007/s00344-023-11154-1.

126. Barajas, H.R., Martínez-Sánchez, S., Romero, M.F., Álvarez, C.H., Servín-González, L., Peimbert, M., Cruz-Ortega, R., García-Oliva, F., and Alcaraz, L.D. 2020. Testing the Two-Step Model of Plant Root Microbiome Acquisition Under Multiple Plant Species and Soil Sources. Front. Microbiol. **11**: 542742. doi:10.3389/fmicb.2020.542742.

127. Mailloux, B.J., and Fuller, M.E. 2003. Determination of In Situ Bacterial Growth Rates in Aquifers and Aquifer Sediments. Appl Environ Microbiol **69**(7): 3798–3808. doi:10.1128/AEM.69.7.3798-3808.2003.

128. Ueta, M., Wada, A., and Wada, C. 2024. The hibernation promoting factor of Betaproteobacteria *Comamonas testosteroni* cannot induce 100S ribosome formation but stabilizes 70S ribosomal particles. Genes to Cells **29**(8): 613–634. doi:10.1111/gtc.13137.

129. Afonso, A.C., Gomes, I.B., Saavedra, M.J., C. Simões, L., and Simões, M. 2023. Drinking-water isolated Delftia acidovorans selectively coaggregates with partner bacteria and facilitates multispecies biofilm development. Science of The Total Environment **875**: 162646. doi:10.1016/j.scitotenv.2023.162646.

130. Hendrickson, E.L., Beck, D.A.C., Wang, T., Lidstrom, M.E., Hackett, M., and Chistoserdova, L. 2010. Expressed Genome of *Methylobacillus flagellatus* as Defined through Comprehensive Proteomics and New Insights into Methylotrophy. J Bacteriol **192**(19): 4859–4867. doi:10.1128/JB.00512-10.

131. Liu, T., Li, P., Ou, Z., Feng, Y., Wang, B., Yu, T., Zhu, Y., and Yu, L. 2025. Insights into the special physiology of Mortierella alpina cultured by agar supported solid state fermentation in enhancing arachidonic acid enriched lipid production. Sci Rep **15**(1): 15967. doi:10.1038/s41598-025-00965-9.

132. Mahata, P.K., Dass, R.S., Pan, A., and Muthusamy, B. 2022. Substantive Morphological Descriptions, Phylogenetic Analysis and Single Nucleotide Polymorphisms of Aspergillus Species From Foeniculum vulgare. Front. Microbiol. **13**: 832320. doi:10.3389/fmicb.2022.832320.

133. Gao, J., Dong, A., Li, J., Xu, J., Liang, Z., and Logrieco, A.F. 2025. Exploring Fungal Communication Mechanisms in the Rhizosphere Microbiome for a Sustainable Green Agriculture. JoF **11**(10): 726. doi:10.3390/jof11100726.

134. Lin, Y.-C., Huang, Y.-M., Huang, Y.-L., Liu, S.-L., He, S.-H., Zhou, L.-W., and Chen, C.-C. 2025. New species and new records of Trechispora (Trechisporales, Basidiomycota) from Taiwan. Bot Stud **66**(1): 21. doi:10.1186/s40529-025-00469-9.

135. Yamaoka, Y. 2017. Taxonomy and pathogenicity of ophiostomatoid fungi associated with bark beetles infesting conifers in Japan, with special reference to those related to subalpine conifers. Mycoscience **58**(4): 221–235. doi:10.1016/j.myc.2017.03.001.

136. Ozimek, E., and Hanaka, A. 2020. Mortierella Species as the Plant Growth-Promoting Fungi Present in the Agricultural Soils. Agriculture **11**(1): 7. doi:10.3390/agriculture11010007.

137. Martens-Uzunova, E.S., and Schaap, P.J. 2009. Assessment of the pectin degrading enzyme network of Aspergillus niger by functional genomics. Fungal Genetics and Biology **46**(1): S170–S179. doi:10.1016/j.fgb.2008.07.021.

138. Waller, P.L., Thornton, C.R., Farley, D., and Groenhof, A. 2008. PATHOGENS AND OTHER FUNGI IN GROWING MEDIA CONSTITUENTS. Acta Hortic. (779): 361–366. doi:10.17660/ActaHortic.2008.779.45.

139. Lebreton, A., Zeng, Q., Miyauchi, S., Kohler, A., Dai, Y.-C., and Martin, F.M. 2021. Evolution of the Mode of Nutrition in Symbiotic and Saprotrophic Fungi in Forest Ecosystems. Annu. Rev. Ecol. Evol. Syst. **52**(1): 385–404. doi:10.1146/annurev-ecolsys-012021-114902.

140. Dunne, W.M. 2002. Bacterial Adhesion: Seen Any Good Biofilms Lately? Clin Microbiol Rev **15**(2): 155–166. doi:10.1128/CMR.15.2.155-166.2002.

141. Nakayasu, M., Takamatsu, K., Yazaki, K., and Sugiyama, A. 2022. Plant specialized metabolites in the rhizosphere of tomatoes: secretion and effects on microorganisms. Bioscience, Biotechnology, and Biochemistry **87**(1): 13–20. doi:10.1093/bbb/zbac181.

142. Schober, I., Koblitz, J., Sardà Carbasse, J., Ebeling, C., Schmidt, M.L., Podstawka, A., Gupta, R., Ilangovan, V., Chamanara, J., Overmann, J., and Reimer, L.C. 2025a. Bac *Dive* in 2025: the core database for prokaryotic strain data. Nucleic Acids Research **53**(D1): D748–D756. doi:https://doi.org/10.13145/bacdive11945.20251217.10.

143. Wiegand, S., Jogler, M., Boedeker, C., Heuer, A., Rast, P., Peeters, S.H., Jetten, M.S.M., Kaster, A.-K., Rohde, M., Kallscheuer, N., and Jogler, C. 2020. Additions to the genus Gimesia: description of Gimesia alba sp. nov., Gimesia algae sp. nov., Gimesia aquarii sp. nov., Gimesia aquatilis sp. nov., Gimesia fumaroli sp. nov. and Gimesia panareensis sp. nov., isolated from aquatic habitats of the Northern Hemisphere. Antonie van Leeuwenhoek **113**(12): 1999–2018. doi:10.1007/s10482-020-01489-0.

144. Schober, I., Koblitz, J., Sardà Carbasse, J., Ebeling, C., Schmidt, M.L., Podstawka, A., Gupta, R., Ilangovan, V., Chamanara, J., Overmann, J., and Reimer, L.C. 2025b. Bac *Dive* in 2025: the core database for prokaryotic strain data. Nucleic Acids Research **53**(D1): D748–D756. doi:https://doi.org/10.13145/bacdive13923.20251217.10.

145. Reichenbach, H. 2015a. *Chondromyces*. *In* Bergey's Manual of Systematics of Archaea and Bacteria, 1st edition. *Edited by* M.E. Trujillo, S. Dedysh, P. DeVos, B. Hedlund, P. Kämpfer, F.A. Rainey, and W.B. Whitman. Wiley. pp. 1–11. doi:10.1002/9781118960608.gbm01051.

146. Reichenbach, H. 2015b. *Polyangium*. *In* Bergey's Manual of Systematics of Archaea and Bacteria, 1st edition. *Edited by* M.E. Trujillo, S. Dedysh, P. DeVos, B. Hedlund, P. Kämpfer, F.A. Rainey, and W.B. Whitman. Wiley. pp. 1–11. doi:10.1002/9781118960608.gbm01059.

147. Schober, I., Koblitz, J., Sardà Carbasse, J., Ebeling, C., Schmidt, M.L., Podstawka, A., Gupta, R., Ilangovan, V., Chamanara, J., Overmann, J., and Reimer, L.C. 2025c. Bac *Dive* in 2025: the core database for prokaryotic strain data. Nucleic Acids Research **53**(D1): D748–D756. doi:https://doi.org/10.13145/bacdive11877.20251217.10.

148. Weon, H.-Y., Kim, B.-Y., Hong, S.-B., Joa, J.-H., Nam, S.-S., Lee, K.H., and Kwon, S.-W. 2007. Skermanella aerolata sp. nov., isolated from air, and emended description of the genus Skermanella. International Journal of Systematic and Evolutionary Microbiology **57**(7): 1539–1542. doi:10.1099/ijs.0.64676-0.

149. Kulichevskaya, I.S., Ivanova, A.O., Belova, S.E., Baulina, O.I., Bodelier, P.L.E., Rijpstra, W.I.C., Sinninghe Damsté, J.S., Zavarzin, G.A., and Dedysh, S.N. 2007. Schlesneria paludicola gen. nov., sp. nov., the first acidophilic member of the order Planctomycetales, from Sphagnum-dominated boreal wetlands. International Journal of Systematic and Evolutionary Microbiology **57**(11): 2680–2687. doi:10.1099/ijs.0.65157-0.

150. Chan, S.H., Ismail, M.H., Tan, C.H., Rice, S.A., and McDougald, D. 2021. Microbial predation accelerates granulation and modulates microbial community composition. BMC Microbiol **21**(1): 91. doi:10.1186/s12866-021-02156-8.

151. MacLean, J., Mayanna, S., Benning, L.G., Horn, F., Bartholomäus, A., Wiesner, Y., Wagner, D., and Liebner, S. 2021. The Terrestrial Plastisphere: Diversity and Polymer-Colonizing Potential of Plastic-Associated Microbial Communities in Soil. Microorganisms **9**(9): 1876. doi:10.3390/microorganisms9091876.

152. Barron, G.L., and Dierkes, Y. 1977. Nematophagous fungi: *Hohenbuehelia* , the perfect state of *Nematoctonus*. Can. J. Bot. **55**(24): 3054–3062. doi:10.1139/b77-345.

153. Rodríguez, C.L., Strub, C., Fontana, A., Verheecke-Vaessen, C., Durand, N., Beugré, C., Guehi, T., Medina, A., and Schorr-Galindo, S. 2024. Biocontrol activities of yeasts or lactic acid bacteria isolated from Robusta coffee against Aspergillus carbonarius growth and ochratoxin A production in vitro. International Journal of Food Microbiology **415**: 110638. doi:10.1016/j.ijfoodmicro.2024.110638.

154. Falvo, A., Levantesi, C., Rossetti, S., Seviour, R.J., and Tandoi, V. 2001. Synthesis of intracellular storage polymers by Amaricoccus kaplicensis, a tetrad forming bacterium present in activated sludge. J Appl Microbiol **91**(2): 299–305. doi:10.1046/j.1365-2672.2001.01384.x.

155. Hamilton, E.F.I. 1982. IGU commission on industrial systems: Reports and announcements. GeoJournal **6**(6): 577–580. doi:10.1007/BF00425331.

156. Parker, E.J. 1975. Some investigations with Beech bark disease Nectria in southern England. Forest Pathol **5**(2): 118–124. doi:10.1111/j.1439-0329.1975.tb00453.x.

157. Seki, T., Matsumoto, A., Ōmura, S., and Takahashi, Y. 2015. Distribution and isolation of strains belonging to the order Solirubrobacterales. J Antibiot **68**(12): 763–766. doi:10.1038/ja.2015.67.

158. Lubian, C., Martinha, D.D., Portz, R.L., Silva Filho, A.G.D.S.E., Cortez, V.G., and Missio, V.C. 2018. Daily Indexes for Predation and Growth of Nematophagous Mushrooms Species of Hohenbuehelia (Pleurotaceae) on Panagrellus redividus. JAS **10**(3): 276. doi:10.5539/jas.v10n3p276.

159. Reichenbach, H. 1999. The ecology of the myxobacteria. Environmental Microbiology **1**(1): 15–21. doi:10.1046/j.1462-2920.1999.00016.x.

160. Hoffmann, T., Krug, D., Bozkurt, N., Duddela, S., Jansen, R., Garcia, R., Gerth, K., Steinmetz, H., and Müller, R. 2018. Correlating chemical diversity with taxonomic distance for discovery of natural products in myxobacteria. Nat Commun **9**(1): 803. doi:10.1038/s41467-018-03184-1.

161. Kündgen, M., Haufschild, T., Kallscheuer, N., Mutter, M., Hammer, J., Jogler, M., Wang, H., Lehmann, R., Lehmann, K., Totsche, K.U., Küsel, K., and Jogler, C. 2026. A novel planctomycetotal isolate from subsurface percolates belongs to the novel species Anatilimnocola aquadivae sp. nov. in the family Pirellulaceae. Sci Rep **16**(1): 9078. doi:10.1038/s41598-026-44018-1.

162. Jung, H.S., Yoon, J.-H., Joh, K., Seong, C.-N., Kim, W.-Y., Im, W.-T., Kim, M.-K., Cha, C.-J., Kim, S.-B., and Jeon, C.-O. 2021. Pseudaminobacter arsenicus. Zenodo. doi:10.5281/ZENODO.8140675.

163. Sun, N., Wang, Y., Chen, J., Wang, P., Song, W., Ma, P., Duan, Y., Jiao, Z., and Li, Y. 2022. Colonization and Interaction of Bacteria Associated With Chinese Chives Affected by Ecological Compartments and Growth Conditions. Front. Microbiol. **13**: 775002. doi:10.3389/fmicb.2022.775002.

164. Lopes, L.D., Futrell, S.L., Bergmeyer, E., Hao, J., and Schachtman, D.P. 2023. Root exudate concentrations of indole-3-acetic acid (IAA) and abscisic acid (ABA) affect maize rhizobacterial communities at specific developmental stages. FEMS Microbiology Ecology **99**(3): fiad019. doi:10.1093/femsec/fiad019.

165. Dove, N.C., Veach, A.M., Muchero, W., Wahl, T., Stegen, J.C., Schadt, C.W., and Cregger, M.A. 2021. Assembly of the *Populus* Microbiome Is Temporally Dynamic and Determined by Selective and Stochastic Factors. mSphere **6**(3): e01316-20. doi:10.1128/mSphere.01316-20.

166. Demirsoy, H., Demirsoy, L., and Öztürk, A. 2005. Improved model for the non-destructive estimation of strawberry leaf area. Fruits **60**(1): 69–73. doi:10.1051/fruits:2005014.

167. Sprangers, K., Avramova, V., and Beemster, G.T.S. 2016. Kinematic Analysis of Cell Division and Expansion: Quantifying the Cellular Basis of Growth and Sampling Developmental Zones in Zea mays Leaves. JoVE (118): 54887. doi:10.3791/54887.

168. Kupe, M., Hacimuftuoglu, F., and Dadasoglu, F. 2026. Effect of some PGPR (Plant Growth Promoting Bacteria) combinations on some soil properties and horticultural characteristics in Albion and Monterey strawberry cultivars. BMC Plant Biol **26**(1): 689. doi:10.1186/s12870-026-08503-z.

169. De Andrade, F.M., De Assis Pereira, T., Souza, T.P., Guimarães, P.H.S., Martins, A.D., Schwan, R.F., Pasqual, M., and Dória, J. 2019. Beneficial effects of inoculation of growth-promoting bacteria in strawberry. Microbiological Research **223–225**: 120–128. doi:10.1016/j.micres.2019.04.005.

170. Rahman, M., Sabir, A.A., Mukta, J.A., Khan, Md.M.A., Mohi-Ud-Din, M., Miah, Md.G., Rahman, M., and Islam, M.T. 2018. Plant probiotic bacteria Bacillus and Paraburkholderia improve growth, yield and content of antioxidants in strawberry fruit. Sci Rep **8**(1): 2504. doi:10.1038/s41598-018-20235-1.

171. Esitken, A., Yildiz, H.E., Ercisli, S., Figen Donmez, M., Turan, M., and Gunes, A. 2010. Effects of plant growth promoting bacteria (PGPB) on yield, growth and nutrient contents of organically grown strawberry. Scientia Horticulturae **124**(1): 62–66. doi:10.1016/j.scienta.2009.12.012.

172. Pırlak, L., and Köse, M. 2009. Effects of Plant Growth Promoting Rhizobacteria on Yield and Some Fruit Properties of Strawberry. Journal of Plant Nutrition **32**(7): 1173–1184. doi:10.1080/01904160902943197.

173. Sangiorgio, D., Cellini, A., Spinelli, F., and Donati, I. 2023. Promoting Strawberry (Fragaria × ananassa) Stress Resistance, Growth, and Yield Using Native Bacterial Biostimulants. Agronomy **13**(2): 529. doi:10.3390/agronomy13020529.

174. Todeschini, V., AitLahmidi, N., Mazzucco, E., Marsano, F., Gosetti, F., Robotti, E., Bona, E., Massa, N., Bonneau, L., Marengo, E., Wipf, D., Berta, G., and Lingua, G. 2018. Impact of Beneficial Microorganisms on Strawberry Growth, Fruit Production, Nutritional Quality, and Volatilome. Front. Plant Sci. **9**: 1611. doi:10.3389/fpls.2018.01611.

175. De Souza Ribeiro, M., Rodrigues, F.A., De Araujo, R.C., Nadal, M.C., Andrade, G.V.S., Pasqual, M., and Rodrigues, J.D. 2023. Growth-Promoting Bacteria Induce Salt Stress Tolerance in Strawberry Plants. J Plant Growth Regul **42**(12): 7606–7613. doi:10.1007/s00344-023-11036-6.

176. Yang, H., Zhang, X., Qiu, X., Chen, J., Wang, Y., Zhang, G., Jia, S., Shen, X., Ye, W., and Yan, Z. 2023. Fusarium Wilt Invasion Results in a Strong Impact on Strawberry Microbiomes. Plants **12**(24): 4153. doi:10.3390/plants12244153.

177. Eccleston, K.L., Brooks, P.R., and Kurtböke, D.İ. 2010. Assessment of the Role of Local Strawberry Rhizosphere—Associated Streptomycetes on the Bacterially—Induced Growth and Botrytis cinerea Infection Resistance of the Fruit. Sustainability **2**(12): 3831–3845. doi:10.3390/su2123831.

178. Pupakdeepan, W., Termsung, N., Ruangwong, O.-U., and Kunasakdakul, K. 2023. Plant Growth Promoting and Colonization of Endophytic Streptomyces albus CINv1 against Strawberry Anthracnose. Horticulturae **9**(7): 766. doi:10.3390/horticulturae9070766.

179. Harsonowati, W., Marian, M., Surono, and Narisawa, K. 2020. The Effectiveness of a Dark Septate Endophytic Fungus, Cladophialophora chaetospira SK51, to Mitigate Strawberry Fusarium Wilt Disease and With Growth Promotion Activities. Front. Microbiol. **11**: 585. doi:10.3389/fmicb.2020.00585.

180. Morales-Quintana, L., Moya, M., Santelices-Moya, R., Cabrera-Ariza, A., Rabert, C., Pollmann, S., and Ramos, P. 2022. Improvement in the physiological and biochemical performance of strawberries under drought stress through symbiosis with Antarctic fungal endophytes. Front. Microbiol. **13**: 939955. doi:10.3389/fmicb.2022.939955.

181. Haggag Wafaa, M., Abd-El-Kreem, F., Singer, S.M., and DEH Aly, M. 2014. Production and Optimization of Rhodotorula glutinis for biocontrolling of Strawberry Blight. RJPBCS **5**(6). 2014/11. Available from https://www.rjpbcs.com/pdf/2014_5%286%29/%5B90%5D.pdf.

182. Ibrahim, Y.A., and Hassan, A.A. 2023. Evaluation of the Rhodotorula glutinis in Controlling the Gray Rot Disease Caused by the Pathogenic Fungus Botrytis cinerea Pre and Post Strawberry Harvesting. IOP Conf. Ser.: Earth Environ. Sci. **1214**(1): 012038. doi:10.1088/1755-1315/1214/1/012038.

183. Liu, W., Tan, M., Qu, P., Huo, C., Liang, W., Li, R., Jia, Y., Fan, X., and Cheng, C. 2022. Use of Piriformospora indica to Promote Growth of Strawberry Daughter Plants. Horticulturae **8**(5): 370. doi:10.3390/horticulturae8050370.

184. Lay, C.-Y., Hamel, C., and St-Arnaud, M. 2018. Taxonomy and pathogenicity of Olpidium brassicae and its allied species. Fungal Biology **122**(9): 837–846. doi:10.1016/j.funbio.2018.04.012.

185. Martin, F.N. 1999. Strawberry root rot and the recovery of Pythium and Rhizoctonia spp. Alternatives and Emissions Reduction **6**. Available from

https://mbao.org/static/docs/confs/1999-sandiego/papers/6martin.pdf#:~:text=One%20root%20disease%20complex%20often,to%20as%20black%20root%20rot.

186. Xu, X., Deakin, G., Zhao, J., Passey, T., and Papp-Rupar, M. 2024. Amplicon-based metagenomics to study the effect of coir age and wood biochar on microbiome in relation to strawberry yield. Front. Agron. **6**: 1397974. doi:10.3389/fagro.2024.1397974.

187. De Cal, A., Martinez-Treceño, A., Salto, T., López-Aranda, J.M., and Melgarejo, P. 2005. Effect of chemical fumigation on soil fungal communities in Spanish strawberry nurseries. Applied Soil Ecology **28**(1): 47–56. doi:10.1016/j.apsoil.2004.06.005.

188. Ataeisalami, T., Shahidibonjar, G., Hosseinipour, A., Abdolshahi, R., Dorrani-Nejad, M., Saadoun, I., and Barka, E.A. 2025. Performance of four Streptomyces root symbionts in the biocontrol of Pythium aphanidermatum in mung bean. Eur J Plant Pathol **173**(3): 731–748. doi:10.1007/s10658-025-03091-4.

189. Sang, M.K., and Kim, K.D. 2012. The volatile-producing Flavobacterium johnsoniae strain GSE09 shows biocontrol activity against Phytophthora capsici in pepper: Biocontrol activity of Flavobacterium johnsoniae. J Appl Microbiol **113**(2): 383–398. doi:10.1111/j.1365-2672.2012.05330.x.

190. Kenderdine, C.M., and Raudales, R.E. 2026. Continuous recirculation of hydroponic-nutrient solutions shifts bacterial communities and induces plant-defense gene expression in lettuce. Appl Environ Microbiol **92**(4): e01647-25. doi:10.1128/aem.01647-25.

191. Abbas, S., Tanwir, K., Hussaan, M., Masood, S., Ali, Q., Raza, A., Shahid, M., Chaudhary, H.J., Mushtaq, S., and Javed, M.T. 2024. In vitro exploration of Acinetobacter strain (SG-5) for antioxidative potential and phytohormone biosynthesis in maize (Zea mays L.) cultivars differing in cadmium tolerance. Environ Sci Pollut Res **31**(33): 45465–45484. doi:10.1007/s11356-024-34181-1.

192. Qadir, M., Hussain, A., Hamayun, M., Shah, M., Iqbal, A., Irshad, M., Ahmad, A., Lodhi, M.A., and Lee, I.-J. 2021. Phytohormones Producing Acinetobacter bouvetii P1 Mitigates Chromate Stress in Sunflower by Provoking Host Antioxidant Response. Antioxidants **10**(12): 1868. doi:10.3390/antiox10121868.

193. Ali, A., Dindhoria, K., and Kumar, R. 2023. *Acinetobacter oleivorans* IRS14 alleviates cold stress in wheat by regulating physiological and biochemical factors. Journal of Applied Microbiology **134**(8): lxad176. doi:10.1093/jambio/lxad176.

194. Chretien, R.L., Burrell, E., Evans, M.R., Lowman, S., and Mei, C. 2024. ACC (1-aminocyclopropane-1-carboxylic acid) deaminase producing endophytic bacteria

improve hydroponically grown lettuce in the greenhouse during summer season. Scientia Horticulturae **327**: 112862. doi:10.1016/j.scienta.2024.112862.

195. Han, L., Zhang, H., Xu, Y., Li, Y., and Zhou, J. 2021. Biological characteristics and salt-tolerant plant growth-promoting effects of an ACC deaminase-producing Burkholderia pyrrocinia strain isolated from the tea rhizosphere. Arch Microbiol **203**(5): 2279–2290. doi:10.1007/s00203-021-02204-x.

196. Liu, W.-H., Chen, F.-F., Wang, C.-E., Fu, H.-H., Fang, X.-Q., Ye, J.-R., and Shi, J.-Y. 2019. Indole-3-Acetic Acid in Burkholderia pyrrocinia JK-SH007: Enzymatic Identification of the Indole-3-Acetamide Synthesis Pathway. Front. Microbiol. **10**: 2559. doi:10.3389/fmicb.2019.02559.

197. De Los Santos-Villalobos, S., Barrera-Galicia, G.C., Miranda-Salcedo, M.A., and Peña-Cabriales, J.J. 2012. Burkholderia cepacia XXVI siderophore with biocontrol capacity against Colletotrichum gloeosporioides. World J Microbiol Biotechnol **28**(8): 2615–2623. doi:10.1007/s11274-012-1071-9.

198. Zhao, K., Penttinen, P., Zhang, X., Ao, X., Liu, M., Yu, X., and Chen, Q. 2014. Maize rhizosphere in Sichuan, China, hosts plant growth promoting Burkholderia cepacia with phosphate solubilizing and antifungal abilities. Microbiological Research **169**(1): 76–82. doi:10.1016/j.micres.2013.07.003.

199. Onofre-Lemus, J., Hernández-Lucas, I., Girard, L., and Caballero-Mellado, J. 2009. ACC (1-Aminocyclopropane-1-Carboxylate) Deaminase Activity, a Widespread Trait in *Burkholderia* Species, and Its Growth-Promoting Effect on Tomato Plants. Appl Environ Microbiol **75**(20): 6581–6590. doi:10.1128/AEM.01240-09.

200. Sarkar, A., Pramanik, K., Mitra, S., Soren, T., and Maiti, T.K. 2018. Enhancement of growth and salt tolerance of rice seedlings by ACC deaminase-producing Burkholderia sp. MTCC 12259. Journal of Plant Physiology **231**: 434–442. doi:10.1016/j.jplph.2018.10.010.

201. Li, W., Fu, Y., Jiang, Y., Hu, J., Wei, Y., Li, H., Li, J., Yang, H., and Wu, Y. 2024b. Synergistic Biocontrol and Growth Promotion in Strawberries by Co-Cultured Trichoderma harzianum TW21990 and Burkholderia vietnamiensis B418. JoF **10**(8): 551. doi:10.3390/jof10080551.

202. Jia, X., Tian, B., Li, J., Li, S., Chen, M., Wang, S., Zhao, Y., Hao, L., and Fu, W. 2026. Paraburkholderia Mediates Salt Stress Alleviation in Cucumber Seedlings. Plants **15**(7): 1104. doi:10.3390/plants15071104.

203. Madhaiyan, M., Selvakumar, G., Alex, T.H., Cai, L., and Ji, L. 2021. Plant Growth Promoting Abilities of Novel Burkholderia-Related Genera and Their Interactions With

Some Economically Important Tree Species. Front. Sustain. Food Syst. **5**: 618305. doi:10.3389/fsufs.2021.618305.

204. Vio, S.A., García, S.S., Casajus, V., Arango, J.S., Galar, M.L., Bernabeu, P.R., and Luna, M.F. 2020. Paraburkholderia. *In* Beneficial Microbes in Agro-Ecology. Elsevier. pp. 271–311. doi:10.1016/B978-0-12-823414-3.00015-0.

205. Herpell, J.B., Alickovic, A., Diallo, B., Schindler, F., and Weckwerth, W. 2023. Phyllosphere symbiont promotes plant growth through ACC deaminase production. The ISME Journal **17**(8): 1267–1277. doi:10.1038/s41396-023-01428-7.

206. Martínez, F., Castillo, S., Borrero, C., Pérez, S., Palencia, P., and Avilés, M. 2013. Effect of different soilless growing systems on the biological properties of growth media in strawberry. Scientia Horticulturae **150**: 59–64. doi:10.1016/j.scienta.2012.10.016.

207. Putra, A.M., Anastasya, N.A., Rachmawati, S.W., Yusnawan, E., Syib`li, M.A., Trianti, I., Setiawan, A., and Aini, L.Q. 2024. Growth performance and metabolic changes in lettuce inoculated with plant growth promoting bacteria in a hydroponic system. Scientia Horticulturae **327**: 112868. doi:10.1016/j.scienta.2024.112868.

208. Dasgan, H.Y., Aldiyab, A., Elgudayem, F., Ikiz, B., and Gruda, N.S. 2022. Effect of biofertilizers on leaf yield, nitrate amount, mineral content and antioxidants of basil (Ocimum basilicum L.) in a floating culture. Sci Rep **12**(1): 20917. doi:10.1038/s41598-022-24799-x.

209. De Freitas, C.C., and Taylor, C.G. 2023. Biological control of hairy root disease using beneficial Pseudomonas strains. Biological Control **177**: 105098. doi:10.1016/j.biocontrol.2022.105098.

210. Durán, D., Bernal, P., Vazquez-Arias, D., Blanco-Romero, E., Garrido-Sanz, D., Redondo-Nieto, M., Rivilla, R., and Martín, M. 2021. Pseudomonas fluorescens F113 type VI secretion systems mediate bacterial killing and adaption to the rhizosphere microbiome. Sci Rep **11**(1): 5772. doi:10.1038/s41598-021-85218-1.

211. Gravel, V., Martinez, C., Antoun, H., and Tweddell, R.J. 2006. Control of greenhouse tomato root rot [*Pythium ultimum*] in hydroponic systems, using plant-growth-promoting microorganisms. Canadian Journal of Plant Pathology **28**(3): 475–483. doi:10.1080/07060660609507322.

212. Oni, F.E., Esmaeel, Q., Onyeka, J.T., Adeleke, R., Jacquard, C., Clement, C., Gross, H., Ait Barka, E., and Höfte, M. 2022. Pseudomonas Lipopeptide-Mediated Biocontrol: Chemotaxonomy and Biological Activity. Molecules **27**(2): 372. doi:10.3390/molecules27020372.

213. Flores-Félix, J.-D., Marcos-García, M., Silva, L.R., Menéndez, E., Martínez-Molina, E., Mateos, P.F., Velázquez, E., García-Fraile, P., Andrade, P., and Rivas, R. 2015. Rhizobium as plant probiotic for strawberry production under microcosm conditions. Symbiosis **67**(1–3): 25–32. doi:10.1007/s13199-015-0373-8.

214. Flores-Félix, J.D., Velázquez, E., García-Fraile, P., González-Andrés, F., Silva, L.R., and Rivas, R. 2018. Rhizobium and Phyllobacterium bacterial inoculants increase bioactive compounds and quality of strawberries cultivated in field conditions. Food Research International **111**: 416–422. doi:10.1016/j.foodres.2018.05.059.

215. Bano, A., Batool, R., and Dazzo, F. 2010. Adaptation of chickpea to desiccation stress is enhanced by symbiotic rhizobia. Symbiosis **50**(3): 129–133. doi:10.1007/s13199-010-0051-9.

216. Halder, A.K., and Chakrabartty, P.K. 1993. Solubilization of inorganic phosphate by Rhizobium. Folia Microbiol **38**(4): 325–330. doi:10.1007/BF02898602.

217. Omar, S.A., and Abd-Alla, M.H. 1998. Biocontrol of fungal root rot diseases of crop plants by the use of rhizobia and bradyrhizobia. Folia Microbiol **43**(4): 431–437. doi:10.1007/BF02818587.

218. Ma, W., Guinel, F.C., and Glick, B.R. 2003. *Rhizobium leguminosarum* Biovar viciae 1-Aminocyclopropane-1-Carboxylate Deaminase Promotes Nodulation of Pea Plants. Appl Environ Microbiol **69**(8): 4396–4402. doi:10.1128/AEM.69.8.4396-4402.2003.

219. Amaradasa, B.S., Chretien, R.L., Lowman, S., and Mei, C. 2026. Transcriptomic and Root Microbiome Responses of Lettuce to Beneficial Endophytic Bacteria in Hydroponic Systems. IJMS **27**(7): 3072. doi:10.3390/ijms27073072.

220. Dong, C.-J., Li, Q., Wang, L.-L., and Shang, Q.-M. 2020. Dynamic changes in bacterial communities in the recirculating nutrient solution of cucumber plug seedlings cultivated in an ebb-and-flow subirrigation system. PLoS ONE **15**(4): e0232446. doi:10.1371/journal.pone.0232446.

221. Liu, W., Zhang, Z., Zhang, B., Zhu, Y., Zhu, C., Chen, C., Zhang, F., Liu, F., Ai, J., Wang, W., Kong, W., Xiang, H., Wang, W., Gong, D., Meng, D., and Zhu, L. 2024. Role of bacterial pathogens in microbial ecological networks in hydroponic plants. Front. Plant Sci. **15**: 1403226. doi:10.3389/fpls.2024.1403226.

222. Zeng, X., Pang, L., Chen, Y., Kong, X., Chen, J., and Tian, X. 2020. Bacteria Sphingobium yanoikuyae Sy310 enhances accumulation capacity and tolerance of cadmium in Salix matsudana Koidz roots. Environ Sci Pollut Res **27**(16): 19764–19773. doi:10.1007/s11356-020-08474-0.

223. Yang, S., Zhang, X., Cao, Z., Zhao, K., Wang, S., Chen, M., and Hu, X. 2014. Growth‐promoting *S phingomonas paucimobilis* ZJSH 1 associated with *D endrobium officinale* through phytohormone production and nitrogen fixation. Microbial Biotechnology **7**(6): 611–620. doi:10.1111/1751-7915.12148.

224. Nivitha, G., Kalaiselvi, T., and Sivakumar, U. 2019. Screening of Rice Apoplast Associated Endophytic Bacterial Isolates for Moisture Stress Tolerance and Plant Growth Promoting Traits. MAJ **106**(1–3): 5–11. doi:10.29321/MAJ.2019.000214.

225. Li, L., Huang, H., Jin, Z., Jiang, K., Zeng, Y., Pathier, D., Cheng, X., and Shen, W. 2024a. Strawberry Yield Improvement by Hydrogen-Based Irrigation Is Functionally Linked to Altered Rhizosphere Microbial Communities. Plants **13**(13): 1723. doi:10.3390/plants13131723.

226. Van Bruggen, A.H.C., Francis, I.M., and Jochimsen, K.N. 2014. Non‐pathogenic rhizosphere bacteria belonging to the genera *Rhizorhapis* and *Sphingobium* provide specific control of lettuce corky root disease caused by species of the same bacterial genera. Plant Pathology **63**(6): 1384–1394. doi:10.1111/ppa.12212.

227. Stouvenakers, G., Massart, S., and Jijakli, M.H. 2023. First Study Case of Microbial Biocontrol Agents Isolated from Aquaponics Through the Mining of High-Throughput Sequencing Data to Control Pythium aphanidermatum on Lettuce. Microb Ecol **86**(2): 1107–1119. doi:10.1007/s00248-022-02126-1.

228. Hu, X., Claerbout, J., Vandecasteele, B., Craeye, S., and Geelen, D. 2025. The bacterial and fungal strawberry root-associated microbiome in reused peat-based substrate. BMC Plant Biol **25**(1): 245. doi:10.1186/s12870-025-06217-2.

229. Kitwetch, B., Rangseekaew, P., Chromkaew, Y., Pathom-Aree, W., and Srinuanpan, S. 2023. Employing a Plant Probiotic Actinomycete for Growth Promotion of Lettuce (Lactuca sativa L. var. longifolia) Cultivated in a Hydroponic System under Nutrient Limitation. Plants **12**(22): 3793. doi:10.3390/plants12223793.

230. Vargas, P., Bosmans, L., Van Calenberge, B., Van Kerckhove, S., Lievens, B., and Rediers, H. 2021. Bacterial community dynamics of tomato hydroponic greenhouses infested with hairy root disease. FEMS Microbiology Ecology **97**(12): fiab153. doi:10.1093/femsec/fiab153.

231. El-Tarabily, K.A. 2008. Promotion of tomato (Lycopersicon esculentum Mill.) plant growth by rhizosphere competent 1-aminocyclopropane-1-carboxylic acid deaminase-producing streptomycete actinomycetes. Plant Soil **308**(1–2): 161–174. doi:10.1007/s11104-008-9616-2.

232. Sadeghi, A., Karimi, E., Dahaji, P.A., Javid, M.G., Dalvand, Y., and Askari, H. 2012. Plant growth promoting activity of an auxin and siderophore producing isolate of Streptomyces under saline soil conditions. World J Microbiol Biotechnol **28**(4): 1503–1509. doi:10.1007/s11274-011-0952-7.

233. Vurukonda, S.S.K.P., Giovanardi, D., and Stefani, E. 2018. Plant Growth Promoting and Biocontrol Activity of Streptomyces spp. as Endophytes. IJMS **19**(4): 952. doi:10.3390/ijms19040952.

234. De Tender, C., Haegeman, A., Vandecasteele, B., Clement, L., Cremelie, P., Dawyndt, P., Maes, M., and Debode, J. 2016. Dynamics in the Strawberry Rhizosphere Microbiome in Response to Biochar and Botrytis cinerea Leaf Infection. Front. Microbiol. **7**. doi:10.3389/fmicb.2016.02062.

235. Yan, K., Ma, Y., Bao, S., Li, W., Wang, Y., Sun, C., Lu, X., and Ran, J. 2024. Exploring the Impact of Coconut Peat and Vermiculite on the Rhizosphere Microbiome of Pre-Basic Seed Potatoes under Soilless Cultivation Conditions. Microorganisms **12**(3): 584. doi:10.3390/microorganisms12030584.

236. Kettongruang, S., Morikawa, M., and Boonmak, C. 2026. Diversity and Plant Growth‐Promoting Potential of Duckweed‐Associated Bacteria on *Wolffia globosa* Biomass Production and Nutritional Quality. Environ Microbiol Rep **18**(2): e70312. doi:10.1111/1758-2229.70312.

237. Wang, Z., Dai, Q., Su, D., Zhang, Z., Tian, Y., Tong, J., Chen, S., Yan, C., Yang, J., and Cui, X. 2024. Comparative analysis of the microbiomes of strawberry wild species Fragaria nilgerrensis and cultivated variety Akihime using amplicon-based next-generation sequencing. Front. Microbiol. **15**: 1377782. doi:10.3389/fmicb.2024.1377782.

238. Zhou, F., Wu, X., Gao, Y., Fan, S., Zhou, H., and Zhang, X. 2022. Diversity Shifts in the Root Microbiome of Cucumber Under Different Plant Cultivation Substrates. Front. Microbiol. **13**: 878409. doi:10.3389/fmicb.2022.878409.

239. Cassán, F., Perrig, D., Sgroy, V., Masciarelli, O., Penna, C., and Luna, V. 2009. Azospirillum brasilense Az39 and Bradyrhizobium japonicum E109, inoculated singly or in combination, promote seed germination and early seedling growth in corn (Zea mays L.) and soybean (Glycine max L.). European Journal of Soil Biology **45**(1): 28–35. doi:10.1016/j.ejsobi.2008.08.005.

240. Mubarik, N.R., Mahagiani, I., and Wahyudi, A.T. 2013. Production of IAA by Bradyrhizobium sp. Engineering and Technology **74**.

241. Okubo, T., Piromyou, P., Tittabutr, P., Teaumroong, N., and Minamisawa, K. 2016. Origin and Evolution of Nitrogen Fixation Genes on Symbiosis Islands and Plasmid in *Bradyrhizobium*. Microbes and environments **31**(3): 260–267. doi:10.1264/jsme2.ME15159.

242. Ríos-Ruiz, W.F., Castro-Tuanama, R., Valdez-Nuñez, R.A., Torres-Bernal, L., Jave-Concepción, H.G., Daza-Pérez, A.C., Barrera-Lozano, M., and Archentti-Reátegui, F. 2024. Co-Inoculation of Phosphate-Solubilizing Bacteria and Rhizobia Increases Phosphorus Availability and Promotes the Development of Forage Legumes. Agronomy **14**(11): 2493. doi:10.3390/agronomy14112493.

243. Ledermann, R., Bartsch, I., Müller, B., Wülser, J., and Fischer, H.-M. 2018. A Functional General Stress Response of *Bradyrhizobium diazoefficiens* Is Required for Early Stages of Host Plant Infection. MPMI **31**(5): 537–547. doi:10.1094/MPMI-11-17-0284-R.

244. Tittabutr, P., Piromyou, P., Longtonglang, A., Noisa-Ngiam, R., Boonkerd, N., and Teaumroong, N. 2013. Alleviation of the effect of environmental stresses using co-inoculation of mungbean by *Bradyrhizobium* and rhizobacteria containing stress-induced ACC deaminase enzyme. Soil Science and Plant Nutrition **59**(4): 559–571. doi:10.1080/00380768.2013.804391.

245. Kim, S., Jung, G., and Nam, I. 2021. Draft genome sequence of Caballeronia jiangsuensis EK, a phosphatesolubilizing bacterium isolated from the rhizosphere of reed. Korean Journal of Microbiology **57**(2): 106–108. 한국미생물학회. doi:10.7845/KJM.2021.1011.

246. Jose, C., Subramaniyan, S., and Sandhia, G.S. 2025. Isolation and characterization of plant growth-promoting bacteria exhibiting ACC deaminase production in soil samples. Proc.Indian Natl. Sci. Acad. doi:10.1007/s43538-025-00537-5.

247. Li, X., Yang, M., Jones, D.L., Du, X., Liu, J., Guo, X., and Tang, Z. 2026. Rhizosphere Metabolites and Microbial Communities Shape Lettuce Responses to Oxytetracycline Stress. J. Agric. Food Chem. **74**(3): 2586–2598. doi:10.1021/acs.jafc.5c10653.

248. Chhetri, G., Kim, I., Kang, M., Kim, J., So, Y., and Seo, T. 2022. Devosia rhizoryzae sp. nov., and Devosia oryziradicis sp. nov., novel plant growth promoting members of the genus Devosia, isolated from the rhizosphere of rice plants. J Microbiol. **60**(1): 1–10. doi:10.1007/s12275-022-1474-8.

249. Du, J., and Yi, T.-H. 2016. Flavobacterium tyrosinilyticum sp. nov., isolated from the rhizosphere of wild strawberry. International Journal of Systematic and Evolutionary Microbiology **66**(7): 2629–2634. doi:10.1099/ijsem.0.001104.

250. Ruiz, A., Scicchitano, D., Palladino, G., Nanetti, E., Candela, M., Furones, D., Sanahuja, I., Carbó, R., Gisbert, E., and Andree, K.B. 2023. Microbiome study of a coupled aquaponic system: unveiling the independency of bacterial communities and their beneficial influences among different compartments. Sci Rep **13**(1): 19704. doi:10.1038/s41598-023-47081-0.

251. Kim, H., Woo, O.-G., Kim, J.B., Yoon, S.-Y., Kim, J.-S., Sul, W.J., Hwang, J.-Y., and Lee, J.-H. 2023. Flavobacterium sp. strain GJW24 ameliorates drought resistance in Arabidopsis and Brassica. Front. Plant Sci. **14**: 1257137. doi:10.3389/fpls.2023.1257137.

252. Yakubovskaya, A.I., Melnychuk, T.N., Kameneva, I.A., Shaposhnikov, A.I., Puhalsky, Y.V., and Sazanova, A.L. 2019. Flavobacterium sp. Strain No. 72 - Associative Symbiont Of Oryza Sativa L. Plants. **21**(3): 566–571. Global Science Publications.

253. Subramanian, P., Krishnamoorthy, R., Chanratana, M., Kim, K., and Sa, T. 2015. Expression of an exogenous 1-aminocyclopropane-1-carboxylate deaminase gene in psychrotolerant bacteria modulates ethylene metabolism and cold induced genes in tomato under chilling stress. Plant Physiology and Biochemistry **89**: 18–23. doi:10.1016/j.plaphy.2015.02.003.

254. Brígido, C., Glick, B.R., and Oliveira, S. 2017. Survey of Plant Growth-Promoting Mechanisms in Native Portuguese Chickpea Mesorhizobium Isolates. Microb Ecol **73**(4): 900–915. doi:10.1007/s00248-016-0891-9.

255. Gamalero, E., and Glick, B.R. 2025. Rhizobia and non-rhizobial nodule bacteria with ACC deaminase increase both nodulation and stress resistance. Front. Microbiol. **16**: 1662592. doi:10.3389/fmicb.2025.1662592.

256. Nagpal, S., Sharma, P., Sirari, A., and Gupta, R.K. 2020. Coordination of Mesorhizobium sp. and endophytic bacteria as elicitor of biocontrol against Fusarium wilt in chickpea. Eur J Plant Pathol **158**(1): 143–161. doi:10.1007/s10658-020-02062-1.

257. Lazcano, C., Boyd, E., Holmes, G., Hewavitharana, S., Pasulka, A., and Ivors, K. 2021. The rhizosphere microbiome plays a role in the resistance to soil-borne pathogens and nutrient uptake of strawberry cultivars under field conditions. Sci Rep **11**(1): 3188. doi:10.1038/s41598-021-82768-2.

258. De Tender, C., Vandecasteele, B., Verstraeten, B., Ommeslag, S., Kyndt, T., and Debode, J. 2021. Biochar-Enhanced Resistance to Botrytis cinerea in Strawberry Fruits

(But Not Leaves) Is Associated With Changes in the Rhizosphere Microbiome. Front. Plant Sci. **12**: 700479. doi:10.3389/fpls.2021.700479.

259. Kasozi, N., Kaiser, H., and Wilhelmi, B. 2020. Metabarcoding Analysis of Bacterial Communities Associated with Media Grow Bed Zones in an Aquaponic System. International Journal of Microbiology **2020**: 1–10. doi:10.1155/2020/8884070.

260. Fan, D., and Smith, D.L. 2022. Mucilaginibacter sp. K Improves Growth and Induces Salt Tolerance in Nonhost Plants via Multilevel Mechanisms. Front. Plant Sci. **13**: 938697. doi:10.3389/fpls.2022.938697.

261. Madhaiyan, M., Poonguzhali, S., Lee, J.-S., Senthilkumar, M., Lee, K.C., and Sundaram, S. 2010. Mucilaginibacter gossypii sp. nov. and Mucilaginibacter gossypiicola sp. nov., plant-growth-promoting bacteria isolated from cotton rhizosphere soils. International Journal of Systematic and Evolutionary Microbiology **60**(10): 2451–2457. doi:10.1099/ijs.0.018713-0.

262. Van Gerrewey, T., El-Nakhel, C., De Pascale, S., De Paepe, J., Clauwaert, P., Kerckhof, F.-M., Boon, N., and Geelen, D. 2021. Root-Associated Bacterial Community Shifts in Hydroponic Lettuce Cultured with Urine-Derived Fertilizer. Microorganisms **9**(6): 1326. doi:10.3390/microorganisms9061326.

263. Lee, S.Y., Lee, Y.-Y., and Cho, K.-S. 2022. Effect of Novosphingobium sp. CuT1 inoculation on the rhizoremediation of heavy metal- and diesel-contaminated soil planted with tall fescue. Environ Sci Pollut Res **30**(6): 16612–16625. doi:10.1007/s11356-022-23339-4.

264. Rangjaroen, C., Sungthong, R., Rerkasem, B., Teaumroong, N., Noisangiam, R., and Lumyong, S. 2017. Untapped Endophytic Colonization and Plant Growth-Promoting Potential of the Genus *Novosphingobium* to Optimize Rice Cultivation. Microbes and environments **32**(1): 84–87. doi:10.1264/jsme2.ME16112.

265. Wang, F., Quo, Q., Wang, L., Ma, Y., Zhang, T., and Li, R. 2018. Nematicidal Activities of Bacterial Volatiles from Pseudoduganella violaceinigra G5-3 and Novosphingobium pokkalii G8-2 against the Pine Wood Nematode Bursaphelenchus xylophilus. Chiang Mai J. Sci. **46**(2): 236–246.

266. Zha, Y., Lai, W., Liu, A., Li, X., Wang, J., Hu, S., Yu, H., Xiao, W., and Chen, X. 2026. Effects of Different Soil DisinfectionMethods on Physicochemical Propertiesand Microbial Community Structure ofStrawberry Continuous Cropping Soils. Pol. J. Environ. Stud. doi:10.15244/pjoes/208865.

267. Boonmak, C., Kettongruang, S., Buranathong, B., Morikawa, M., and Duangmal, K. 2024. Duckweed-associated bacteria as plant growth-promotor to enhance growth of

Spirodela polyrhiza in wastewater effluent from a poultry farm. Arch Microbiol **206**(1): 43. doi:10.1007/s00203-023-03778-4.

268. Lei, Z., Zhang, H., Liu, W., Sheng, J., Zhang, H., Wang, Y., Tang, Y., Wang, H., Ding, C., Qiao, W., Zhu, Y., Yang, G., Zhang, Y., Liu, Z., Zhou, N., Hu, C., and Zhao, X. 2025. Dynamic and Stable Core Microbiota Assist Plants in Enriching Selenium and Reducing Cadmium Absorption. Advanced Science **12**(25): e00862. doi:10.1002/advs.202500862.

269. Thijs, S., Weyens, N., Sillen, W., Gkorezis, P., Carleer, R., and Vangronsveld, J. 2014. Potential for plant growth promotion by a consortium of stress‐tolerant 2,4‐dinitrotoluene‐degrading bacteria: isolation and characterization of a military soil. Microbial Biotechnology **7**(4): 294–306. doi:10.1111/1751-7915.12111.

270. Woo, H., Kim, I., Chhetri, G., Park, S., Lee, H., Yook, S., and Seo, T. 2024. Two Novel Bacterial Species, Rhodanobacter lycopersici sp. nov. and Rhodanobacter geophilus sp. nov., Isolated from the Rhizosphere of Solanum lycopersicum with Plant Growth-Promoting Traits. Microorganisms **12**(11): 2227. doi:10.3390/microorganisms12112227.

271. Huo, Y., Kang, J.-P., Park, J.-K., Li, J., Chen, L., and Yang, D.-C. 2018. Rhodanobacter ginsengiterrae sp. nov., an antagonistic bacterium against root rot fungal pathogen Fusarium solani, isolated from ginseng rhizospheric soil. Arch Microbiol **200**(10): 1457–1463. doi:10.1007/s00203-018-1560-9.

272. Hassani, M.A., Gonzalez, O., Hunter, S.S., Holmes, G.J., Hewavitharana, S.S., Ivors, K., and Lazcano, C. 2023. Microbiome Network Connectivity and Composition Linked to Disease Resistance in Strawberry Plants. Phytobiomes Journal: PBIOMES-10-22-0069-R. doi:10.1094/PBIOMES-10-22-0069-R.

273. Legein, M., Smets, W., Wuyts, K., Bosmans, L., Samson, R., and Lebeer, S. 2022. The Greenhouse Phyllosphere Microbiome and Associations with Introduced Bumblebees and Predatory Mites. Microbiol Spectr **10**(4): e01755-22. doi:10.1128/spectrum.01755-22.

274. Chen, B., Shen, J., Zhang, X., Pan, F., Yang, X., and Feng, Y. 2014. The Endophytic Bacterium, Sphingomonas SaMR12, Improves the Potential for Zinc Phytoremediation by Its Host, Sedum alfredii. PLoS ONE **9**(9): e106826. doi:10.1371/journal.pone.0106826.

275. Lombardino, J., Bijlani, S., Singh, N.K., Wood, J.M., Barker, R., Gilroy, S., Wang, C.C.C., and Venkateswaran, K. 2022. Genomic Characterization of Potential Plant Growth-Promoting Features of *Sphingomonas* Strains Isolated from the International Space Station. Microbiol Spectr **10**(1): e01994-21. doi:10.1128/spectrum.01994-21.

276. Mazoyon, C., Catterou, M., Alahmad, A., Mongelard, G., Guénin, S., Sarazin, V., Dubois, F., and Duclercq, J. 2023. Sphingomonas sediminicola Dae20 Is a Highly Promising Beneficial Bacteria for Crop Biostimulation Due to Its Positive Effects on Plant Growth and Development. Microorganisms **11**(8): 2061. doi:10.3390/microorganisms11082061.

277. Wachowska, U., Irzykowski, W., Jędryczka, M., Stasiulewicz-Paluch, A.D., and Głowacka, K. 2013. Biological control of winter wheat pathogens with the use of antagonistic *Sphingomonas* bacteria under greenhouse conditions. Biocontrol Science and Technology **23**(10): 1110–1122. doi:10.1080/09583157.2013.812185.

278. Yang, Z., Liu, T., Fan, J., Chen, Y., Wu, S., Li, J., Liu, Z., Yang, Z., Li, L., Liu, S., Yang, H., Yin, H., Meng, D., and Tang, Q. 2024. Biocontrol agents modulate phyllosphere microbiota interactions against pathogen Pseudomonas syringae. Environmental Science and Ecotechnology **21**: 100431. doi:10.1016/j.ese.2024.100431.

279. Kumari, A., Patel, A.K., Banjare, U., and Pandey, K.D. 2020. Growth promoting characteristics of endophytic bacteria isolated from Costus igneus plant. Plant Archive **20**(1): 2991–3001.

280. Deng, X., Zhang, N., Shen, Z., Zhu, C., Li, R., Salles, J.F., and Shen, Q. 2020. Rhizosphere bacteria assembly derived from fumigation and organic amendment triggers the direct and indirect suppression of tomato bacterial wilt disease. Applied Soil Ecology **147**: 103364. doi:10.1016/j.apsoil.2019.103364.

281. Fu, L., Xiong, W., Dini-Andreote, F., Wang, B., Tao, C., Ruan, Y., Shen, Z., Li, R., and Shen, Q. 2020. Changes in bulk soil affect the disease-suppressive rhizosphere microbiome against Fusarium wilt disease. Front. Agr. Sci. Eng. **7**(3): 307. doi:10.15302/J-FASE-2020328.

282. Rani, V., Bhatia, A., Nain, L., Tomar, G.S., and Kaushik, R. 2021. Methane utilizing plant growth-promoting microbial diversity analysis of flooded paddy ecosystem of India. World J Microbiol Biotechnol **37**(4): 56. doi:10.1007/s11274-021-03018-1.

283. Chen, X., Li, F.-L., and Kong, C.-H. 2023. Rhizosphere bacteria mediate flowering time of two genotypes of Arabidopsis with and without root-secreted signaling (−)-loliolide. Rhizosphere **27**: 100774. doi:10.1016/j.rhisph.2023.100774.

284. Guevara, F., Frey, T., Malacrinò, A., and Benitez Ponce, M.S. 2025. Influence of System Type and Management Practices on Bacterial and Fungal Community Structure in Hydroponic Systems: Insights from Commercial Facilities in Ohio. Phytobiomes Journal **9**(2): 302–316. doi:10.1094/PBIOMES-07-24-0070-R.

285. Schmidt, C.S., Mrnka, L., Frantík, T., Lovecká, P., and Vosátka, M. 2018. Plant growth promotion of Miscanthus × giganteus by endophytic bacteria and fungi on non-polluted and polluted soils. World J Microbiol Biotechnol **34**(3): 48. doi:10.1007/s11274-018-2426-7.

286. Wang, L., Li, Z., Zhang, G., Liang, X., Hu, L., Li, Y., He, Y., and Zhan, F. 2023. Dark septate endophyte Exophiala pisciphila promotes maize growth and alleviates cadmium toxicity. Front. Microbiol. **14**: 1165131. doi:10.3389/fmicb.2023.1165131.

287. Anzalone, A., Mosca, A., Dimaria, G., Nicotra, D., Tessitori, M., Privitera, G.F., Pulvirenti, A., Leonardi, C., and Catara, V. 2022. Soil and Soilless Tomato Cultivation Promote Different Microbial Communities That Provide New Models for Future Crop Interventions. IJMS **23**(15): 8820. doi:10.3390/ijms23158820.

288. Abd Alhakim, A., Hashem, A., Abdelaziz, A., and Attia, M. 2022. Impact of plant growth promoting fungi on biochemical defense performance of Tomato under Fusarial infection. Egypt. J. Chem. **0**(0): 0–0. doi:10.21608/ejchem.2022.124008.5532.

289. Attia, M.S., Abdelaziz, A.M., Al-Askar, A.A., Arishi, A.A., Abdelhakim, A.M., and Hashem, A.H. 2022. Plant Growth-Promoting Fungi as Biocontrol Tool against Fusarium Wilt Disease of Tomato Plant. JoF **8**(8): 775. doi:10.3390/jof8080775.

290. Abdelaziz, A.M., Sharaf, M.H., Hashem, A.H., Al-Askar, A.A., Marey, S.A., Mohamed, F.A., Abdelstar, M.N., Zaki, M.A., Abdelgawad, H., and Attia, M.S. 2023. Biocontrol of Fusarium wilt disease in pepper plant by plant growth promoting Penicillium expansum and Trichoderma harzianum. Not Bot Horti Agrobo **51**(3): 13302. doi:10.15835/nbha51313302.

291. Mahadevamurthy, M., Channappa, T., Sidappa, M., Raghupathi, M., and Nagaraj, A. 2016. Isolation of phosphate solubilizing fungi from rhizosphere soil and its effect on seed growth parameters of different crop plants. J App Biol Biotech: 022–026. doi:10.7324/JABB.2016.40604.

292. Tarroum, M., Romdhane, W.B., Al-Qurainy, F., Ali, A.A.M., Al-Doss, A., Fki, L., and Hassairi, A. 2022. A novel PGPF Penicillium olsonii isolated from the rhizosphere of Aeluropus littoralis promotes plant growth, enhances salt stress tolerance, and reduces chemical fertilizers inputs in hydroponic system. Front. Microbiol. **13**: 996054. doi:10.3389/fmicb.2022.996054.

293. Hossain, Md.M., Sultana, F., Miyazawa, M., and Hyakumachi, M. 2014. The Plant Growth-promoting Fungus Penicillium spp. GP15-1 Enhances Growth and Confers Protection against Damping-off and Anthracnose in the Cucumber. J. Oleo Sci. **63**(4): 391–400. doi:10.5650/jos.ess13143.

294. Hossain, Md.M., Sultana, F., and Hyakumachi, M. 2017. Role of ethylene signalling in growth and systemic resistance induction by the plant growth‐promoting fungus *Penicillium viridicatum* in Arabidopsis. Journal of Phytopathology **165**(7–8): 432–441. doi:10.1111/jph.12577.

295. Kaewkrajay, C., Kotabaru, T., and Dethoup, T. 2025. Characterization of indole-3-acetic acid-producing marine yeasts and their effect on tomato (Solanum lycopersicum L.) seedlings. ANRES **59**(4). doi:10.34044/j.anres.2025.59.4.13.

296. Poorniammal, R. 2022. Plant Growth Promoting Activity and Biocontrol Potential of Soil Yeast. IJAEB **15**(1). doi:10.30954/0974-1712.01.2022.9.

297. Mundra, S., Arora, R., and Stobdan, T. 2011. Solubilization of insoluble inorganic phosphates by a novel temperature-, pH-, and salt-tolerant yeast, Rhodotorula sp. PS4, isolated from seabuckthorn rhizosphere, growing in cold desert of Ladakh, India. World J Microbiol Biotechnol **27**(10): 2387–2396. doi:10.1007/s11274-011-0708-4.

298. Moharrami, F., Bolandnazar, S., Salteh, S.A., and Sarikhani, M. 2026. Plant growth-promoting microorganisms and phosphorus levels influence growth, nutrient uptake, and secondary metabolites in hydroponic basil. Sci Rep. doi:10.1038/s41598-026-45285-8.

299. Rahbari, A., Esmaielpour, B., Azarmi, R., Fatemi, H., Lajayer, H.M., Panahirad, S., Gohari, G., and Vita, F. 2025. Symbiotic Fungus Serendipita indica as a Natural Bioenhancer Against Cadmium Toxicity in Chinese Cabbage. Plants **14**(17): 2773. doi:10.3390/plants14172773.

300. Batool, A., Wang, C., Xia, Y., Xiao, L., Ahmad, J., Liu, L., Ge, L., and Chen, C. 2025. Transcriptional profiles of endophyte Serendipita indica associated with plant growth improvement in watermelon. BMC Plant Biol **25**(1): 1776. doi:10.1186/s12870-025-07659-4.

301. Kushwaha, A.S., Maurya, A., and Kumar, M. 2025. Analysis of the phosphate solubilization efficiency of different phosphorus sources by Endophytic fungus Serendipita indica under arsenic stress. Plant Soil **516**(2): 1383–1396. doi:10.1007/s11104-025-07801-z.

302. Dagher, D., Taskos, D., Mourouzidou, S., and Monokrousos, N. 2025. Microbial-Enhanced Abiotic Stress Tolerance in Grapevines: Molecular Mechanisms and Synergistic Effects of Arbuscular Mycorrhizal Fungi, Plant Growth-Promoting Rhizobacteria, and Endophytes. Horticulturae **11**(6): 592. doi:10.3390/horticulturae11060592.

303. Del Barrio-Duque, A., Samad, A., Nybroe, O., Antonielli, L., Sessitsch, A., and Compant, S. 2020. Interaction between endophytic Proteobacteria strains and Serendipita indica enhances biocontrol activity against fungal pathogens. Plant Soil **451**(1–2): 277–305. doi:10.1007/s11104-020-04512-5.

304. Kumla, J., Nundaeng, S., Suwannarach, N., and Lumyong, S. 2020. Evaluation of Multifarious Plant Growth Promoting Trials of Yeast Isolated from the Soil of Assam Tea (Camellia sinensis var. assamica) Plantations in Northern Thailand. Microorganisms **8**(8): 1168. doi:10.3390/microorganisms8081168.

305. Taiebikhah, N., Mirtalebi, M., and Gharin, R. 2026. Antagonistic potential of arugula vermicompost-derived fungi for controlling tomato crown and root rot caused by Fusarium oxysporum f. sp. radicis-lycopersici. Physiological and Molecular Plant Pathology **141**: 102982. doi:10.1016/j.pmpp.2025.102982.

306. Bi, B., Xiao, Y., Xu, X., Chen, Q., Li, H., Zhao, Z., and Li, T. 2024. Diversity and Functional Roles of Root-Associated Endophytic Fungi in Two Dominant Pioneer Trees Reclaimed from a Metal Mine Slag Heap in Southwest China. Microorganisms **12**(10): 2067. doi:10.3390/microorganisms12102067.

307. Oh, Y., Cheon, W., Goh, J., Lee, C.S., and Mun, H.Y. 2024. Characterization of Four Unrecorded Cadophora Species from Freshwater in Korea. The Korean Journal of Mycology **52**(4): 239–245. 한국균학회. doi:10.4489/KJM.520402.

308. Khastini, R.O., Ogawara, T., Sato, Y., and Narisawa, K. 2014. Control of Fusarium wilt in melon by the fungal endophyte, Cadophora sp. Eur J Plant Pathol **139**(2): 339–348. doi:10.1007/s10658-014-0389-6.

309. Shah, S., Shah, B., Sharma, R., Rekadwad, B., Shouche, Y.S., Sharma, J., and Pant, B. 2022. Colonization with non-mycorrhizal culturable endophytic fungi enhances orchid growth and indole acetic acid production. BMC Microbiol **22**(1): 101. doi:10.1186/s12866-022-02507-z.

310. Zheng, W., Yang, C., Zhou, C., Ma, T., Zhu, Q., and Li, Z. 2025. Disruption of MAPK signalling and amino acid biosynthesis underlies the antifungal biocontrol mechanism of *Coniochaeta velutina* against *Colletotrichum gloeosporioides* : a transcriptome and metabolome analysis. Can. J. Microbiol. **71**: 1–13. doi:10.1139/cjm-2023-0223.

311. Su, D., Chen, S., Zhou, W., Yang, J., Luo, Z., Zhang, Z., Tian, Y., Dong, Q., Shen, X., Wei, S., Tong, J., and Cui, X. 2022. Comparative Analysis of the Microbial Community Structures Between Healthy and Anthracnose-Infected Strawberry Rhizosphere Soils

Using Illumina Sequencing Technology in Yunnan Province, Southwest of China. Front. Microbiol. **13**: 881450. doi:10.3389/fmicb.2022.881450.

312. Ozimek, E., Jaroszuk-Ściseł, J., Bohacz, J., Korniłłowicz-Kowalska, T., Tyśkiewicz, R., Słomka, A., Nowak, A., and Hanaka, A. 2018. Synthesis of Indoleacetic Acid, Gibberellic Acid and ACC-Deaminase by Mortierella Strains Promote Winter Wheat Seedlings Growth under Different Conditions. IJMS **19**(10): 3218. doi:10.3390/ijms19103218.

313. Li, F., Zhang, S., Wang, Y., Li, Y., Li, P., Chen, L., Jie, X., Hu, D., Feng, B., Yue, K., and Han, Y. 2020. Rare fungus, Mortierella capitata, promotes crop growth by stimulating primary metabolisms related genes and reshaping rhizosphere bacterial community. Soil Biology and Biochemistry **151**: 108017. doi:10.1016/j.soilbio.2020.108017.

314. Sang, Y., Jin, L., Zhu, R., Yu, X.-Y., Hu, S., Wang, B.-T., Ruan, H.-H., Jin, F.-J., and Lee, H.-G. 2022. Phosphorus-Solubilizing Capacity of Mortierella Species Isolated from Rhizosphere Soil of a Poplar Plantation. Microorganisms **10**(12): 2361. doi:10.3390/microorganisms10122361.

315. Zhu, R., Jin, L., Sang, Y., Hu, S., Wang, B.-T., and Jin, F.-J. 2024. Characterization of potassium-solubilizing fungi, Mortierella spp., isolated from a poplar plantation rhizosphere soil. Arch Microbiol **206**(4): 157. doi:10.1007/s00203-024-03912-w.

316. Johnson, J.M., Ludwig, A., Furch, A.C.U., Mithöfer, A., Scholz, S., Reichelt, M., and Oelmüller, R. 2019. The Beneficial Root-Colonizing Fungus *Mortierella hyalina* Promotes the Aerial Growth of *Arabidopsis* and Activates Calcium-Dependent Responses That Restrict *Alternaria brassicae* –Induced Disease Development in Roots. MPMI **32**(3): 351–363. doi:10.1094/MPMI-05-18-0115-R.

317. Qiu, Z., Wang, Z., Wang, S., Fei, J., Qu, Z., Wu, H., Zhao, M., and Yang, H. 2024b. Protective role of Mortierella alpina-derived lipids in resisting root rot in Panax ginseng. Rhizosphere **32**: 100994. doi:10.1016/j.rhisph.2024.100994.

318. Debode, J., De Tender, C., Cremelie, P., Lee, A.S., Kyndt, T., Muylle, H., De Swaef, T., and Vandecasteele, B. 2018. Trichoderma-Inoculated Miscanthus Straw Can Replace Peat in Strawberry Cultivation, with Beneficial Effects on Disease Control. Front. Plant Sci. **9**: 213. doi:10.3389/fpls.2018.00213.

319. Duan, Y., Wang, M., Wang, L., Wu, G., Mao, T., Sun, H., Pang, H., Zhang, M., Jiao, Z., Wang, Y., Kong, X., Cai, Y., and Tan, Z. 2024. Mushroom residue and sheep manure fermentation with Bacillus promoted tomato growth via nutrient release and favorable

microbial conditions. Chem. Biol. Technol. Agric. **11**(1): 94. doi:10.1186/s40538-024-00618-5.

320. Kacem, I. 2023. Effect of soil management on rhizosphere microbial structure and function in olive grove. MSc, Escola Superior Agraria de Braganca, Braganca. Available from https://bibliotecadigital.ipb.pt/server/api/core/bitstreams/f91cc3d5-9a8e-4d92-9470-435f98f7cb06/content.

321. Montanares, M., Jiménez, C., Rodríguez, J., Diaz, A., Ageitos, L., Chávez, R., and Vaca, I. 2025. Siderophore Activity of Partially Acetylated Fusarinines from the Sponge-Derived Fungus *Pseudogymnoascus verrucosus*. J. Nat. Prod. **88**(7): 1643–1652. doi:10.1021/acs.jnatprod.5c00399.

322. David, D.R., Mendelsohn, O., Dubeshko, S., Bierman, R., Jacob, D., Levi, N.O., Kiyar, M., Shtienberg, D., and Elad, Y. 2007. Development of biocontrol of powdery mildew diseases. IOBC **30**(6): 11–15.

323. Kriem, L.S., Pietzka, C., Beckett, M., Gärtling, L., and Wriedt, B. 2023. Electrochemical In Situ Hydrogen Peroxide Production Can Reduce Microbial Load in Bioponic Nutrient Solutions Derived from Organic Waste. Agriculture **13**(11): 2122. doi:10.3390/agriculture13112122.

324. Endes, A. 2024. The Effect of Phytophthora citrophthora Infection of Strawberry Physiology and Histology in the Presence of Calcium, Iron, and Zinc Deficiencies. Applied Fruit Science **66**(5): 1767–1775. doi:10.1007/s10341-024-01160-2.

325. Punja, Z.K., Scott, C., and Lung, S. 2022. Several *Pythium* species cause crown and root rot on cannabis (*Cannabis sativa* L., marijuana) plants grown under commercial greenhouse conditions. Canadian Journal of Plant Pathology **44**(1): 66–81. doi:10.1080/07060661.2021.1954695.

326. Wang, S., Zhu, Y., Yang, Y., Li, J., and Hoffmann, M.R. 2020. Electrochemical cell lysis of gram-positive and gram-negative bacteria: DNA extraction from environmental water samples. Electrochimica Acta **338**: 135864. doi:10.1016/j.electacta.2020.135864.

327. Zhang, Y., Song, Z., and Schilling, J.S. 2024. Evaluation of DNA Extraction Methods for Microbial Community Profiling in Deadwood Decomposition. MicrobiologyOpen **13**(6): e70007. doi:10.1002/mbo3.70007.

328. Rathod, D.R., and Silverman, J.D. 2026. PCR bias impacts microbiome ecological analyses. PLoS Comput Biol **22**(1): e1013908. doi:10.1371/journal.pcbi.1013908.

329. Delahaye, C., and Nicolas, J. 2021. Sequencing DNA with nanopores: Troubles and biases. PLoS ONE **16**(10): e0257521. doi:10.1371/journal.pone.0257521.

330. Kastanis, G.J., Santana‐Quintero, L.V., Sanchez‐Leon, M., Lomonaco, S., Brown, E.W., and Allard, M.W. 2019. In‐depth comparative analysis of Illumina® MiSeq run metrics: Development of a wet‐lab quality assessment tool. Molecular Ecology Resources **19**(2): 377–387. doi:10.1111/1755-0998.12973.

331. Nearing, J.T., Comeau, A.M., and Langille, M.G.I. 2021. Identifying biases and their potential solutions in human microbiome studies. Microbiome **9**(1): 113. doi:10.1186/s40168-021-01059-0.

332. Gloor, G.B., Macklaim, J.M., Pawlowsky-Glahn, V., and Egozcue, J.J. 2017. Microbiome Datasets Are Compositional: And This Is Not Optional. Front. Microbiol. **8**: 2224. doi:10.3389/fmicb.2017.02224.

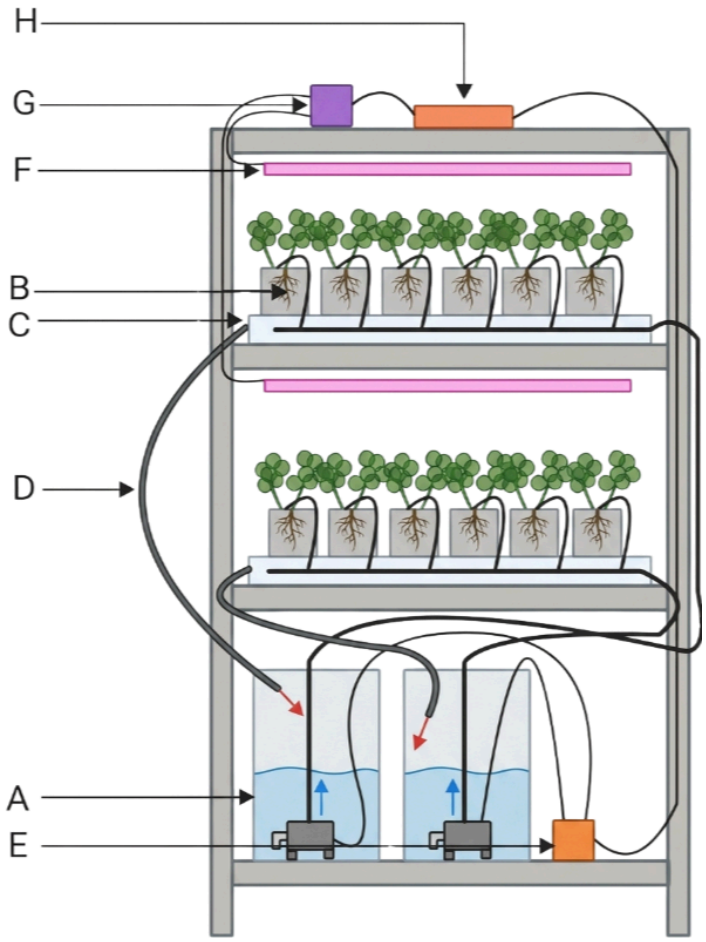
333. Gloor, G.B., and Reid, G. 2016. Compositional analysis: a valid approach to analyze microbiome high-throughput sequencing data. Can. J. Microbiol. **62**(8): 692–703. doi:10.1139/cjm-2015-0821.

334. Gómez Expósito, R., Postma, J., Raaijmakers, J.M., and De Bruijn, I. 2015. Diversity and Activity of Lysobacter Species from Disease Suppressive Soils. Front. Microbiol. **6**. doi:10.3389/fmicb.2015.01243.

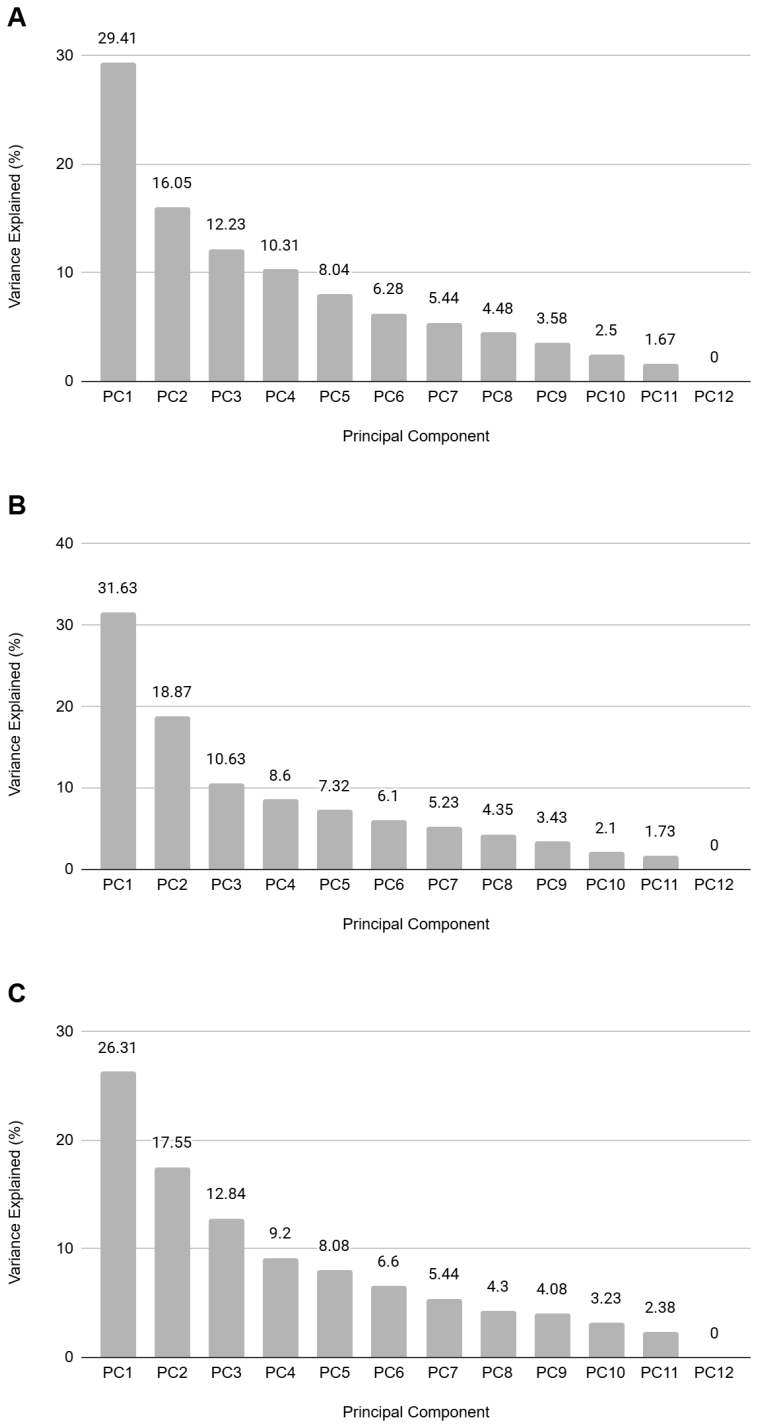
335. Aparicio, M.A., Lucena, C., García, M.J., Ruiz-Castilla, F.J., Jiménez-Adrián, P., López-Berges, M.S., Prieto, P., Alcántara, E., Pérez-Vicente, R., Ramos, J., and Romera, F.J. 2023. The nonpathogenic strain of Fusarium oxysporum FO12 induces Fe deficiency responses in cucumber (Cucumis sativus L.) plants. Planta **257**(3): 50. doi:10.1007/s00425-023-04079-2.

336. Pu, X., Xie, B., Li, P., Mao, Z., Ling, J., Shen, H., Zhang, J., Huang, N., and Lin, B. 2014. Analysis of the defence-related mechanism in cucumber seedlings in relation to root colonization by nonpathogenic *Fusarium oxysporum* CS-20. FEMS Microbiol Lett **355**(2): 142–151. doi:10.1111/1574-6968.12461.

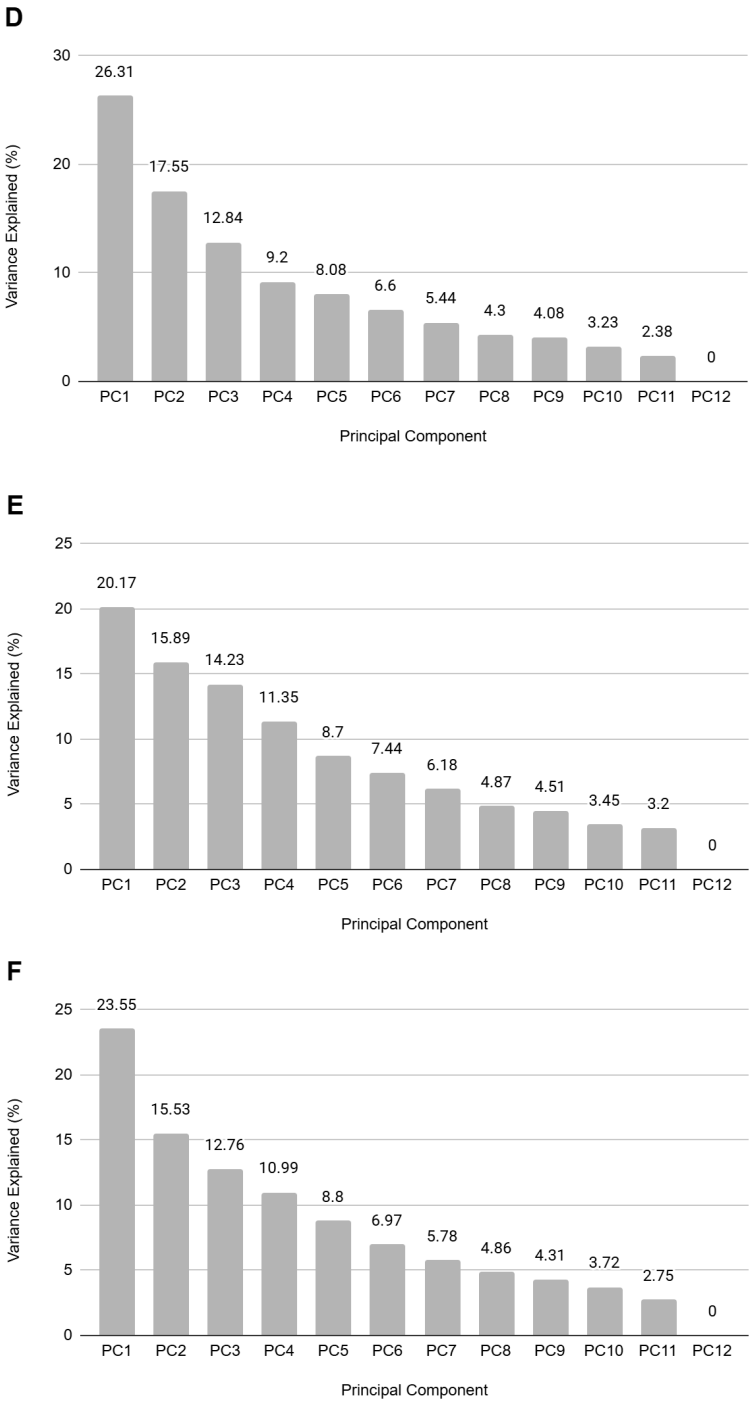
Appendix A: Supplementary Figures



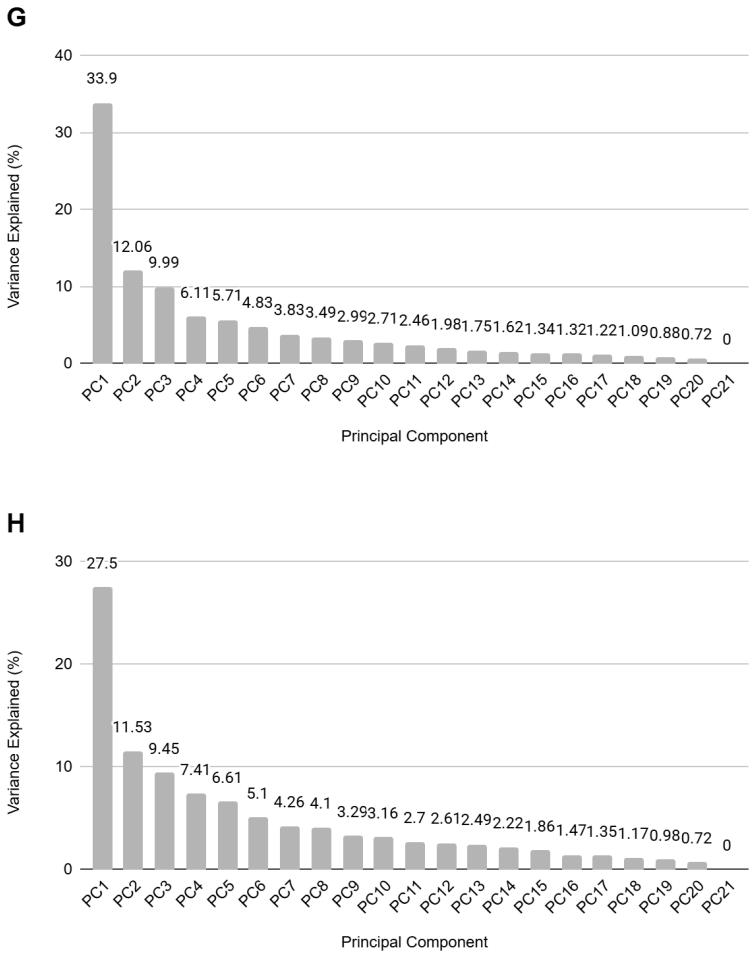
Supplementary Figure A1. Schematic of hydroponic strawberry cropping systems. Each experimental unit contained two shelves and housed up to 24 plants. Each shelf received nutrients from a 15 L reservoir. Each reservoir contained a submersible pump to pump nutrient solution up to the shelf via black vinyl tubing (1/2" inner diameter) (A). Nutrient solution was administered twice daily to each pot via drip lines and drip stakes inserted into the substrate (B). Excess nutrient solution flowed out the bottom of each pot, into a collector trough (C). Excess nutrient solution flows down a collector tube back into the reservoir (D). Each submersible pump was connected to a programmable timer, which activated the pumps for 30 seconds at 6:00 pm and 2:00 am, daily (E). Each pot on the top rack received roughly 200 mL of nutrient solution (mean = 192.1 mL, SD = 8.8 mL), while each pot on the bottom rack received roughly 300 mL of nutrient solution (mean = 291.9 mL, SD = 8.7 mL). Each shelf contained three grow lights, equidistant from one another, to provide sufficient light to each plant (F). The grow lights were connected to a second programmable timer; lights were on for 16 hours, and off for eight hours. The top rack was lined with an opaque liner to minimize light from the top rack reaching plants on the bottom rack (G). Both timers received constant power from a power pack on top of the rack (H).



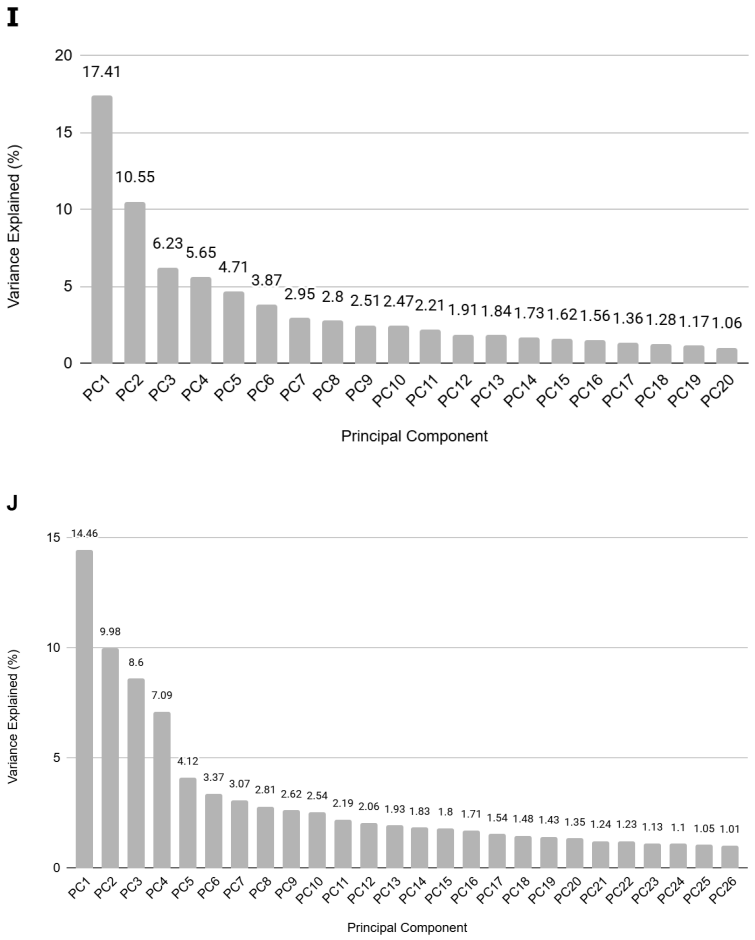
Supplementary Figure A2. Scree plots for Figure 3.1 PCAs. Panels A, B, and C correspond to PCAs A, B and C in Figure 3.1, respectively. Scree plots summarize variance captured by all computed eigenvectors.



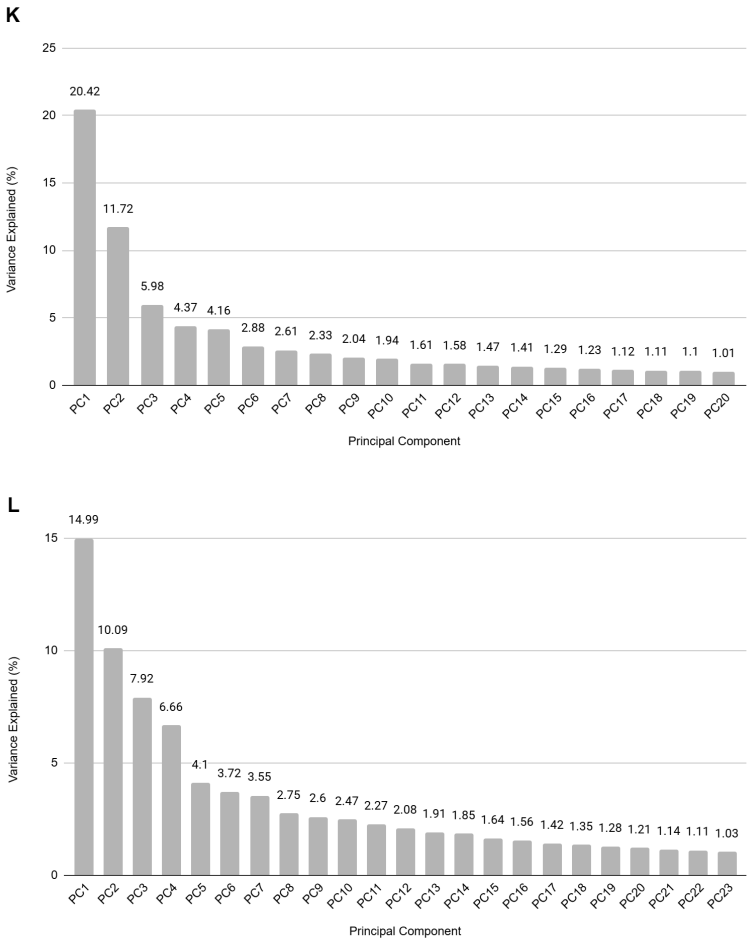
Supplementary Figure A3. Scree plots for Figure 3.2 PCAs. Panels D, E, and F correspond to PCAs A, B, and C in Figure 3.2, respectively. Scree plots summarize variance captured by all computed eigenvectors.



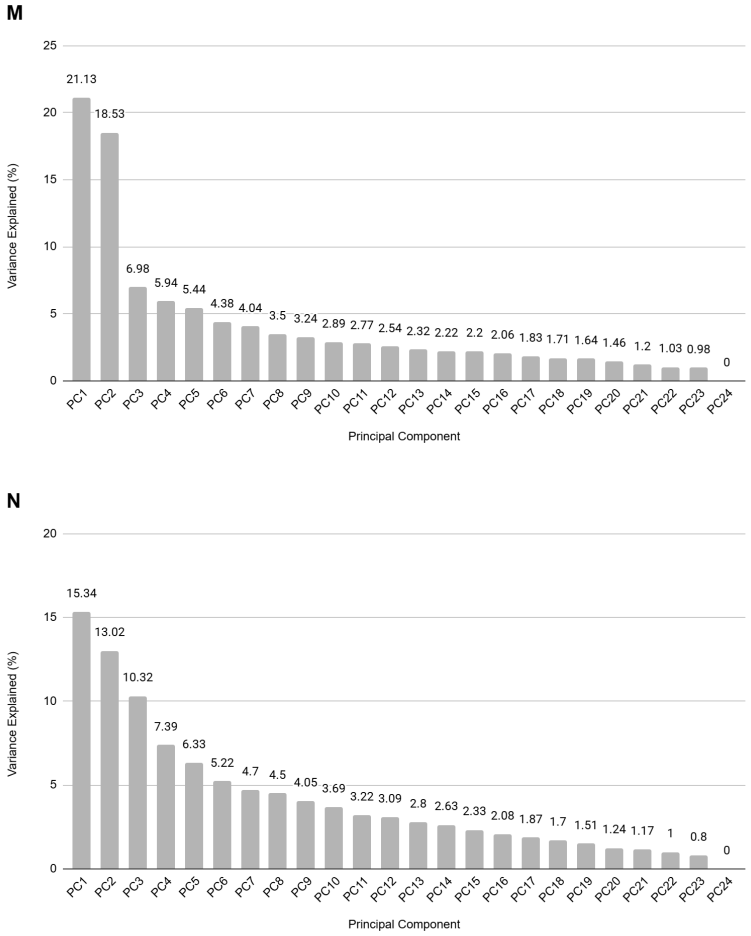
Supplementary Figure A4. Scree plots for Figure 4.1 (G) and 4.2 (H) PCAs. Panels G and H correspond to PCAs in Figures 4.1 and 4.2, respectively. Scree plots summarize variance captured by all computed eigenvectors.



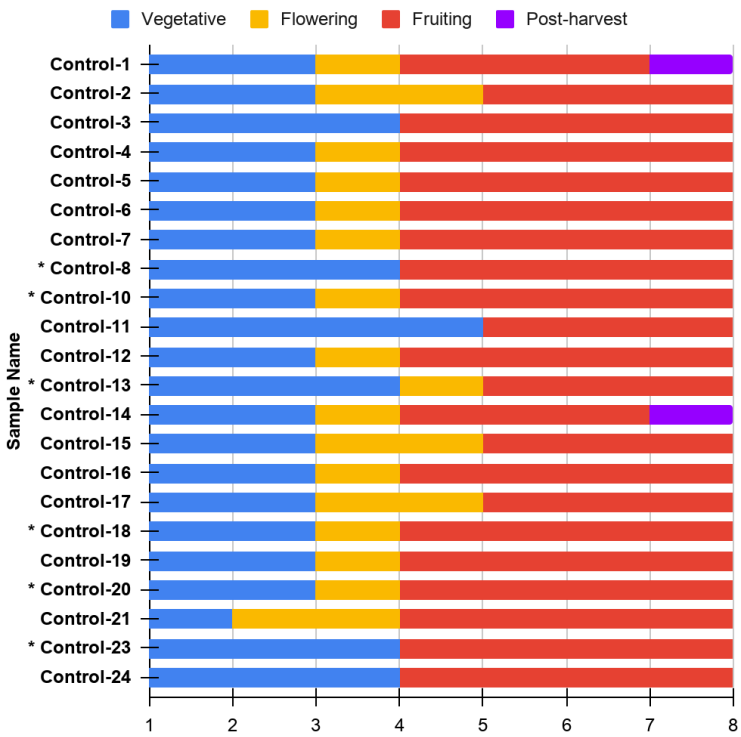
Supplementary Figure A5. Scree plots for Figure 7.1 (I) and 7.2 (J) PCAs. Scree plots I and J summarize all eigenvectors that capture more than 1% of variance. Remaining principle components (up to PC96) capture less than 1% of variance and are not shown.



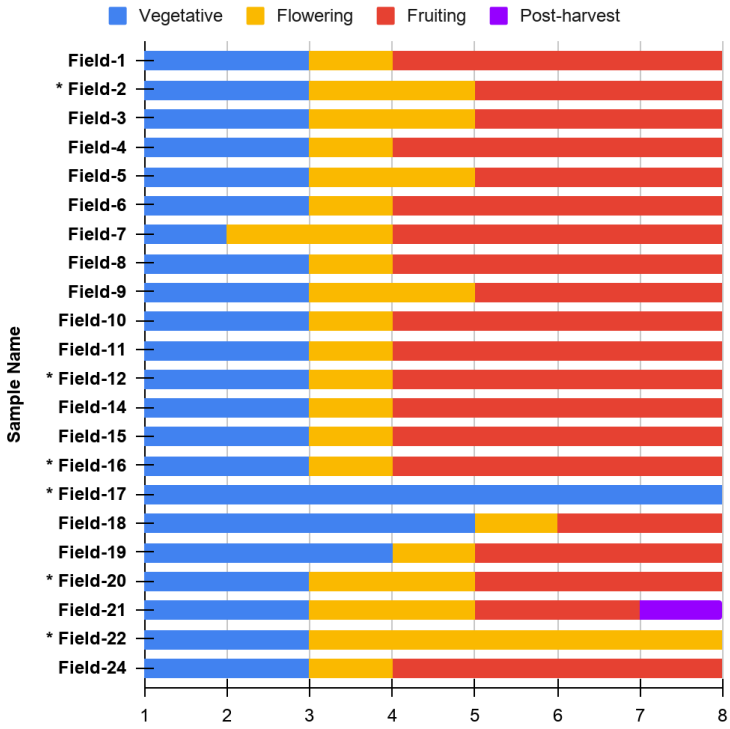
Supplementary Figure A6. Scree plots for Figure 9.1A (K) and 9.2A (L) PCAs. Scree plots K and L summarize all eigenvectors that capture more than 1% of variance. Remaining principle components (up to PC96) capture less than 1% of variance each and are not shown.



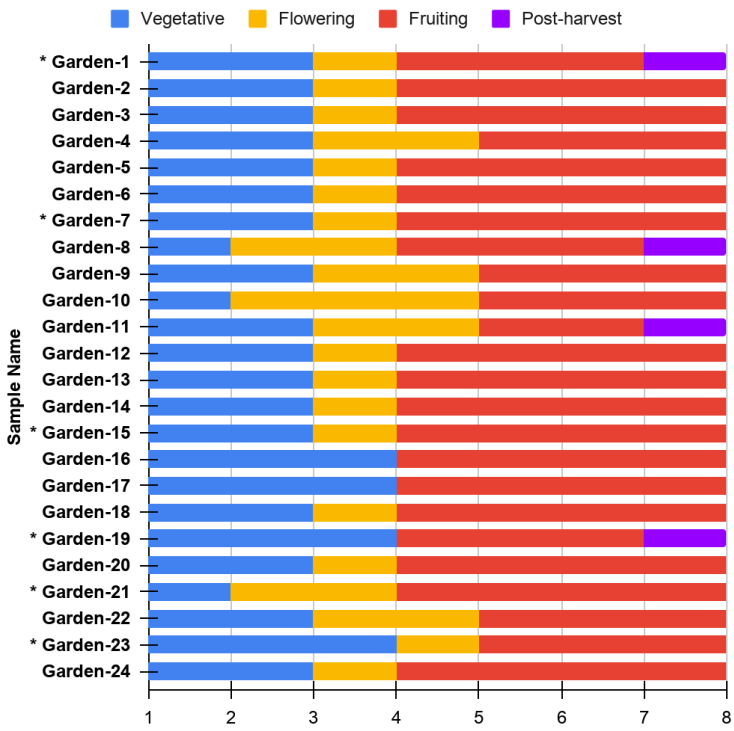
Supplementary Figure A7. Scree plots for Figure 10.1A (M) and 10.2A (N) PCAs. Scree plots summarize variance captured by all computed eigenvectors.



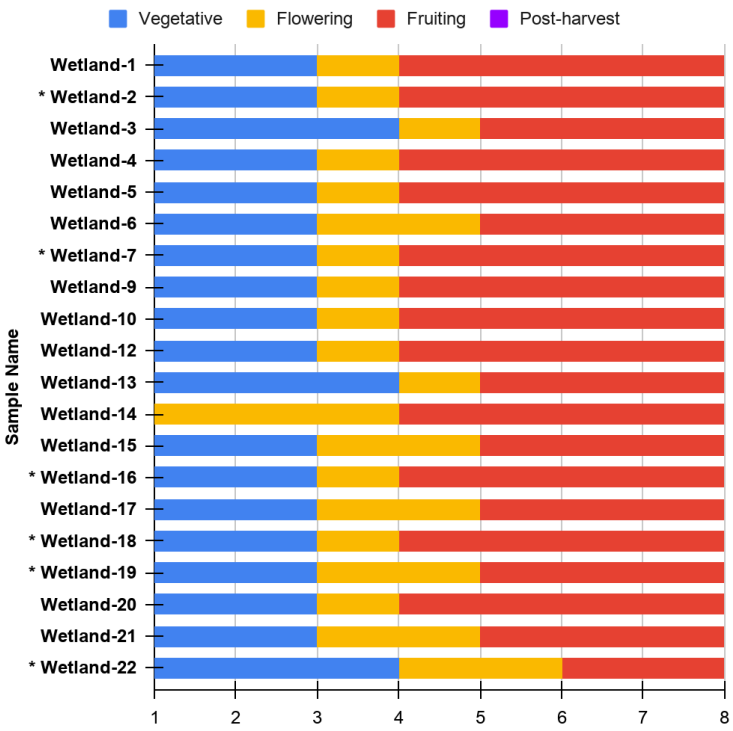
Supplementary Figure A8. Growth state tracking for the no-soil control strawberry plants. Each bar summarizes the progression through vegetative (blue), flowering (yellow), fruiting (red), and post-harvest (purple) growth states for one plant over eight weeks. Growth state was determined weekly via visual inspection based on the following criteria: "vegetative" for plants that have not yet produced a mature flower, "flowering" began at observation of first mature, pollinatable flower, "fruiting" began at observation of first developing marketable berry (i.e. all petals have fallen away and berry is uniformly green with no visual imperfections), and "post-harvest" when all berries have been harvested and no new flowers or berries are developing. Six plants (denoted with *) from each treatment were selected for analysis as previously described. Two plants died during the trial (Control-9 and Control-22), and thus did not contribute any data to this study.



Supplementary Figure A9. Growth state tracking for Field treatment strawberry plants. Each bar summarizes the progression through vegetative (blue), flowering (yellow), fruiting (red), and post-harvest (purple) growth states for one plant over eight weeks. Growth state was determined weekly via visual inspection based on the criteria described above (Supplementary Figure A8). Six plants (denoted with *) from each treatment were selected for analysis as previously described. Two plants died during the trial (Field-13 and Field-23), and thus did not contribute any data to this study.



Supplementary Figure A10. Growth state tracking for Garden treatment strawberry plants. Each bar summarizes the progression through vegetative (blue), flowering (yellow), fruiting (red), and post-harvest (purple) growth states for one plant over eight weeks. Growth state was determined weekly via visual inspection based on the criteria described above (Supplementary Figure A8). Six plants (denoted with *) from each treatment were selected for analysis as previously described.



Supplementary Figure A11. Growth state tracking for Wetland treatment strawberry plants. Each bar summarizes the progression through vegetative (blue), flowering (yellow), fruiting (red), and post-harvest (purple) growth states for one plant over eight weeks. Growth state was determined weekly via visual inspection based on the criteria described above (Supplementary Figure A8). Six plants (denoted with *) from each treatment were selected for analysis as previously described. Four plants died during the trial (Wetland-8, Wetland-11, Wetland-23, and Wetland-24), and thus did not contribute any data to this study.

Appendix B: Supplementary Tables

Supplementary Table B1. Hydroponic strawberry nutrient solutions for three developmental stages. Separate A/B concentrated stock solutions were prepared in 10 L of sterile RO water, then diluted in hydroponic reservoirs to generate the final nutrient solution (i.e. 150 mL A stock and 150 mL B stock in 15 L RO water). Chemical components are separated into A/B designations to prevent formation of ionic precipitates in the stock solution, which would sequester essential nutrients out of solution, and thus decrease nutrient availability to the plants.

Nutrient			Mass (g) per 10 L stock		
Part	Name	Formula	Vegetative	Flowering	Fruiting
A	Iron EDDHA	Fe EDDHA	15.23	30.79	30.15
	Monoammonium Phosphate (MAP)	12-61-0	90.97	106.33	107.49
	Magnesium Nitrate (Hexahydrate)	Mg(NO3)2.6H2O	165.33	151.07	333.82
	Calcium Nitrate (Ag grade)	5Ca(NO3)2.NH4NO3.10H2O	431.83	629.02	455.26
B	Boric Acid	H3BO3	0.34	0.67	0.63
	Mn EDTA	MnEDTA	0.93	2.07	0.00
	Zinc Sulfate (Monohydrate)	ZnSO4.H2O	0.85	1.09	1.10
	Potassium Sulfate	K2SO4	243.94	270.08	426.05
	Sodium Molybdate (Dihydrate)	Na2MoO4.2H2O	0.05	0.26	0.25
	Copper Sulfate (pentahydrate)	CuSO4.5H2O	0.08	0.14	0.13

Supplementary Table B2. PCR reagents and primer sequences for separate amplification of 16S and ITS rRNA amplicons. All primers were obtained from Integrated DNA Technologies Inc (IDT, USA).

Reagent	Volume (µL)
2X Master Mix (FroggaBio, #FBTAQM)	10
Forward Primers (10 µM): 16S-27F: 5'-AGAGTTTGATCCTGGCTCAG-3' ITS1catta: 5'-ACCWGCGGARGGATCATTA-3'	1
Reverse Primers (10 µM): 16S 1492R: 5'-TACGGYTACCTTGTTACGACTT-3' ITS4ngsuni: 5'-CCTSCSCTTANTDATATGC-3'	1
UltraPure H_2O (Invitrogen, #10977015)	7
Template gDNA	1

Supplementary Table B3. PCR cycling specifications for amplification of 16S and ITS rRNA amplicons.

Cycle Specifications
1. Initial denaturation: 95 ºC, 5 min
2. Denaturation: 95 ºC, 45 s
3. Annealing: 57 ºC, 45 s for 16S amplicon; 47 ºC, 45 s for ITS amplicon
4. Elongation: 72 ºC, 1 min
5. Repeat steps 2-4 x 34 (35 cycles total)
6. Final elongation: 72 ºC, 5 minutes

Supplementary Table B4. Summary of bacterial differential abundance between soil and hydroponic sample groups. Effect size and FDR were calculated in ALDEx2 as previously described. Positive and negative effect size correspond to enrichment in hydroponic or soil samples, respectively. Taxa with effect size >|1| and FDR <0.05 are considered significantly differentially abundant. There are 60 significant differentially abundant bacterial genera between groups. "BCP Group" represents the tri-genus group *Burkholderia-Caballeronia-Paraburkholderia*.

Enriched in Soil Sample Group			Enriched in Hydroponic Sample Group		
Bacterial Genera	Effect Size	FDR p-value	Bacterial Genera	Effect Size	FDR p-value
Terrimicrobium	-2.12	0.001	Sphingobium	2.74	0.031
Micrococcus	-2.24	0.002	Hyphomicrobium	2.56	0.031
Luteolibacter	-2.3	0.002	Asticcacaulis	2.5	0.031
Gemmata	-2.31	0.002	Rhizomicrobium	2.43	0.03
Pedomicrobium	-2.12	0.003	Novosphingobium	2.31	0.06
Aquihabitans	-2.43	0.004	Shinella	2.07	0.032
Nocardioides	-2.05	0.005	Spirochaeta	1.95	0.041
Roseimicrobium	-2.13	0.005	Labrys	1.84	0.044
Ramlibacter	-2.51	0.005	Methylophilus	1.83	0.035
Rhodoplanes	-1.69	0.006	Rhodoferax	1.73	0.049
Stenotrophobacter	-1.96	0.009	Mucilaginibacter	1.69	0.052
Niabella	-1.93	0.01	Methylovorus	1.68	0.038
Labilithrix	-1.95	0.013	Chroococcopsis	1.67	0.036
Pseudonocardia	-2.05	0.014	Rhodanobacter	1.54	0.109
Flavisolibacter	-2.22	0.014	Phenylobacterium	1.54	0.076
Bradyrhizobium	-1.5	0.016	Devosia	1.46	0.051
Chryseolinea	-1.7	0.02	Ereboglobus	1.42	0.046
Flavobacterium	-1.71	0.02	Granulicella	1.36	0.091
Flavitalea	-1.64	0.021	BCP Group	1.3	0.109
Chthoniobacter	-1.69	0.021	Schlesneria	1.3	0.182
Ferruginibacter	-1.7	0.024	Micropepsis	1.3	0.076
Vibrio	-1.57	0.029	Stanieria PCC-7437	1.29	0.092
Sandaracinus	-2.17	0.03	Uliginosibacterium	1.28	0.099
Sorangium	-1.92	0.035	Acidicapsa	1.28	0.141
Fimbriiglobus	-1.72	0.036	Terriglobus	1.26	0.129
Lysobacter	-1.53	0.041	Solimonas	1.22	0.197
Ancylobacter	-1.62	0.047	Oleiharenicola	1.19	0.097
Aurantisolimonas	-1.4	0.053	Rhizobium	1.11	0.225
Micromonospora	-1.52	0.059	Methylobacillus	1.06	0.175
Oligoflexus	-1.44	0.079	Cephaloticoccus	1.06	0.23

Tundrisphaera	-1.25	0.087	Curvibacter	1.04	0.183
Candidatus Solibacter	-1.27	0.088	Oharaeibacter	1.03	0.206
Arthrobacter	-1.29	0.089	Acidocella	1.02	0.283
Pseudarthrobacter	-1.11	0.095	Flexilinea	1.02	0.281
Rhodoblastus	-1.24	0.098			
Aetherobacter	-1.17	0.108			
Caldilinea	-1.05	0.111			
Arboricoccus	-1.06	0.127			
Demequina	-1.09	0.148			
Blastopirellula	-1.27	0.152			
Achromobacter	-1.1	0.156			
Bryobacter	-1.08	0.165			
Parasegetibacter	-1.1	0.167			
Aeromicrobium	-1.05	0.196			
Chitinophaga	-1.15	0.221			
Ensifer	-1.02	0.28			
Conexibacter	-2.26	<0.001			
Reyranella	-2.67	<0.001			
Gemmatimonas	-2.69	<0.001			
Patulibacter	-2.78	<0.001			
Paenibacillus	-2.84	<0.001			
Parviterribacter	-2.93	<0.001			
Tepidisphaera	-3.13	<0.001			
Candidatus Anammoximicrobium	-3.14	<0.001			
Mycobacterium	-3.55	<0.001			
Candidatus Tremblaya	-3.65	<0.001			
Pirellula	-3.72	<0.001			
Zavarzinella	-3.75	<0.001			
Pseudorhodoplanes	-3.77	<0.001			
Ilumatobacter	-4.11	<0.001			
Methyloceanibacter	-4.31	<0.001			
Bacillus	-4.61	<0.001			
Vicinamibacter	-4.75	<0.001			
Microlunatus	-4.8	<0.001			
Microvirga	-4.93	<0.001			
Solirubrobacter	-5.99	<0.001			
Gaiella	-6.09	<0.001			

Supplementary Table B5. Summary of fungal/oomycete differential abundance between soil and hydroponic sample groups. Positive and negative effect size correspond to enrichment in hydroponic or soil samples, respectively. There are 51 differentially abundant fungal genera between groups.

Enriched in Soil Sample Group			Enriched in Hydroponic Sample Group		
Fungal Genera	Effect Size	FDR p-value	Fungal Genera	Effect Size	FDR p-value
Sistotrema	-1.02	0.074	Simocybe	3.14	0.017
Subulicystidium	-1.08	0.236	Achroceratosphaeria	3.09	0.017
Ophiostoma	-1.12	0.106	Tubeufia	2.72	0.017
Cladophialophora	-1.24	0.094	Rhodosporidiobolus	2.67	0.017
Fusarium	-1.35	0.072	Archaeorhizomyces	2.55	0.026
Mucor	-1.36	<0.001	Cutaneotrichosporon	2.54	0.018
Agroathelia	-1.48	0.026	Hohenbuehelia	2.42	0.023
Clonostachys	-1.49	0.004	Podospora	2.34	0.017
Dactylonectria	-1.51	0.04	Apiotrichum	2.25	0.024
Coprinopsis	-1.52	0.007	Atractospora	2.12	0.021
Rhizophagus	-1.6	0.003	Neohelicosporium	1.9	0.025
Ambispora	-1.64	0.102	Nectria	1.7	0.063
Chondrogaster	-1.7	0.011	Pascua	1.64	0.048
Colletotrichum	-1.95	0.02	Sporothrix	1.63	0.025
Syncephalis	-2.17	<0.001	Conlarium	1.48	0.062
Ganoderma	-2.3	0.003	Kirschsteiniothelia	1.42	0.077
Akanthomyces	-2.31	0.016	Pseudogymnoascus	1.36	0.069
Alternaria	-2.43	<0.001	Olpidium	1.33	0.122
Schizothecium	-2.5	<0.001	Leucosporidium	1.3	0.065
Betamyces	-2.59	<0.001	Cadophora	1.28	0.178
Trichoderma	-2.69	<0.001	Savoryella	1.28	0.066
Neosetophoma	-3.21	<0.001	Cuphophyllus	1.18	0.124
Psathyrella	-3.3	<0.001	Phytopythium	1.17	0.155
Cladosporium	-3.53	<0.001	Mycochaetophora	1.05	0.268
Clavaria	-3.65	<0.001			
Marquandomyces	-4.06	<0.001			
Globisporangium	-5.77	<0.001			

Supplementary Table B6. Summary of effect size and FDR for significant differentially abundant bacterial genera between growth states. Effect size and FDR calculated in ALDEx2 as previously described. Taxa with effect size >|1| and FDR <0.05 are considered significantly differentially abundant.

Taxon	Enriched In...	Relative To...	|Effect Size|	FDR
Methylotenera	Vegetative	Fruiting	1.000461657	3.67E-06
Edaphobaculum	Flowering	Fruiting	1.021547712	6.56E-04
Amaricoccus	Fruiting	Vegetative	1.017669565	1.33E-06
Polyangium	Fruiting	Vegetative	1.168211688	2.81E-07

Supplementary Table B7. Summary of microbial differential abundance between week two and week eight sample groups. Effect size and FDR were calculated in ALDEx2 as previously described. Taxa with effect size >|1| and FDR <0.05 are considered significantly differentially abundant. Taxa are listed in order of most-positive to most-negative effect size. Positive and negative effect size correspond to enrichment in week eight or week two, respectively. There are 22 differentially abundant bacterial genera and 9 differentially abundant fungal genera.

Bacterial Genera	Effect Size	FDR p-value	Fungal Genera	Effect Size	FDR p-value
Polyangium	2.06	<0.001	Nectria	1.54	<0.001
Amaricoccus	1.38	<0.001	Hohenbuehelia	1.48	<0.001
Solirubrobacter	1.28	<0.001	Cutaneotrichosporon	1.25	<0.001
Chondromyces	1.28	<0.001	Rhodosporidiobolus	1.04	<0.001
Candidatus Solibacter	1.21	<0.001	Mortierella	-1.07	<0.001
Oleiharenicola	1.21	<0.001	Ophiostoma	-1.17	<0.001
Candidatus Obscuribacter	1.21	<0.001	Aspergillus	-1.28	<0.001
Schlesneria	1.13	<0.001	Trechispora	-1.3	<0.001
Zoogloea	1.12	<0.001	Clavaria	-1.42	<0.001
Mariniblastus	1.11	<0.001			
Pseudaminobacter	1.1	<0.001			
Skermanella	1.1	<0.001			
Gimesia	1.05	<0.001			
Natronohydrobacter	1.02	<0.001			
Acidovorax	-1.04	<0.001			
Nemorincola	-1.1	<0.001			
Asticcacaulis	-1.12	<0.001			
Comamonas	-1.25	<0.001			
Methylobacillus	-1.25	<0.001			
Luteolibacter	-1.27	<0.001			
Delftia	-1.3	<0.001			
Methylotenera	-1.33	<0.001			

Supplementary Table B8. Summary of yield and vegetative growth results for plants selected for analysis. Briefly, six plants per treatment were selected for inclusion in sequencing analysis according to the following parameters: three high-yielding and three-low yielding plants per treatment, all from separate pots, with an additional constraint that two plants from each yield category were located on the bottom-rack of the hydroponic system and one was from the top-rack to account for possible microbiome differences due to differences in irrigation volume.

Treatment	Plant	Total Yield (g)	Total Yield (count)	Shoot Fresh Weight (g)	Shoot Height (cm)
Control	8	123.24	10	175.5	39.12
	10	67.20	8	144.5	34.93
	13	46.17	2	124.4	39.37
	18	65.41	6	67.2	33.02
	20	117.66	9	236.2	40.64
	23	42.95	3	146.1	35.31
Field	2	38.66	7	188.9	38.1
	12	168.83	7	142.9	34.29
	16	154.76	13	138.4	35.56
	17	0.00	0	197.2	34.54
	20	255.52	20	292.5	40.39
	22	1.88	1	132.9	39.37
Garden	1	50.90	4	118.2	41.66
	7	158.37	10	113.3	39.12
	15	146.38	13	97.6	34.29
	19	74.87	5	229.9	43.18
	21	153.56	11	114.4	33.78
	23	41.21	6	120.6	42.16
Wetland	2	69.44	4	144.5	31.24
	7	190.24	16	158.3	39.37
	16	179.82	11	169.2	36.07
	18	97.16	7	30.2	22.23
	19	119.29	9	168.0	33.78
	22	46.97	5	121.5	31.75

Supplementary Table B9. Nutrient content (ppm) in soil samples and hydroponic nutrient solution. Hydroponic reservoirs contained 15 L of vegetative nutrient solution at time of inoculation. Soil nutrient quantification was performed by A&L Canada Laboratories (London, Ontario, Canada).

Sample	K	P	Fe	Mg	Ca	B	Mn	Zn	S	Na	Cu
Vegetative Nutrient Solution	22.86	106.85	0.85	14.64	0.02	0.06	0.13	0.3	43.97	0.01	0.02
Field	0.57	0.15	0.23	0.97	7.48	0.004	0.28	0.04	0.05	0.09	0.004
Wetland	0.23	0.05	0.14	0.38	5.03	0.002	0.12	0.02	0.01	0.03	0.003
Garden	0.13	0.06	0.14	0.42	4.4	0.003	0.08	0.03	0.03	0.04	0.005

Appendix C: Full-Resolution Figures

The following appendix contains single-panel full-resolution versions of all multi-panel figures included in the body of this manuscript to maximize interpretability. An appendix-specific list of figures is presented below:

Figure 3.1A. Pairwise principal component analysis (PCA) for genus-level 16S CLR abundance data from control and Field treatment groups at week eight……. 121
Figure 3.1B. Pairwise principal component analysis (PCA) for genus-level 16S CLR abundance data from control and Garden treatment groups at week eight……. 122
Figure 3.1C. Pairwise principal component analysis (PCA) for genus-level 16S CLR abundance data from control and Wetland treatment treatment groups at week eight….. 123
Figure 3.1D. ALDEx2 effect plot for genus-level 16S CLR abundance data from control and Field treatment groups at week eight……... 124
Figure 3.1E. ALDEx2 effect plot for genus-level 16S CLR abundance data from control and Garden treatment groups at week eight…… 125
Figure 3.1F. ALDEx2 effect plot for genus-level 16S CLR abundance data from control and Wetland treatment groups at week eight…….. 126
Figure 3.2A. Pairwise principal component analysis (PCA) for genus-level ITS CLR abundance data from control and Field treatment groups at week eight……. 127
Figure 3.2B. Pairwise principal component analysis (PCA) for genus-level ITS CLR abundance data from control and Garden treatment groups at week eight……. 128
Figure 3.2C. Pairwise principal component analysis (PCA) for genus-level ITS CLR abundance data from control and Wetland treatment groups at week eight…… 129
Figure 3.2D. ALDEx2 effect plot for genus-level ITS CLR abundance data from control and Field treatment groups at week eight……... 130
Figure 3.2E. ALDEx2 effect plot for genus-level ITS CLR abundance data from control and Garden treatment groups at week eight…… 131
Figure 3.2F. ALDEx2 effect plot for genus-level ITS CLR abundance data from control and Wetland treatment groups at week eight…….. 132
Figure 4.1A. Principal component analysis (PCA) for genus-level 16S CLR abundance data from initial soil samples and week eight inoculated hydroponic root samples……... 133
Figure 4.1B. ALDEx2 effect plot for genus-level 16S CLR abundance data from initial soil samples and week eight inoculated root samples……. 134
Figure 4.2A. Principal component analysis (PCA) for genus-level ITS CLR abundance data from initial soil samples and week eight inoculated hydroponic root samples…… 135
Figure 4.2B. ALDEx2 effect plot for genus-level ITS CLR abundance data from initial soil samples and week eight inoculated root samples……. 136
Figure 6.1A. Stacked bar chart of genus-level bacterial relative abundance in each baseline microbiome sample……... 137
Figure 6.1B. Heat map of genus-level bacterial community composition in each baseline microbiome sample……... 138
Figure 6.2A. Stacked bar chart of genus-level fungal/oomycete relative abundance in each baseline microbiome sample……... 139

Figure 6.2B. Heat map of genus-level fungal/oomycete community composition in each baseline microbiome sample……... 140
Figure 8.1A. Stacked bar chart summary of hydroponic strawberry rhizomicrobiome bacterial composition with respect to growth stage…… 141
Figure 8.1B. Prevalence-abundance plot of bacterial genera across all growth stages…. 142
Figure 8.1C. Core occupancy heat map of prevalence and abundance of bacterial genera across all growth stages……... 143
Figure 8.2A. Stacked bar chart summary of hydroponic strawberry rhizomicrobiome fungal/oomycete composition with respect to growth stage……... 144
Figure 8.2B. Prevalence-abundance plot of fungal/oomycete genera across all growth stages……... 145
Figure 8.2C. Core occupancy heat map of prevalence and abundance of fungal/oomycete genera across all growth stages……... 146
Figure 9.1A. Principal component analysis (PCA) of species-level 16S CLR-abundance at four biweekly timepoints……. 147
Figure 9.1B. ALDEx2 effect plot for genus-level 16S CLR abundance data at week two and week eight…….. 148
Figure 9.1C. Stacked bar chart summary of hydroponic strawberry rhizomicrobiome bacterial composition with respect to time in weeks…….. 149
Figure 9.2A. Principal component analysis (PCA) of species-level ITS CLR-abundance at four biweekly timepoints……. 150
Figure 9.2B. ALDEx2 effect plot for genus-level ITS CLR abundance data at week two and week eight……. 151
Figure 9.2C. Stacked bar chart summary of hydroponic strawberry rhizomicrobiome fungal/oomycete composition with respect to time in weeks……. 152
Figure 10.1A. Principal component analysis (PCA) of species-level 16S CLR abundance data for high- and low-yielding groups……. 153
Figure 10.1B. ALDEx2 effect plot for species-level 16S CLR abundance data for high- and low-yielding groups…….. 154
Figure 10.1C. Volcano plot of associations between yield (g) and 16S CLR abundance…… 155
Figure 10.2A. Principal component analysis (PCA) of species-level ITS CLR abundance data for high- and low-yielding groups……. 156
Figure 10.2B. ALDEx2 effect plot for species-level ITS CLR abundance data for high- and low-yielding groups…….. 157
Figure 10.2C. Volcano plot of associations between yield (g) and ITS CLR abundance…… 158

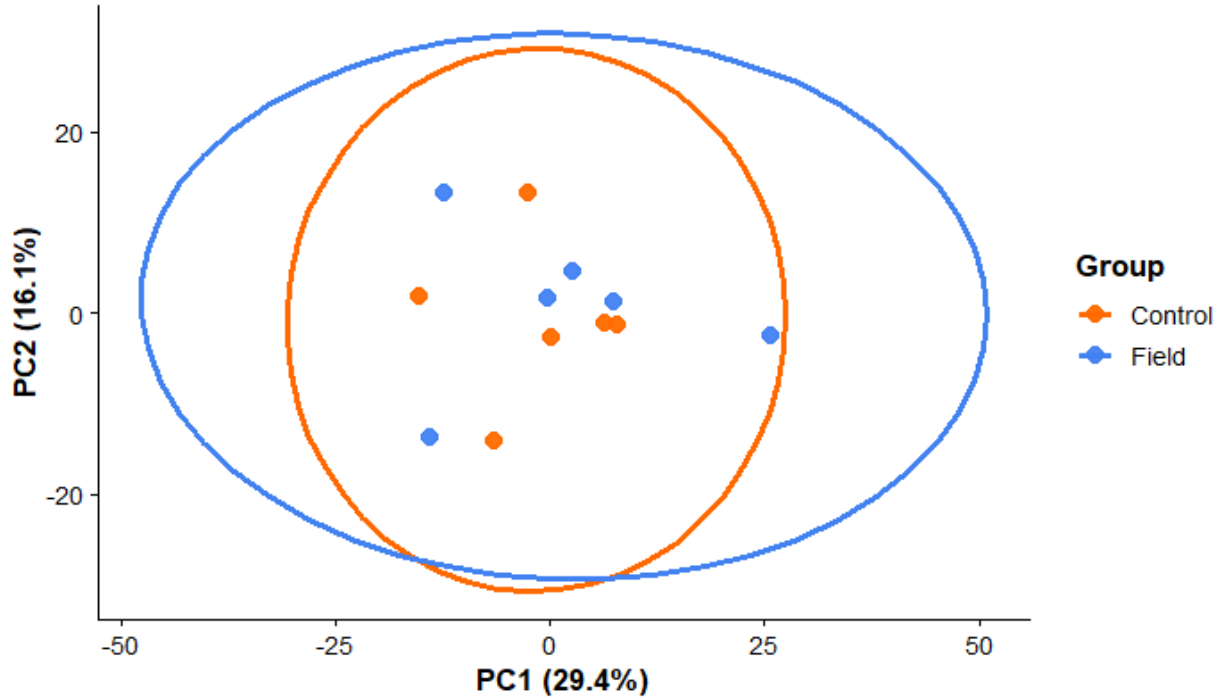


Figure 3.1A. Pairwise principal component analysis (PCA) for genus-level 16S CLR abundance data from control and Field treatment groups at week eight. Each point represents the bacterial community of one sample; orange and blue ellipses represent 95% confidence intervals for control (n = 6) and Field groups (n = 6), respectively.

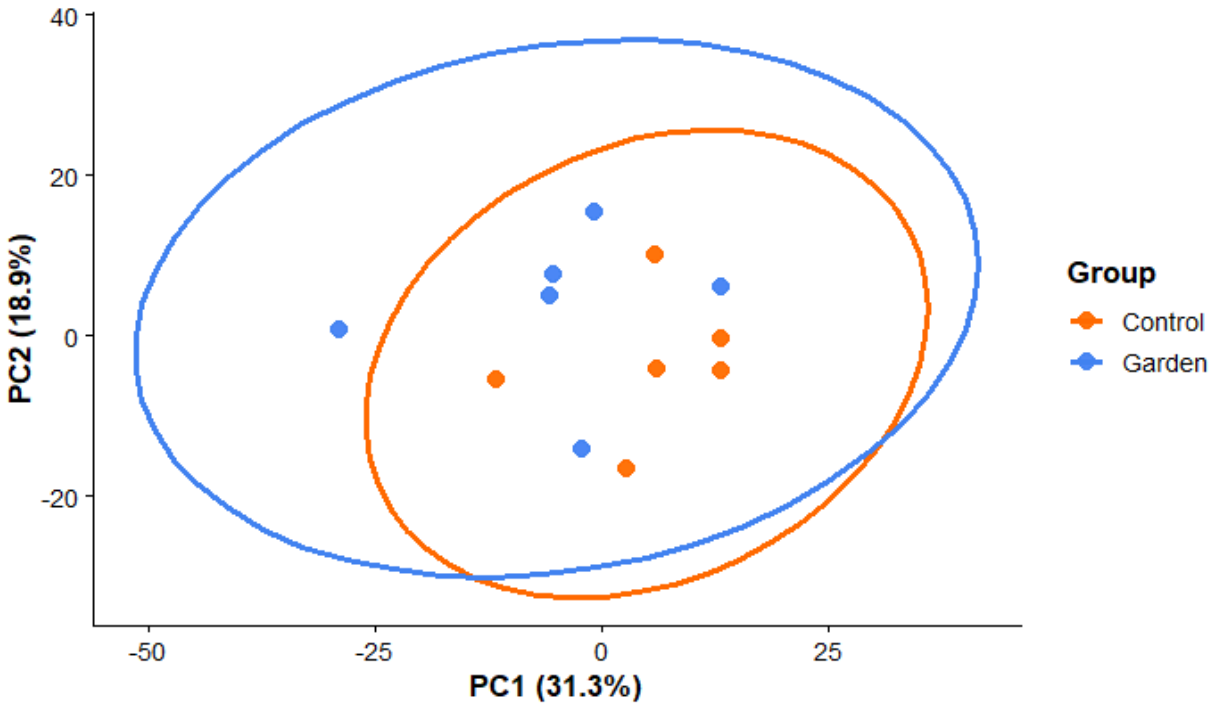


Figure 3.1B. Pairwise principal component analysis (PCA) for genus-level 16S CLR abundance data from control and Garden treatment groups at week eight. Each point represents the bacterial community of one sample; orange and blue ellipses represent 95% confidence intervals for control (n = 6) and garden treatment groups (n = 6), respectively.

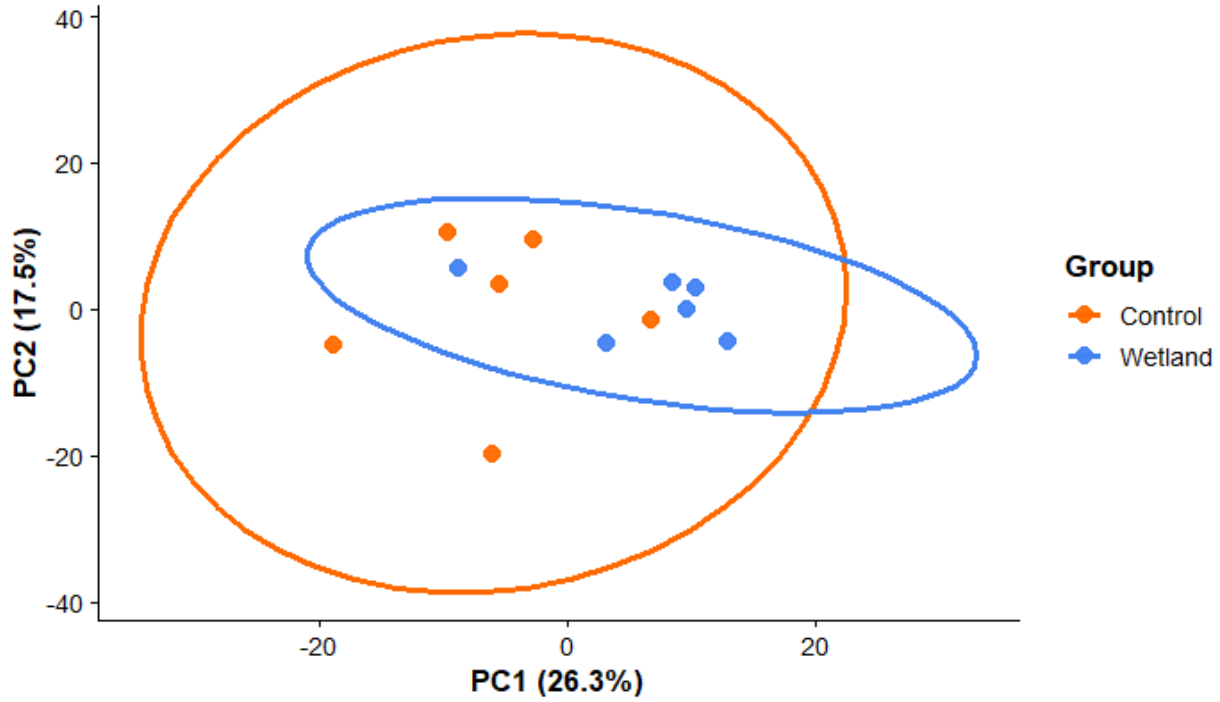


Figure 3.1C. Pairwise principal component analysis (PCA) for genus-level 16S CLR abundance data from control and Wetland treatment treatment groups at week eight. Each point represents the bacterial community of one sample; orange and blue ellipses represent 95% confidence intervals for control (n = 6) and Wetland treatment groups (n = 6), respectively.

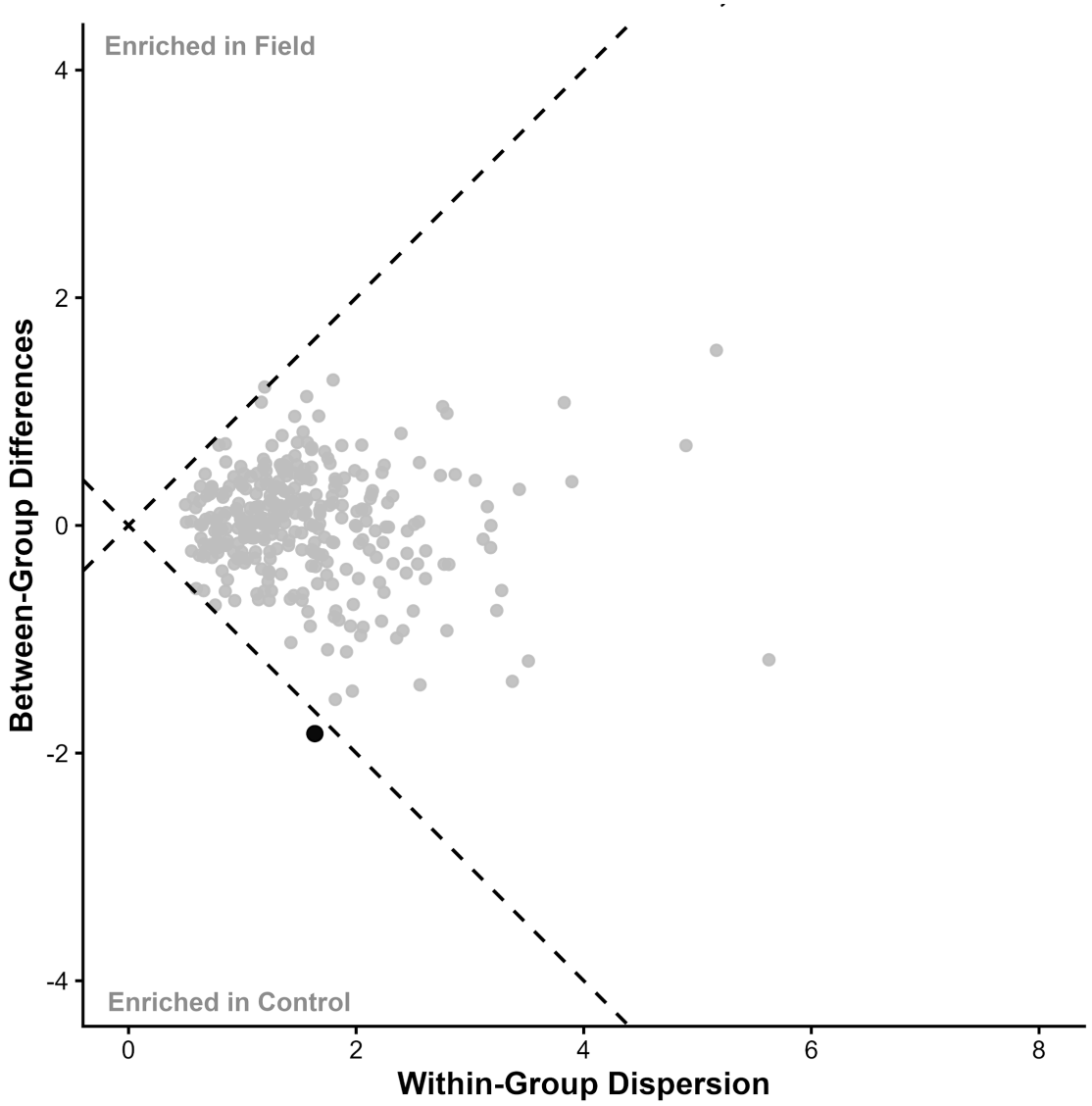


Figure 3.1D. ALDEx2 effect plot for genus-level 16S CLR abundance data from control and Field treatment groups at week eight. Each point represents a genus plotted according to between-group difference and within-group dispersion. Black points indicate genera with effect size >|1| and FDR >0.05. Red points, though none are identified in this analysis, indicate genera with effect size >|1| and FDR <0.05.

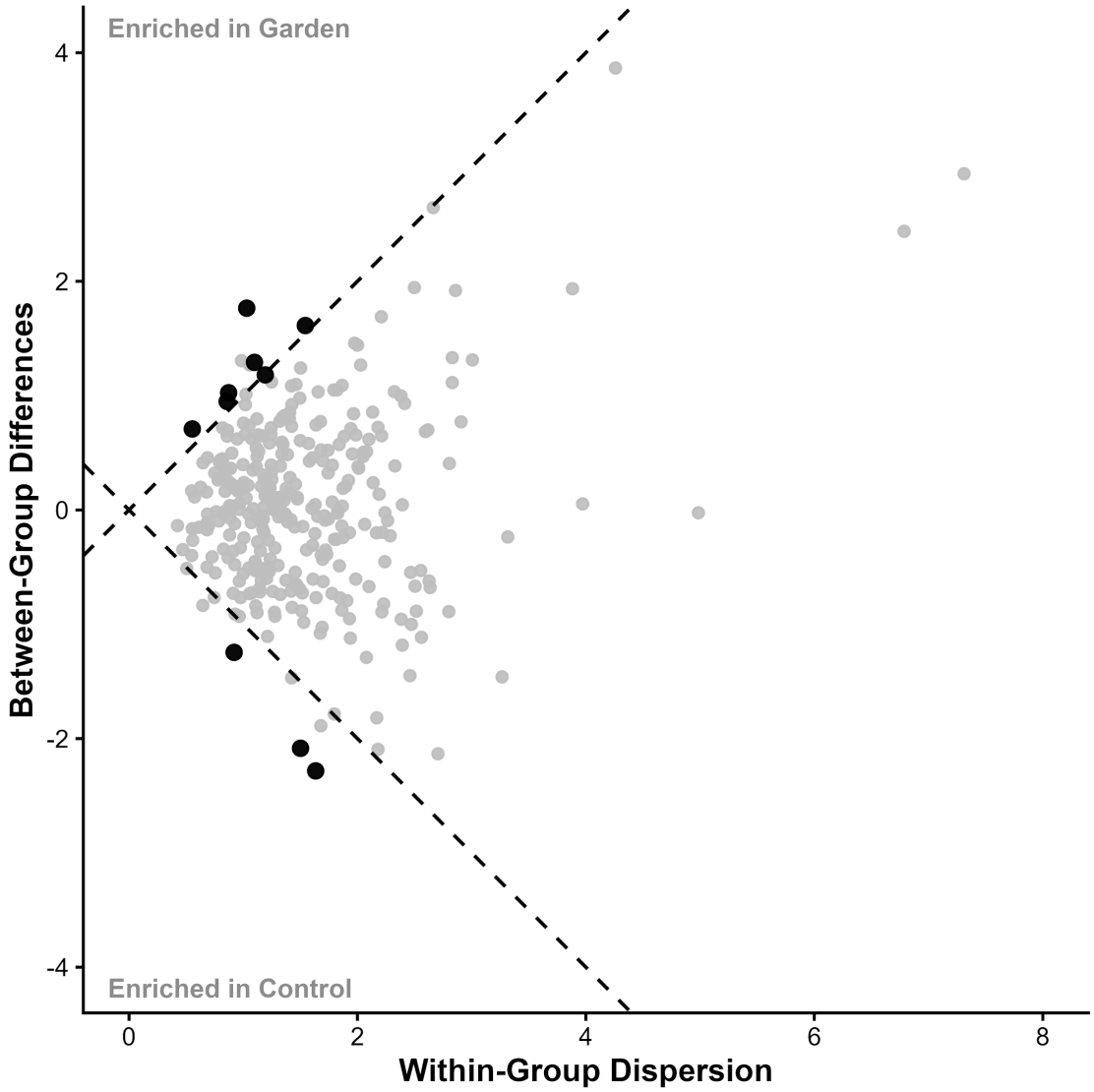


Figure 3.1E. ALDEx2 effect plot for genus-level 16S CLR abundance data from control and Garden treatment groups at week eight. Each point represents a genus plotted according to between-group difference and within-group dispersion. Black points indicate genera with effect size >|1| and FDR >0.05. Red points, though none are identified in this analysis, indicate genera with effect size >|1| and FDR <0.05.

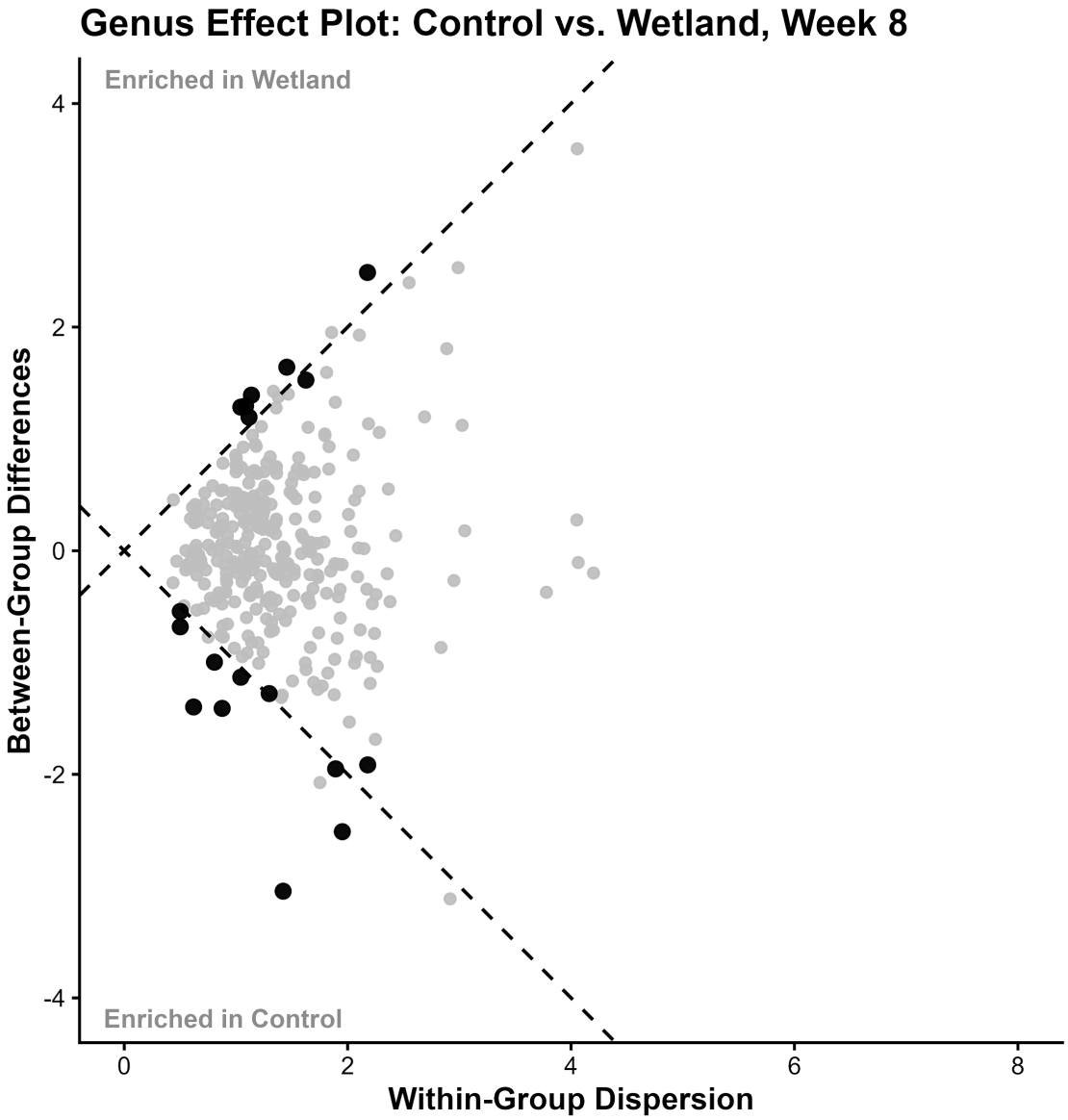


Figure 3.1F. ALDEx2 effect plot for genus-level 16S CLR abundance data from control and Wetland treatment groups at week eight. Each point represents a genus plotted according to between-group difference and within-group dispersion. Black points indicate genera with effect size >|1| and FDR >0.05. Red points, though none are identified in this analysis, indicate genera with effect size >|1| and FDR <0.05.

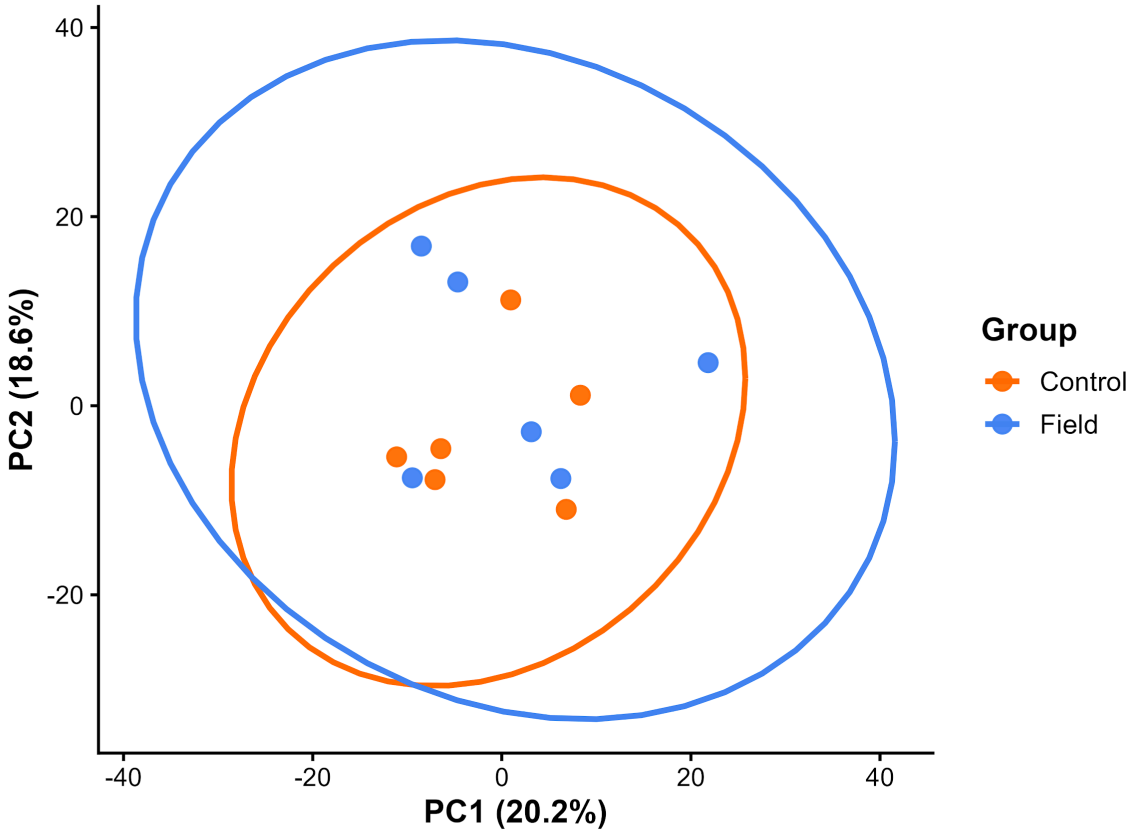


Figure 3.2A. Pairwise principal component analysis (PCA) for genus-level ITS CLR abundance data from control and Field treatment groups at week eight. Each point represents the fungal/oomycete community of one sample; orange and blue ellipses represent 95% confidence intervals for control (n = 6) and Field treatment groups (n = 6), respectively.

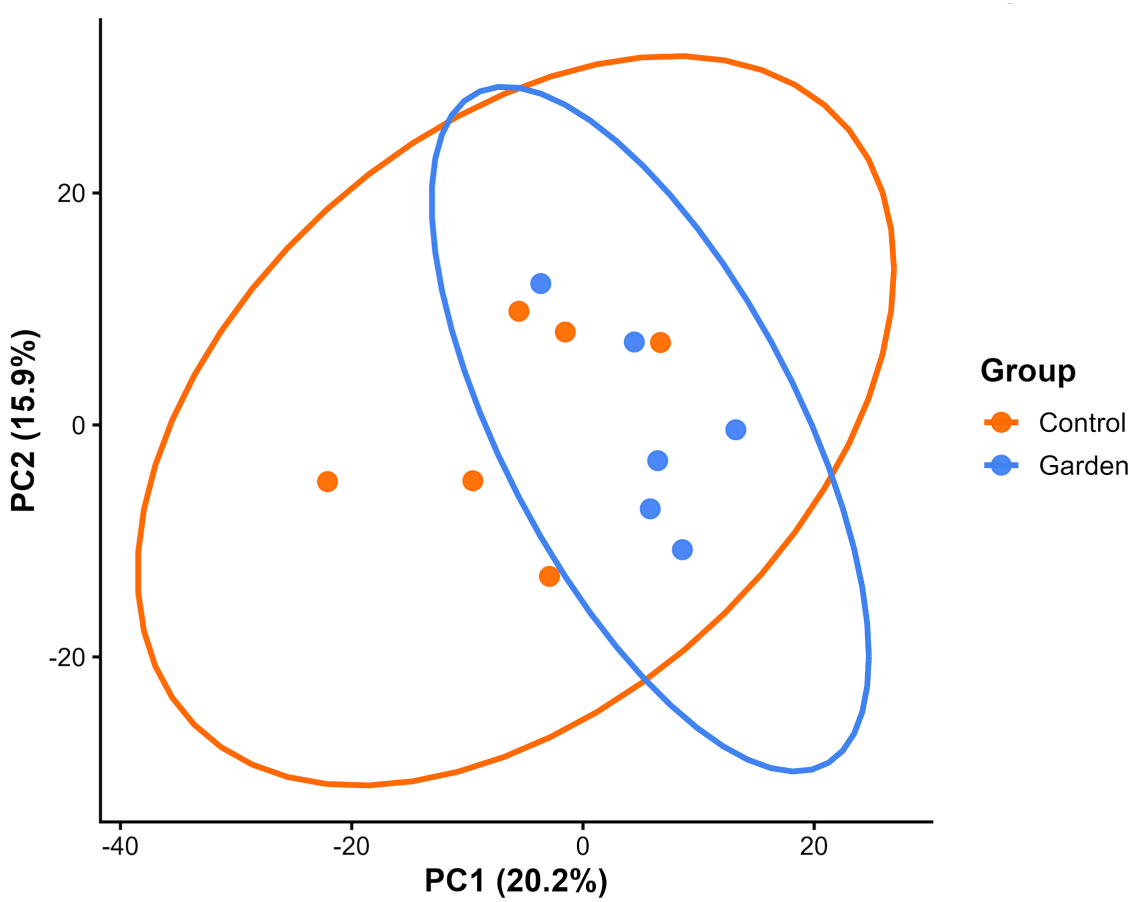


Figure 3.2B. Pairwise principal component analysis (PCA) for genus-level ITS CLR abundance data from control and Garden treatment groups at week eight. Each point represents the fungal/oomycete community of one sample; orange and blue ellipses represent 95% confidence intervals for control (n = 6) and Garden treatment groups (n = 6), respectively.

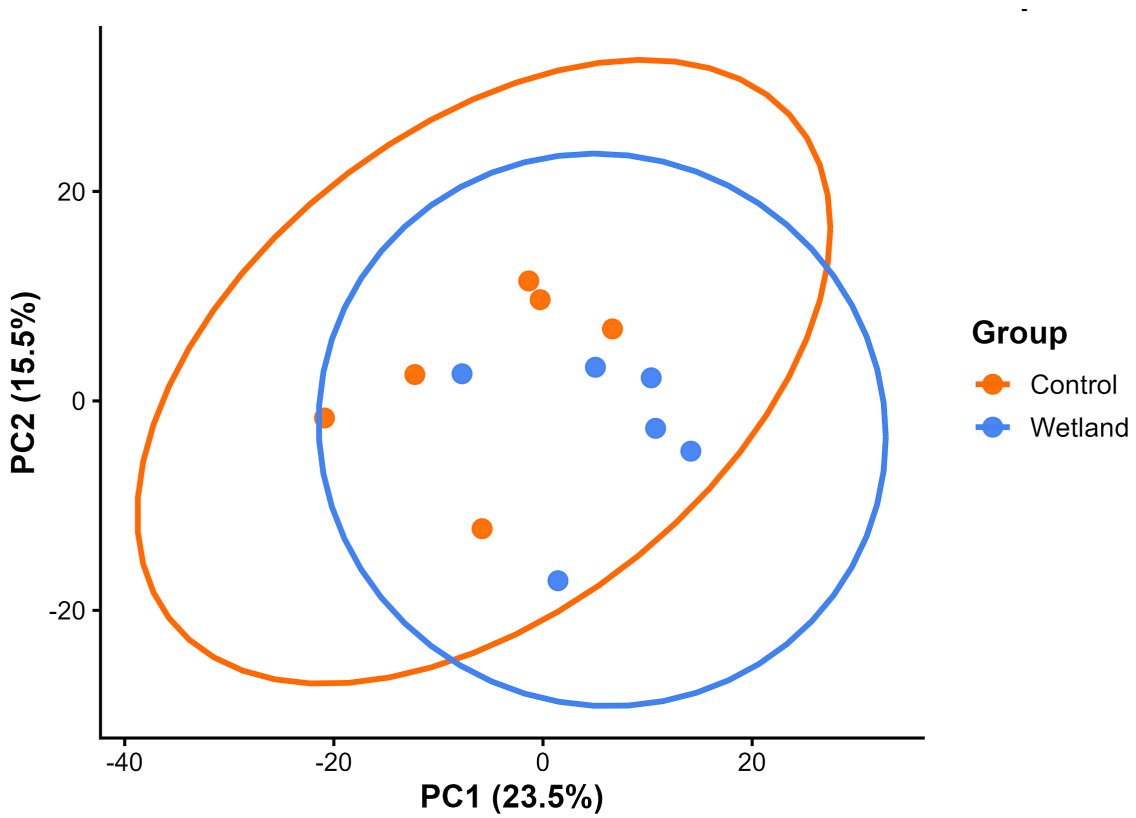


Figure 3.2C. Pairwise principal component analysis (PCA) for genus-level ITS CLR abundance data from control and Wetland treatment groups at week eight. Each point represents the fungal/oomycete community of one sample; orange and blue ellipses represent 95% confidence intervals for control (n = 6) and Wetland treatment groups (n = 6), respectively.

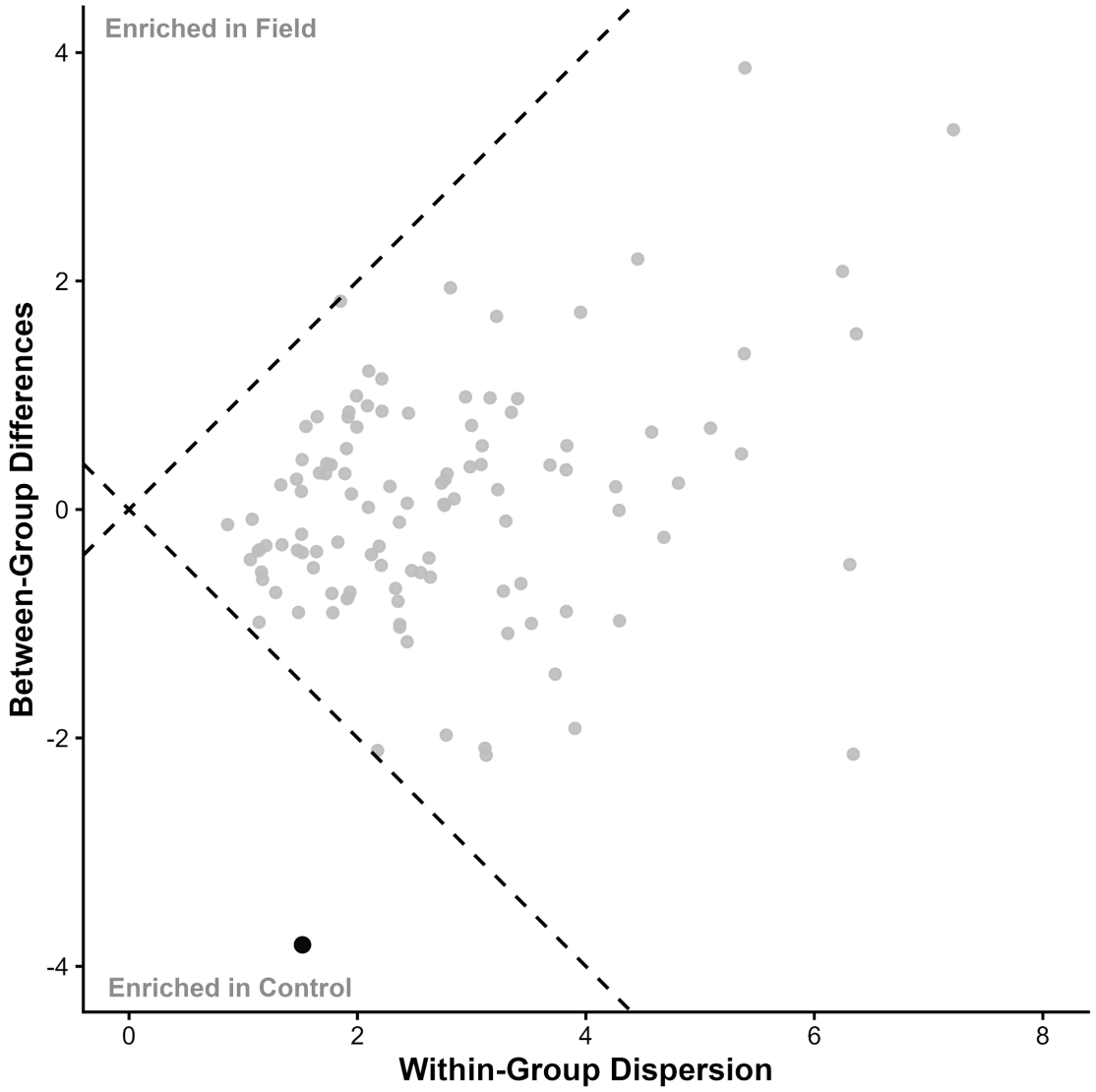


Figure 3.2D. ALDEx2 effect plot for genus-level ITS CLR abundance data from control and Field treatment groups at week eight. Each point represents a genus plotted according to between-group difference and within-group dispersion. Black points indicate genera with effect size >|1| and FDR >0.05. Red points, though none are identified in this analysis, indicate genera with effect size >|1| and FDR <0.05.

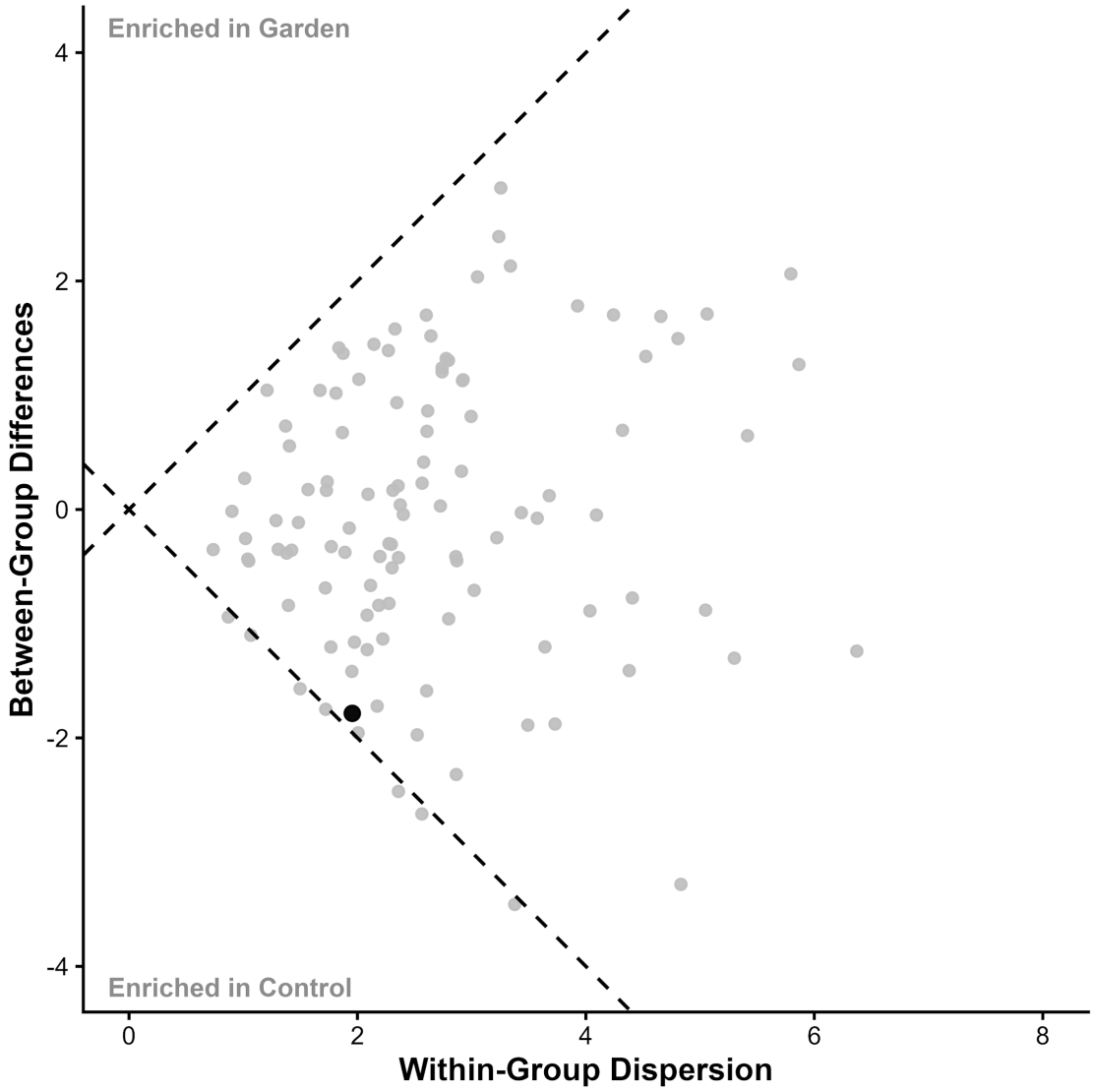


Figure 3.2E. ALDEx2 effect plot for genus-level ITS CLR abundance data from control and Garden treatment groups at week eight. Each point represents a genus plotted according to between-group difference and within-group dispersion. Black points indicate genera with effect size >|1| and FDR >0.05. Red points, though none are identified in this analysis, indicate genera with effect size >|1| and FDR <0.05.

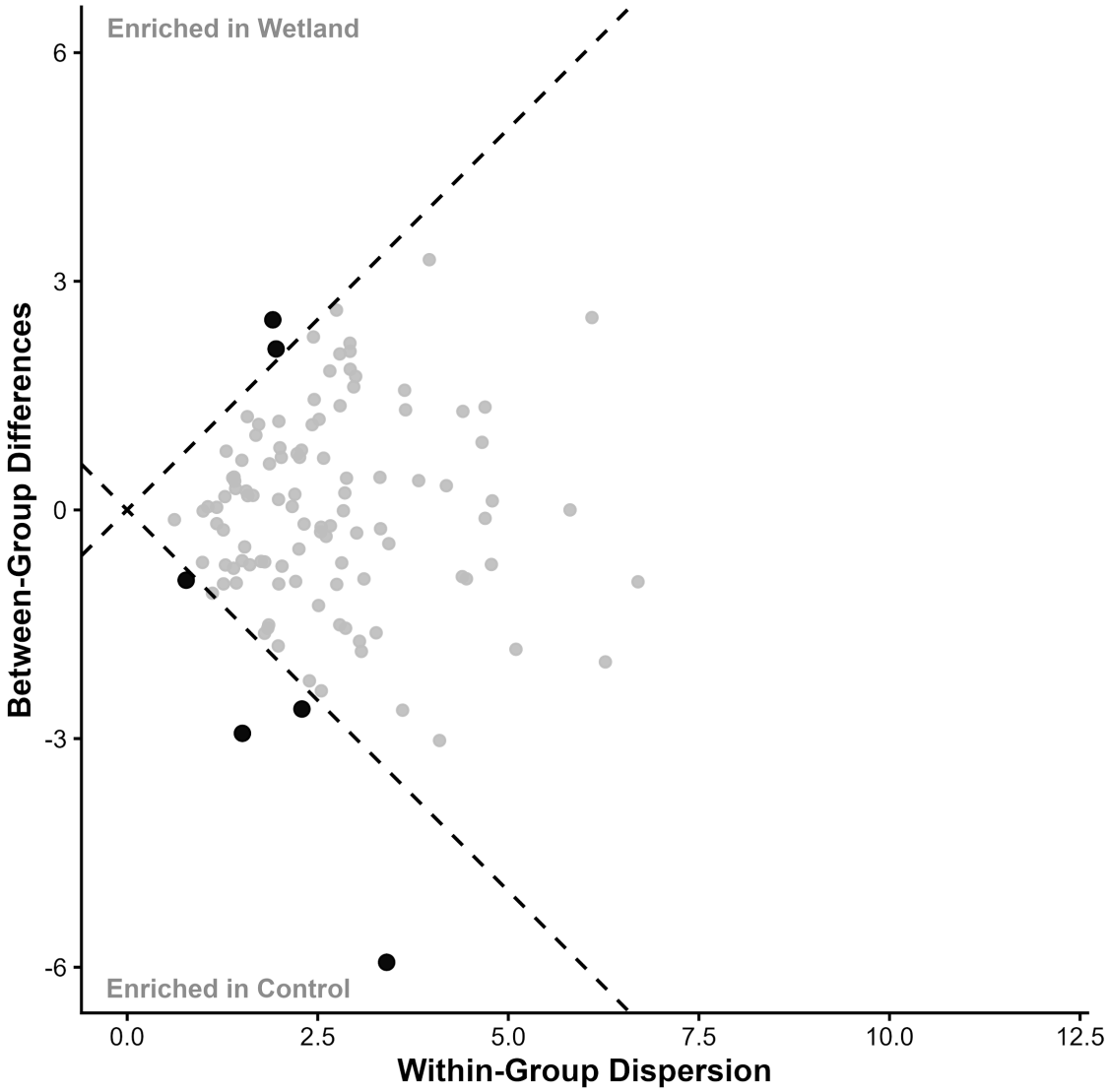


Figure 3.2F. ALDEx2 effect plot for genus-level ITS CLR abundance data from control and Wetland treatment groups at week eight. Each point represents a genus plotted according to between-group difference and within-group dispersion. Black points indicate genera with effect size >|1| and FDR >0.05. Red points, though none are identified in this analysis, indicate genera with effect size >|1| and FDR <0.05.

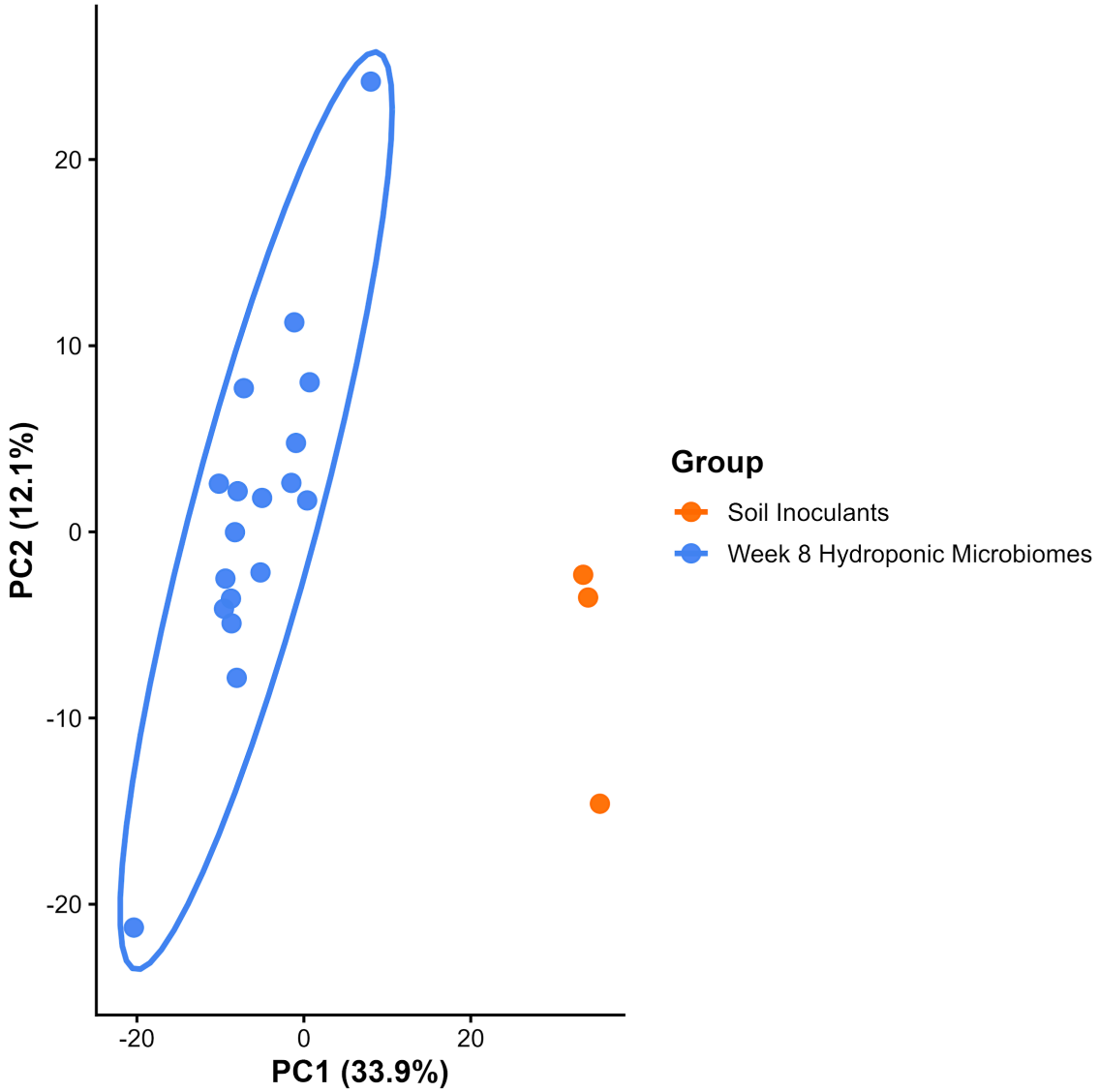


Figure 4.1A. Principal component analysis (PCA) for genus-level 16S CLR abundance data from initial soil samples and week eight inoculated hydroponic root samples. Each point represents the bacterial community of one sample. Week eight hydroponic samples are coloured in blue. Soil samples are coloured in orange and lack an ellipse due to small sample size.

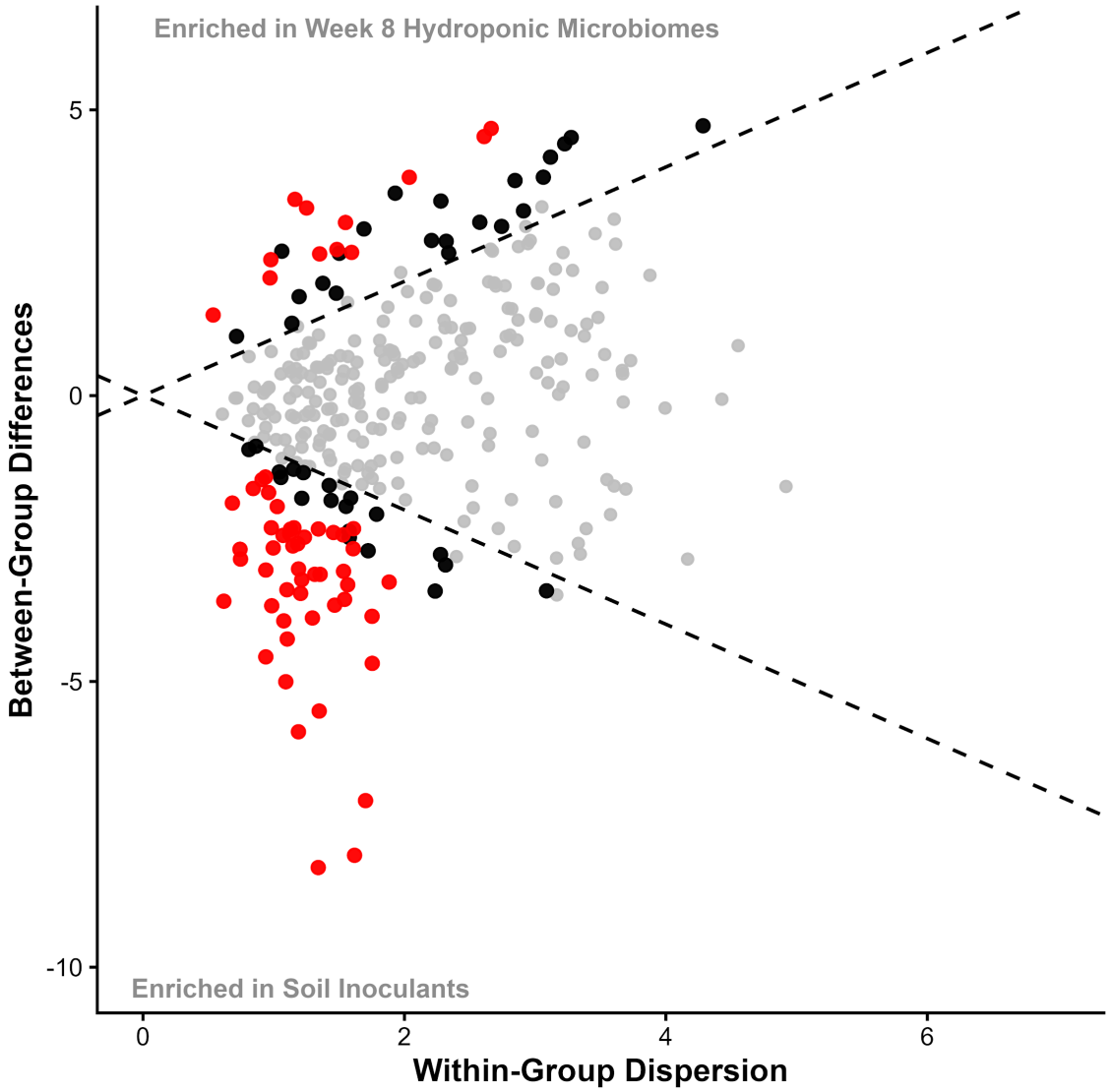


Figure 4.1B. ALDEx2 effect plot for genus-level 16S CLR abundance data from initial soil samples and week eight inoculated root samples. Each point represents a genus plotted according to between-group difference and within-group dispersion. Location of points outside of the dashed lines indicates enrichment of that taxon in one group, relative to the other, as labelled on the effect plot. Both black and grey points indicate statistical insignificance (FDR >0.05). Black points indicate genera with effect size >|1|, while grey points indicate genera with effect size <|1|. Red points indicate significant differentially abundant genera, with effect size >|1| and FDR <0.05.

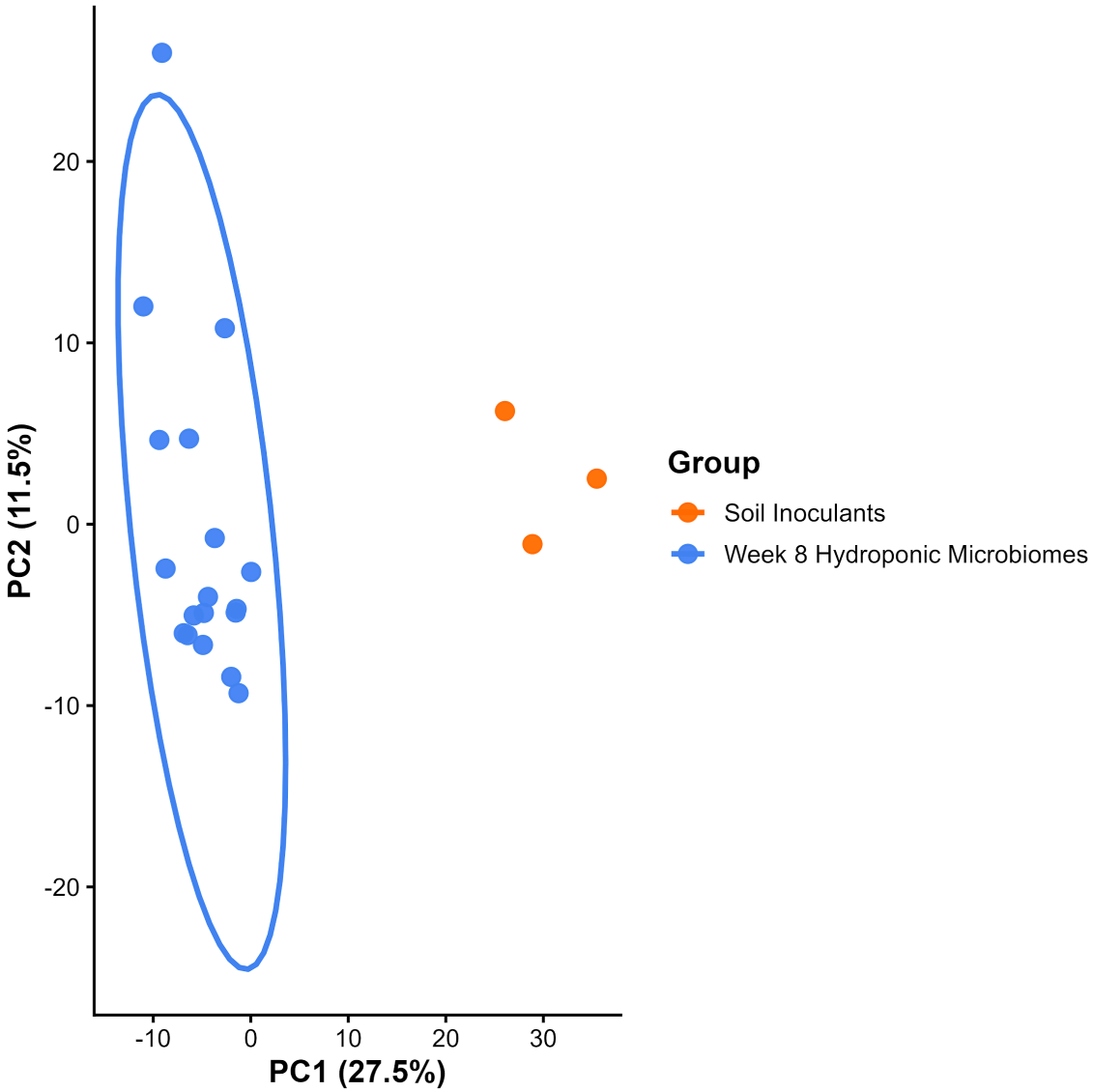


Figure 4.2A. Principal component analysis (PCA) for genus-level ITS CLR abundance data from initial soil samples and week eight inoculated hydroponic root samples. Each point represents the fungal/oomycete community of one sample. Week eight hydroponic samples are coloured in blue. Soil samples are coloured in orange and lack an ellipse due to small sample size.

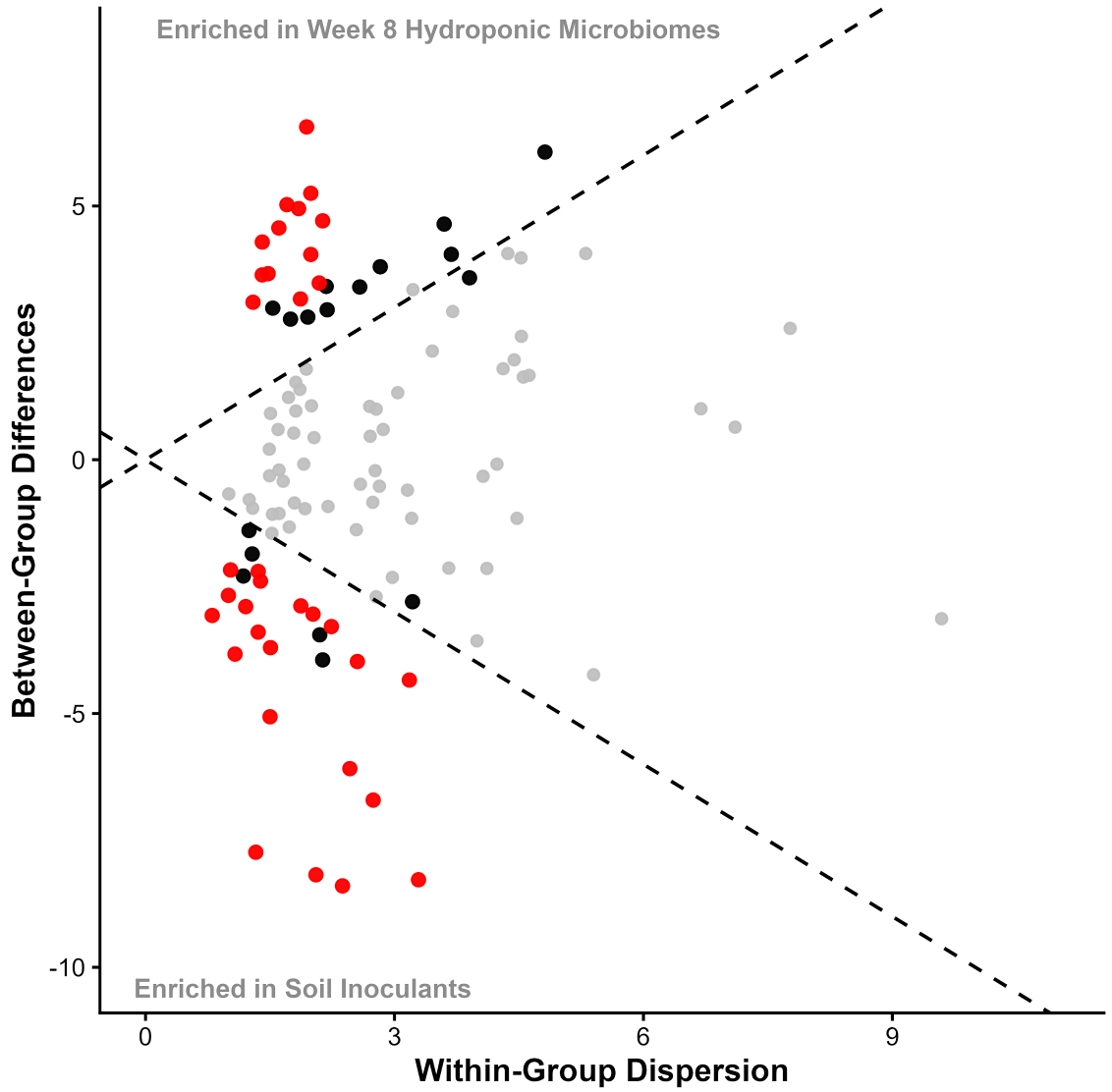


Figure 4.2B. ALDEx2 effect plot for genus-level ITS CLR abundance data from initial soil samples and week eight inoculated root samples. Each point represents a genus plotted according to between-group difference and within-group dispersion. Location of points outside of the dashed lines indicates enrichment of that taxon in one group, relative to the other, as labelled on the effect plot. Both black and grey points indicate statistical insignificance (FDR >0.05). Black points indicate genera with effect size >|1|, while grey points indicate genera with effect size <|1|. Red points indicate significant differentially abundant genera, with effect size >|1| and FDR <0.05.

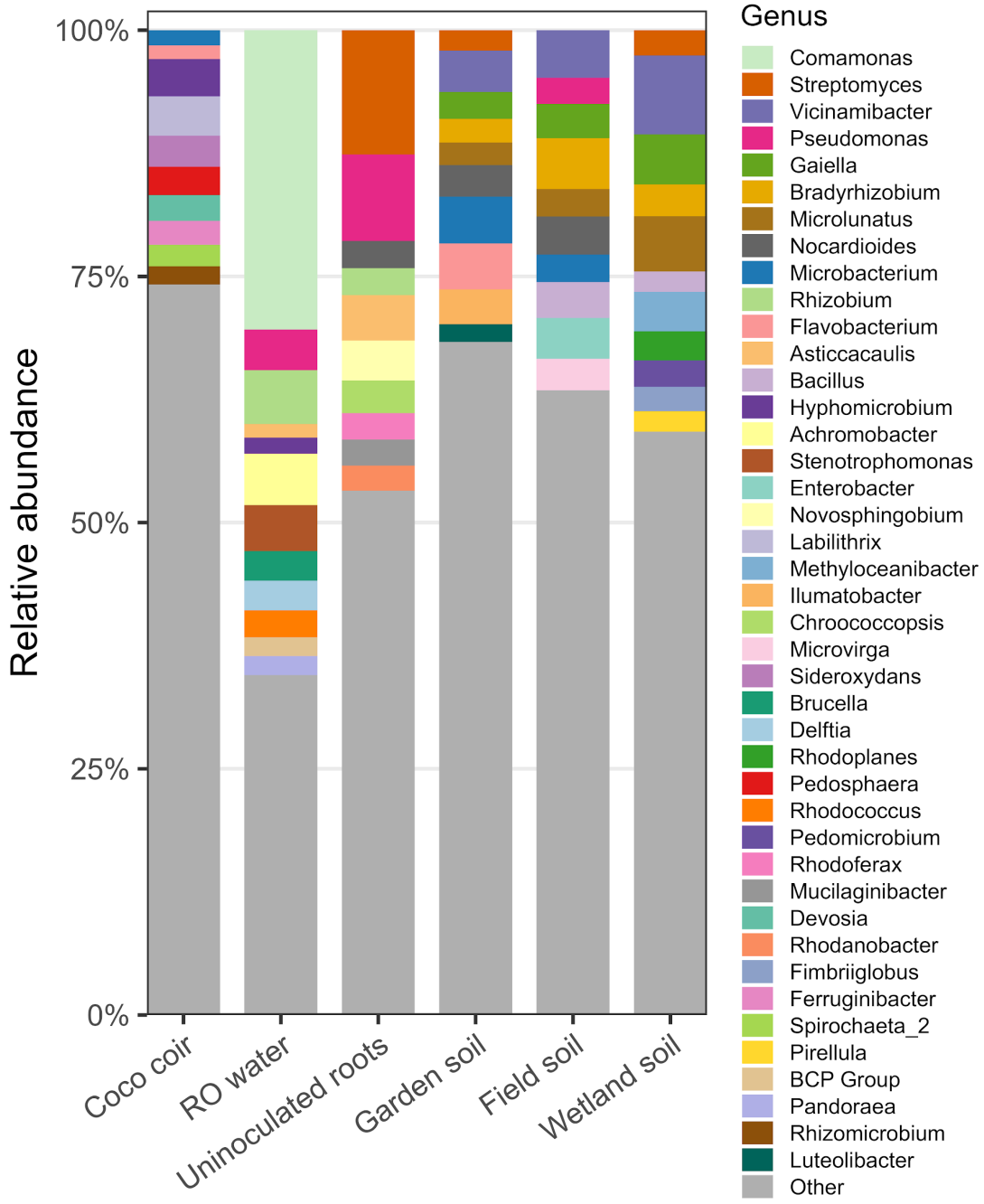


Figure 6.1A. Stacked bar chart of genus-level bacterial relative abundance in each baseline microbiome sample. Relative abundance (%) is displayed for the 10 most relatively abundant bacterial genera; all others are collapsed into the "Other" category. Note, "BCP Group" is an acronym for the tri-genus group "*Burkholderia- Caballeronia-Paraburkholderia*."

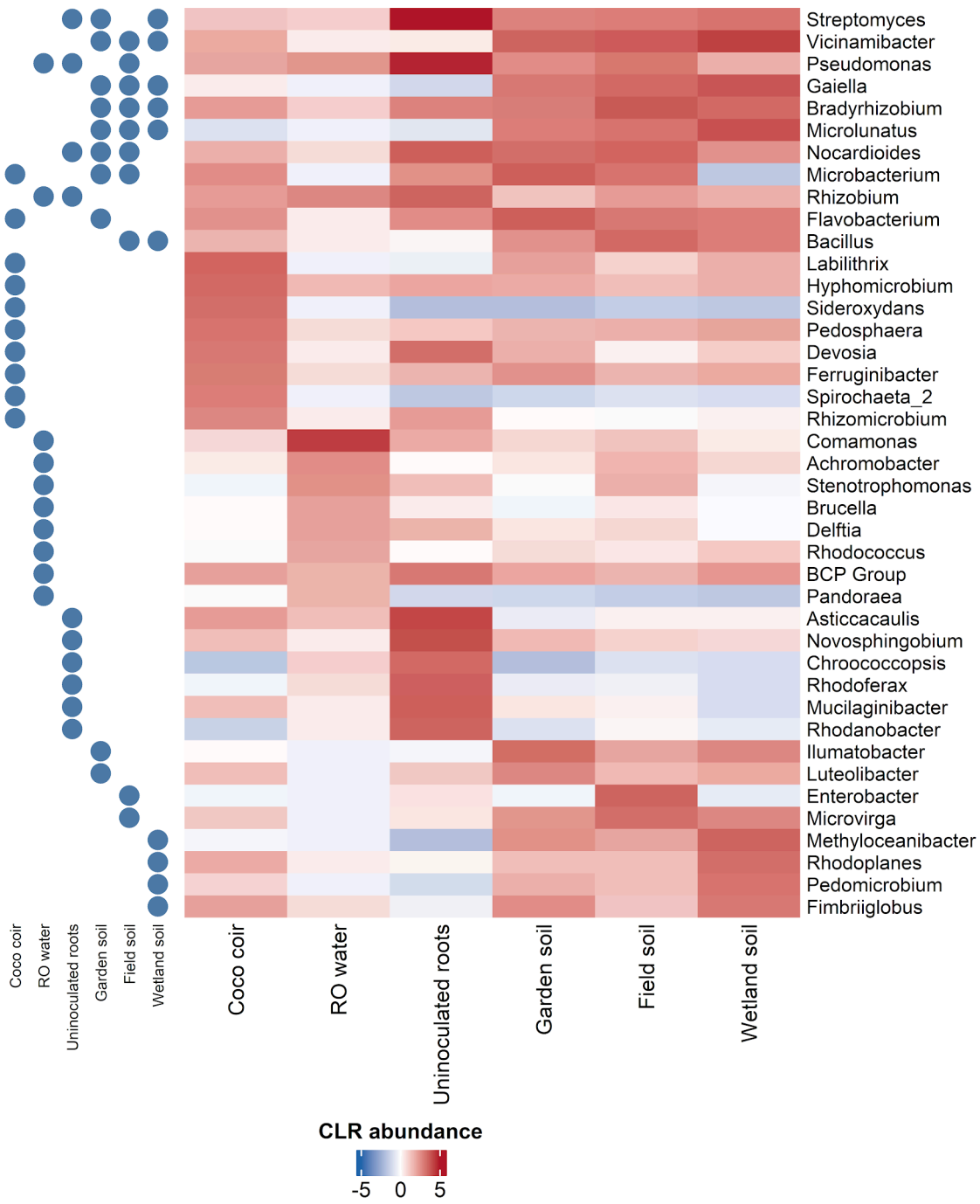


Figure 6.1B. Heat map of genus-level bacterial community composition in each baseline microbiome sample. Each row represents one of the top ten most relatively abundant genera identified in Figure 6.1A. In the dot-map (left), dot indicates which baseline communities each taxa was within the top ten genera for relative abundance. Tile colours of red and blue indicate high or low CLR abundance per sample, which can be interpreted in relative terms, as higher or lower than the geometric mean abundance (white) of the dataset, respectively.

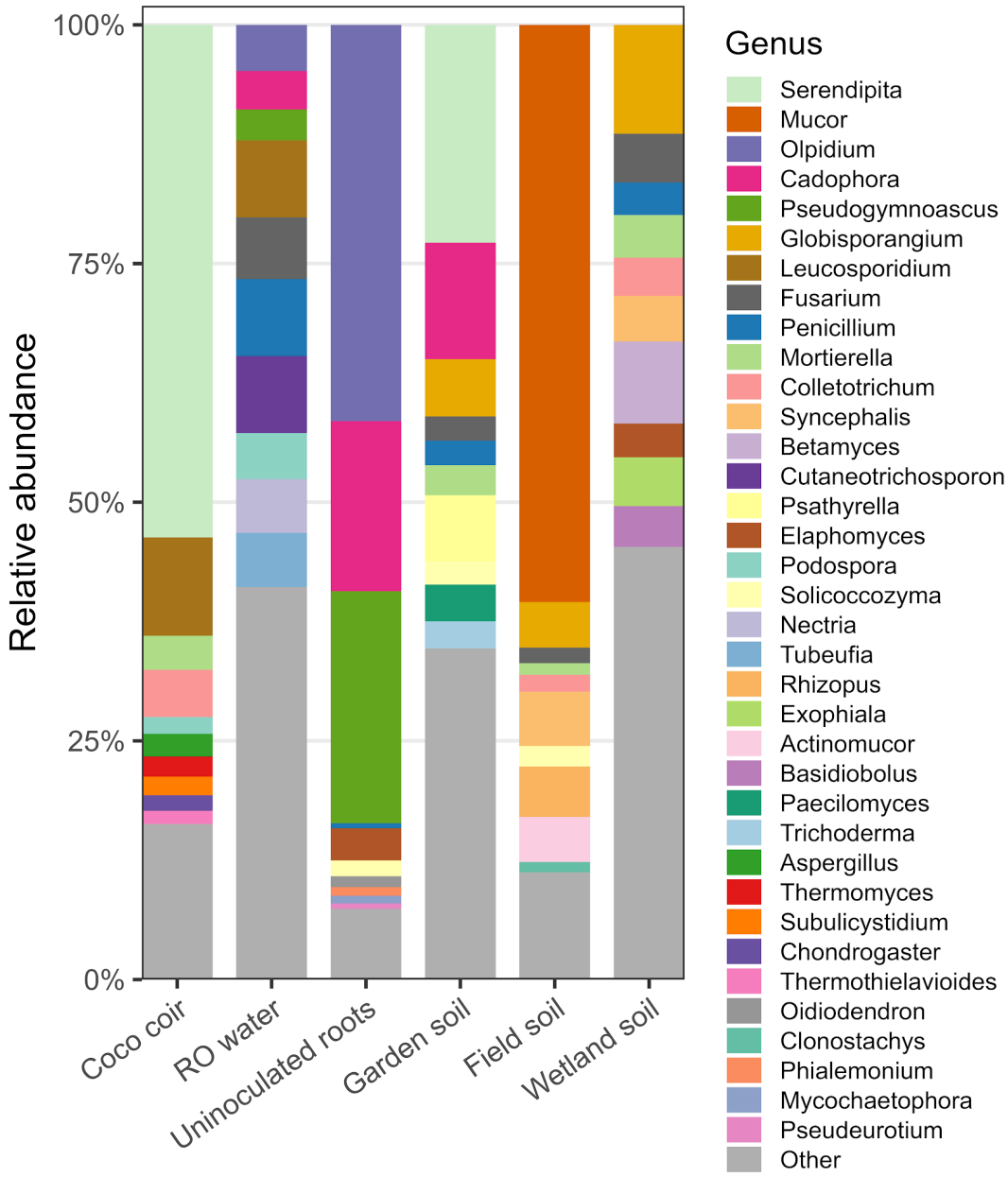


Figure 6.2A. Stacked bar chart of genus-level fungal/oomycete relative abundance in each baseline microbiome sample. Relative abundance (%) is displayed for the 10 most relatively abundant genera; all others are collapsed into the "Other" category.

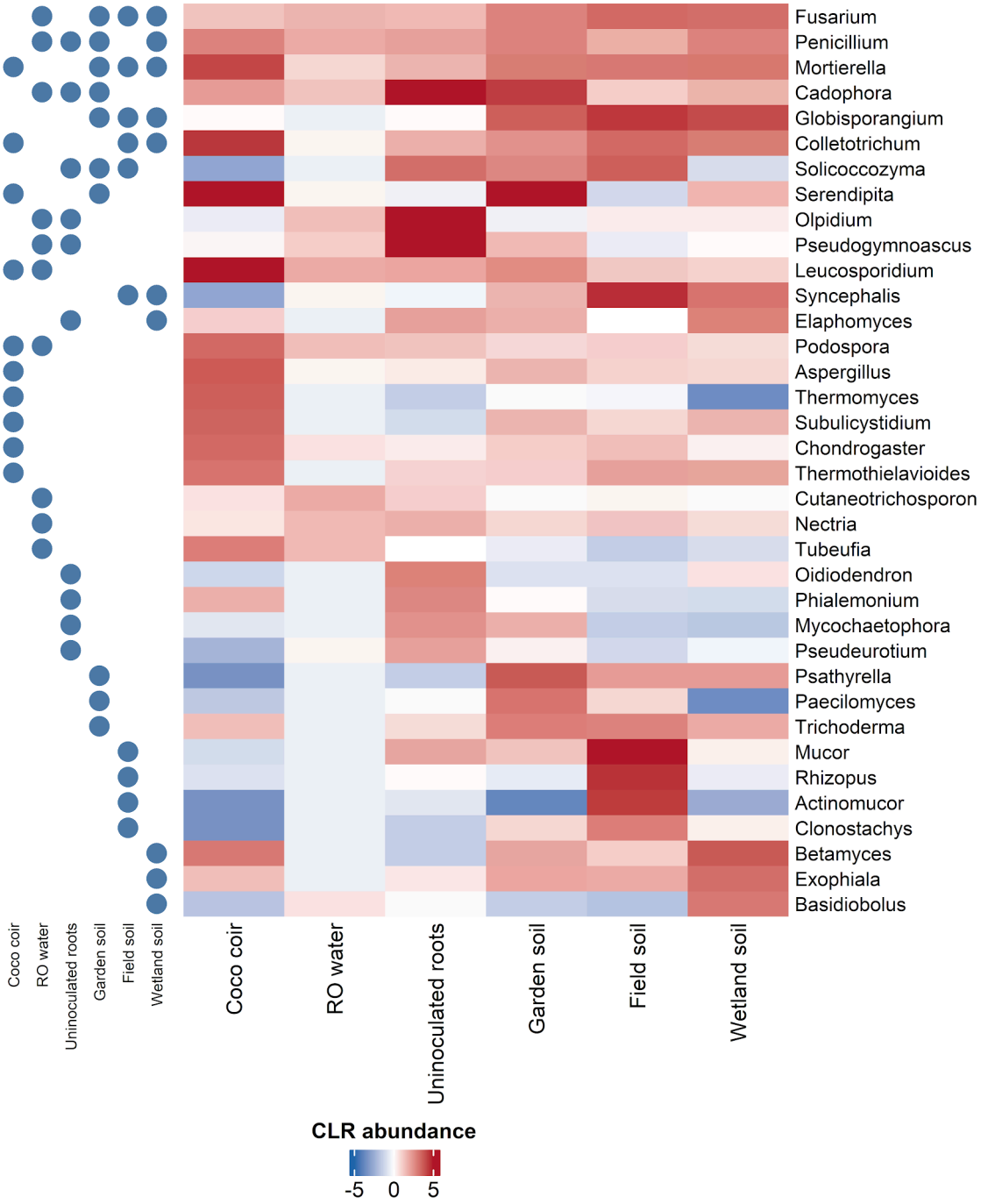


Figure 6.2B. Heat map of genus-level fungal/oomycete community composition in each baseline microbiome sample. Each row represents one of the top ten most relatively abundant genera identified in Figure 6.2A. In the dot-map (left), dot indicates which baseline communities each taxa was within the top ten genera for relative abundance. Tile colours of red and blue indicate high or low CLR abundance per sample, which can be interpreted in relative terms, as higher or lower than the geometric mean abundance (white) of the dataset, respectively.

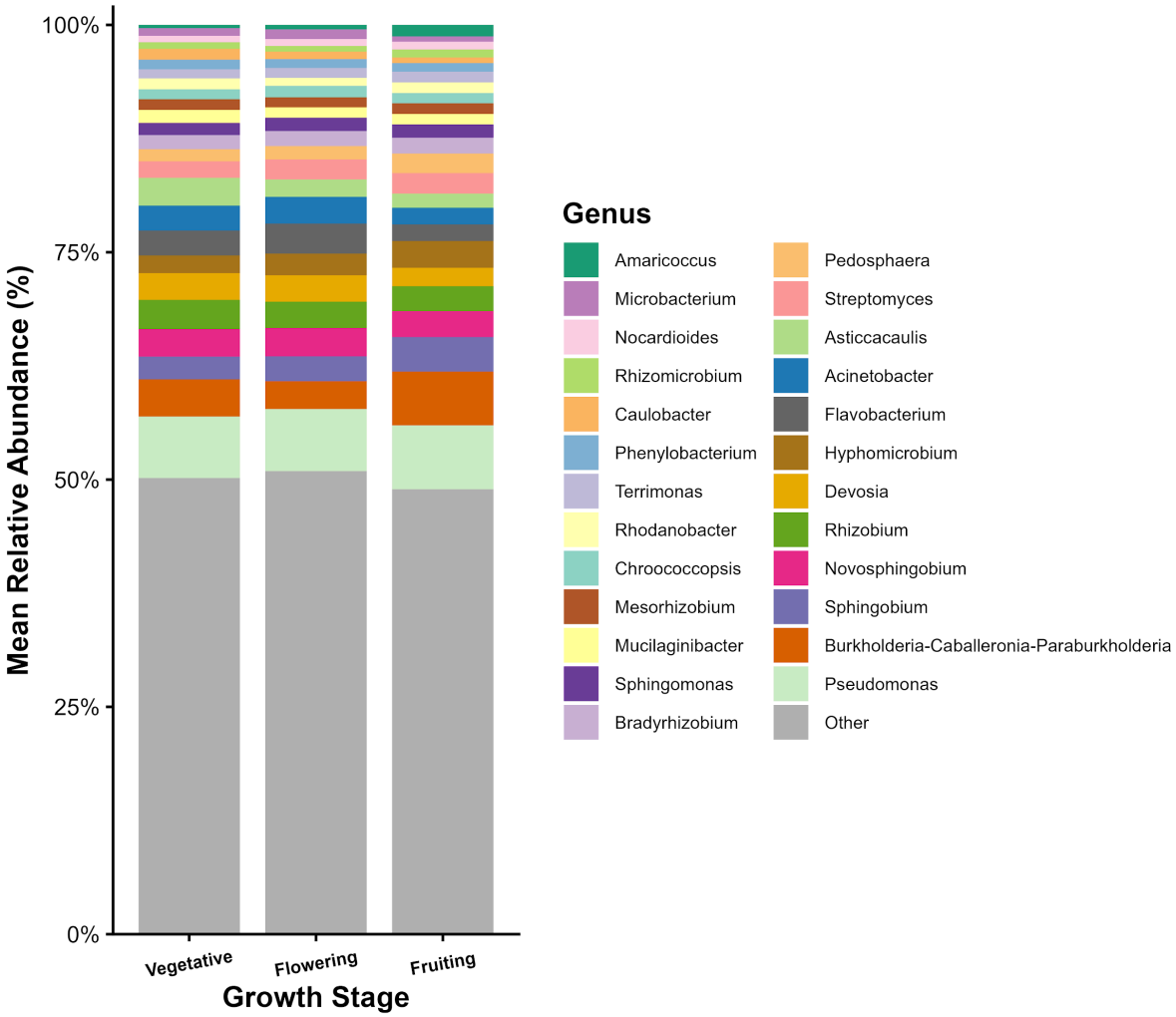


Figure 8.1A. Stacked bar chart summary of hydroponic strawberry rhizomicrobiome bacterial composition with respect to growth stage. Each bar summarizes mean relative abundance (%) for the top 25 most abundant bacterial genera at one of three strawberry growth stages. Left to right, the bars summarize data for all samples collected at vegetative (n = 34), flowering (n = 19), and fruiting (n = 41) growth stages. The 25 most abundant genera are ordered top to bottom in the legend and each bar. All other genera are collapsed into the "Other" category.

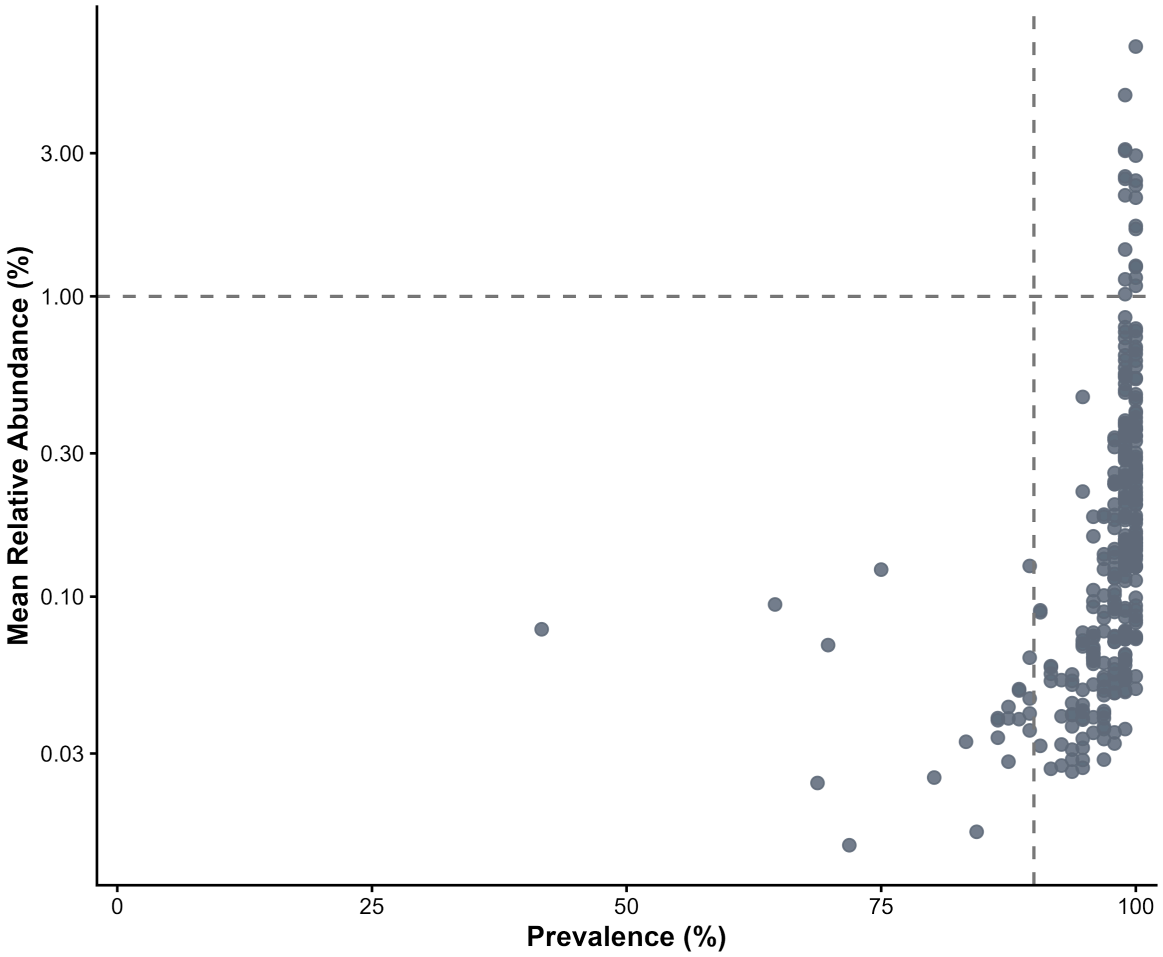


Figure 8.1B. Prevalence-abundance plot of bacterial genera across all growth stages. Each dot represents a bacterial genus plotted according to prevalence (%) and mean relative abundance (%) within all samples (n = 94). Taxa that surpass both dashed thresholds are highly prevalent (i.e. detected in ≥ 90% of samples) and highly abundant (i.e. ≥ 1% mean relative abundance).

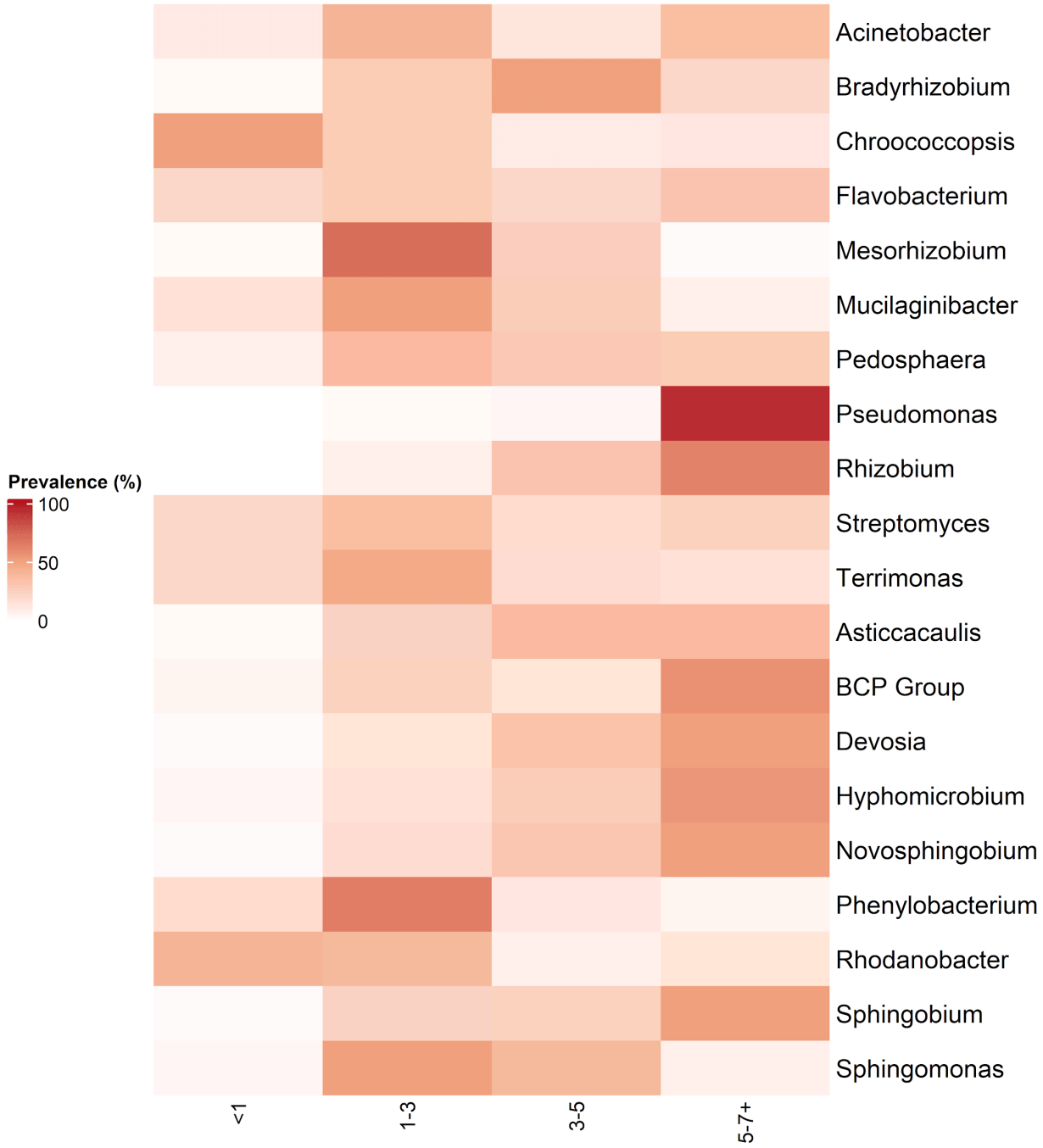


Figure 8.1C. Core occupancy heat map of prevalence and abundance of bacterial genera across all growth stages. Each row represents a highly prevalent, highly abundant taxon identified in figure 8.1B. Each column represents a range of mean relative abundance (%). Colour intensity represents the percent of samples in which that taxon is identified at the given relative abundance level. Note, "BCP Group" is an acronym for the tri-genus group "*Burkholderia-Caballeronia-Paraburkholderia*."

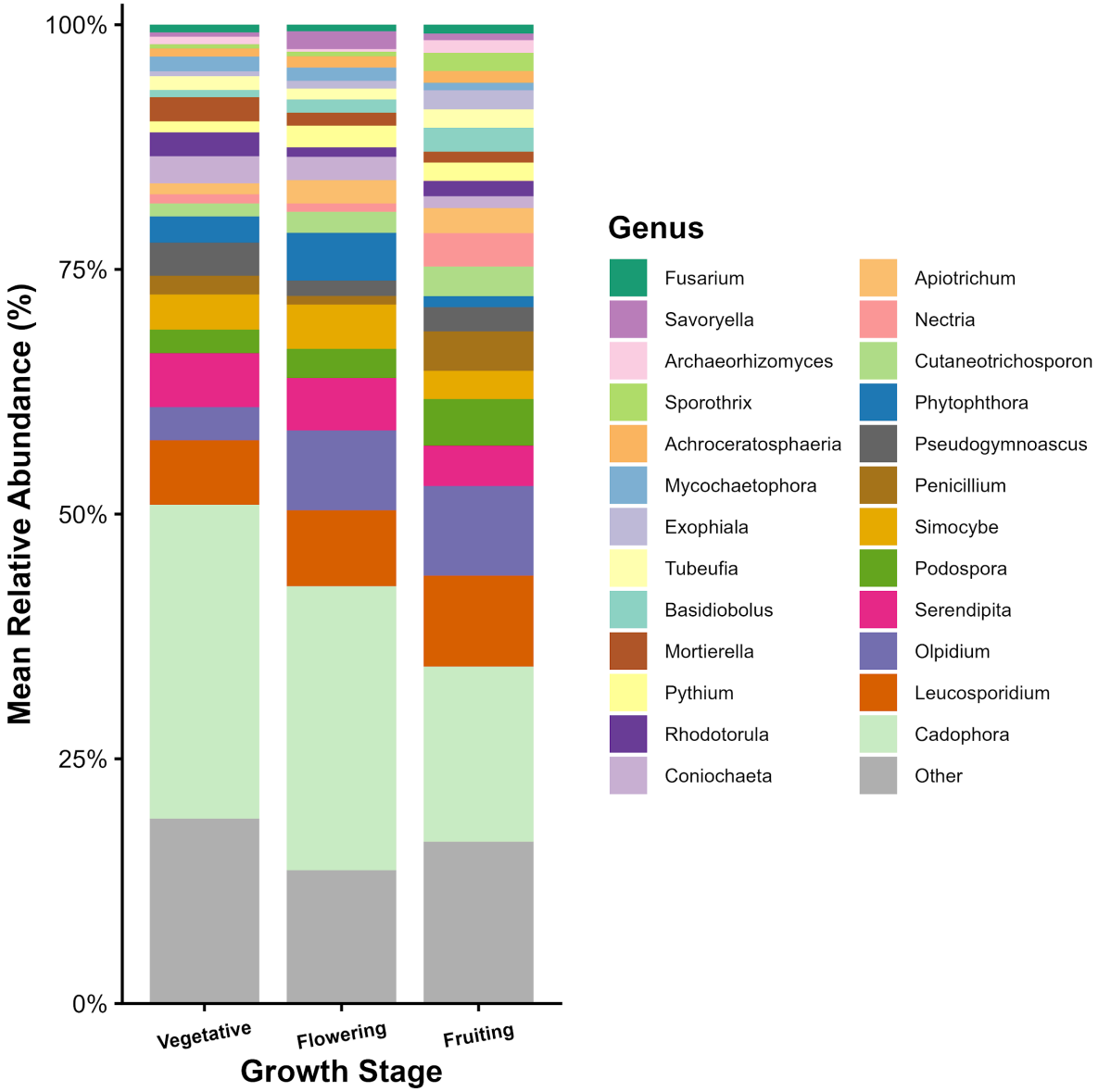


Figure 8.2A. Stacked bar chart summary of hydroponic strawberry rhizomicrobiome fungal/oomycete composition with respect to growth stage. Each bar summarizes mean relative abundance (%) for the top 25 most abundant fungal/oomycete genera at one of three strawberry growth stages. Left to right, the bars summarize data for all samples collected at vegetative (n = 34), flowering (n = 19), and fruiting (n = 41) growth stages. The 25 most abundant genera are ordered top to bottom in the legend and each bar. All other genera are collapsed into the "Other" category.

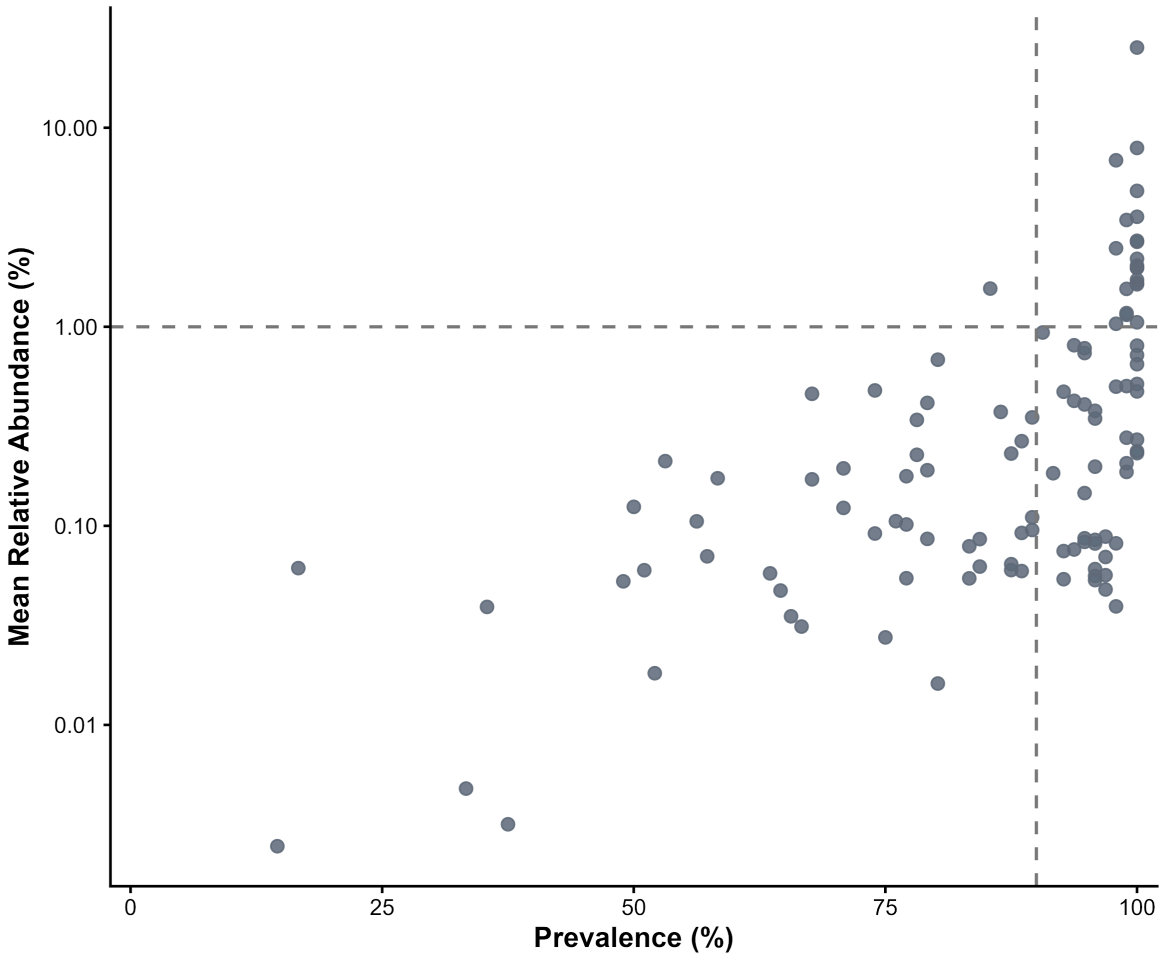


Figure 8.2B. Prevalence-abundance plot of fungal/oomycete genera across all growth stages. Each dot represents a genus plotted according to prevalence (%) and mean relative abundance (%) within all samples (n = 94). Taxa that surpass both dashed thresholds are highly prevalent (i.e. detected in ≥ 90% of samples) and highly abundant (i.e. ≥ 1% mean relative abundance).

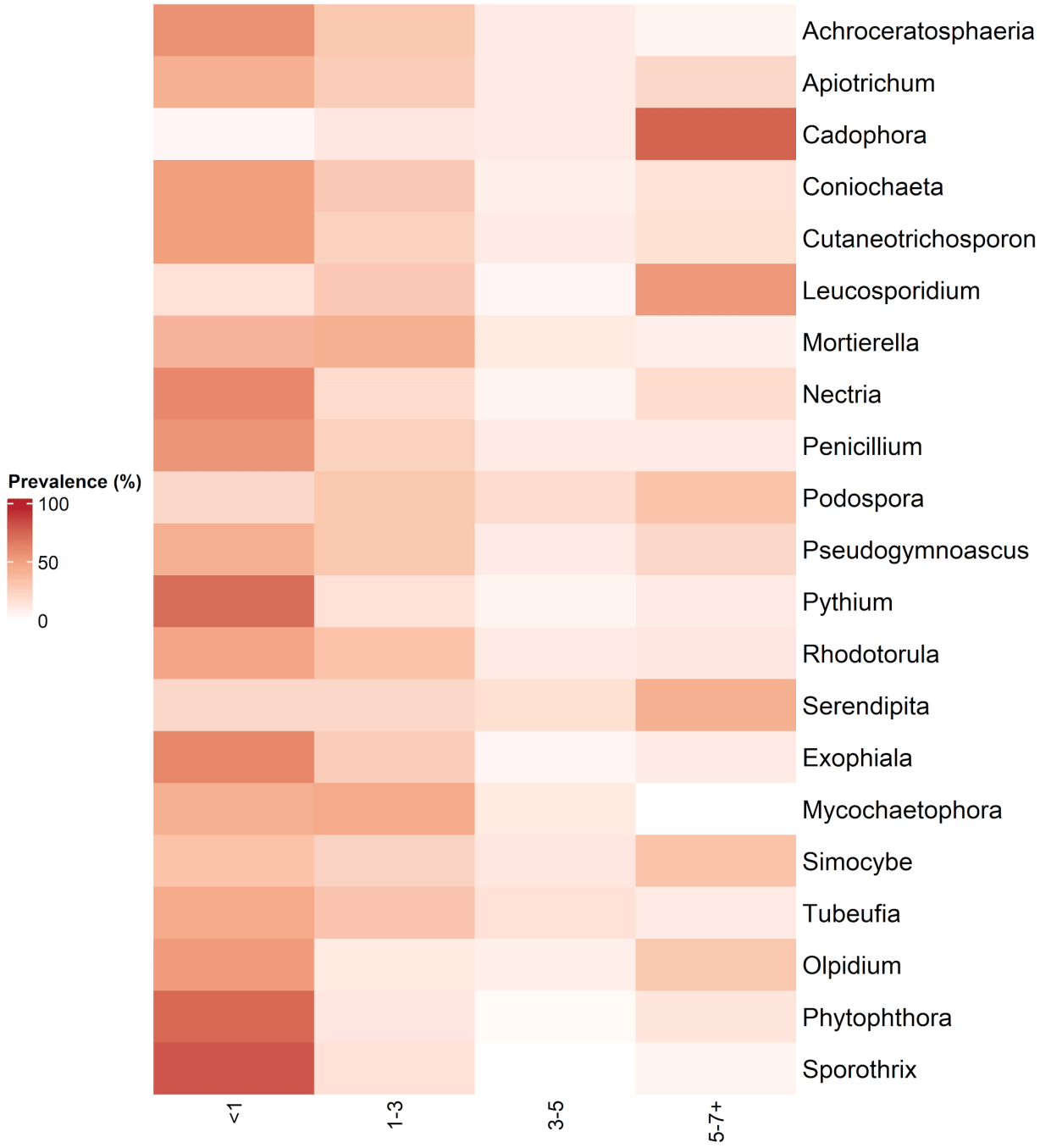


Figure 8.2C. Core occupancy heat map of prevalence and abundance of fungal/oomycete genera across all growth stages. Each row represents a highly prevalent, highly abundant taxon identified in Figure 8.2B. Each column represents a range of mean relative abundance (%). Colour intensity represents the percent of samples in which that taxon is identified at the given relative abundance level.

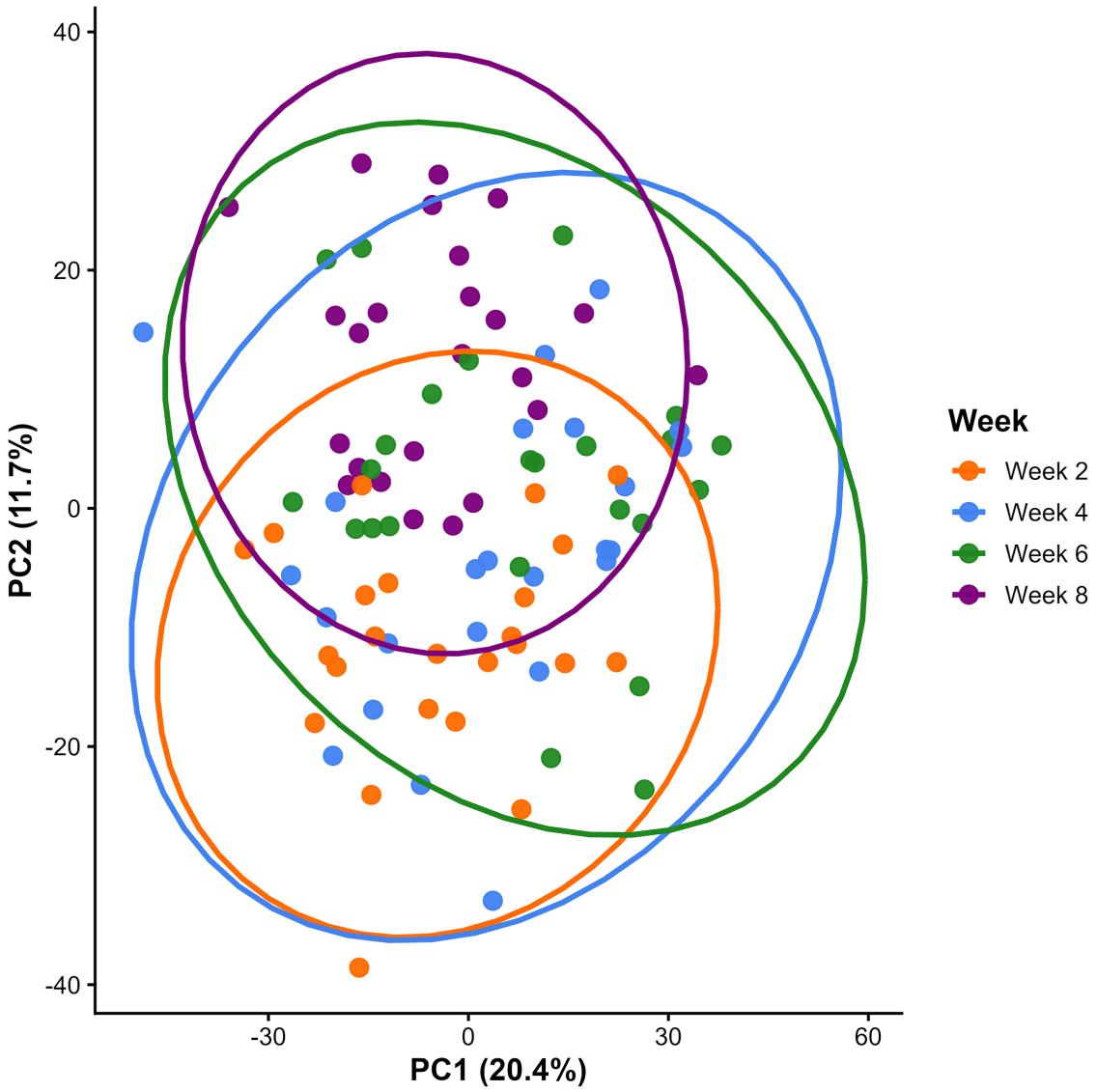


Figure 9.1A. Principal component analysis (PCA) of species-level 16S CLR-abundance at four biweekly timepoints. Each point represents the bacterial community of one sample. Sample points are coloured based on timepoint, week two (orange), week four (blue), week six (green), and week eight (purple), with corresponding 95% confidence interval ellipses (n = 24).

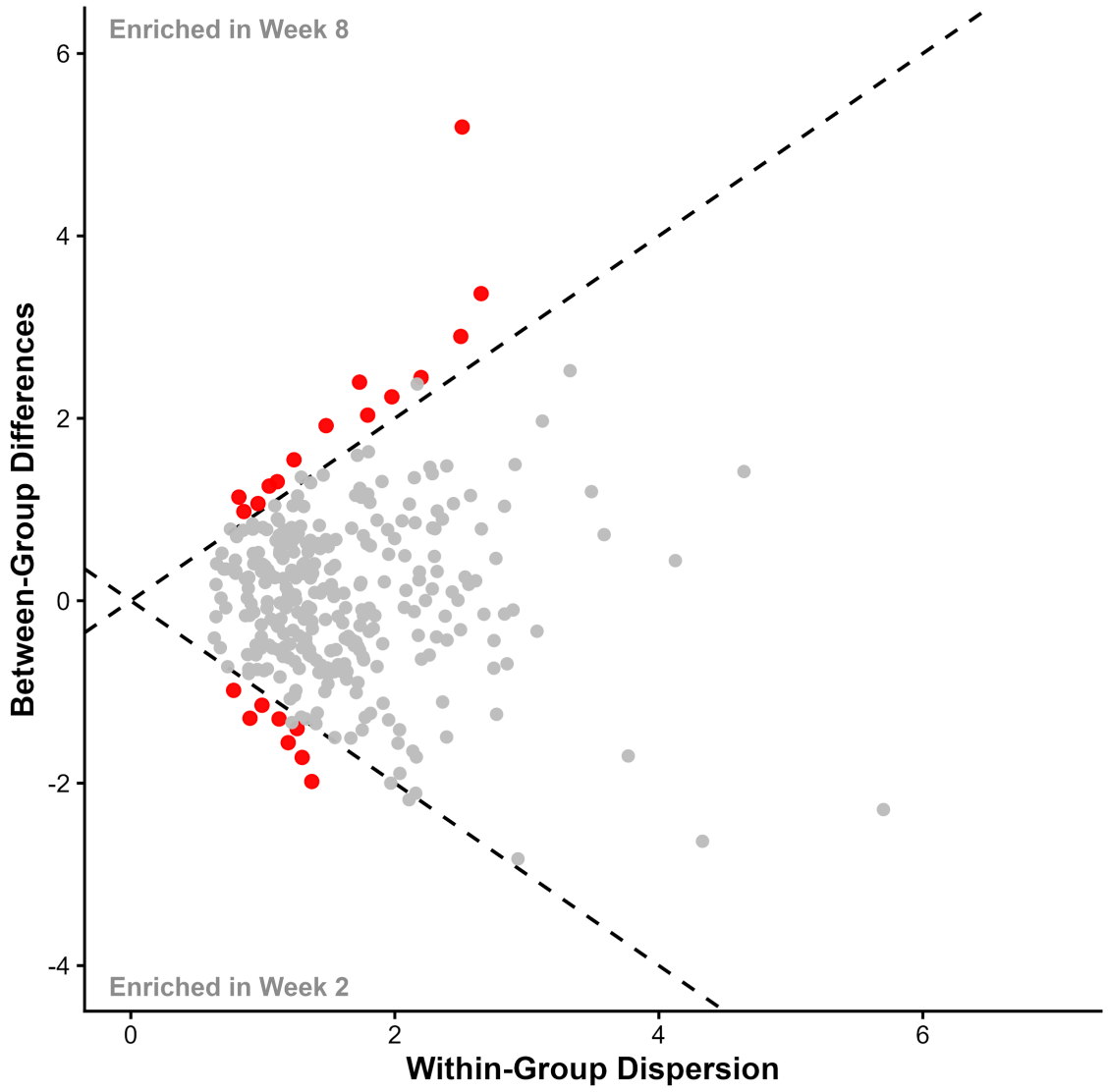


Figure 9.1B. ALDEx2 effect plot for genus-level 16S CLR abundance data at week two and week eight. Each point represents a bacterial genus, plotted based on median within-group dispersion (i.e. variance) and median between-group difference of CLR abundance data between week two and week eight timepoints. Location of points outside of the dashed lines indicates enrichment of that taxon in one group, relative to the other, as labelled on the plot. Both black and grey points indicate statistical insignificance (FDR >0.05), with effect sizes of >|1| and <|1|, respectively. Red points denote significant differentially abundant taxa, with effect size >|1| and FDR <0.05.

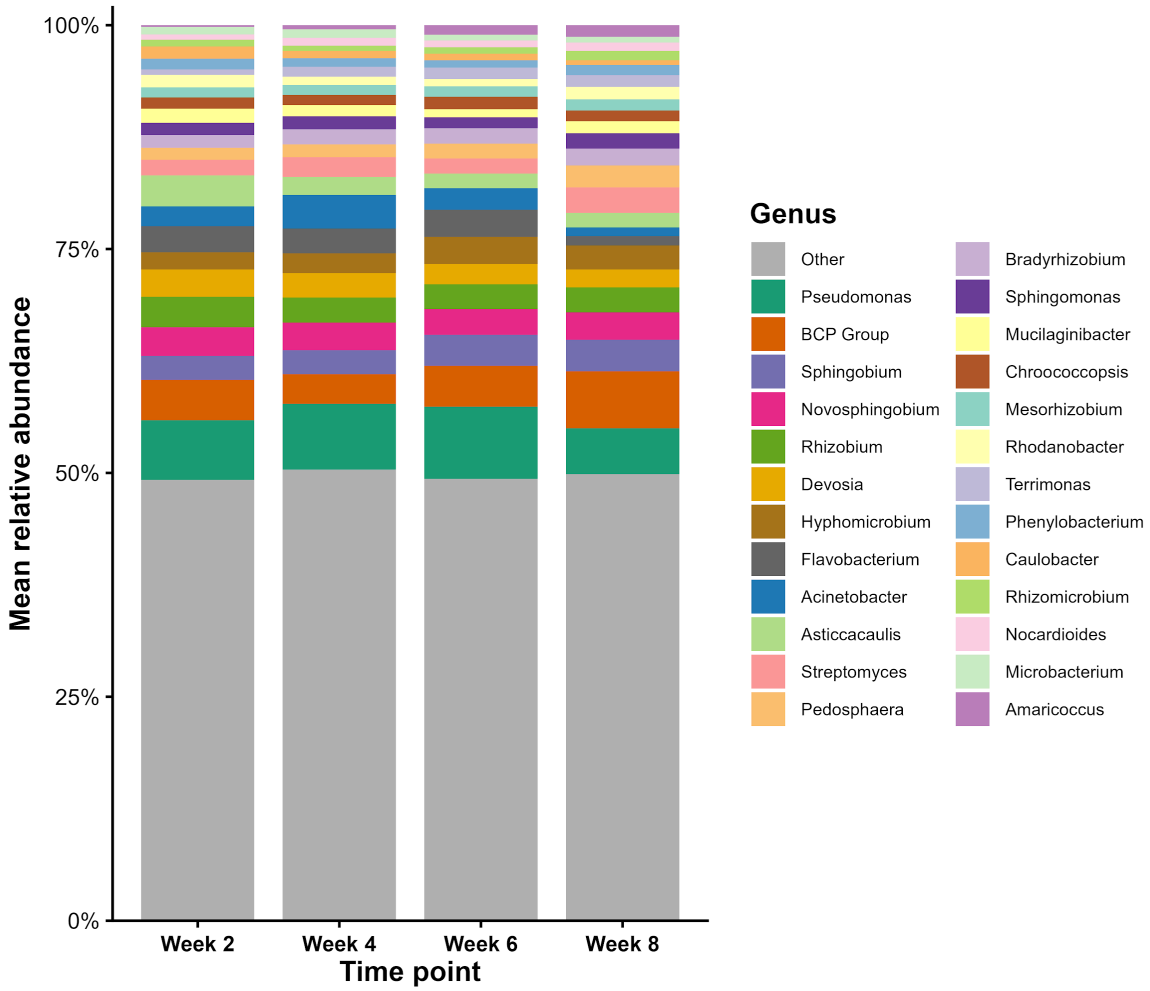


Figure 9.1C. Stacked bar chart summary of hydroponic strawberry rhizomicrobiome bacterial composition with respect to time in weeks. Each bar summarizes mean relative abundance (%) for the top 25 most abundant genera at one of four biweekly timepoints. All other genera are collapsed into the "Other" category. Note, "BCP Group" is an acronym for the tri-genus group "*Burkholderia- Caballeronia-Paraburkholderia*."

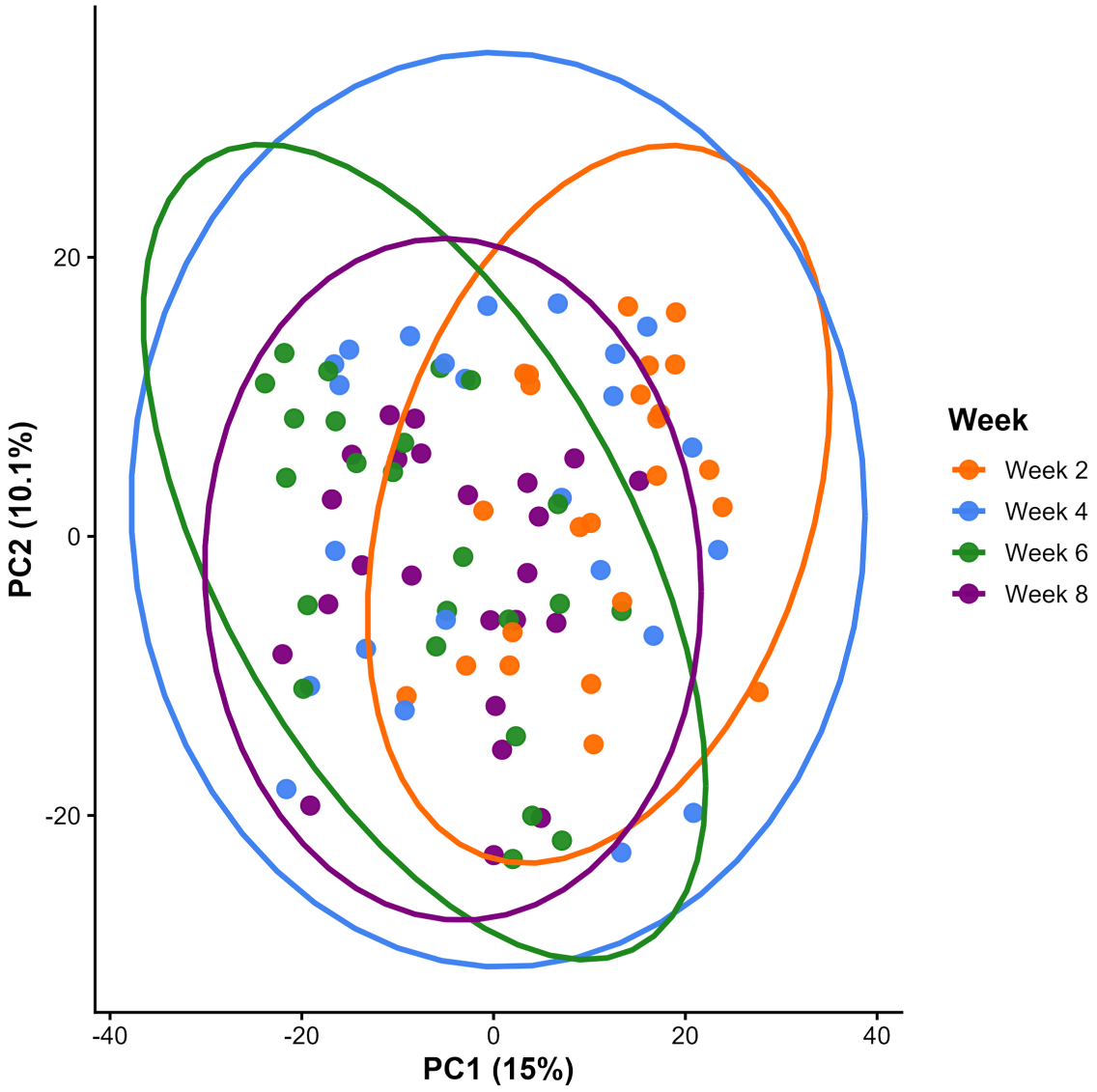


Figure 9.2A. Principal component analysis (PCA) of species-level ITS CLR-abundance at four biweekly timepoints. Each point represents the fungal/oomycete community of one sample. Sample points are coloured based on timepoint, week two (orange), week four (blue), week six (green), and week eight (purple), with corresponding 95% confidence interval ellipses (n = 24).

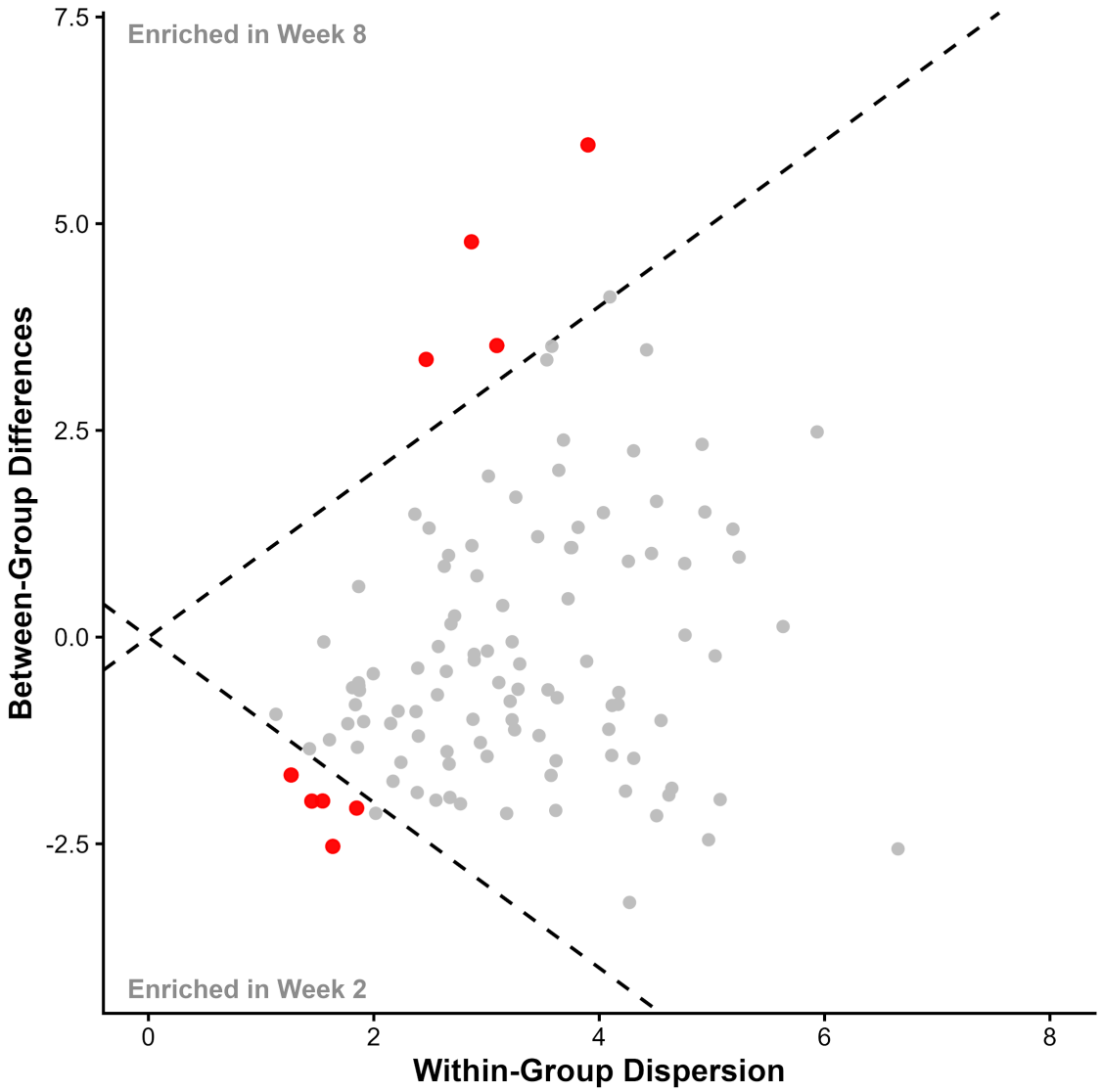


Figure 9.2B. ALDEx2 effect plot for genus-level ITS CLR abundance data at week two and week eight. Each point represents a fungal/oomycete genus, plotted based on median within-group dispersion (i.e. variance) and median between-group difference of CLR abundance data between week two and week eight timepoints. Location of points outside of the dashed lines indicates enrichment of that taxon in one group, relative to the other, as labelled on the plot. Both black and grey points indicate statistical insignificance (FDR >0.05), with effect sizes of >|1| and <|1|, respectively. Red points denote significant differentially abundant taxa, with effect size >|1| and FDR <0.05.

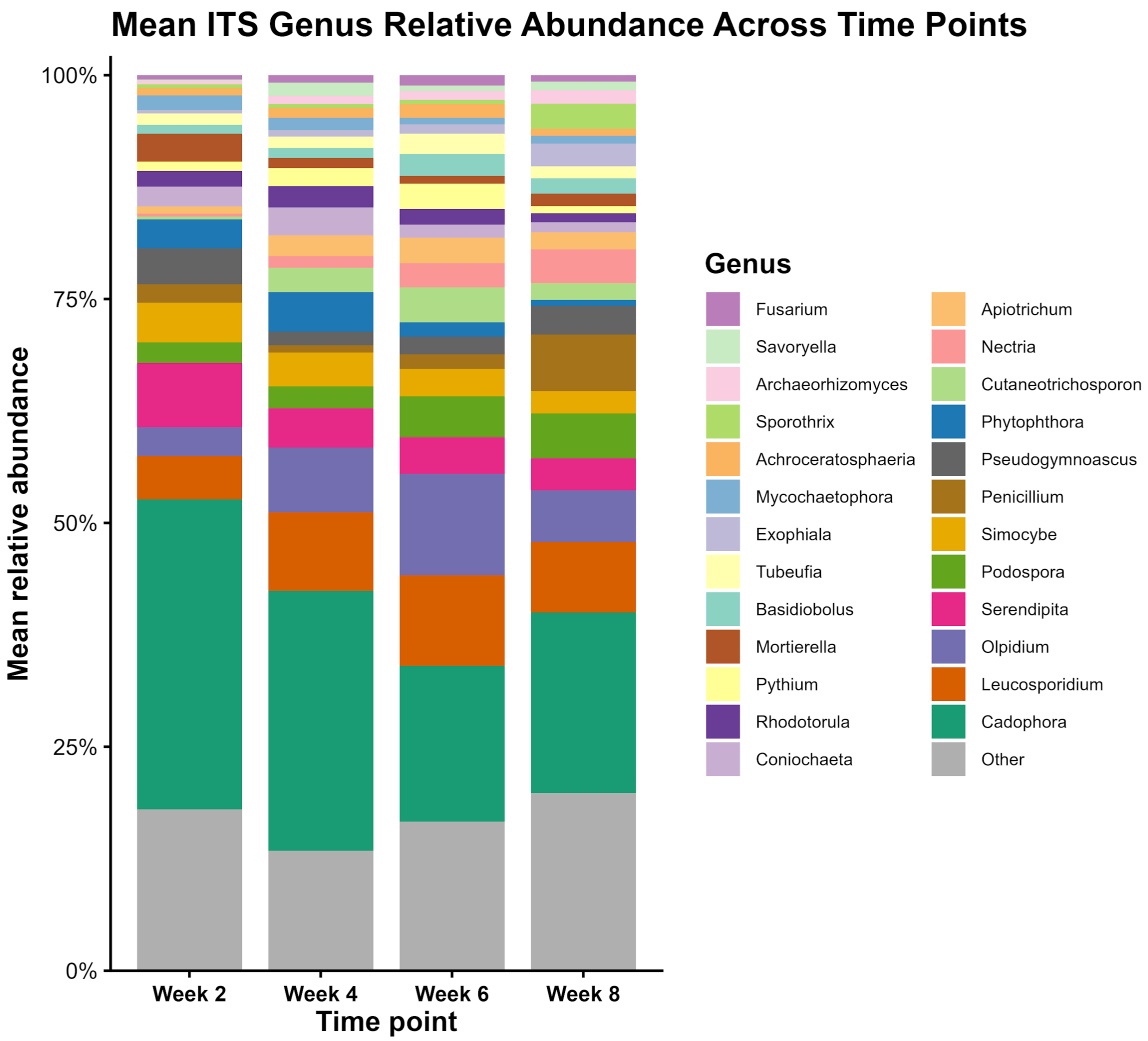


Figure 9.2C. Stacked bar chart summary of hydroponic strawberry rhizomicrobiome fungal/oomycete composition with respect to time in weeks. Each bar summarizes mean relative abundance (%) for the top 25 most abundant genera at one of four biweekly timepoints. All other genera are collapsed into the "Other" category.

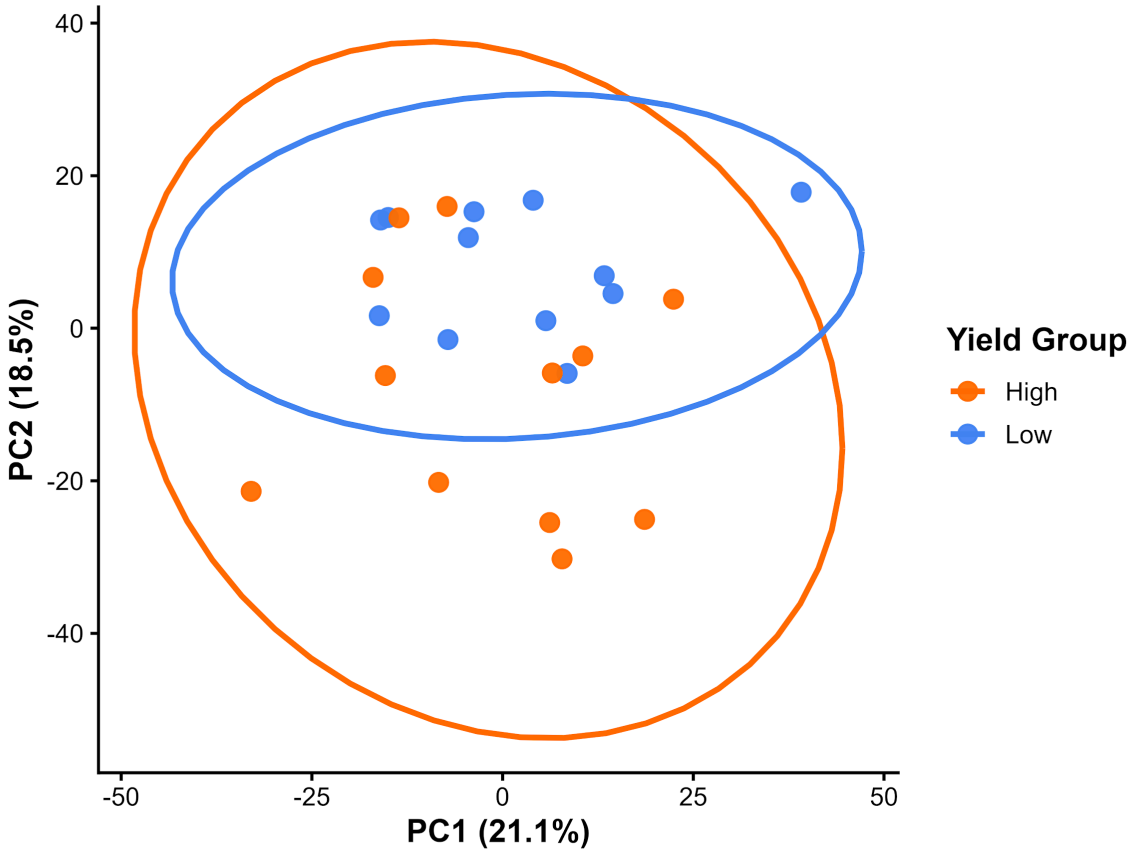


Figure 10.1A. Principal component analysis (PCA) of species-level 16S CLR abundance data for high- and low-yielding groups. Each point represents the bacterial community of one sample. Sample points are coloured based on yield category; orange and blue for high- and low-yielding groups, respectively.

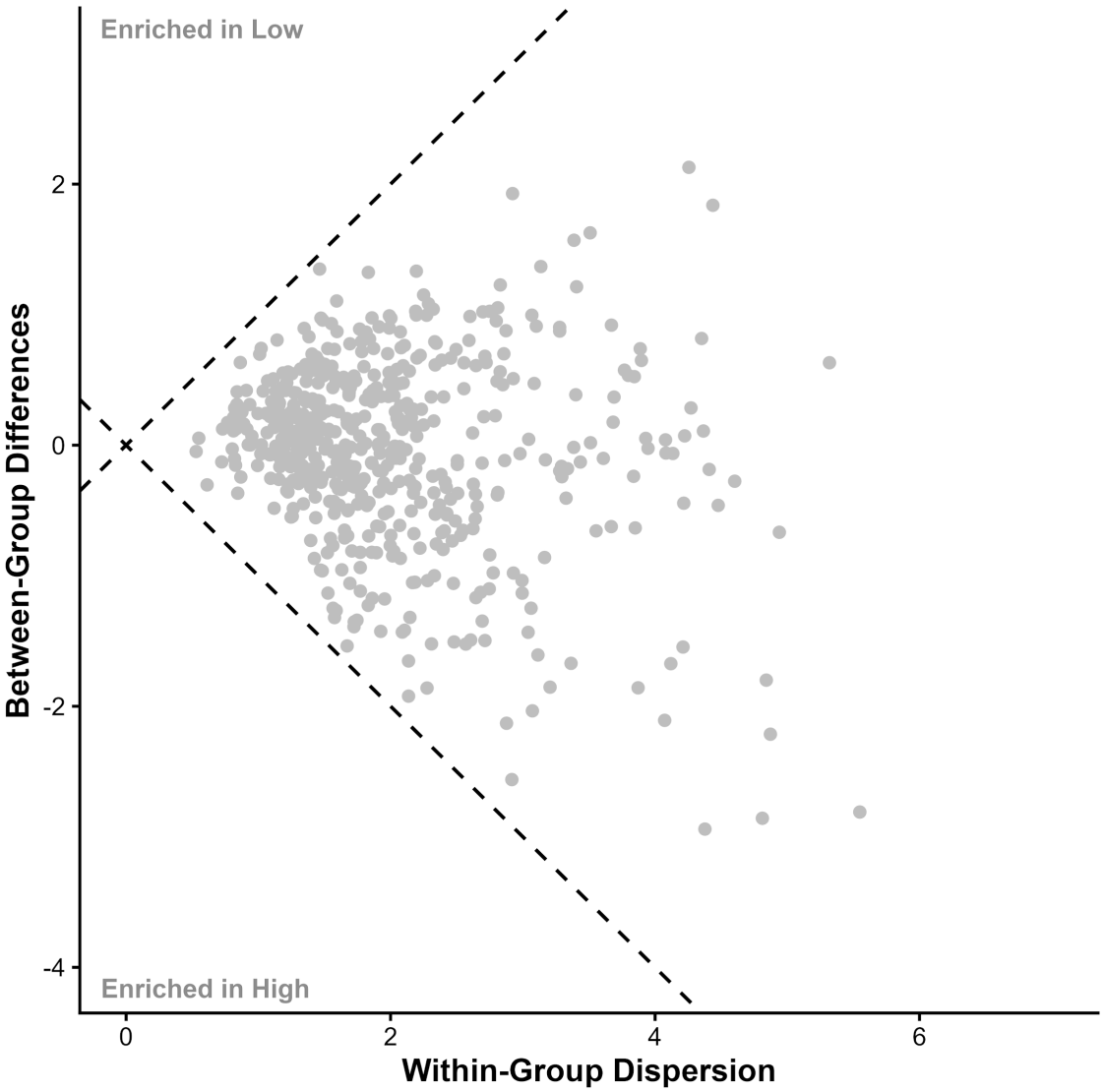


Figure 10.1B. ALDEx2 effect plot for species-level 16S CLR abundance data for high- and low-yielding groups. Each point represents a bacterial species, plotted based on median within-group dispersion (i.e. variance) and median between-group difference of 16S CLR abundance data for sample groups of high- and low-yielding plants. Location of points outside of the dashed lines indicates enrichment of that taxon in one group, relative to the other, as labelled on the plot. Both black and grey points indicate statistical insignificance (FDR >0.05), with effect sizes of >|1| and <|1|, respectively. Red points denote significant differentially abundant taxa, with effect size >|1| and FDR <0.05; no red points are observed in this figure.

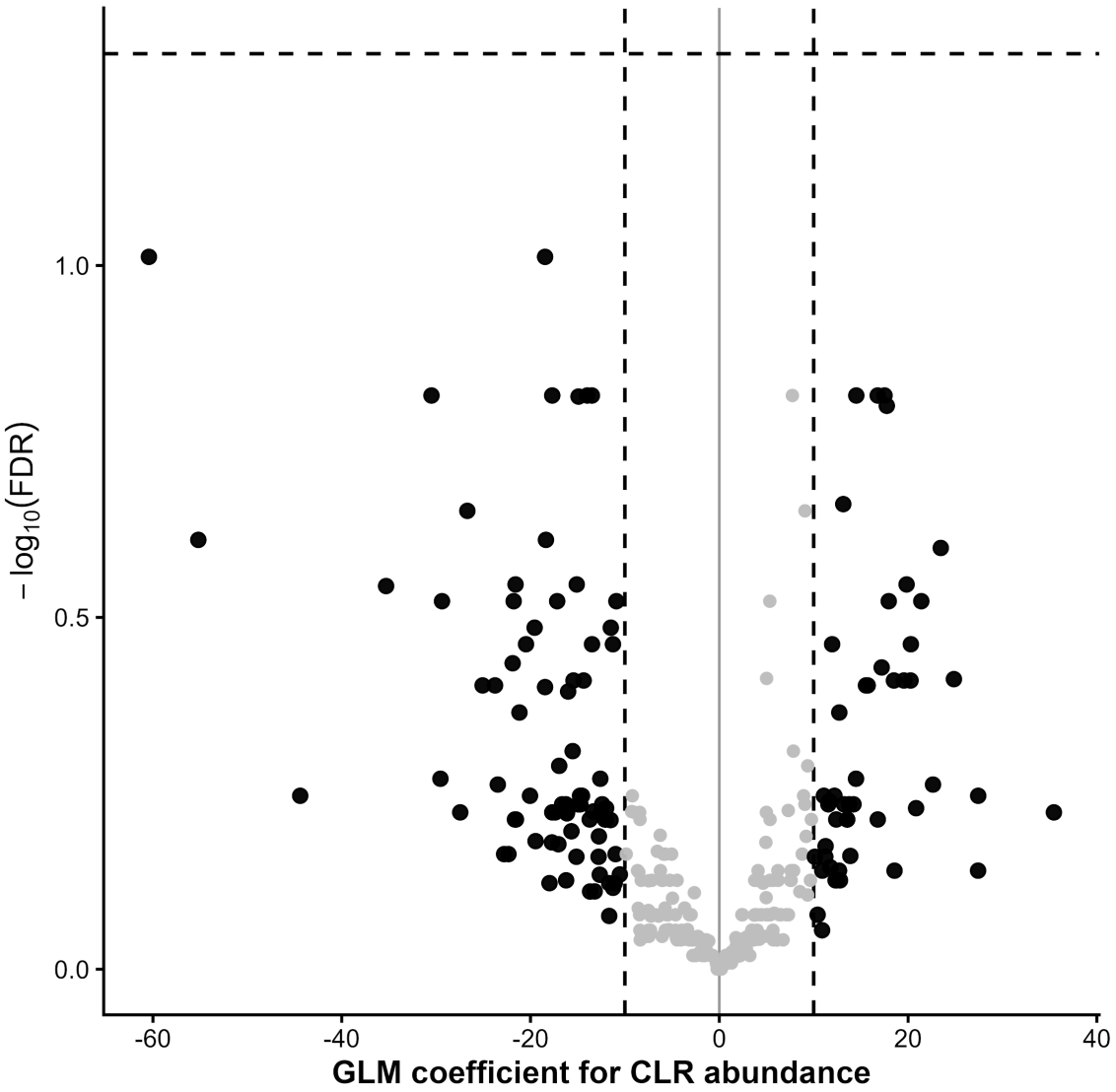


Figure 10.1C. Volcano plot of associations between yield (g) and 16S CLR abundance. Each point represents one bacterial genus, plotted according to Gaussian GLM coefficient on the x-axis and log-transformed FDR value on the y-axis. The horizontal dashed threshold represents FDR = 0.05. The vertical dashed thresholds represent the GLM coefficients at which a taxon is associated with a yield increase or decrease of 5 g per 1-unit increase in CLR abundance. Black and grey points indicate statistical insignificance (FDR >0.05), with GLM coefficients >|5| or <|5|, respectively. Red points denote significantly associated taxa with FDR <0.05 and GLM coefficient >|5|; no red points are observed in this figure.

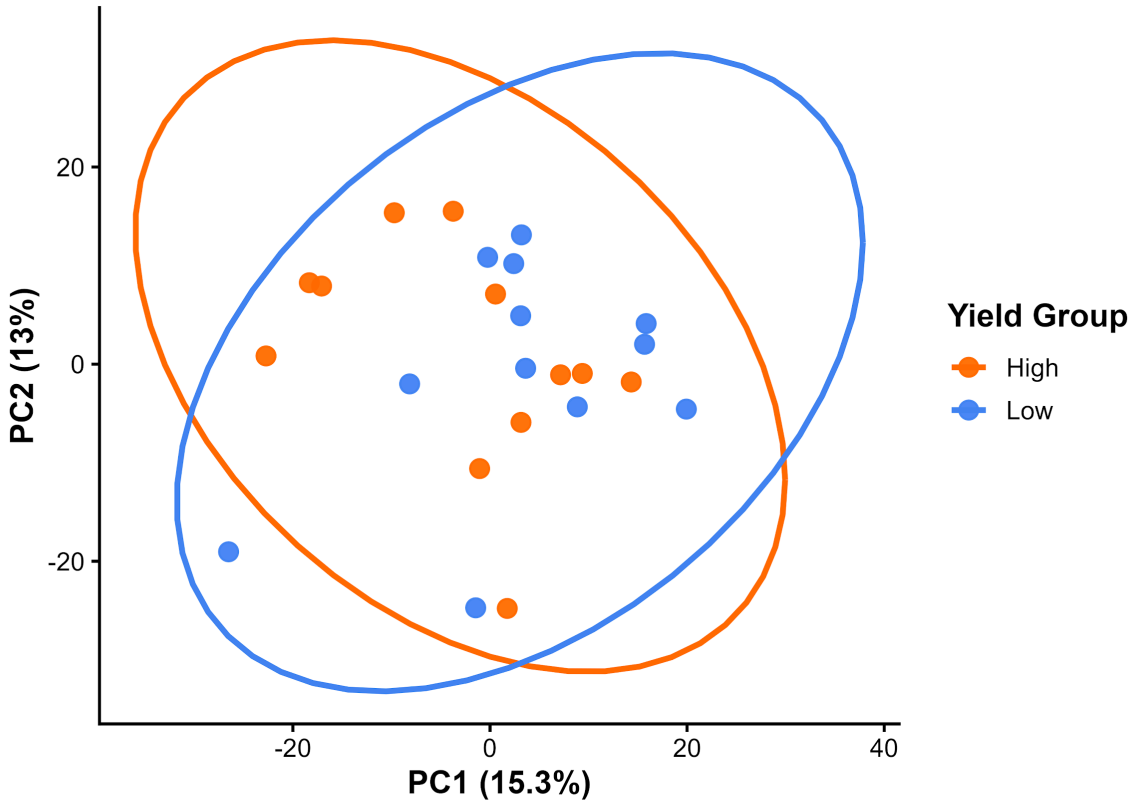


Figure 10.2A. Principal component analysis (PCA) of species-level ITS CLR abundance data for high- and low-yielding groups. Each point represents the fungal/oomycete community of one sample. Sample points are coloured based on yield category; orange and blue for high- and low-yielding groups, respectively.

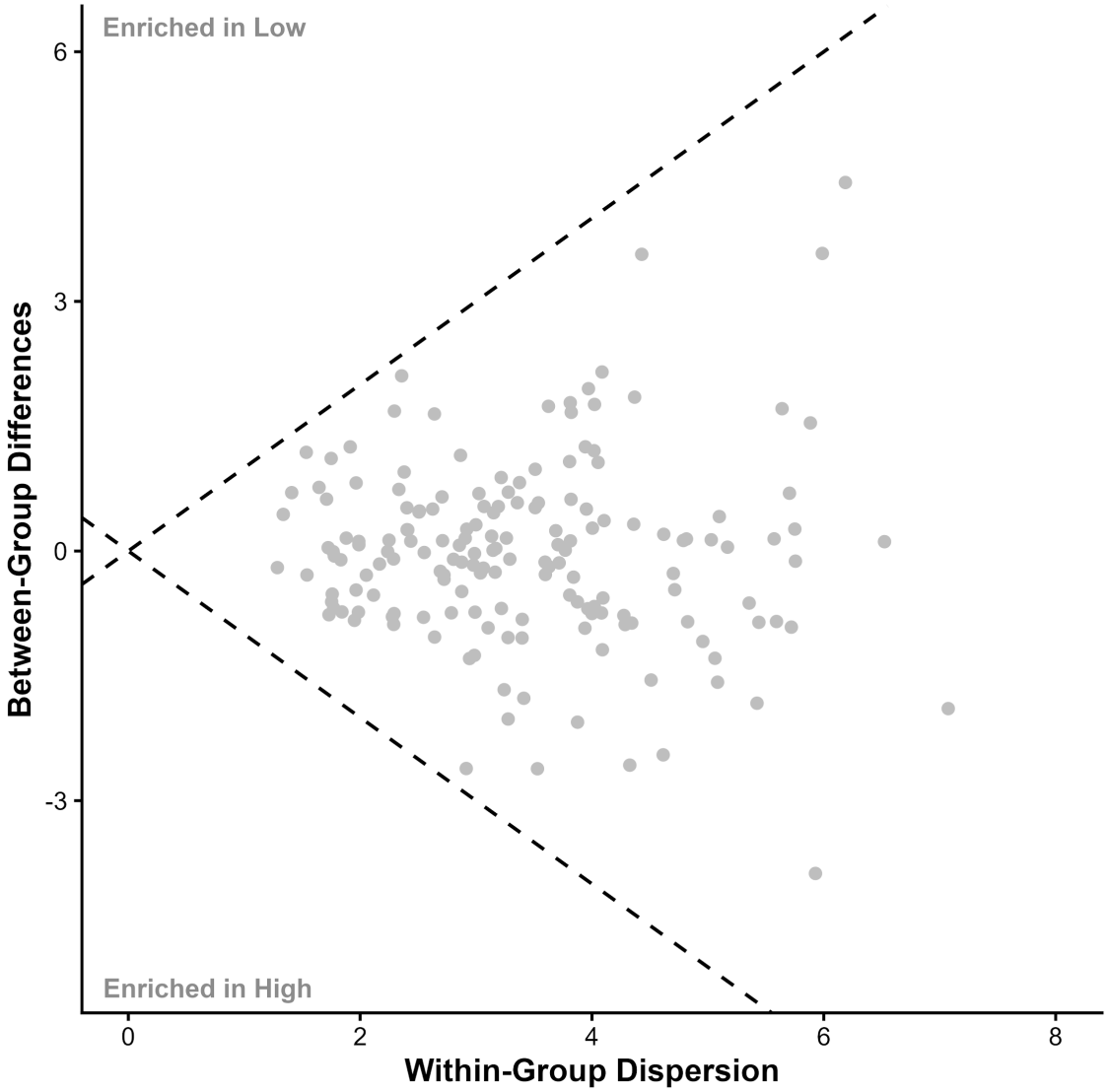


Figure 10.2B. ALDEx2 effect plot for species-level ITS CLR abundance data for high- and low-yielding groups. Each point represents a fungal/oomycete species, plotted based on median within-group dispersion (i.e. variance) and median between-group difference of 16S CLR abundance data for sample groups of high- and low-yielding plants. Location of points outside of the dashed lines indicates enrichment of that taxon in one group, relative to the other, as labelled on the plot. Both black and grey points indicate statistical insignificance (FDR >0.05), with effect sizes of >|1| and <|1|, respectively. Red points denote significant differentially abundant taxa, with effect size >|1| and FDR <0.05; no red points are observed in this figure.

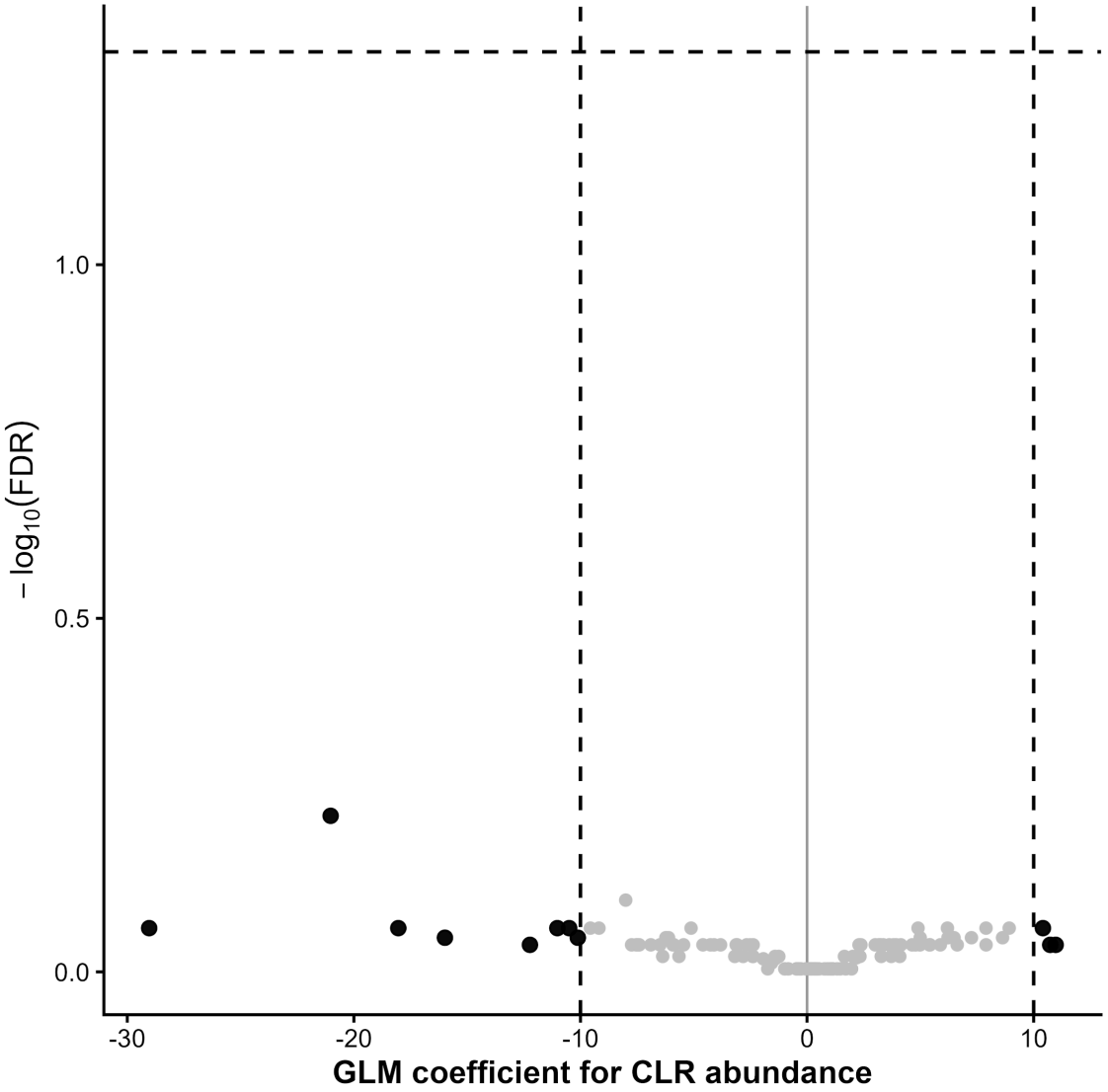


Figure 10.2C. Volcano plot of associations between yield (g) and ITS CLR abundance. Each point represents one fungal/oomycete genus, plotted according to Gaussian GLM coefficient on the x-axis and log-transformed FDR value on the y-axis. The horizontal dashed threshold represents FDR = 0.05. The vertical dashed thresholds represent the GLM coefficients at which a taxon is associated with a yield increase or decrease of 5 g per 1-unit increase in CLR abundance. Black and grey points indicate statistical insignificance (FDR >0.05), with GLM coefficients >|5| or <|5|, respectively. Red points denote significantly associated taxa with FDR <0.05 and GLM coefficient >|5|; no red points are observed in this figure.